



EX LIBRIS
UNIVERSITATIS
ALBERTENSIS

The Bruce Peel
Special Collections
Library



Digitized by the Internet Archive
in 2025 with funding from
University of Alberta Library

<https://archive.org/details/0162014920464>

University of Alberta

Library Release Form

Name of Author: Donald Alan Finlay Colwell

Title of Thesis: Horizontal Directional Drilling Field Tests: Response of Drilling Rig Pressures, Loading, and Strain on High-Density Polyethylene Pipelines

Degree: Master of Science

Year this Degree Granted: 2001

Permission is hereby granted to the University of Alberta Library to reproduce single copies of this thesis and to lend or sell such copies for private, scholarly or scientific research purposes only.

The author reserves all other publication and other rights in association with the copyright in the thesis, and except as herein before provided, neither the thesis nor any substantial portion thereof may be printed or otherwise reproduced in any material form whatever without the author's prior written permission.

University of Alberta

**Horizontal Directional Drilling Field Tests: Response of Drilling Rig Pressures,
Loading, and Strain on High-Density Polyethylene Pipelines**

by



Donald Alan Finlay Colwell

A thesis submitted to the Faculty of Graduate Studies and Research in partial fulfillment
of the requirements for the degree of Master of Science

in

Construction Engineering & Management

Department of Civil and Environmental Engineering

Edmonton, Alberta

Fall 2001

University of Alberta

Faculty of Graduate Studies and Research

The undersigned certify that they have read, and recommend to the Faculty of Graduate Studies and Research for acceptance, a thesis entitled **Horizontal Directional Drilling Field Tests: Response of Drilling Rig Pressures, Loading, and Strain on High-Density Polyethylene Pipelines** submitted by **Donald Alan Finlay Colwell** in partial fulfillment of the requirements for the degree of **Master of Science in Construction Engineering & Management**.

ABSTRACT

This thesis presents the results of a field and laboratory testing program that was utilized to understand the strain and load applied on high-density polyethylene pipes (HDPE) installed in a cohesive and cohesionless soil medium through the horizontal directional drilling process. Additionally, the response of several drilling rig parameters was captured during these installations, which included the pullback, rotational, and drilling fluid pressures. Three different pipe diameters were installed in each soil medium: 114 mm outside diameter (O.D) SDR 17 HDPE pipe, 219 mm O.D. SDR 17 HDPE pipe, and 324 mm O.D. SDR 17 HDPE pipe. Samples of the pipe material were collected both prior to and following installation to manufacture testing coupons. The sample coupons were tested in a tensile testing machine to determine the modulus of elasticity through the 2% secant method. Conclusions on the data developed through both the field and laboratory testing are subsequently presented.

ACKNOWLEDGEMENT

I would like to foremost thank my wife Julie for all her patience and support during the many hours required to write this thesis. Also, I would like to thank her for her invaluable contribution in assisting in the proofreading and revision processes.

Thank-you to the members of my family, Mom, Dad, Rose, Greg, Kelsey, Jeremy, and Dara, who encouraged me during this process.

I would like to express my appreciation for my supervisor, Dr. Samuel Ariaratnam, for his support, and assistance throughout this research.

Thank-you to the members of my examination committee, Dr. Hamid Soleymani and Dr. John Whittaker, for taking time out of their busy schedules to participate in the oral defense.

I also would like to thank the two technicians that assisted in the field and laboratory testing programs. Gerry Cyre was a great help in providing the technical knowledge for the field instrumentation and testing program. Bob Billey was very helpful during the laboratory testing of the high-density coupons. Thank-you both for your assistance and help.

For their financial support during my studies and research I would like to thank the Natural Sciences and Engineering Research Council of Canada.

TABLE OF CONTENTS

CHAPTER 1: INTRODUCTION	1
1.1 INTRODUCTION.....	1
1.2 RESEARCH SCOPE	2
1.3 RESEARCH OBJECTIVES	3
1.4 THESIS ORGANIZATION.....	4
 CHAPTER 2: BACKGROUND & LITERATURE REVIEW	 6
2.1 INTRODUCTION.....	6
2.2 HORIZONTAL DIRECTIONAL DRILLING	6
2.2.1 <i>Background</i>	6
2.2.2 <i>Drilling Procedure</i>	9
2.3 HIGH-DENSITY POLYETHYLENE	13
2.3.1 <i>Background</i>	13
2.3.2 <i>Viscoelasticity</i>	14
2.3.3 <i>Tensile Testing</i>	15
2.3.4 <i>Butt Fusion Welding Process</i>	16
2.4 MECHANICS OF THE HDD PROCESS	17
2.5 HDPE MONITORING DURING HDD INSTALLATION	19
2.5.1 <i>University of Waterloo – 1997 Installation</i>	19
2.5.2 <i>University of Waterloo – 2000 Installation</i>	22
2.5.3 <i>University of Western Ontario</i>	23
 CHAPTER 3: FIELD TESTING	 24
3.1 INTRODUCTION.....	24
3.2 FIELD TESTING LOCATIONS	24
3.2.1 <i>University of Alberta Farms, Edmonton, Alberta</i>	24
3.2.2 <i>Sil Silica Sand Pit, Bruderheim, Alberta</i>	25
3.3 FIELD SETUP	26
3.4 STRAIN MONITORING SYSTEM.....	27

3.4.1	<i>Linear Potentiometers</i>	27
3.4.2	<i>Installation Procedure</i>	28
3.4.3	<i>Calibration</i>	29
3.5	LOAD CELL DEVICE	29
3.5.1	<i>Load Cell Construction</i>	30
3.5.2	<i>Load Cell Calibration</i>	30
3.5.3	<i>Field Connection Procedure</i>	31
3.6	PRESSURE TRANSDUCERS FOR HYDRAULIC PRESSURES.....	32
3.6.1	<i>Pressure Transducers</i>	32
3.6.2	<i>Connection Procedure</i>	33
3.7	DATA DOLPHIN DATA COLLECTION SYSTEM	34
3.7.1	<i>Data Dolphin Collection Unit</i>	34
3.8	HORIZONTAL DIRECTIONAL DRILLING RIG	35
3.8.1	<i>Specifications</i>	35
3.8.2	<i>Tracking System</i>	36
3.9	FIELD INSTALLATION PROCESS	36
 CHAPTER 4: LABORATORY TESTING		38
4.1	INTRODUCTION.....	38
4.2	COUPON MANUFACTURING PROCESS	38
4.3	TESTING EQUIPMENT	40
4.4	TESTING PROCEDURE	41
 CHAPTER 5: FIELD TESTING RESULTS		43
5.1	INTRODUCTION.....	43
5.2	UNIVERSITY OF ALBERTA FARMS INSTALLATION 1 – CLAY	43
5.2.1	<i>114 mm Diameter Pipe</i>	43
5.2.2	<i>219 mm Diameter Pipe</i>	46
5.2.3	<i>324 mm Diameter Pipe</i>	48
5.3	UNIVERSITY OF ALBERTA FARMS INSTALLATION 2 – CLAY	51
5.3.1	<i>114 mm Diameter Pipe</i>	51

5.3.2	219 mm Diameter Pipe.....	54
5.4	SIL SILICA INSTALLATION – SAND	57
5.4.1	114 mm Diameter Pipe.....	57
5.4.2	219 mm Diameter Pipe.....	60
5.4.3	324 mm Diameter Pipe.....	63
CHAPTER 6: ANALYSIS OF FIELD TESTING RESULTS		68
6.1	INTRODUCTION.....	68
6.2	114 mm DIAMETER PIPE – SOIL MEDIUM COMPARISON	68
6.2.1	Drilling Fluid Pressure	68
6.2.2	Rotational Torque Pressure	69
6.2.3	Pullback Pressure	70
6.2.4	Load Cell.....	71
6.2.5	Strain Results.....	72
6.3	219 mm DIAMETER PIPE – SOIL MEDIUM COMPARISON	74
6.3.1	Drilling Fluid Pressure	74
6.3.2	Rotational Torque Pressure	75
6.3.3	Pullback Pressure	76
6.3.4	Load Cell.....	77
6.3.5	Strain Results.....	78
6.4	324 mm DIAMETER PIPE – SOIL MEDIUM COMPARISON	80
6.4.1	Drilling Fluid Pressure	80
6.4.2	Rotational Torque Pressure	82
6.4.3	Pullback Pressure	84
6.4.4	Load Cell.....	86
6.4.5	Strain Results.....	87
6.5	DISCUSSION OF SOIL MEDIUM COMPARISON	89
6.6	CLAY SOIL MEDIUM – DIAMETER OF PIPE COMPARISON	92
6.6.1	Drilling Fluid Pressure	92
6.6.2	Rotational Pressure.....	93
6.6.3	Pullback Pressure	94

6.6.4	<i>Load Cell</i>	95
6.6.5	<i>Strain Results</i>	96
6.7	SAND SOIL MEDIUM – DIAMETER OF PIPE COMPARISON	98
6.7.1	<i>Drilling Fluid Pressure</i>	98
6.7.2	<i>Rotational Pressure</i>	99
6.7.3	<i>Pullback Pressure</i>	100
6.7.4	<i>Load Cell</i>	101
6.7.5	<i>Strain Results</i>	103
6.8	DISCUSSION OF PIPE DIAMETER COMPARISON	105
6.9	CORRELATIONS OF LOAD, STRAIN, AND PULLBACK PRESSURE	107
6.9.1	<i>Clay Soil Medium</i>	107
6.9.2	<i>Sand Soil Medium</i>	109
6.10	DISCUSSION OF LOAD, STRAIN, AND PRESSURE CORRELATION	111
CHAPTER 7: ANALYSIS OF LAB TESTING RESULTS		113
7.1	INTRODUCTION	113
7.2	HDPE PIPE INSTALLED IN CLAY	113
7.2.1	<i>219 mm Diameter</i>	113
7.2.2	<i>324 mm Diameter</i>	115
7.3	HDPE PIPE INSTALLED IN SAND	117
7.3.1	<i>219 mm Diameter</i>	117
7.3.2	<i>324 mm Diameter</i>	119
7.4	DISCUSSION OF TENSILE TESTING RESULTS	121
CHAPTER 8: CONCLUSIONS		124
8.1	CONCLUSIONS	124
8.1.1	<i>Applied Strain and General Observations</i>	124
8.1.2	<i>Cohesionless Versus Cohesive Soil Medium</i>	125
8.1.3	<i>Effect of Pipe Diameter</i>	126
8.1.4	<i>Tensile Testing of HDPE Coupons</i>	127
8.2	AREAS FOR FUTURE RESEARCH	128

REFERENCES	131
BIBLIOGRAPHY	134
APPENDIX A	141
APPENDIX B	152

LIST OF TABLES

Table 2.1: Breakdown of Pipeline Product Installed.....	7
Table 2.2: Drilling Rig Segmentation	9
Table 3.1: Drilling Fluid Mixes Utilized For The Installations	37
Table 7.1: Summary of Elastic Modulus Values from Tensile Testing	122
Table 7.2: Percent Difference Between the Mean Elastic Modulus Values	123

LIST OF FIGURES

Figure 2.1: Vermeer Midi Size Drilling Rig	8
Figure 2.2: American Augers Large Size Drilling Rig	8
Figure 2.3: Pilot Boring Phase of the HDD Installation	10
Figure 2.4: Assorted Reamers	11
Figure 2.5: Reaming and Pullback Phase of the HDD Installation	12
Figure 2.6: Production of Polyethylene	13
Figure 2.7: Secant Method for Calculation of the Elastic Modulus.....	16
Figure 2.8: Butt Fusion Welding of a 200 mm Diameter HDPE Pipe	17
Figure 2.9: Key Stress Areas on Pipelines During the Pullback Phase	18
Figure 2.10: Forces on the Pipe During Pullback	19
Figure 3.1: University of Alberta Farms Site – Clay Soil Medium	25
Figure 3.2: Sil Silica Sand Pit – Sand Soil Medium	26
Figure 3.3: Plan View of the Typical Installation Layout.....	27
Figure 3.4: Linear Potentiometer	28
Figure 3.5: Linear Potentiometer Placement in the HDPE Pipes.....	28
Figure 3.6: Linear Potentiometer Configuration for the 200 mm (8 in.) Pipe	29
Figure 3.7: Manufactured Load Cell	30
Figure 3.8: Calibration Curve for the Load Cell	31
Figure 3.9: Load Cell Connected to the 200 mm Pipe in the Sand Medium	32
Figure 3.10: Pictures of the Pressure Transducers	33
Figure 3.11: Connection of the Pressure Transducers to the Drilling Rig.....	33
Figure 3.12: Data Dolphin Data Collection Unit	34
Figure 3.13: Vermeer D24-40A Horizontal Directional Drilling Rig.....	35
Figure 4.1: Typical HDPE Coupon	39
Figure 4.2: Completed HDPE Coupons	39
Figure 4.3: MTS 810 Structural Testing Machine	40
Figure 4.4: MTS Model 632 Extensometer.....	41
Figure 4.5: Testing of a Sample Coupon	42
Figure 5.1: 114 mm Bore Path Profile – Clay 1	43

Figure 5.2: 114 mm Drilling Rig Pressures During Pullback – Clay 1.....	45
Figure 5.3: 219 mm Bore Path Profile – Clay 1.....	46
Figure 5.4: 219 mm Drilling Rig Pressures During Pullback – Clay 1.....	47
Figure 5.5: 219 mm Strain During Pullback – Clay 1.....	48
Figure 5.6: 324 mm Bore Path Profile - Clay	48
Figure 5.7: 324 mm Drilling Rig Pressure During Pre-Ream - Clay.....	49
Figure 5.8: 324 mm Drilling Rig Pressure During Pullback - Clay.....	50
Figure 5.9: 324 mm Strain During Pullback - Clay	51
Figure 5.10: 114 mm Bore Path Profile – Clay 2.....	51
Figure 5.11: 114 mm Rig Pressure During Pullback – Clay 2.....	52
Figure 5.12: 114 mm Load Cell Results During Pullback – Clay 2	53
Figure 5.13: 114 mm Strain During Pullback – Clay 2.....	54
Figure 5.14: 219 mm Bore Path Profile – Clay 2.....	54
Figure 5.15: 219 mm Rig Pressure During Pullback – Clay 2.....	55
Figure 5.16: 219 mm Load Cell Results During Pullback – Clay 2	56
Figure 5.17: 219 mm Strain During Pullback – Clay 2.....	57
Figure 5.18: 114 mm Bore Path Profile - Sand.....	57
Figure 5.19: 114 mm Rig Pressure During Pullback – Sand	58
Figure 5.20: 114 mm Load Cell Results During Pullback – Sand.....	59
Figure 5.21: 114 mm Strain During Pullback – Sand	60
Figure 5.22: 219 mm Bore Path Profile – Sand	60
Figure 5.23: 219 mm Rig Pressure During Pullback – Sand	61
Figure 5.24: 219 mm Load Cell Results During Pullback – Sand.....	62
Figure 5.25: 219 mm Strain During Pullback – Sand	63
Figure 5.26: 324 mm Bore Path Profile - Sand.....	63
Figure 5.27: 324 mm Drilling Rig Pressure During Pre-Ream - Sand	64
Figure 5.28: 324 mm Drilling Rig Pressure During Pullback - Sand	65
Figure 5.29: 324 mm Load Cell Results During Pullback – Sand.....	66
Figure 5.30: 324 mm Strain During Pullback – Sand	67
Figure 6.1: Pullback Drilling Fluid Pressures for 114 mm Pipes	69
Figure 6.2: Pullback Rotational Pressures for 114 mm Pipes.....	70

Figure 6.3: Pullback Pressures for 114 mm Pipes.....	71
Figure 6.4: Load Cell Comparisons for 114 mm Pipes.....	72
Figure 6.5: Average Strain During Pullback for 114 mm Pipes	73
Figure 6.6: Maximum Recorded Strain During Pullback for 114 mm Pipes.....	74
Figure 6.7: Pullback Drilling Fluid Pressures for 219 mm Pipes	75
Figure 6.8: Pullback Rotational Pressures for 219 mm Pipes.....	76
Figure 6.9: Pullback Pressures for 219 mm Pipes.....	77
Figure 6.10: Load Cell Comparisons for 219 mm Pipes.....	78
Figure 6.11: Average Strain During Pullback for 219 mm Pipes	79
Figure 6.12: Maximum Recorded Strain During Pullback for 219 mm Pipes.....	80
Figure 6.13: Pre-Ream Drilling Fluid Pressures for 324 mm Pipes	81
Figure 6.14: Pullback Drilling Fluid Pressures for 324 mm Pipes	82
Figure 6.15: Pre-Ream Rotational Pressures for 324 mm Pipes.....	83
Figure 6.16: Pullback Rotational Pressures for 324 mm Pipes.....	84
Figure 6.17: Pre-Ream Pullback Pressures for 324 mm Pipes.....	85
Figure 6.18: Pullback Pressures for 324 mm Pipes.....	86
Figure 6.19: Load Cell Comparisons for 324 mm Pipes.....	87
Figure 6.20: Average Strain During Pullback for 324 mm Pipes	88
Figure 6.21: Maximum Recorded Strain During Pullback for 324 mm Pipes.....	89
Figure 6.22: Drilling Fluid Pressure by Diameter for the Clay Installations	93
Figure 6.23: Rotational Pressure by Diameter for the Clay Installations	94
Figure 6.24: Pullback Pressure by Diameter for the Clay Installations	95
Figure 6.25: Load Cell Results by Diameter for the Clay Installations	96
Figure 6.26: Average Strain by Diameter for the Clay Installations.....	97
Figure 6.27: Maximum Absolute Strain by Diameter for the Clay Installations.....	98
Figure 6.28: Drilling Fluid Pressure by Diameter for the Sand Installations.....	99
Figure 6.29: Rotational Pressure by Diameter for the Sand Installations	100
Figure 6.30: Pullback Pressure by Diameter for the Sand Installations.....	101
Figure 6.31: Load Cell Results by Diameter for the Sand Installations.....	102
Figure 6.32: Average Strain by Diameter for the Sand Installations	104
Figure 6.33: Maximum Absolute Strain by Diameter for the Sand Installations.....	105

Figure 6.34: Correlation of Installation Results for 219 mm Pipe in Clay	108
Figure 6.35: Correlation of Installation Results for 324 mm Pipe in Clay	109
Figure 6.36: Correlation of Installation Results for 219 mm Pipe in Sand.....	110
Figure 6.37: Correlation of Installation Results for 324 mm Pipe in Sand.....	111
Figure 7.1: Stress-Strain Graphs for 219 mm Coupons – Clay Before Installation.....	114
Figure 7.2: Stress-Strain Graphs for 219 mm Coupons – Clay Following Installation .	115
Figure 7.3: Stress-Strain Graphs for 324 mm Coupons – Clay Before Installation.....	116
Figure 7.4: Stress-Strain Graphs for 324 mm Coupons – Clay Following Installation .	117
Figure 7.5: Stress-Strain Graphs for 219 mm Coupons – Sand Before Installation	118
Figure 7.6: Stress-Strain Graphs for 219 mm Coupons – Sand Following Installation.	119
Figure 7.7: Stress-Strain Graphs for 324 mm Coupons – Sand Before Installation	120
Figure 7.8: Stress-Strain Graphs for 324 mm Coupons – Sand Following Installation.	121

LIST OF SYMBOLS

HDD	Horizontal Directional Drilling
HDPE	High-Density Polyethylene
ϵ	Strain
δ	Deformation
L	Unit Length
σ	Stress
E	Elastic Modulus (Young's Modulus)
MTS	Material Test System

1.1 INTRODUCTION

New underground infrastructure construction is an important aspect for a developing municipal environment. Installing this new infrastructure using traditional trenching techniques, particularly open cut construction, can equate to high social costs. These social costs include noise pollution, traffic disruption, aesthetic factors, and negative public perception. The use of trenchless technologies can enable installation of pipelines and other conduits under these sensitive areas while providing minimal disruption in comparison to traditional trenching methods.

Horizontal directional drilling (HDD) is a trenchless technology that has the capacity to install a wide variety of pipe materials into the ground. This process provides an alternative over the traditional open cut methodology while providing a number of benefits. For example, the HDD process can decrease the social costs of installing underground conduit as the operation can be performed more quickly, require less working space, and can be conducted without disruption to surface activities (traffic and pedestrian areas). When utilized under a watercourse, the HDD method can provide reduced environmental impacts and increased productivity in comparison to an open cut operation.

High-Density Polyethylene (HDPE) is becoming one of the most common pipe materials utilized for HDD operations. Allouche et al. (2000) conducted a survey of 49 HDD contractors which found that approximately 62% of the total length of pipe installed by the respondents was HDPE. Additionally, contractors prefer using HDPE for three key reasons: 1) segments of the pipe can be connected through the butt-fusion welding process in a timely fashion, 2) the high tensile strength of the pipe, and 3) the flexibility of the pipe complements the steering ability of the HDD operation.

While HDD has been employed in North America since the 1970's, there are still some municipalities and regulatory bodies that are wary of allowing the process. Also, some of

these municipalities do not allow the installation of HDPE pipe because they believe that the pipes will be structurally damaged during the pullback operation. It is hoped that the results of this research will make these municipalities and regulatory agencies more aware of the capabilities of the HDD process. Thus, these bodies can consider the use of HDD for new infrastructure development programs. Also, by understanding the magnitude of the loading and mechanical response of HDPE piping, engineers and other decision makers can confidently install this product in their development programs.

1.2 RESEARCH SCOPE

There are many issues and concerns related to the installation of pipelines through the HDD process. This research will focus on four distinct issues surrounding the installation of HDPE pipe through the use of HDD methodology.

The first area is the strain that is imposed on HDPE pipe during the pullback phase of the drilling process. Currently, industry experts suggest that to prevent structural damage during the HDD operation the pipe strain on a HDPE pipe should not exceed 5% (Svetlik 1993, Kirby et al. 1996). Therefore in this study, the magnitudes of the strain on different sizes of HDPE pipe will be measured during the pullback phase in both a cohesive and cohesionless soil medium. The strain experienced on the pipe during the installation process is influenced mainly by the interaction of the soil medium with the pipe. Different soil mediums will provide different frictional resistances to the pipe, interactions with the reamer, and resulting differences in the strain imposed on the pipe.

The second and third research areas focus on the load that is transferred through the reamer to the product pipeline during the pullback phase of the drilling operation and the effects of the drilling operation on the drilling rig. The force of the drilling rig is distributed through both the reamer and the product line being installed. The actual loading on the product pipeline can be compared to the strain experienced by the product pipe during the installation process. Additionally, the loading can be compared to the drilling rig pullback pressures. HDD contractors often rely on the hydraulic pressure gauges located on the drilling rig to assess the condition of the loading on the pipe. These

hydraulic gauges only give an indication of the exertion by the machine and not the actual loading or subsequent strain on the pipe. Three different pressure gauges thrust/pullback, rotational, and drilling fluid provide the operator with indications of the drilling operation. These pressures will be collected for all the installations along with the pullback force on the product pipeline.

The last area will focus on the mechanical properties of the HDPE pipe and how they change following the pullback process of the HDD operation. Segments of HDPE pipe have been collected both prior to and following installation. From these segments, coupons will be manufactured to be tested in a tensile testing machine. Through these tests, an analysis of the change in mechanical properties of the HDPE pipes can be conducted.

1.3 RESEARCH OBJECTIVES

The main objective of this research is to quantify the strain behaviour and loading on HDPE pipelines during their installation in different soil conditions. This is to try to establish that proper drilling practices can enable pipe strain to be kept below the 5% threshold, and the mechanical properties of the pipe are not adversely affected. These results may provide confidence to municipalities and other agencies in the use of the HDD process and the use of HDPE piping.

Subsequently, there are three components of this objective that will be analyzed in this thesis. The first component is to observe the changes in the drill rig pressures, the loading condition on the HDPE pipe during the pullback phase, and the strain on the HDPE pipe during the pullback phase that occur between a cohesive and a cohesionless soil medium. The second component is to observe the impact that the pipe diameter has on the drill rig pressures, loading condition of the HDPE pipe, and the strain experienced by the HDPE pipe during the pullback process for both a cohesive and a cohesionless soil medium. The final component is to determine whether or not the mechanical properties of the HDPE pipe are changed through the installations in these two soil mediums. Understanding the

behaviour of all of the identified parameters could benefit engineers and contractors that participate in HDD installations involving HDPE.

The secondary objective of this research is to increase the knowledge of the HDD industry for the benefit of contractors, municipalities, engineers, designers, public agencies, university staff, students, and other interested parties.

1.4 THESIS ORGANIZATION

Chapter 2 provides an introduction to all of the components of this research program and identifies some of the previous research that has been performed in this area. The background of the HDD industry is covered and the directional drilling procedure is explained. The installed pipe material is HDPE and subsequently the background and production process of HDPE is covered. Additionally, HDPE is a viscoelastic material and some basic viscoelastic theory is presented along with the components of a tensile testing program. Research on the strains and behaviour of HDPE pipe in HDD operations is relatively new and therefore minimal research has been performed to date. Summaries of the research developed at the University of Waterloo and the University of Western Ontario are presented.

Chapter 3 describes the testing program that was conducted to install the HDPE pipelines into the ground. Descriptions of the two testing locations are presented identifying the number of pipelines that were installed in each soil medium. To ensure reproduction of these tests the drilling procedure for each installation is identified along with the drilling fluid mixes that were used for the installation. Introductions to the various testing equipment is accomplished providing specifications and detailed photos taken during the testing program.

Chapter 4 describes the laboratory testing that was conducted for the coupon samples from the HDPE pipes. The coupon manufacturing process is introduced, and schematics of these coupons are shown. Additionally, the testing equipment is presented along with

the testing procedure that was adapted from ASTM D 638-98 *Standard Test Method for Tensile Properties of Plastics*.

Chapter 5 presents the entire field testing results that were collected from the two test sites. These results are displayed in graphical form and have been transformed from the time-based system that is presented in Appendix A to a bore path location based system. Discussion on the trends of each of the properties is conducted and the maximum values stated.

Chapter 6 provides the comparisons between the different soil mediums for the pipelines that were installed. Comparisons are made across the soil mediums for each of the 114 mm, 219 mm, and 324 mm diameter pipes. These comparisons are made based on drilling fluid pressures, rotational torque pressures, pullback pressures, load cell results, and strain results. Additional comparisons on these same parameters are made between the three pipe diameters installed in each of the soil mediums. Lastly, the pullback pressures, strain, and loading are graphically represented to allow comparisons of each parameter and how they relate to one another for the 219 and 324 mm pipes.

Chapter 7 provides the results and discussion from the laboratory testing on the HDPE coupon samples. The 2% secant method is used to calculate the elastic modulus of the HDPE pipe material and this modulus is compared between each of the samples. Comparisons are made between the uninstalled product pipe samples and the installed pipe samples to determine the change in the modulus of elasticity of the pipe material.

Chapter 8 contains the conclusions that were derived from the field and the laboratory testing programs. Recommendations for future research directions are presented based upon the discoveries made in this thesis.

2.1 INTRODUCTION

This chapter provides an introduction to horizontal directional drilling, the high-density polyethylene pipe material that was employed in the research program, and a summary of previous work that has been performed. The background of the HDD industry is given along with the typical drilling procedure employed on a directional drilling project. For the HDPE piping a brief history along with the production process is presented. The theory of viscoelasticity is presented and discussed in relation to components of a tensile testing program. Additionally, the butt-fusion welding process that bonds two segments of HDPE pipe together is discussed. Following this, the mechanics of the pullback process for HDD is presented including the key stress areas that act on the product pipe and the forces inside the borehole are presented. Finally, a summary of previous research on strain analysis and loading on HDPE pipes is presented examining each research's methodology, results, and conclusions.

2.2 HORIZONTAL DIRECTIONAL DRILLING

2.2.1 Background

Horizontal directional drilling is a member of the family of trenchless installation techniques that has evolved from the combination of the water well, oil field, and utility industries (Allouche et al. 2000). This installation technique allows for wide design flexibility through the steering capabilities of the drilling rig; bore paths may be straight or curved, and the depth and orientation may be adjusted during the drilling process. The HDD method has become a preferred choice for crossings of watercourses and roads through this wide flexibility and the ability to be non-disruptive to the surface. The HDD industry has experienced rapid growth following the first known water crossing utilizing HDD that occurred in 1971 near Watsonville, California (Allouche et al. 2000). This growth encompasses several thousand drilling rigs operated by many contractors and more variation of installation materials. Recently, HDD has seen increased use in the installation of fiber-optic cable conduits.

The nature of the HDD process lends itself well to installing a wide variety of pipe materials into the ground. The size of these installed materials depends on a number of factors including: size of the drilling rig used, soil conditions encountered, and overall length of the installation (Ariaratnam et al. 1998). Typical sizes of pipe installations range from 50 mm (fiber-optic cable conduit) to 1200 mm (pipelines) in diameter. Allouche et al. (2000) conducted a survey of forty-nine HDD contractors, across North America, to quantify the types of pipe materials installed, diameters of the installed material, and the total length installed.

Table 2.1 contains the results from this survey broken down by pipe material and diameter of the installed product. The most widely installed material, as indicated by the respondents, was HDPE at 62% of the total, followed by steel at 23%, and polyvinyl chloride (PVC) at 15%. In regard to the diameters, the range of 50–100 mm accounted for 72% of the total length installed, followed by pipes greater than 300 mm at 12%, the range of 150–200 mm at 11%, and the range of 250–300 mm for the remaining 5%.

Table 2.1: Breakdown of Pipeline Product Installed (Allouche et al. 2000)

Diameter (mm)	PVC (m)	HDPE (m)	Steel (m)	Other (m)	Total (m)	Percent of Total
50 – 100	241,428	891,494	64,573	4,500	1,201,994	72
150 – 200	6,686	11,688	55,717	0	179,288	11
250 – 300	457	7,730	72,042	0	80,229	5
> 300	0	13,146	180,144	0	193,290	12
Total installed	248,572	1,029,253	372,476	4,500	1,654,800	
Percent of Total	15	62	23	0.3		

The main piece of equipment used in an HDD operation is the horizontal directional drilling rig. There are a wide variety of manufacturers of drilling rigs, but they all operate by “pushing or pulling a carriage through the use of hydraulics, cable, chain, or rack and pinion drive” (Ariaratnam et al. 1998). The mobility of an individual drilling rig depends on its size and whether or not it is self-propelling. Figure 2.1 shows a medium size drilling rig that is outfitted with treads to navigate adverse ground conditions. These types of rigs can access remote locations and drill in more difficult terrain. The larger drilling

rigs, (Figure 2.2) are not capable of self-propulsion and therefore require level site conditions and a good access road to the site.

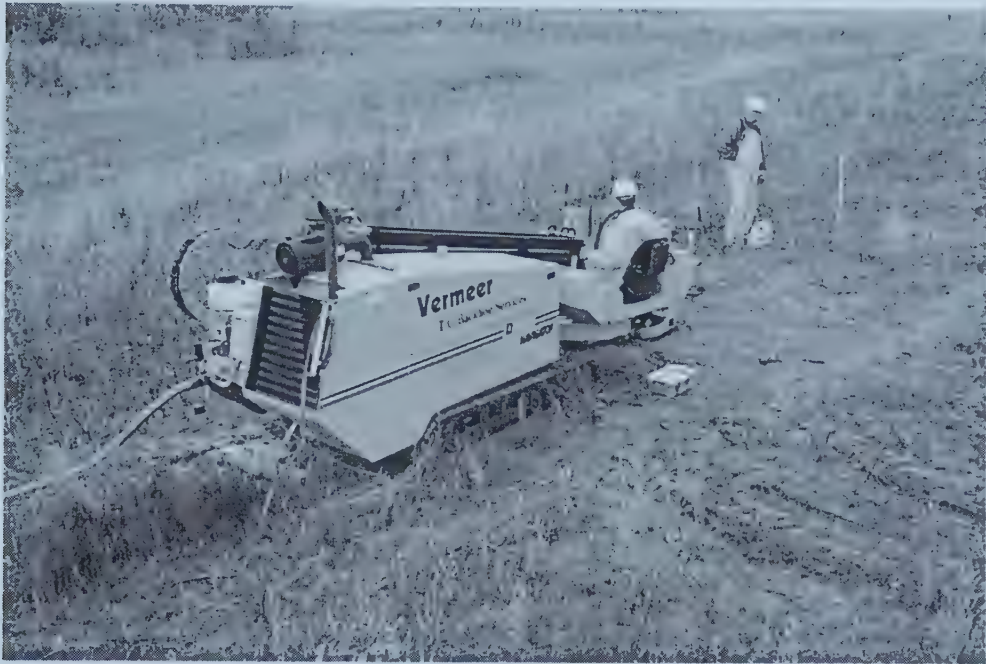


Figure 2.1: Vermeer Midi Size Drilling Rig

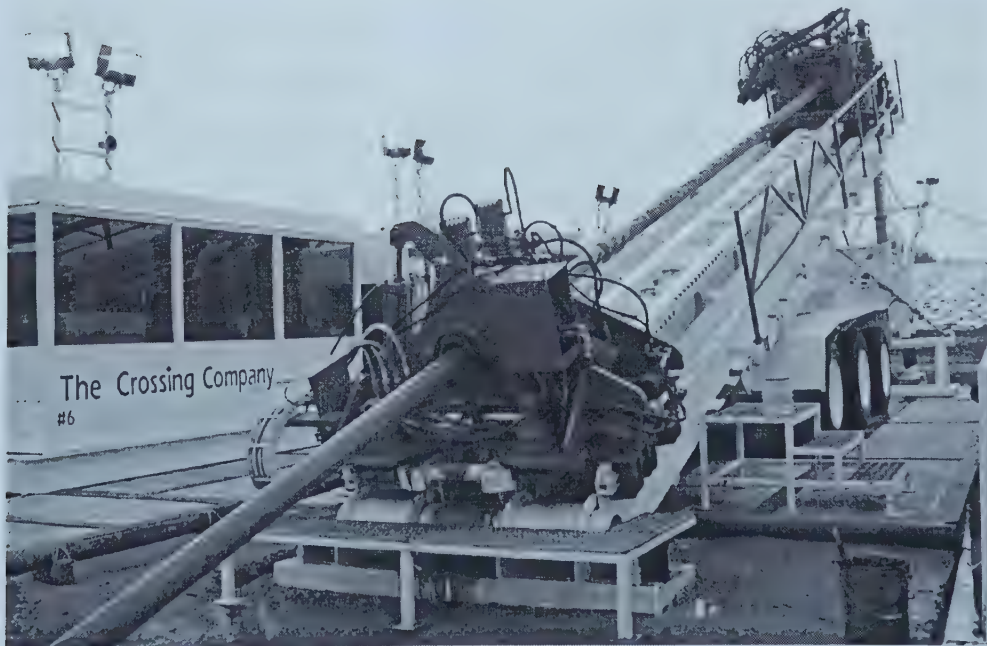


Figure 2.2: American Augers Large Size Drilling Rig

Segmentation of the different types of drilling rigs has been performed to allow for quick reference between the different types of drilling rigs. Initially, May (1994) created three segmentations of mini, midi, and maxi. More recently, this segmentation has been revised by Bennett et al. (2001) as shown in Table 2.2. The newer segmentation covers more attributes of the drilling rigs and has changed the labeling of the categories.

Table 2.2: Drilling Rig Segmentation (Adapted from Bennett et al. 2001)

	Small Rigs	Medium Rigs	Large Rigs
Thrust/Pullback	< 40,000 lbs.	40,000 – 100,000 lbs.	> 100,000 lbs.
Maximum Torque	< 4,000 ft.-lbs.	4,000 – 20,000 ft.-lbs	> 20,000 ft.-lbs
Rotational Speed	> 130 rpm	90 – 210 rpm	< 210 rpm
Carriage Speed	> 100 ft/min	90 – 100 ft/min	< 90 ft/min
Carriage Drive	Chain, Cylinder	Chain or Rack & Pinion	Rack & Pinion
Drill Pipe Length	5 – 15 ft	10 – 30 ft	30 – 40 ft
Drilling Distance	< 700 ft	< 2000 ft	< 6000 ft
Power Source	< 150 hp	150 – 250 hp	> 250 hp
Mud Pump	< 75 gpm	50 – 200 gpm	> 200 gpm
Weight of Drill Rig	< 15,000 lbs.	< 60,000 lbs.	> 60,000 lbs.

2.2.2 Drilling Procedure

The installation of pipe and conduit is typically performed in three distinct phases: pilot bore, reaming, and pipe pullback (DCCA 1998). The pilot bore phase (Figure 2.3) consists of using a small diameter drill head that is launched from the surface at an entry angle between 8 and 20° to the horizontal. The drill head proceeds downwards until the desired depth of the installation is reached and the orientation of the drill is brought to horizontal. The drilling will proceed horizontally along the pre-determined bore path before it is brought to the surface along a curvilinear path. The drilling head has the ability to be steered during the installation phase due to a sloped head design. When the drill is to go in a straight line, the operator will rotate the drilling head and push with the drill. If the drill head is to turn, the drill bit will be rotated such that the sloped face is in the direction of the desired turn. The HDD operator will then push the drill head, without rotation, until the desired alignment is achieved.

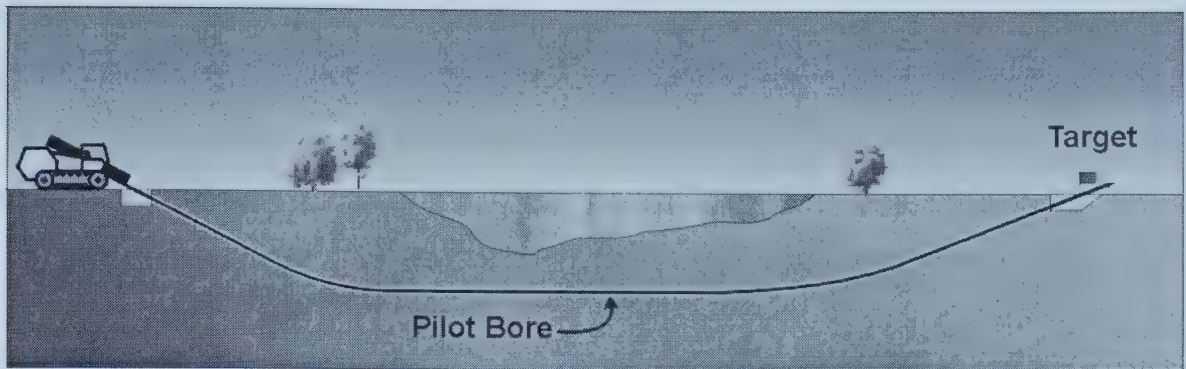


Figure 2.3: Pilot Boring Phase of the HDD Installation (Courtesy of Jason Lueke)

During the drilling process, the location, orientation, rotation, and depth of the drill head is tracked by either a walkover or wireline location system. Typically, a magnetic device, known as a transmitter, or sonde, is placed inside the drill bit housing. The transmitter emits an electromagnetic signal field that can be tracked using a hand-held locating device. These hand-held devices display the depth, orientation, and location of the drill head. Until recently, the hand held units had to be operated along the installation path of the HDD profile. This made it difficult to track the drilling head when it passed under above-ground obstacles such as busy roads or buildings. Recently, several manufacturers have introduced systems that mitigate this problem. Through the unique orientation of the receiving magnets, these systems can enable the user to locate the drill head anywhere in proximity of the drill line. For example, the locator can walk at a distance parallel to the drill stem when encountering surface obstacles.

These tracking systems have some limitations for use, as they can be influenced by magnetic interference. Typical sources of magnetic interference include steel structures and power lines. Care needs to be taken when operating a drilling operation in an area with high magnetic interference, as the drill head may not be located as shown on the hand-held unit. Additionally, the hand-held tracking units have a maximum tracking depth of around 20 m depending upon the outside interference in the area.

When hand-held tracking systems are unable to be employed, the directional drilling contractor can implement the use of a wireline system. The wireline system consists of a

measuring instrument that is mounted inside the drill head similar to the walkover system. The measuring device will track the azimuth and inclination of the drilling head during the HDD operation. This information is transmitted through wires that run inside the drill pipe and is collected and calibrated with a computer system. The wireline system is extremely accurate but is also time consuming, as a new connection needs to be made with every drill rod put into the ground. However, they are useful when the bore path lies under a deep-water body, where conventional tracking units would not be effective.

Once the pilot hole has reached the exit pit, the drill head is removed and a reamer is attached. Reamers come in a variety of sizes and types as shown in Figure 2.4. The reaming operation enlarges the borehole prior to the pipe pullback process to reduce the frictional effects that are imposed on the product pipe during the pullback process and can reduce the associated bending stresses near the entry and exit regions. The borehole is typically enlarged to 1.5 times the diameter of the product line that is to be installed; however, this can be adjusted according to the overall length of the installation and the soil conditions encountered. For larger diameter pipes, several reaming passes, known as pre-reaming, typically occur with increasing reamer sizes used to reach the desired upsizing. The last reaming pass is conducted coincidentally with the pipe pullback process, as shown in Figure 2.5.



Figure 2.4: Assorted Reamers

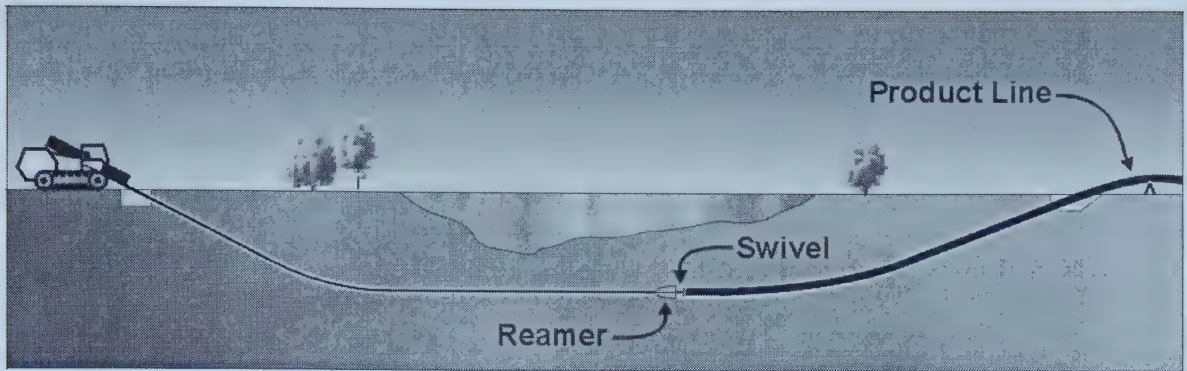


Figure 2.5: Reaming and Pullback Phase of the HDD Installation (Lueke et al. 2001)

During the pipe pullback process and the last reaming pass, the product line is attached to the reamer with a swivel link assembly. The swivel link prevents the reamer from rotating the product pipe during the installation process thus helping to decrease the torsional stress on the pipe. Additionally, swivel links can be “breakaway” links that are designed to break if the force on the product pipe exceeds a pre-calculated limit. This prevents the product pipeline from being overstressed, as the breakaway link will fail prior to any structural damage of the pipe. Additionally, during a pullback operation, it is preferable that the pipe is completely fabricated prior to the pullback operation if sufficient space is available. The risk of the pipe becoming stuck in the borehole can increase substantially if the pulling operation is stopped for connection of the pipe segments (Richard 1996).

Drilling fluid is utilized in all stages of the HDD operation and plays an important role in the success of the directional drilling operation. The most common drilling fluid is composed of bentonite clay mixed with water and may have polymers and other agents added. During the pilot bore phase, the drilling fluid serves several purposes: to stabilize the borehole, remove the cuttings, reduce the torque on the drill, lubricate the drill pipe, and cool the drill housing containing the electromagnetic sonde (Plexco 1999). During the reaming phase the drilling fluid is dispersed through the reamer and provides lubrication in the borehole, aids in the cutting and transport of the soil, and prevents collapse of the borehole. During the pullback phase and final reaming phase, the drilling fluid not only aids in the reaming action as mentioned previously, but also provides

lubrication to the product pipe. The lubrication of the drilling fluid reduces the chances of the product line becoming stuck as it decreases the frictional forces between the pipe and the borehole wall.

2.3 HIGH-DENSITY POLYETHYLENE

2.3.1 Background

Polymeric materials are defined as either thermoplastic or thermosetting. The main difference between these two classifications is the response to heat. A solid thermoplastic material can change to a liquid state through the application of heat and back again to the solid phase upon cooling. On the other hand, thermosetting materials will not soften upon application of heat following the setting process. This setting process creates cross-links between the molecular chains that prevent phase change during heating. Further applications of heat will subsequently degrade the properties of the material.

Polyethylene is a synthetically created thermoplastic material that was first invented by the Imperial Chemical Company in 1933 (PPI Chapter 3 1993). Polyethylene is formed from the combination of ethylene and a catalyst. The exact temperature and pressure applied during the manufacturing process depends upon the type of catalyst that is used. During this manufacturing process the double-bonded carbon atom in the ethylene molecule is broken to allow each of the ethylene molecules to bond to one another to form the chain structure of the polyethylene molecule, as shown in Figure 2.6.

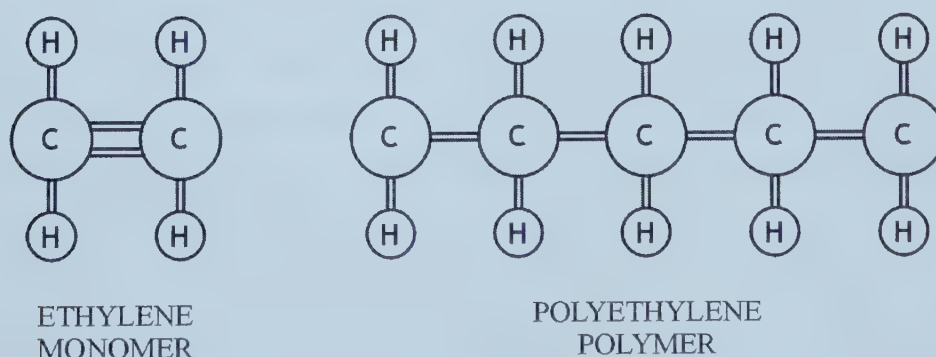


Figure 2.6: Production of Polyethylene

Polyethylene can be produced in a variety of different densities including low (0.910 – 0.925), medium (0.926 – 0.940), high (0.941 – 0.959), and high homopolymer (0.960 and above) (PPI Chapter 3 1993). These different densities are produced through varying degrees of side branching. Side branching occurs when a shorter polymer chain is attached to the main chain. The density of polyethylene impacts the apparent modulus of elasticity of the material along with the stress resistance capabilities.

2.3.2 Viscoelasticity

Polymers, plastics, and other synthetic materials exhibit stress-strain characteristics that cannot be classified as either elastic or viscous. The viscoelastic model combines both the theory of elasticity and the theory of a viscous fluid to attempt to define these polymers, plastics, and other synthetic materials.

Axial strain (ϵ) in a structural element is described as the deformation, δ , of the member per unit length, L , and is denoted by Equation 2.1. The strain is often expressed as a percentage of the deformation that is experienced over a specific gauge length of the material in question.

$$\epsilon = \frac{\delta}{L} \quad (2.1)$$

If the material is linear-elastic, Hooke's law governs, as shown in Equation 2.2. The perfect example of linear elastic behaviour is to examine the response of a spring under a loading condition. When a load is applied, the spring subsequently deforms to an amount proportional to this load. Upon removal of the load this spring will return to the original length prior to receiving the load. Hooke's law was developed based upon this theory and forms a linear relation between stress and strain. This linear relation is affected by the elastic modulus (E), also known as Young's modulus, as seen in Equation 2.2.

$$\sigma = E\epsilon \quad (2.2)$$

The viscous model also relates a force to the deformation of a structural element. In this case, the deformation of the element is not proportional to the force applied but the rate of change of the strain and the velocity of the applied force. The real world example is the dashpot that holds a viscous fluid and has time rate dependence. A dashpot can be described as a piston that contains a viscous fluid.

Viscoelastic behaviour is modeled through the combination of spring elements and dashpot elements comprising the behaviour identified above. A variety of models have been developed through the combination of these elements: most notably the Maxwell and Kelvin models. However, discussion of these and other models are beyond the scope of this thesis.

2.3.3 Tensile Testing

The mechanical properties of HDPE depend upon the load applied, temperature, and total length of time that the load is applied. Owing to its viscoelastic properties, the resistance of a HDPE pipe to an applied load slowly decreases. Additionally, a long term loading will cause the material to “creep”. Creep is the decreasing of the apparent modulus of elasticity during the loading duration. Therefore, during the duration of the loading, the structural resistance of the HDPE will change due to this decreasing apparent modulus of elasticity.

Tensile testing can be conducted on HDPE to determine the response to different loading and time conditions. Testing is accomplished through the application of a load in a testing machine on HDPE coupons. ASTM D 638-98 *Standard Test Method for Tensile Properties of Plastics* identifies standard coupon shapes and testing procedures that can be utilized for tensile testing on HDPE materials. Testing of the coupons develops load-deformation curves that can be transformed into stress-strain curves. From these curves, the mechanical properties of the HDPE can be identified. The Plastics Pipe Institute (PPI Chapter 3 1993) suggests that to calculate the elastic modulus the 2% secant method should be utilized. Secant lines are constructed at the 2% strain point to define the elastic region. This is shown in Figure 2.7 where a straight line is drawn from the origin to the

point on the stress-strain graph that intersects with the 2% strain mark. Subsequent calculation of the elastic modulus is conducted by dividing the stress that is read from this intersection by the 2% strain. Additionally, the speed of testing will impact the elastic modulus and therefore any comparative tests need to ensure that the same speed of testing is used (PPI Chapter 3 1993).

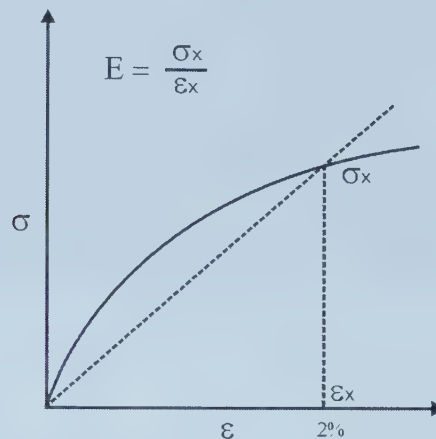


Figure 2.7: Secant Method for Calculation of the Elastic Modulus (PPI Chapter 3 1993)

2.3.4 *Butt Fusion Welding Process*

Polyethylene piping can be transported to the job site in two forms. The first method for smaller diameter lines is where the pipe is placed on a roll providing a continuous length for installment. Larger diameter pipes are created in segments that come in various lengths. Before being installed in the ground these pipe segments can be joined together with mechanical fittings or a heat fusion process. HDD contractors typically employ the heat fusion process to connect these segments of HDPE pipe. There are three heat fusion methods that can be used, but most often HDD contractors utilize the butt fusion welding process. The contractors prefer this process as special machines, shown in Figure 2.8, have been developed for field fusing of polyethylene pipes. These machines are relatively easy to use and are very mobile.

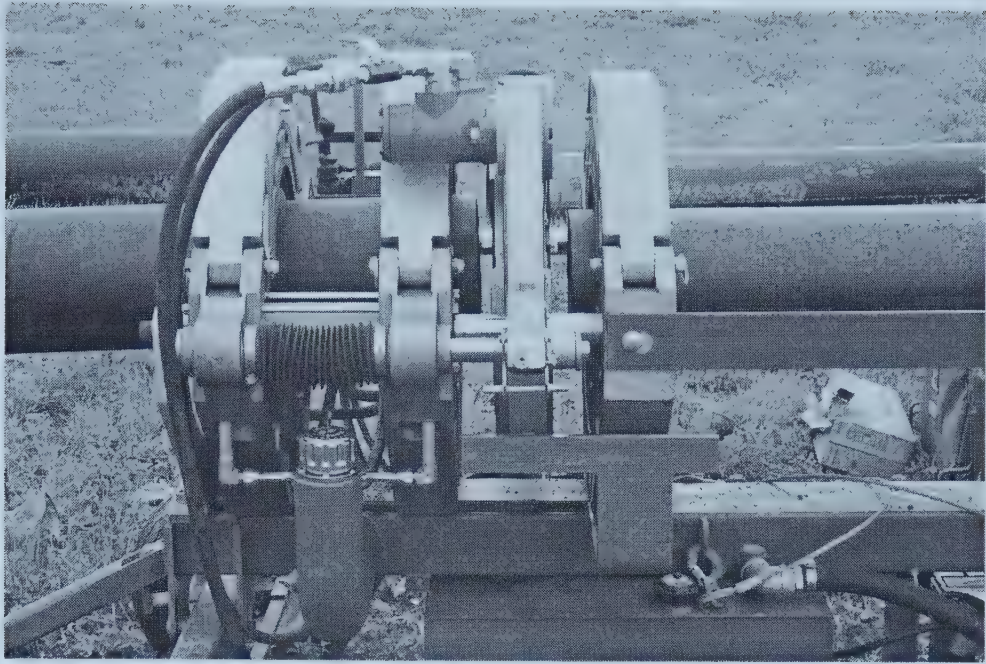


Figure 2.8: Butt Fusion Welding of a 200 mm Diameter HDPE Pipe

Six steps are required in order to make a quality butt fusion joint as identified by PPI Chapter 6 (1993), these are: secure the individual segments in each side of the fusion-welding machine, face the ends of the pipe with the mechanical cutting tool that is incorporated into the machine, align the pipe profile to ensure contact between both segment faces, melt the pipe ends to form a molten “bead” with the heating tools, join the two segments together at the specified pressure, and hold the two segments together until the joint has cooled.

2.4 MECHANICS OF THE HDD PROCESS

During the HDD pullback process the product pipeline experiences a variety of stresses as illustrated in Figure 2.9. These stresses are comprised of tension, bending, external hoop, pipe support spanning, and pipe overbend at entry (Harper 1999). The tension stress encompasses the frictional drag between the borehole wall and the product pipe, pullback force from the drilling rig, and the fluidic drag imparted by the drilling fluid in the annular space. Curvatures of the borehole, both vertically and horizontally, induce bending stresses during the negotiating of these curves in the borehole. Additional bending stresses are encountered outside the borehole through the pipe overbend at the

entry pit and from pipe support spanning. Pipe support spanning stress is caused by deflection of the pipe between the pipe supports. The pipe may also experience external hoop stress caused by the pressurized drilling fluid that is pumped into the borehole during the pullback operation.

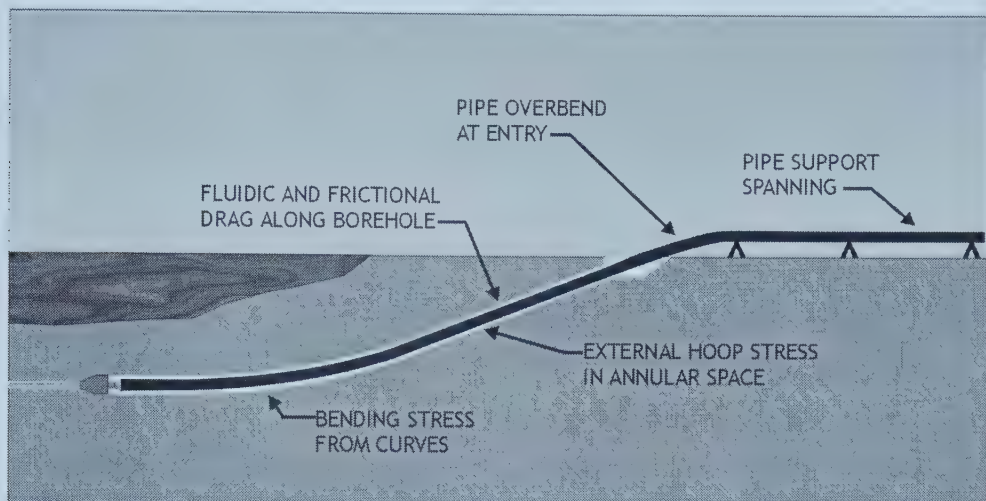


Figure 2.9: Key Stress Areas on Pipelines During the Pullback Phase

A free body diagram of a pipe segment inside the borehole is shown in Figure 2.10. This diagram illustrates the various forces that may act on the pipe inside the borehole during the pullback operation. Tensile forces are generated from the drilling rig and are transmitted through the drill string and the reamer onto the product pipeline. Frictional forces are present where the wall of the product pipeline contacts the borehole wall. At these contact locations a normal force will also be applied to the product pipeline. The drilling fluid inside the borehole imparts drag forces along the entire length of the submerged product line. Additionally, the self-weight of the pipe provides either a downward or upward force depending on the buoyancy of the product line.

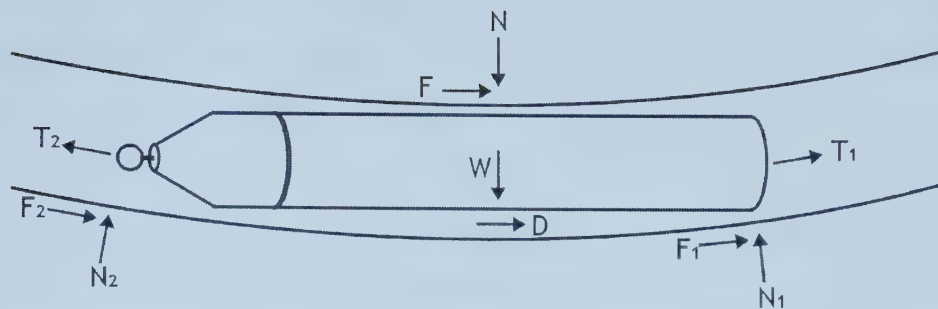


Figure 2.10: Forces on the Pipe During Pullback (Adapted from Huey et al. 1996)

Where:	T_1, T_2	tensile forces acting on the pipe
	F, F_1, F_2	frictional forces between the borehole and the pipe
	N, N_1, N_2	normal forces between the borehole and the pipe
	D	drag force exerted by the drilling fluid on the pipe
	W	weight of the pipe (may be reversed due to buoyancy)

2.5 HDPE MONITORING DURING HDD INSTALLATION

The monitoring of pipe strain on HDPE pipes during HDD installation is a new research field comprising only a small number of installations. The University of Waterloo has commenced work through several authors and installations. The University of Western Ontario has conducted research on the statistical correlation of pulling loads through a load cell, mounted in a HDD operation.

2.5.1 University of Waterloo – 1997 Installation

The first known set of research comprising the analysis of strain effects on HDPE pipe during HDD drilling was conducted by the University of Waterloo in 1997 and has been widely published (Gelinas 1998-a, Gelinas 1998-b, Polak et al. 1999, Gelinas et al. 2000). This research consists of two installations of 200 mm (8 in.) diameter SDR 17 HDPE pipes in a fine sand soil medium, at a depth of 2 m, with installed lengths of 55 m (180 ft) and 90 m (295 ft) respectively.

The measurement of the strain on the HDPE pipes was accomplished through the use of 1 m test sections that were placed at various locations along the installed pipe; three test

sections were used in the 55 m installation, and 4 test sections were used in the 90 m installation (Gelinas 1998-a). The test sections were connected to the non-instrumented portions of the pipe through the butt-fusion welding process. Each of the test sections contained four “metal-use” strain gauges located at the crown, invert, and springlines of the installed pipe (Gelinas 1998-a). These “metal-use” strain gauges were calibrated through HDPE coupon testing to determine the stiffening effects that the strain gauge imparts upon the plastic material. The readings on the strain gauges were collected and run from the free end of the pipe to the data acquisition equipment.

Each of the installed pipes was pre-reamed prior to the pullback phase using a 200 mm (8 in.) beaver tail reamer for the pre-ream (Gelinas et al. 2000). The final ream conducted during the pullback phase consisted of a 355 mm (14 in.) stackable reamer for the 55 m test and a 305 mm (12 in.) beavertail reamer for the 90 m test. Additionally, the 90 m installation had a second pre-ream performed with the same reamer prior to pullback as the drilling and first pre-ream had been performed on the previous day.

During the drilling phases the thrust/pullback pressure of the directional drilling rig was monitored. A pressure transducer was installed to measure the reading of the thrust/pullback gauge of the drilling rig. These readings are only indicative of machine effort and not the actual force exerted by the rig (Gelinas 1998-a). During the pilot bore phase the thrust pressures remained relatively constant, approximately 750 psi, over the length of the bore path for both installations. The pre-ream operation yielded relatively constant pressures for the 55 m installation averaging 350 psi while the 90 m installation began at 350 psi, increased to 800 psi at the 65 m point, and decreased to 500 psi at the end of the installation. In the pullback phase there was an increasing pressure trend along the length of installation for both test pipes. The 55 m installation began at 400 psi and increased steadily to 1100 psi at the end of the bore path, while the 90 m installation began at 400 psi and finished at 900 psi at the end.

The strain results were presented in three formats: measured strain, bending strain, and axial strain (Gelinas 1998-a). The measured strain is the reading collected from the strain

gauges during the installations, while the bending strain is determined from the borehole geometry, and the axial strain is the strain resulting from the subtraction of the bending strain from the measured strain. During the 55 m installation the measured strain peaked, to a maximum of 1.2%, during the initial bending portion of the bore path and gradually returned to a negligible amount during the horizontal section to the end bending section where it peaked, to a maximum of approximately 0.3%. For the 90 m installation the measured strain peaked, to a maximum of 1%, during the initial bending portion and declined to approximately 0.3% for the initial level portion where it increased steadily to approximately 0.6% at the end of the installation. The highest strains that were attributed to the bending phase of the installations were 1.0% for the 55 m test and 0.9% for the 90 m test. The maximum axial strains encountered for the installations were 0.18% and 0.55% for the 55 m and 90 m tests respectively.

Several conclusions were found through the installation and monitoring of the two HDPE pipes. For the drill rig pressures it was found that the “amount of thrust required for pullback will increase as the length of pipe within the borehole increases” and the type of reamer employed will affect the amount of thrust required (Gelinas 1998-a). The curvature of the borehole will “impose bending deformations on the pipe” and “larger borehole diameters decrease the bending deformations” (Gelinas et al. 2000). The strains developed through the pullback operation will be approximately the same for any single point in the bore path (Gelinas 1998-a). A large amount of strain will remain in the installed pipe following the pullback operation (Polak et al. 1999).

The results of this research are useful in providing an individual look at how the thrust pressure on the drilling rig and the strain acts on the HDPE pipe during the HDD installation process. However, due to the fact that there are differences between the installations there can be no direct correlation between the two installations. For example, two different reamer types were utilized during the final reaming and pullback phase of the installations. Additionally, the 90 m installation was pre-reamed twice, once on one day, and again on the following day. This creates different borehole conditions for the two installed pipelines and as a consequence the interaction between the pipe, drilling

fluid, and the soil will be different. Also, installation of the test pipes was conducted under “highly ideal” conditions as the contractor was “given considerable freedom with timelines, supplies, and equipment” (Gelinas 1998-a). This “highly ideal” approach is useful for quantifying the strain under perfect loading conditions, but may not be useful for real-world applications as many contractors may not take the time to make the installation “perfect.”

2.5.2 University of Waterloo – 1999 Installation

The second set of installations conducted by the University of Waterloo is a continuation of the previous installations and were conducted in 1999. This second set of installations comprises two 90 m (295 ft) long 200 mm (8 in.) HDPE SDR 17 pipes in the same soil medium as the previous installations (Duyvestyn et al. 2001). The researchers are varying one parameter between each installation to determine how each parameter affects the drilling operation. Akin to the previous tests, data was gathered on the pipe strain and machine pressures. Additionally, an internal load cell was used to measure the loading on the pipe during these tests.

The first installation was to utilize water as the drilling fluid. During the pilot bore phase the drilling rods become stuck in the ground and had to be excavated to be removed. Subsequently the pilot bore operation, and the pullback, was unable to be completed. The second installation utilized a 200 mm (8 in.) reamer for the pre-ream, and a 250 mm (10 in.) reamer during the pullback (Duyvestyn et al. 2001). Instrumentation was used to collect strain, pullback pressures, drilling fluid pressures, and load on the pipe during the pullback. These instruments were similar to the first set of installations with exception that plastic-use strain gauges were utilized and an internal load cell was installed inside the butt cap of the HDPE pipe. Similar to the first set of installations, five test sections were fused at various locations in the HDPE pipe.

Through this research it was found that the pipe load data from the load cell correlates with the strain data and the drilling rig hydraulic pressures, pipe loading estimated by the directional drilling rig pressures have some correlation with the actual pipe loading, and

the predicted load from the strain gauge measurements are approximately 70% higher than those actually experienced by the product pipe (Duyvestyn et al. 2001). However, additional installations should be conducted to support these conclusions.

2.5.3 University of Western Ontario

The University of Western Ontario has conducted research on the pulling loads that are associated with an HDD operation. The purpose of this research was to analyze some of the models that have been developed for predicted loads on installed pipes and to compare these models with the actual loading experienced through the external load cell device. This comparison was performed on an HDD project that installed a twin barrel siphon, which consisted of 508 and 660 mm diameter HDPE pipes with installed lengths of 420 m (Allouche and Baumert 2001).

To measure the loads in the field an external load cell was developed to measure the tensile forces that are transferred from the reamer to the pull head (Allouche and Baumert 2001). This load cell contains an electronic system that records the pulling loads during the installation and has a maximum capacity of 245 kN. The data can be downloaded after the installation through the use of a computer.

Through this research Allouche and Baumert (2001) have found that the loading shows a strong correlation with the profile of the installation rather than the installed length of pipe in the ground. Additionally, the Pipeline Research Council International's (PRCI) design model and the Drillpath software program do not accurately predict the tensile forces that occur during the installation process. For the PRCI model the loading at the start of the installation is overly conservative but declines below the actual loading discovered during the test. The Drillpath software predicted load was less than the actual loading experienced. Therefore, the authors suggest that more realistic models need to be developed that can accurately predict the loading experienced during the installation process.

3.1 INTRODUCTION

This chapter describes the horizontal directional field testing program that was conducted for comparisons on pipe strain, loading, and rig pressures between a cohesive and a cohesionless soil medium. Descriptions of the soil classification and the number of installations performed for each site are presented along with the schematic of the performed installations. An introduction and description of the methodology employed for the instrumentation used in the field testing program is given. This instrumentation includes linear potentiometers for the collection of strain data in the HDPE pipes, pressure transducers for the collection of rig pressures during the installation process, a load cell to record the loading on the HDPE pipe during the pullback phase, and the data collection unit that was used to record the information from each of these instruments. Next, the horizontal drilling rig that was employed for all the installations is introduced along with the tracking system that was employed during the pilot bore phase are described. Finally, to allow repeatability of the field tests, the field installation process is presented along with the drilling fluid mixtures utilized for each installation.

3.2 FIELD TESTING LOCATIONS

Field testing was performed at two different locations in order to provide both a cohesive and a cohesionless soil medium for installation. Field locations were chosen based upon the proximity to the University of Alberta, consistent soil conditions, topography of the site, and the ability to leave the pipe in the ground for a period of one year. The two locations utilized for this research were the University of Alberta Farms and the Sil Silica sand pit.

3.2.1 *University of Alberta Farms, Edmonton, Alberta*

The University of Alberta Farm site is shown in Figure 3.1. This site was chosen to provide the cohesive soil medium for this research. The upper 4 m of the soil at this site consists of uniform lacustrine Lake Edmonton Clay with a unit weight of approximately 18 kN/m^3 (Zhang 1999). There were five installations performed at this location including

two 114 mm (4 in.) diameter SDR 17 HDPE pipes, two 219 mm (8 in.) diameter SDR 17 HDPE pipes, and one 324 mm (12 in.) diameter SDR 17 HDPE pipe. The first three installations were performed on June 13 and 14, 2000, consisting of a 114, 219, and 324 mm diameter pipe. During this installation the strain data for the 114 mm pipe was lost, and therefore the second set of installations was performed to capture this missing data. This second installation was conducted on August 29, 2000, and consisted of a 114 and 219 mm diameter pipeline.



Figure 3.1: University of Alberta Farms Site – Clay Soil Medium

3.2.2 *Sil Silica Sand Pit, Bruderheim, Alberta*

The sand site was located in one of Sil Silica's sand pits located West of Bruderheim, Alberta (Figure 3.2). The site was not completely level but had consistently fine sand, satisfying the cohesionless requirement, from the surface to beyond the testing depths. The classification of the soil is medium grained sand to silty sand with an approximate unit weight of 18 to 19 kN/m³ (Zhang 1999). The installations were performed over a period of two days July 11 and 12, 2000. Three installations were conducted over this time period including one 114 mm (4 in.) diameter SDR 17 HDPE pipe, one 219 mm (8 in.) diameter SDR 17 HDPE pipe, and one 324 mm (12 in.) diameter SDR 17 HDPE

pipe. The load cell was first employed for the 114 mm diameter installation and was utilized for all of the installations.



Figure 3.2: Sil Silica Sand Pit – Sand Soil Medium

3.3 FIELD SETUP

All setups were done in the same manner as shown in Figure 3.3. The overall length of each borehole and subsequent product line was approximately 60 m (200 ft). Laterally, the pipes were spaced 5 m apart from the centerline of one installation to the centerline of the next. This 5 m spacing was maintained for the surface heave monitoring that was running consecutively with this research program. The sites were surveyed prior to installation and during this time, survey stakes were placed at the beginning, intermediate, and end points of each installation. The survey stakes were utilized to ensure that the bore path proceeded in a straight line and were necessary for the ground surface monitoring that was being conducted during the installation process.

The placement of the drilling rig and the layout of the installation lines was determined by the access location for each site. For the University of Alberta Farms site the pipe was set out and welded at the opposite end of the drilling rig setup area. For the Sil Silica

Sand site the pipe was welded on the main road and then dragged to the exit pit due to the topological constraints of performing the butt-welding operation on the exit pit side.

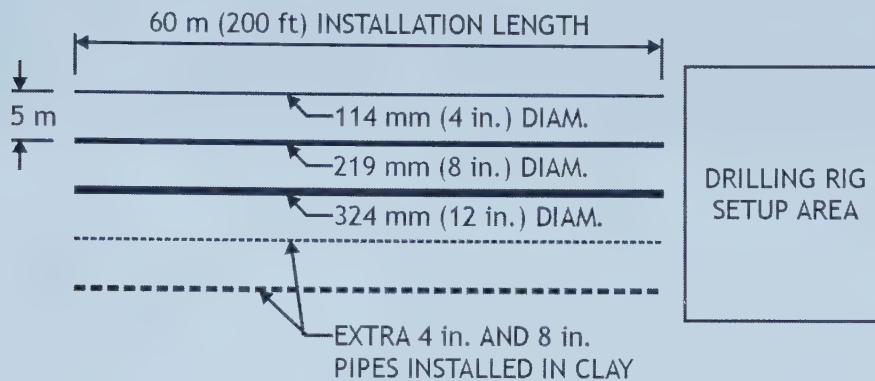


Figure 3.3: Plan View of the Typical Installation Layout

3.4 STRAIN MONITORING SYSTEM

3.4.1 *Linear Potentiometers*

The measurement of strain was accomplished through the use of linear potentiometers that were attached to the interior of the product pipe. The linear potentiometer measures strain through the changes in electrical current. The translation into strain is accomplished by recording the initial gauge length that the linear potentiometer is recording. The deformation of the linear potentiometer can be divided by this gauge length and transferred into a percentage to represent the strain. The advantage of using linear potentiometers are that they are easy to install and do not generate reinforcing effects on the HDPE pipeline.

The linear potentiometers utilized for these experiments were TR-50 position transducers manufactured by Novotechnik. Figure 3.4 shows a picture of one of these linear potentiometers. The TR-50 has a defined electrical range of 50 mm with a nominal resistance of 5 k Ω .

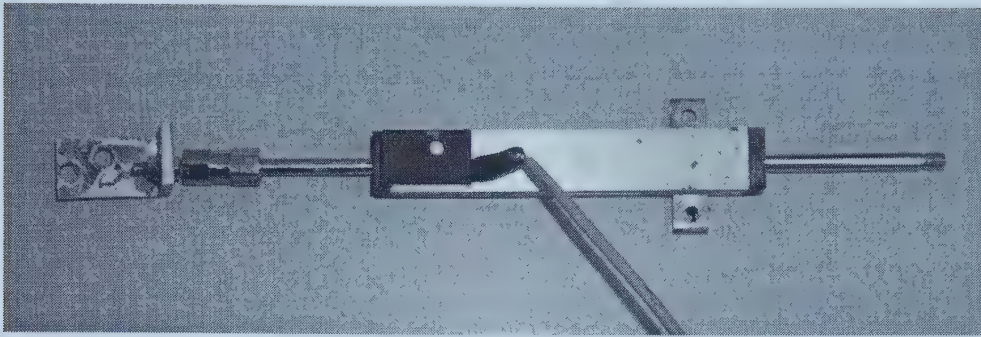


Figure 3.4: Linear Potentiometer

3.4.2 *Installation Procedure*

The linear potentiometers were mechanically attached to the interior of the HDPE pipe wall in the configuration shown in Figure 3.5. The 114 mm (4 in.) diameter pipe had two linear potentiometers installed at opposite points on the pipe profile. Both the 219 mm (8 in.) diameter and the 324 mm (12 in.) diameter pipes had four linear potentiometers installed at the crown, invert, and the springline points in the pipe profile.

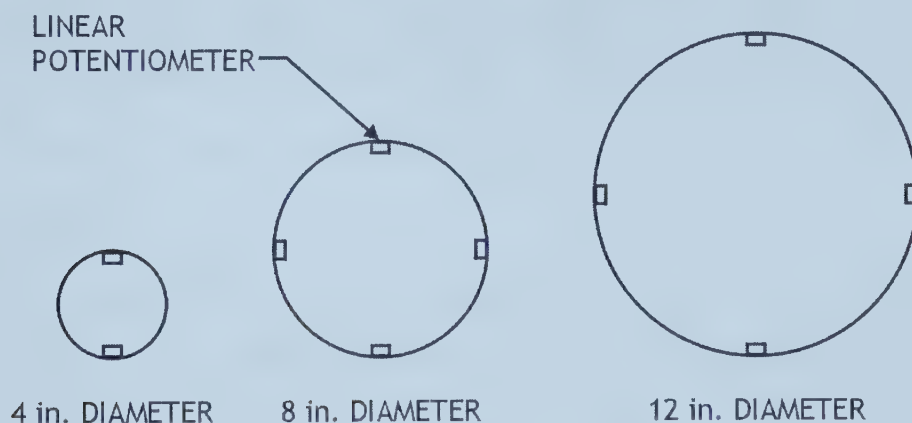


Figure 3.5: Linear Potentiometer Placement in the HDPE Pipes

Several steps were followed to attach the linear potentiometers to the inside of the HDPE pipe walls. First, a linear potentiometer was positioned on the outside of the pipe corresponding to its interior location. The proper gauge length was set, to allow movement in both directions, and a common drill was used to drill the fastener holes through the pipe wall. Silicon gel was then injected into the holes, to prevent drilling

fluid from leaking into the pipe during the pullback phase. Following this, the linear potentiometer was attached on the inside of the HDPE pipe using common carpentry screws placed in the holes that were previously drilled. The completed configuration of the 214 mm diameter pipe is shown in Figure 3.6.

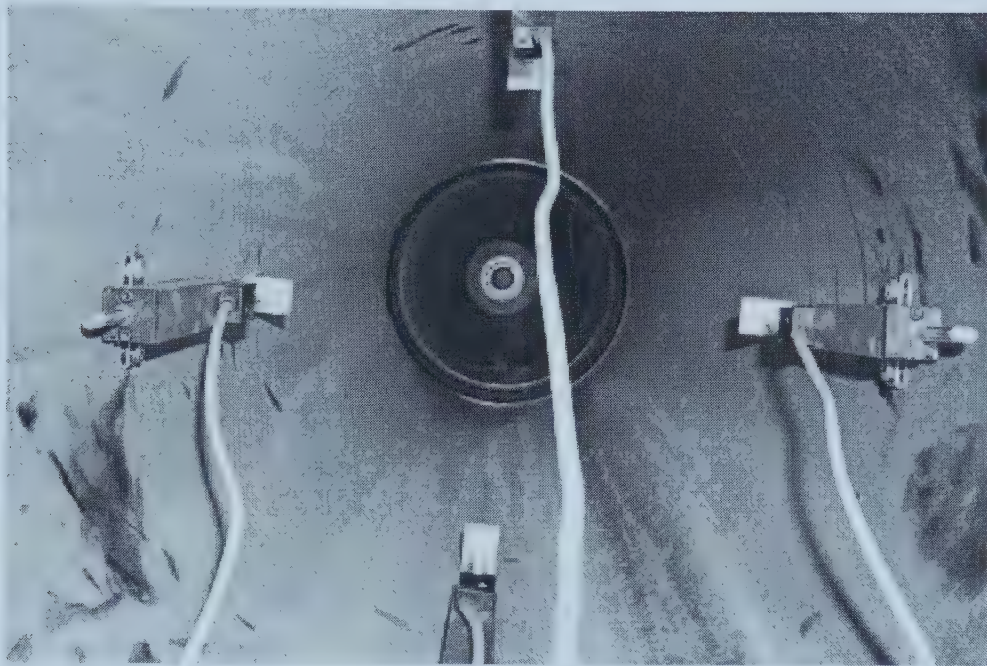


Figure 3.6: Linear Potentiometer Configuration for the 214 mm Pipe

3.4.3 Calibration

Following installation, the linear potentiometers were connected to the Data Dolphin data collection device described later in this chapter. The preliminary readings from the linear potentiometers were recorded for the baseline reference point. Additionally, the pipe was loaded slightly to ensure that the linear potentiometers were transmitting data to the data collection unit.

3.5 LOAD CELL DEVICE

Quantification of the loading applied on the product pipeline is difficult to achieve because of the interaction of the reamer and the soil medium. The force that is transmitted from the drilling rig is split between both the reamer and the product pipeline. The exact split of this force is unknown and may change in differing soil conditions. Therefore,

contractors may not know exactly how much load is being transferred to the product pipe during the installation process. The load cell device is intended to measure the load that is transferred between the reamer and the product pipeline.

3.5.1 Load Cell Construction

The load cell was constructed at the University of Alberta between the first installation at the University of Alberta Farms site and the Sil Silica Sand pit installations. The load cell, shown in Figure 3.7, is comprised of eight tee rosette strain gauges mounted inside a 76 mm (3 in.) diameter schedule 80 steel pipe. The strain gauges were connected to a modified Data Dolphin data collection unit that was also housed inside the steel pipe. Threaded end caps were utilized to allow the retrieval of the Data Dolphin for the download of the data following the installation. Care was taken to ensure that the load cell was completely waterproof as any penetration of water could short circuit either the strain gauges or the data collection unit.



Figure 3.7: Manufactured Load Cell

3.5.2 Load Cell Calibration

Following fabrication, the load cell was calibrated using a structural testing machine. Different compressive loads were placed upon the load cell noting the time of the loading because the data collection unit stores information based upon time. These loads and the readings given by the load cell were plotted, as shown in Figure 3.8. The equation relating the output in milli-volts corresponding to the load encountered is also given. A

straight line is fit through the testing points to develop an equation that can be used to translate the voltage information from the data collection unit to the load (kN). A regression analysis was also performed during the equation fitting to determine how close to linear the fit was. A perfectly linear fit is defined by $R^2 = 1$. In this case the regression coefficient is 0.9997, which is sufficiently close to accept this as a linear fit.

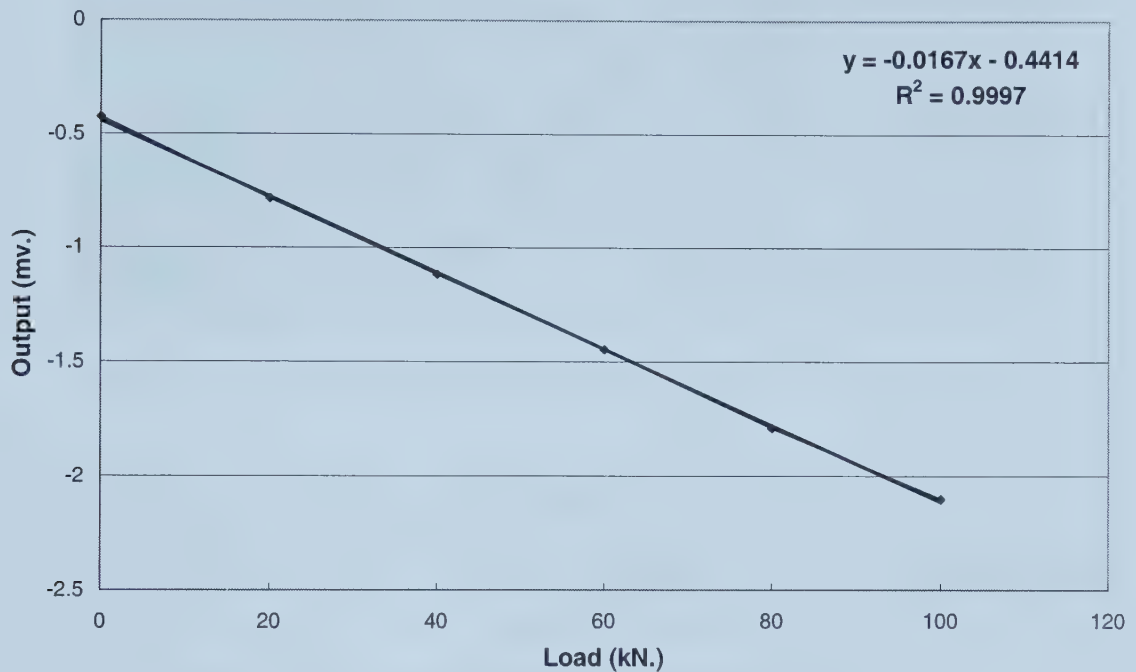


Figure 3.8: Calibration Curve for the Load Cell

3.5.3 Field Connection Procedure

The load cell was connected to the reamer and the product pipeline during the pullback phase of the HDD installations (Figure 3.9). The connection was accomplished through the use of steel shackles to both the reamer and the product pipeline.



Figure 3.9: Load Cell Connected to the 200 mm Pipe in the Sand Medium

3.6 PRESSURE TRANSDUCERS FOR HYDRAULIC PRESSURES

Pressure transducers were used to measure the hydraulic fluid pressures encountered by the drilling rig during the HDD operation. Transducers were connected to the thrust/pullback system, rotational torque system, and the drilling fluid system to record the pressures that are shown on the directional drilling rig's gauges. These pressures are only an indication of the machine effort and not of any quantifiable force exerted by the machine. Therefore, they are useful in comparing the effects that differing soil mediums have on the drilling rig.

3.6.1 *Pressure Transducers*

The pressure transducers used for this research were 892.23.510-300 pressure transmitters manufactured by Wika. Figure 3.10 illustrates one of these pressure transducers.



Figure 3.10: Pressure Transducer

3.6.2 Connection Procedure

The pressure transducers were connected inline with the directional drilling rig's hydraulic system. The transducers were placed between the hydraulic cables and the inlet of the pressure gauges mounted on the operator's console. Therefore, the pressure gauges are able to collect the information that is displayed on the operator's pressure gauges. The existing caps on the pressure gauges were removed and coupling units were installed. To allow the connection of the pressure transducer to the pressure gauge.



Figure 3.11: Connection of the Pressure Transducers to the Drilling Rig

3.7 DATA DOLPHIN DATA COLLECTION SYSTEM

The collection of data is required from the recording devices mentioned earlier in this chapter. The selection of a data collection unit was based upon cost, ease of use, reliability, previous experience, and durability. The Data Dolphin data collection unit was chosen based upon these requirements. Additionally, the Data Dolphin manufacturers were based in Edmonton, Alberta and were able to provide technical support if any malfunctions occurred.

3.7.1 *Data Dolphin Collection Unit*

The Data Dolphin data collection unit, shown in Figure 3.12, provides a resolution of 90 nanovolts. The data that is recorded by the unit is stored in a flash memory module that can be removed to allow for easier downloading of the data. The unit is powered by three “C” size batteries or can be connected to an external power source.

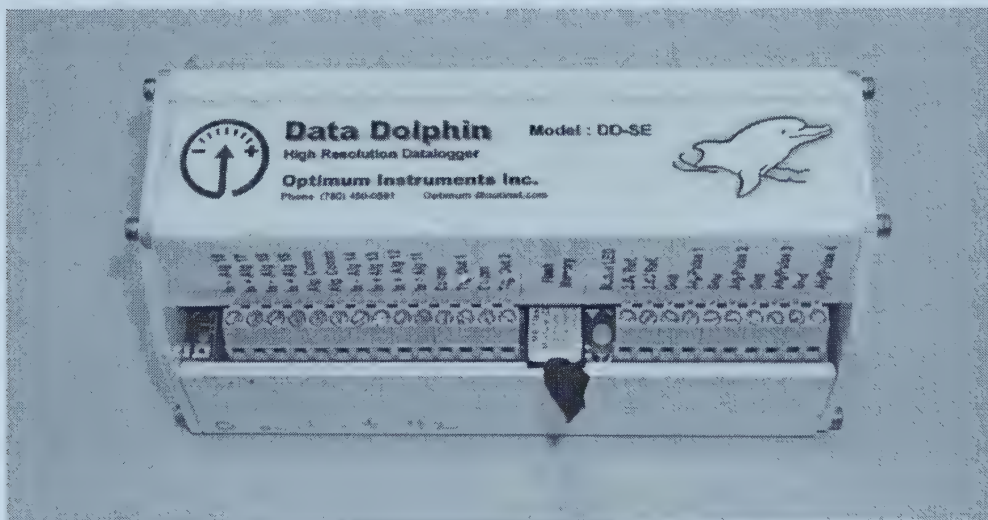


Figure 3.12: Data Dolphin Data Collection Unit

Each of the data collection units needed to be calibrated and setup, prior to instrumentation connection. Interaction with the collection unit was accomplished through a parallel port connection with a laptop computer and the supplier’s proprietary software system. During this calibration process, the unit was set to take readings every

ten seconds during the duration of the tests. Additionally, each of the unit's internal clocks was calibrated to ensure the cross-compatibility of the data.

3.8 HORIZONTAL DIRECTIONAL DRILLING RIG

The drilling rig used for all installations was a Vermeer model D24x40A horizontal directional drilling rig (Figure 3.13). The D24x40A features a track propulsion system and automated rod loader to increase the productivity of the directional drilling installation. Vermeer FIRESTICK® drilling rods were utilized for all stages of the installation.

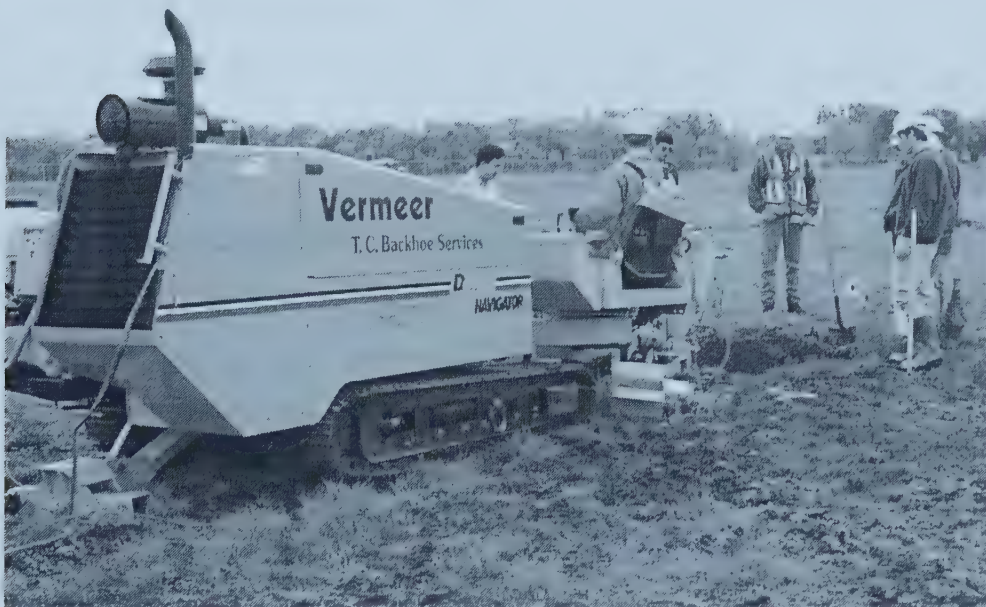


Figure 3.13: Vermeer D24-40A Horizontal Directional Drilling Rig

3.8.1 Specifications

The D24x40A is classified as a small drilling rig following the classification scheme presented in Chapter 2. The dimensions of the drilling rig were 516 cm (203 in.) length and 188 cm (74 in.) width. Drilling rotational torque is variable with a 3-speed gearbox that accommodates the following specifications: 5424 Nm (4000 ft-lb) at 131 RPM, 4060 Nm (3000 ft-lb) at 174 RPM, and 1760 Nm (1300 ft-lb) at 262 RPM. The maximum

pullback load is 10796 kg (23800 lbs). A two-speed valve in the mudflow system allows either 72 Lpm (19 gpm) at 1600 psi or 144 Lpm (38 gpm) at 800 psi.

3.8.2 Tracking System

The tracking system employed was a DigiTrak Mark III walkover location system. The system comprises a handheld walkover unit and an electromagnetic sonde that is placed in the drill housing. This handheld walkover unit runs on a battery and has a depth range of 42.7 m (140 ft). Data is displayed on the digital display that is located on the handheld unit and is stored in its memory for retrieval at a later date. The manufacturer states that this system can achieve an accuracy of $\pm 5\%$ (Digital Control 1999).

3.9 FIELD INSTALLATION PROCESS

This section describes the installation procedure that was followed for each of the installed pipelines. Since consistency is required between each of the soil mediums, the same tooling and drilling procedures were established to ensure similarity between the installations. For each of the sites the installation order of the product lines started from the smallest diameter to the largest diameter. Additionally, both the 114 mm diameter pipe and the 219 mm diameter pipe were installed on the same day while the 324 mm diameter pipe was installed the following day.

All installations began with the directional drilling rig positioned at the entry location with its position secured through anchoring rods that penetrate the ground. Pilot hole drilling was conducted with a Vermeer flat faced drilling bit. For the 114 mm diameter pipes, a 150 mm (6 in.) fluted reamer was attached to the drill stem for the reaming operation. To connect the pipe to the reamer, a steel pulling head was attached to the HDPE pipe and connected with shackles to the swivel assembly. For the 219 mm diameter pipes, a 300 mm (12 in.) fluted reamer was attached to the drill stem for the pullback operation. The HDPE pipe was fused to a special pulling head that was connected to the swivel assembly of the reamer. For the 324 mm diameter pipes, following the pilot-bore phase an additional 200 ft of rods were pushed through the borehole to allow for the pre-ream operation. The rods were disconnected at the exit

location and the 300 mm (12 in.) fluted reamer was attached for the pre-ream operation and connected to the extra string of rods. Following the pre-ream, a 450 mm (18 in.) fluted reamer was attached to the end of the extra rods, which were now at the exit pit. Similar to the 219 mm installations, an HDPE pulling head was fused to the pipe and attached to the reamer for the pullback operation.

Table 3.1 contains the drilling fluid mixes that were utilized during the installations. A representative from Baroid Industrial Drilling Products, who was present during all stages of each installation, conducted all of the drilling fluid designs. Additionally, all of the drilling fluid components were supplied by Baroid (Baroid 1998). Bore-GelTM was the primary component, along with water, that was utilized for the installations. Bore-GelTM is comprised mainly of sodium bentonite, which provides the primary function of stabilizing the borehole and removing the cuttings. EZ-Mud[®] is a liquid polymer that is used as a borehole stabilizer and prevents reactive clay from swelling. Con Det[®] is a wetting agent that aids in the cleaning of the drill bit and counteracts the sticking tendencies of clays. No-SagTM is a gel strength enhancer that enables better suspension of cuttings and increases the carrying capacity for solids suspension. The drilling fluid mixes for the second series of installations conducted at the University of Alberta Farms site are not included, as they were not recorded during the installation process.

Table 3.1: Drilling Fluid Mixes Utilized For The Installations

Pipe Designation	# of Batches	Water	Bore-Gel TM	EZ-Mud [®]	Con Det [®]	Other
114 mm – Clay 1	1	900gal	150lbs	2L	2L	-
219 mm – Clay 1	2	900gal	150lbs	2L	2L	-
324 mm – Clay 1	2	900gal	150lbs	4L	2L	2 lbs No-Sag TM
114 mm – Clay 2	N.R.	N.R.	N.R.	-	-	-
219 mm – Clay 2	N.R.	N.R.	N.R.	-	-	-
114 mm – Sand	1	900gal	250lbs	-	-	-
219 mm – Sand	1	900gal	250lbs	-	-	2.5 lbs No-Sag TM
324 mm – Sand	2	900gal	250lbs	-	-	5 lbs No-Sag TM

N.R. – Not Recorded

4.1 INTRODUCTION

This chapter details the equipment and procedures utilized for the tensile testing of the coupon samples that were manufactured from the 219 and 324 mm HDPE pipes. The coupon manufacturing process is presented along with the specification used to create the coupons. Next, the equipment required for this tensile testing is introduced. Finally, the coupon testing procedure that was utilized for these samples is described

4.2 COUPON MANUFACTURING PROCESS

To allow for tensile testing comparisons, samples of the HDPE pipe that were installed in the field were collected. For each of the installed pipes, both an un-pulled and pulled specimen of approximate length of 900 mm were collected. From each of these samples, three coupons were fabricated for tensile testing. Unfortunately, the coupons manufactured from the 114 mm pipe were unsuitable for testing. Therefore, only the coupons manufactured from the 219 and 324 mm pipes were included in the tensile testing program.

The samples of the HDPE pipes were cleaned and delivered to the Technical Resources Group, a machine shop located on the University of Alberta campus. From each of the samples, three coupons were required to bring the total number of coupons to twenty-four for the 219 mm and 324 mm pipes. Figure 4.1 illustrates how the coupons were manufactured from the pipe wall and the finished dimensions of each coupon. The coupon dimensions were based upon the Type I coupon as specified in the ASTM D638-98 standard. However, the overall length of the coupon was increased to allow the connection of the extensometer that was utilized during this testing.

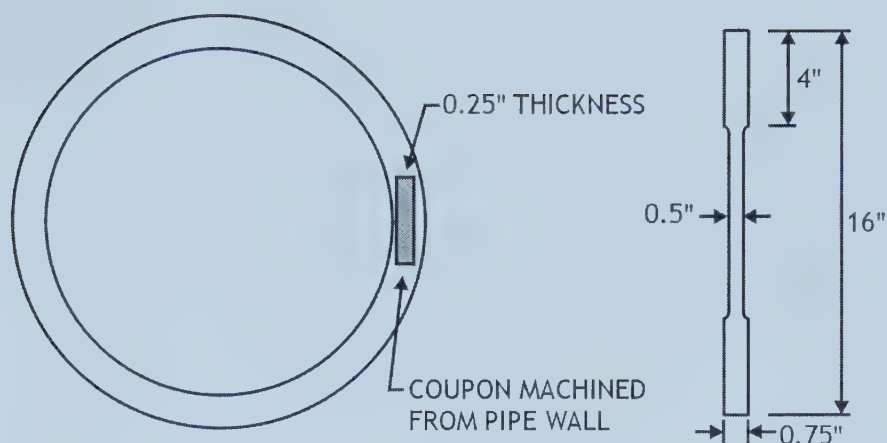


Figure 4.1: Typical HDPE Coupon

The process of manufacturing the coupons started by cutting the length and width of the coupon from the pipe wall. Once these segments were removed, machining of the coupons commenced to reduce the cross-section to the proper thickness. Following this, the rectangular bar was placed in a jig and the dog-bone profile was created. Figure 4.2 illustrates a number of completed HDPE coupons prior to tensile testing.

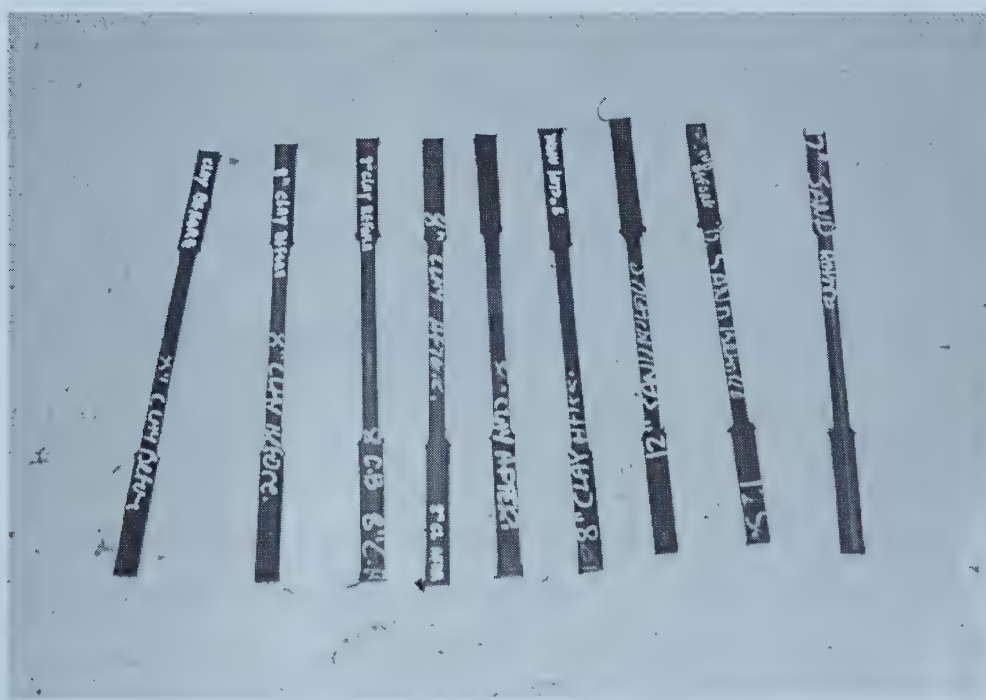


Figure 4.2: Completed HDPE Coupons

4.3 TESTING EQUIPMENT

The tensile testing of the HDPE coupons was conducted through the use of a Material Test Systems (MTS) 810 structural testing machine, shown in Figure 4.3. The testing machine is capable of performing both tensile and compression tests for a variety of material specimens. The tensile test is accomplished by first securing the coupon into the grips of the testing machine and then allowing the piston below the bottom grip to move in a downward direction. The MTS testing machine is connected to a computer system that contains software that automatically records the parameters of the tensile test. This proprietary software records the load, carriage position, and movement of the extensometer, and automatically calculates the stress based upon the input cross-sectional area.

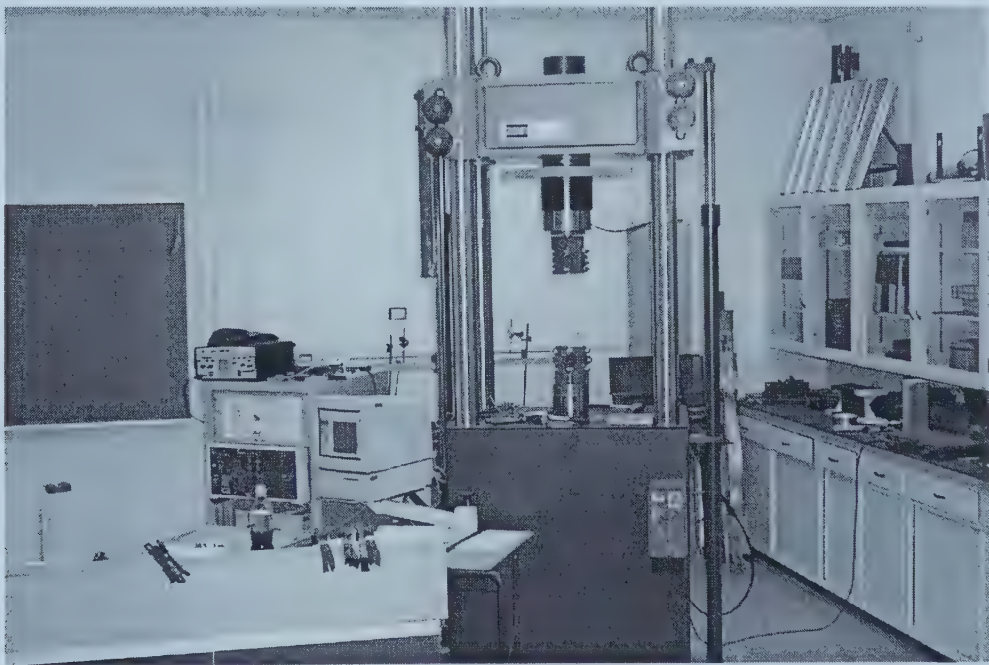


Figure 4.3: MTS 810 Structural Testing Machine

Figure 4.4 illustrates the extensometer that was used to record the elongation of the HDPE coupon samples during the tensile testing. The extensometer is an MTS Model 632 extensometer that measures elongation over a gauge length of 50 mm. The extensometer is attached to the side of the coupon sample and held in place by looping

elastics through the hooks in the body of the unit. At the end of the unit there are two fine bars that rest against the coupon sample.

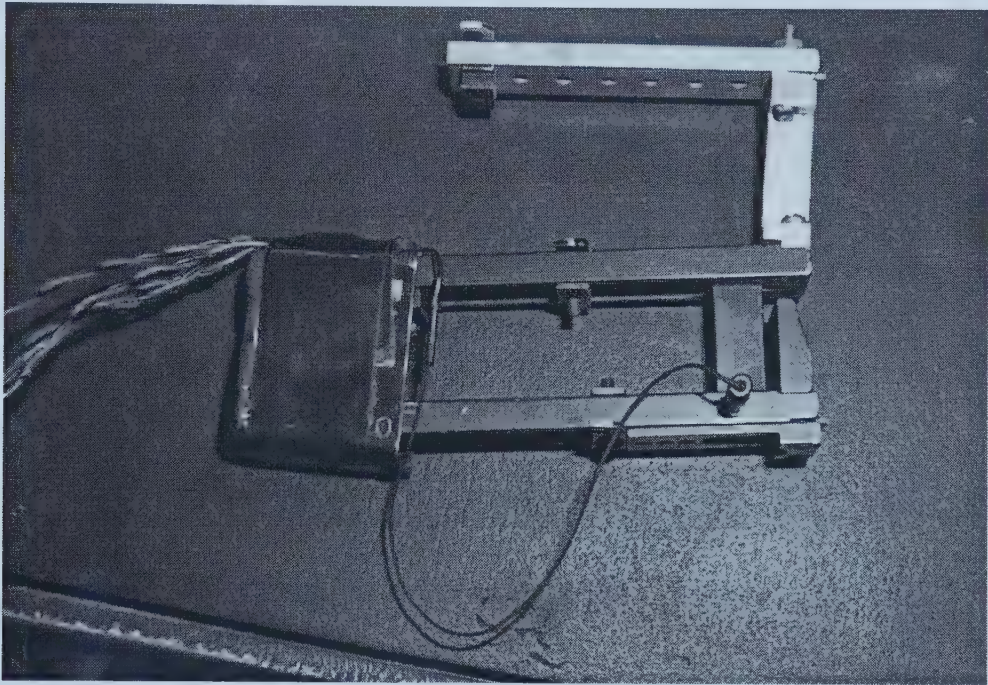


Figure 4.4: MTS Model 632 Extensometer

4.4 TESTING PROCEDURE

This section identifies the tensile testing procedure, illustrated in Figure 4.5, conducted for each of the HDPE test specimens. The testing procedure consisted of the following steps:

- 1) The width and thickness of each coupon was measured at three separate locations in the narrow section of the coupon. This measurement was conducted to calculate the average cross-sectional area and was accomplished with the use of a digital caliper.
- 2) The coupon was placed into the grips of the testing machine and was secured into place. Care was taken to ensure that the center of the coupon was aligned with the center of the grips.

- 3) The MTS 632 extensometer was attached to the edge of the coupon sample using elastic bands (illustrated in Figure 4.5).
- 4) The average cross-sectional area was input into the proprietary software and the data values were set to zero.
- 5) Testing of the specimen was conducted at a cross-head speed of 15 mm/min. The testing continued until the strain reached a value of 10%.
- 6) The data collected by the proprietary software program was exported into a spreadsheet application that allowed the plotting of the stress-strain graphs.
- 7) The extensometer was removed and the tested coupon was retrieved to allow setup for the next test.

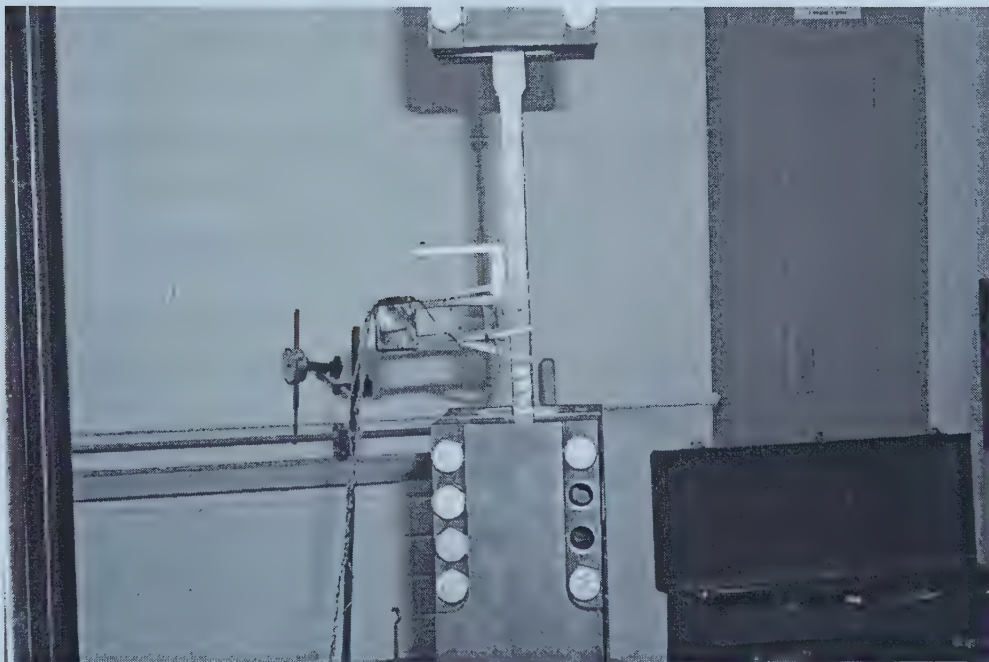


Figure 4.5: Testing of a Sample Coupon

5.1 INTRODUCTION

This chapter contains the testing results for installations in the two different soil mediums. The individual bore path profiles are presented to allow for direct comparison with the data presented. A number of graphical representations of the data are presented illustrating the drilling rig pressures, load cell results, and strain experienced during the pullback operation. The drilling rig results include the rotational, pullback, and drilling fluid pressures that were experienced during the pullback phases for the 114 and 219 mm pipes, and the pre-ream and pullback phases for the 324 mm pipes. The load cell results encompass the pulling force on the load cell, which was placed between the reamer and the product pipe. Additionally, the strain results are presented for each of the pipes.

5.2 UNIVERSITY OF ALBERTA FARMS INSTALLATION 1 – CLAY

5.2.1 114 mm Diameter Pipe

The bore path profile of the 114 mm diameter pipe installed during the first installation set in the clay soil medium is shown in Figure 5.1. This figure shows the ground topography and the as-built profile of the installed pipe. The ground topography was generated using a Vermeer laser level system with an electronic distance measurement device and was input into ATLAS Bore Planner. The as-built information about the pipe depth was retrieved from the information stored by the Digi-Trak Mark III tracking unit.

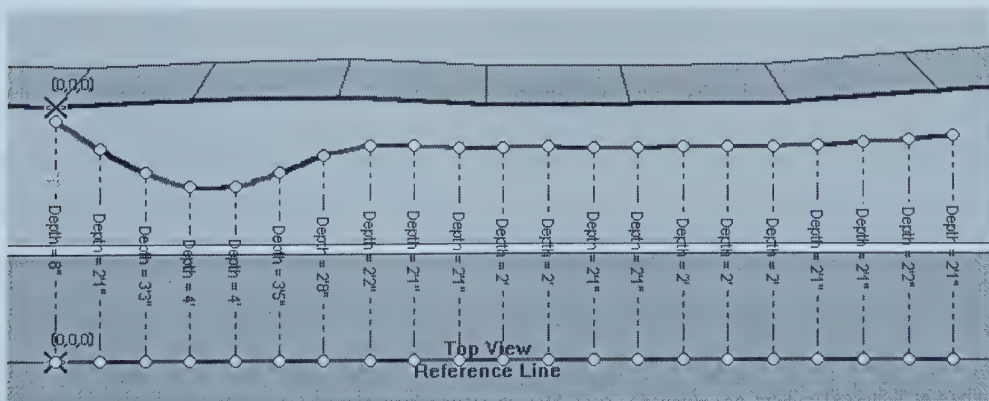


Figure 5.1: 114 mm Bore Path Profile – Clay 1

The “X” point on the surface (left hand side of the figure) shows the location where the drill entered the ground. The “X” point corresponds to the 60 m point for all the graphs in this thesis. Following this entry point the pipe is shown to continue downwards and approaches the horizontal depth required for the installation (for the 114 mm diameter pipe, it is 2 ft). This dip is required, as the drilling rods have a minimum-bending radius, and this radius needs to be satisfied before the horizontal drilling stage can begin. Following this dip it can be observed that the pipe remained close to the desired 2 ft depth of installation.

During the pilot bore phase of the HDD installation the drilling rig pressures were monitored and collected by the Data Dolphin collection system. The pilot phase rig pressures are not presented due to the fact that they could not be converted into a bore path location. When these pressures were plotted by time they consisted of many peaks and valleys, which made it difficult to interpret when the drilling rig was moving, and when it was stopped. The results of the drilling rig pressures during the pilot-boring phase are shown in Appendix A along with all additional field results.

For both the pre-reaming phase and the pullback phase the rig pressures were collected. Initially the rig pressure data was plotted versus time, as mentioned previously, and needed to be converted to the bore path location to eliminate times when the rig was not moving. Two methods could be used to accomplish this conversion of data. The first method consisted of looking at the drilling fluid pressures during the pullback phase of the HDD process. During the drilling process the drilling fluid pressure was approximately constant during the movement of one entire rod. During the “breaking” process the drilling fluid pressure dipped substantially, providing a series of peaks and valleys, where the peaks coincided with the drilling operation. Since the length of each rod was known and the number of peaks coincided with the number of rods, the data could be converted from time-based to bore path (location-based). The second method could look at the pullback pressures experienced by the drilling rig during the pullback operation. During the “breaking” process the pullback pressure would spike and therefore the data could be transformed in the same fashion as the drilling fluid pressure.

Both the strain and load cell data was converted from a time-based system to a location-based system using the drilling rig pressures as identified above. The times from the drilling rig pressure analysis were transposed to the strain and load cell data to incorporate the same location changes.

The drilling rig pressures for the pullback phase of the 114 mm pipe installed in the first series of clay installations is shown in Figure 5.2. It can be seen that the drilling fluid pressure remains quite constant at 70 psi during the range of the installation until it dips down to 50 psi at the end of the installation. The pullback pressure is seen to increase from 315 psi, at the start of the installation, to 475 psi at the 50 m point where it drops down to approximately 375 psi at the end of the installation. The rotational pressure also increased steadily from around 1200 psi to around 1400 psi just beyond the halfway point of the installation. Following this, the pressure stayed around 1300 psi until it dropped below 1200 psi to finish the installation.

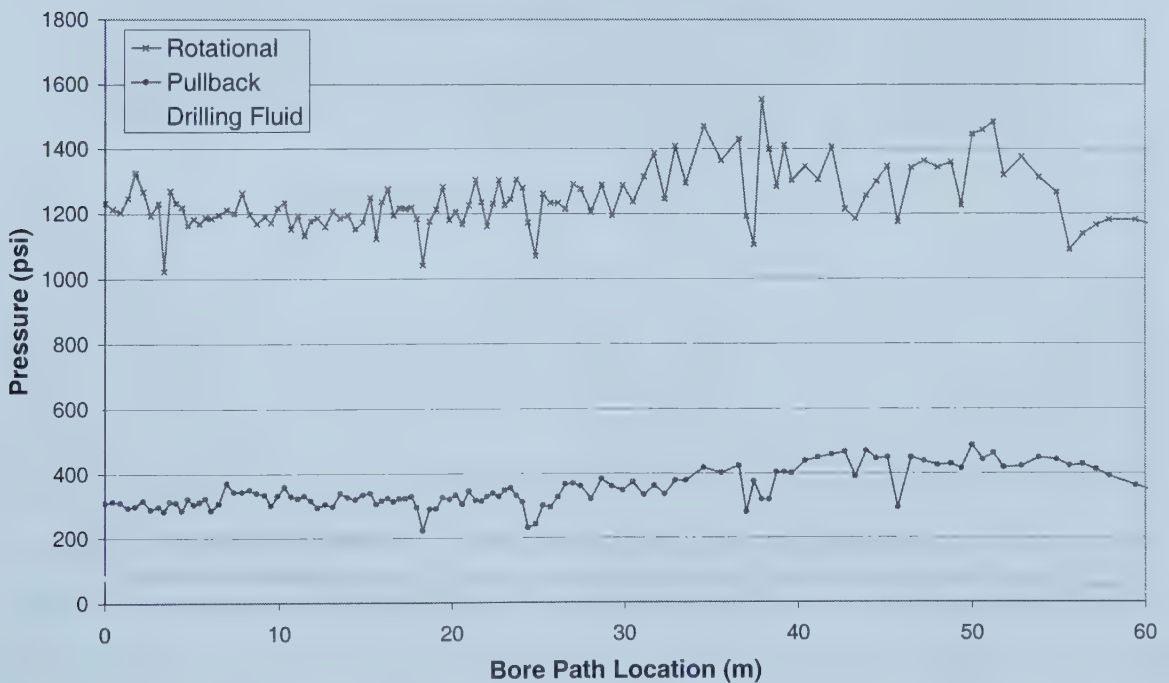


Figure 5.2: 114 mm Drilling Rig Pressures During Pullback – Clay 1

The strain information for the 114 mm pipe installed in the first series at the clay site could not be included. The information was lost due to failure of the data collection device during the installation process. It is believed that water was allowed to infiltrate the pipe during the pullback process. The water caused the data collection unit to short out and erase the flash memory. The second series of tests, conducted in August 2000, were used to replace this lost strain data.

5.2.2 219 mm Diameter Pipe

The bore path profile of the 219 mm pipe installed in the first series of clay is shown in Figure 5.3. It can be seen that the pipe remained at the 3 ft mark for the majority of the installation.

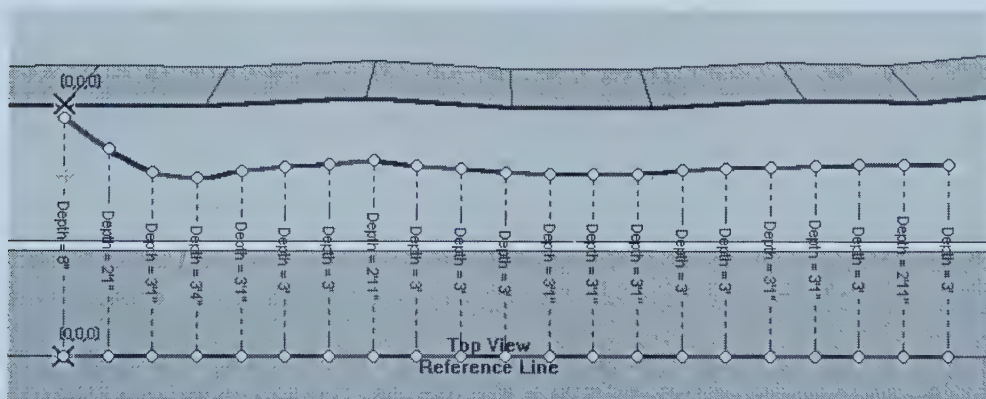


Figure 5.3: 219 mm Bore Path Profile – Clay 1

The drilling rig pressures for the pullback phase of the 219 mm pipe installed in the first series of clay installations is shown in Figure 5.4. The drilling fluid pressure remained relatively constant, at 90 psi, during the installation. One peak is evident at the 33 m mark where the drilling pressure was 200 psi during that individual rod. Also at the end of the installation, the drilling fluid pressure peaked again to approximately 200 psi. The pullback pressure rose dramatically from around 300 psi at the start of the installation to over 2400 psi at the end of the installation. The rotational pressure fluctuated during the course of the installation, ranging from as low as 900 psi to as high as 1950 psi.

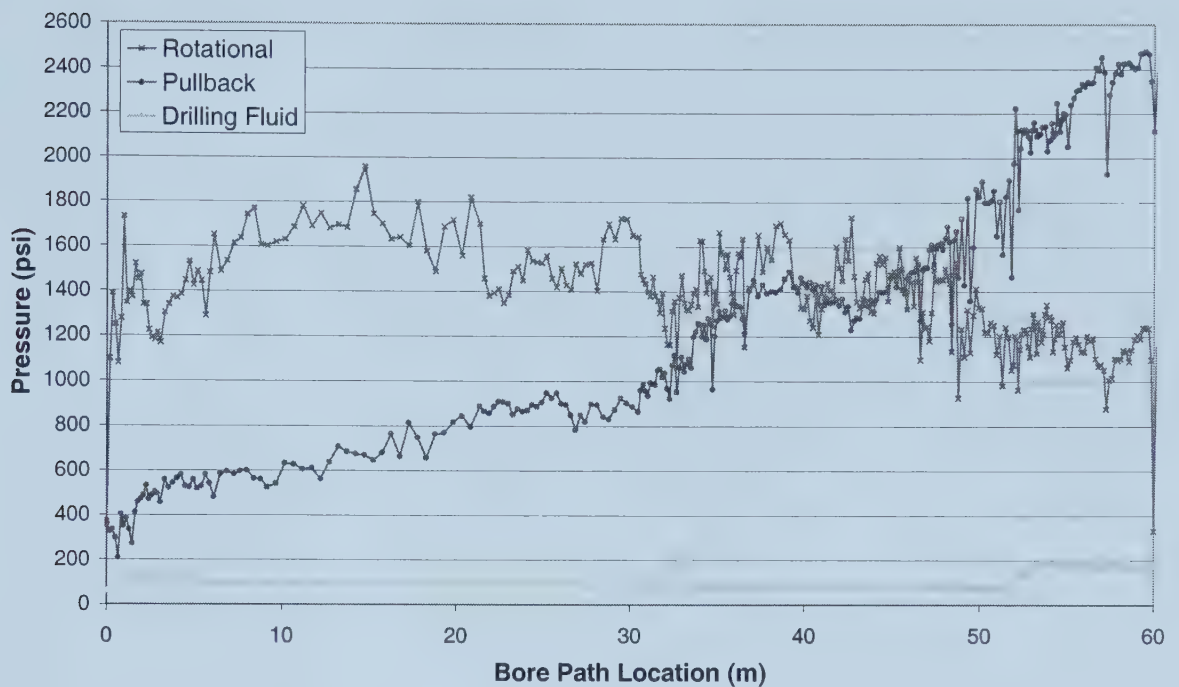


Figure 5.4: 219 mm Drilling Rig Pressures During Pullback – Clay 1

The strain experienced by the 219 mm pipe during the installation in clay is shown in Figure 5.5. It should be noted that the individual linear potentiometers were not recorded during the connection phase to the data collection device and therefore are not indicated in the Figure. However, by observing the behaviour of the strain response of each linear potentiometer during the bending portion of the installation the approximate location can be determined. This determination is due to the fact that during the bending portion the linear potentiometers that are in the upper half of the pipe will experience a compressive stress while the ones in the lower half will experience a tensile stress. Therefore, the linear potentiometers that exhibit a positive reading are located in the lower half and the other linear potentiometers are in the upper half. During the initial portion of the bore path it can be seen that the bending of the pipe imposed strains to a maximum of 0.35%. Following this initial bending portion, the strain subsided to a negligible level until the halfway point of the installation. Following this point, the strains rose to 0.8% at the end of the installation.

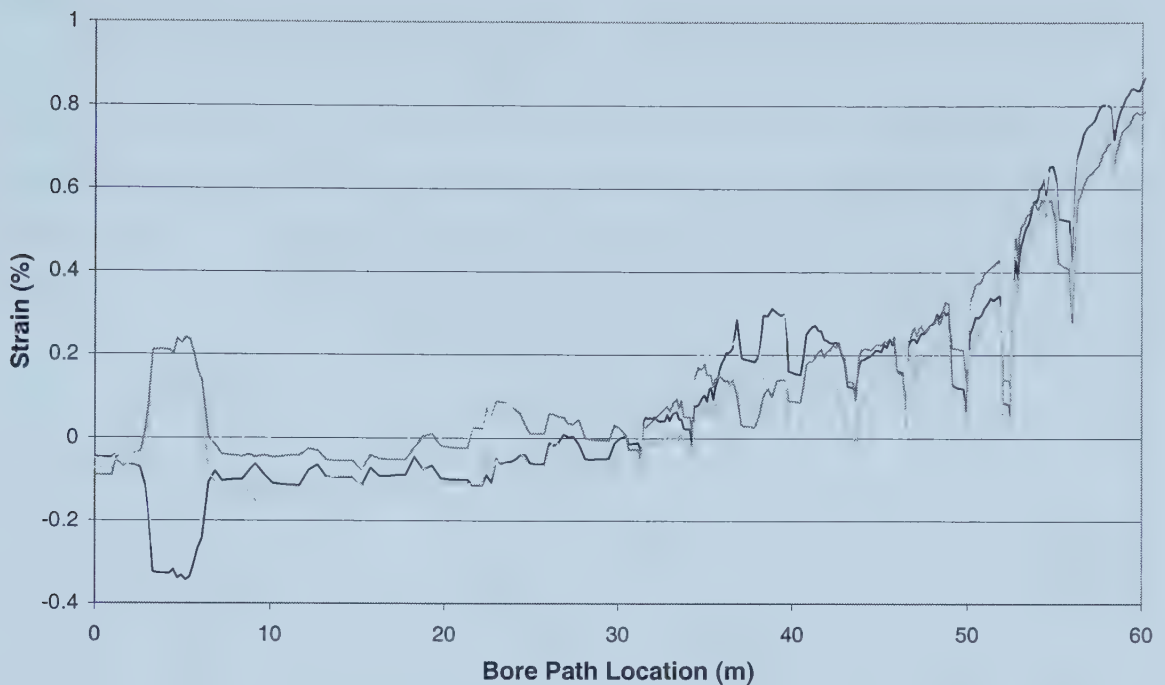


Figure 5.5: 219 mm Strain During Pullback – Clay 1

5.2.3 324 mm Diameter Pipe

Figure 5.6 contains the installed bore path profile for the 324 mm diameter pipe installed in the clay soil medium. The installed pipe deviated a maximum of 2 in. from the required installation depth of 4 ft over the duration of the installation.

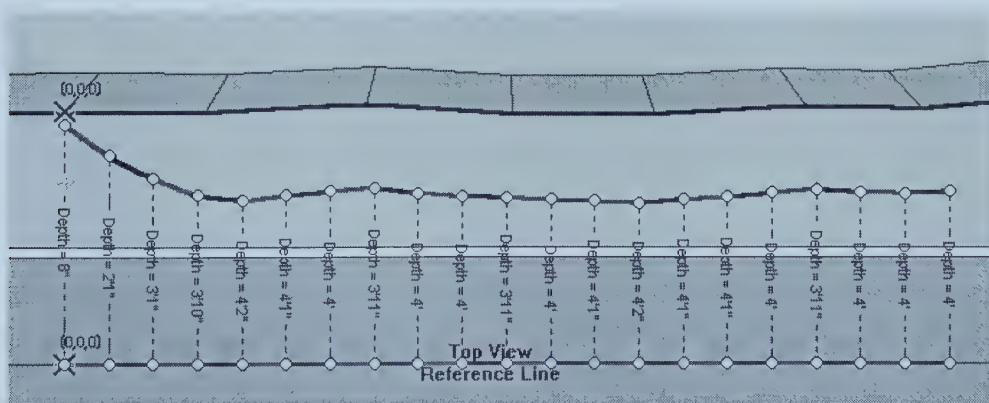


Figure 5.6: 324 mm Bore Path Profile - Clay

The drilling rig pre-ream pressures for the 324 mm pipe installed in the clay soil medium are shown in Figure 5.7. The drilling fluid pressure is absent from this graph as the pressure transducer was not connected to the drilling fluid system during the installation. Therefore, only the rotational and pullback pressures are displayed. During the pre-ream phase the pullback pressure remained constant at about 575 psi. The trend of this pullback pressure tends to be horizontal to slightly downward sloping. The rotational torque varied along the installation path, but the main trend remained close to 1800 psi until the 50 m point where it decreased to 1400 psi at the end of the installation.

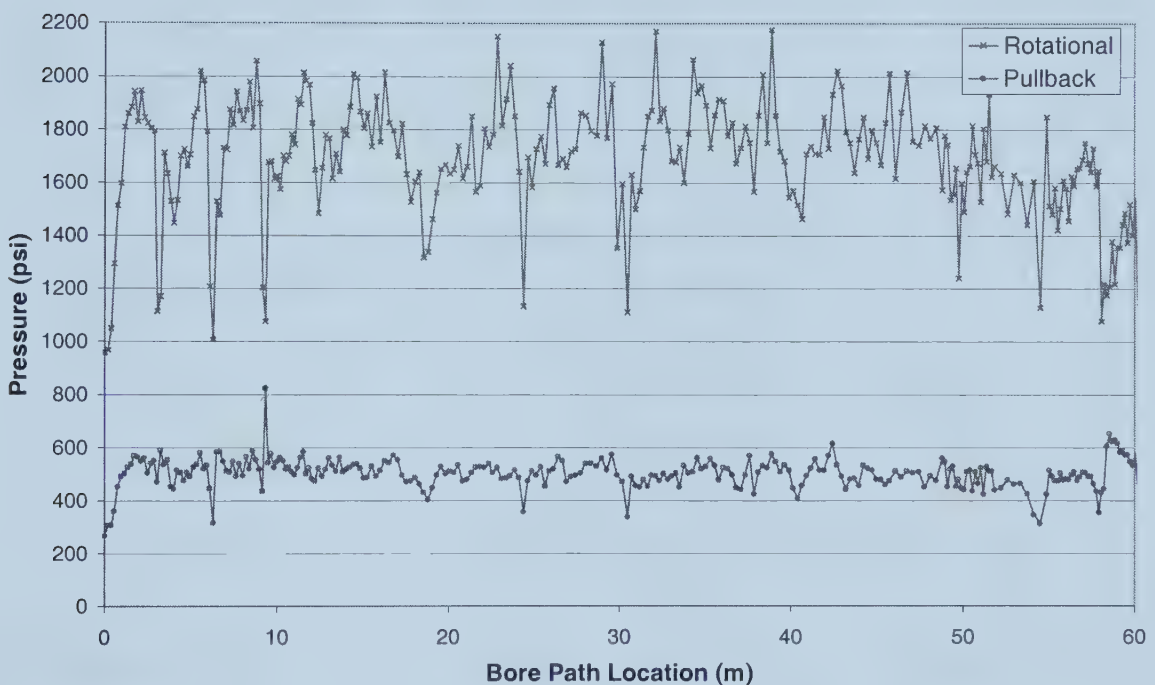


Figure 5.7: 324 mm Drilling Rig Pressure During Pre-ream – Clay

The drilling rig pressures for the pullback phase of the 324 mm pipe installed in clay are shown in Figure 5.8. The pullback pressure during the pullback phase did not remain constant as it did for the pre-ream phase. Initially, the pullback pressure started around 400 psi and peaked at approximately the 5 m point at around 1000 psi. Following this peak, the pressure decreased to around 650 psi and steadily rose to about 775 psi at the 30 m point in the installation. After the 30 m point the pullback pressure jumped to 900 psi and remained around that level for the rest of the installation. The rotational pressure

varied as evidenced before with the trend of the line starting at around 1800 psi and increasing to 2800 psi at around the 23 m point of the installation. The rotational pressure fluctuated about this point until the 30 m mark where it decreased to approximately 2200 psi and remained at that point for the rest of the installation.

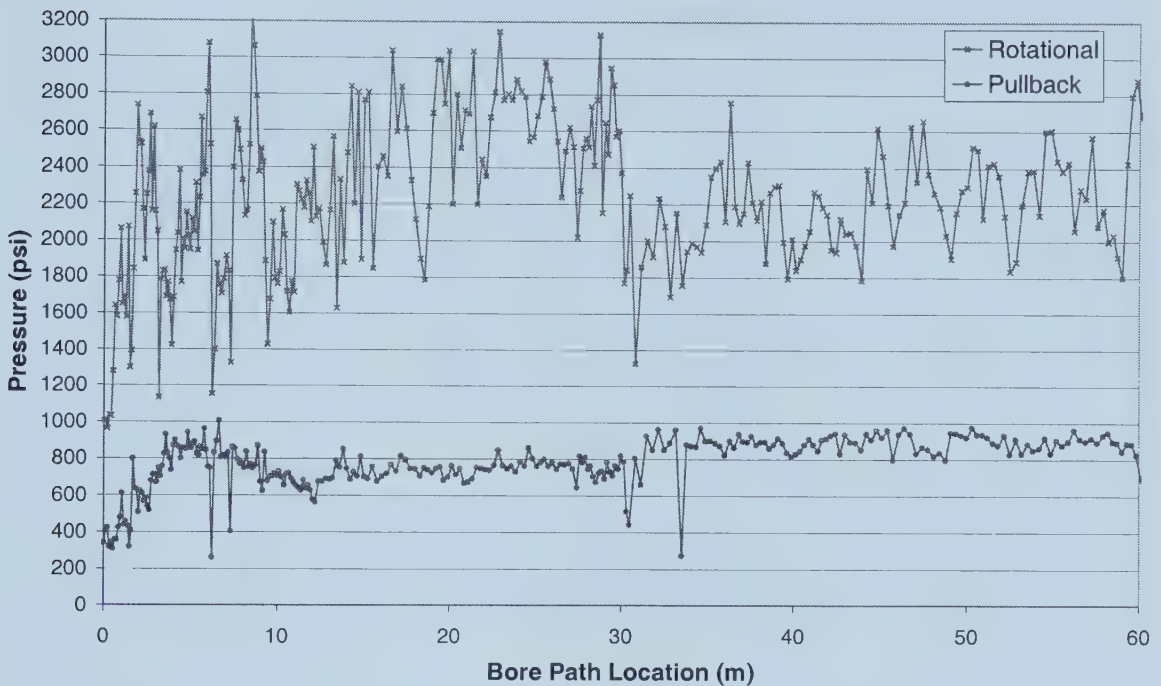


Figure 5.8: 324 mm Drilling Rig Pressure During Pullback – Clay

The strain experienced by the 324 mm pipe installed in the clay soil medium is shown in Figure 5.9. The majority of the strain effects experienced by the pipe during the installation phase can be attributed to the initial bending portion of the installation where the strain peaked at almost 0.4%. Following this initial bending portion, the strain subsided within the 0.1% range for the remainder of the installation.

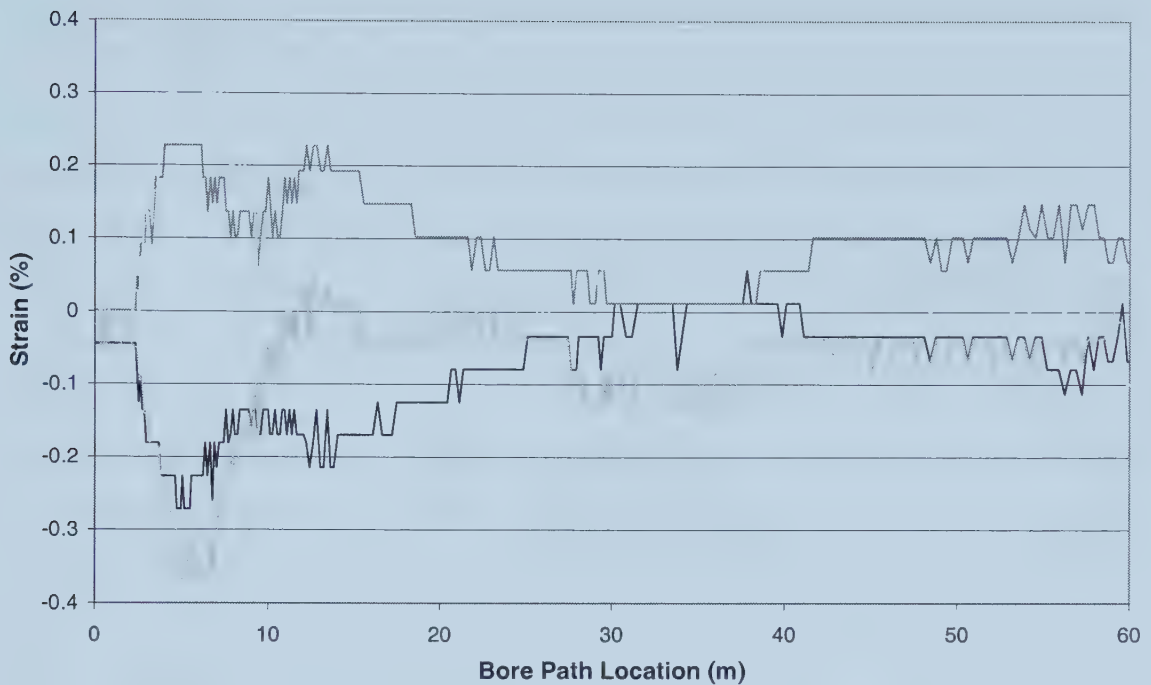


Figure 5.9: 324 mm Strain During Pullback - Clay

5.3 UNIVERSITY OF ALBERTA FARMS INSTALLATION 2 – CLAY

5.3.1 114 mm Diameter Pipe

The bore path profile for the 114 mm pipe installed in the second series of clay installations is shown in Figure 5.10.

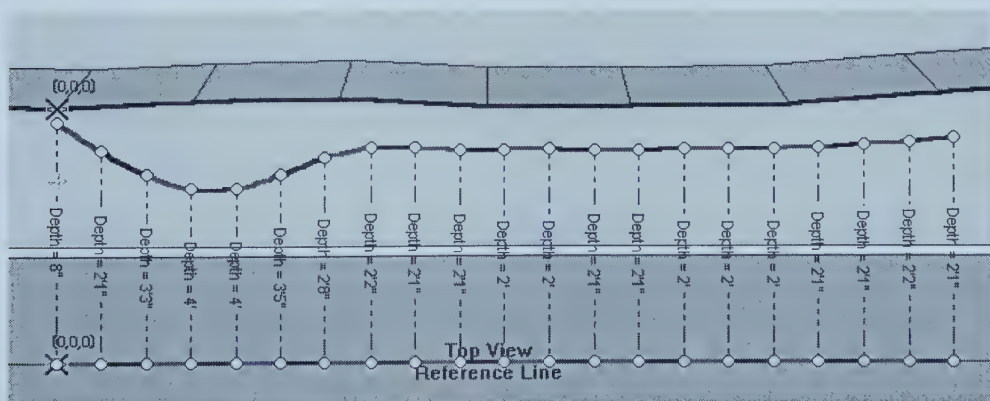


Figure 5.10: 114 mm Bore Path Profile – Clay 2

Figure 5.11 shows the drilling rig pressures that were recorded during the installation of the 114 mm pipe in the second series of clay installations. The drilling fluid pressure is not shown on the graph, as there was a malfunction with the data that was collected by the pressure transducer for this installation. The drilling fluid pressure data collected was similar to the pullback pressure that was recorded during the installation. Therefore, the drilling rig pressure was omitted from the plotted data due to this error. Additionally, it was difficult to convert the other pressures from the time-based system to the location-based system due to the absence of the drilling fluid data. The pullback pressure experienced by the drilling rig during the pullback phase was constant over the length of the installation. During the installation the pullback pressure remained in the 200 – 250 psi range with a slight increase from start to finish. The rotational pressures were very erratic and no noticeable trend can be established due to the wide range between the points on the upper and lower ends.

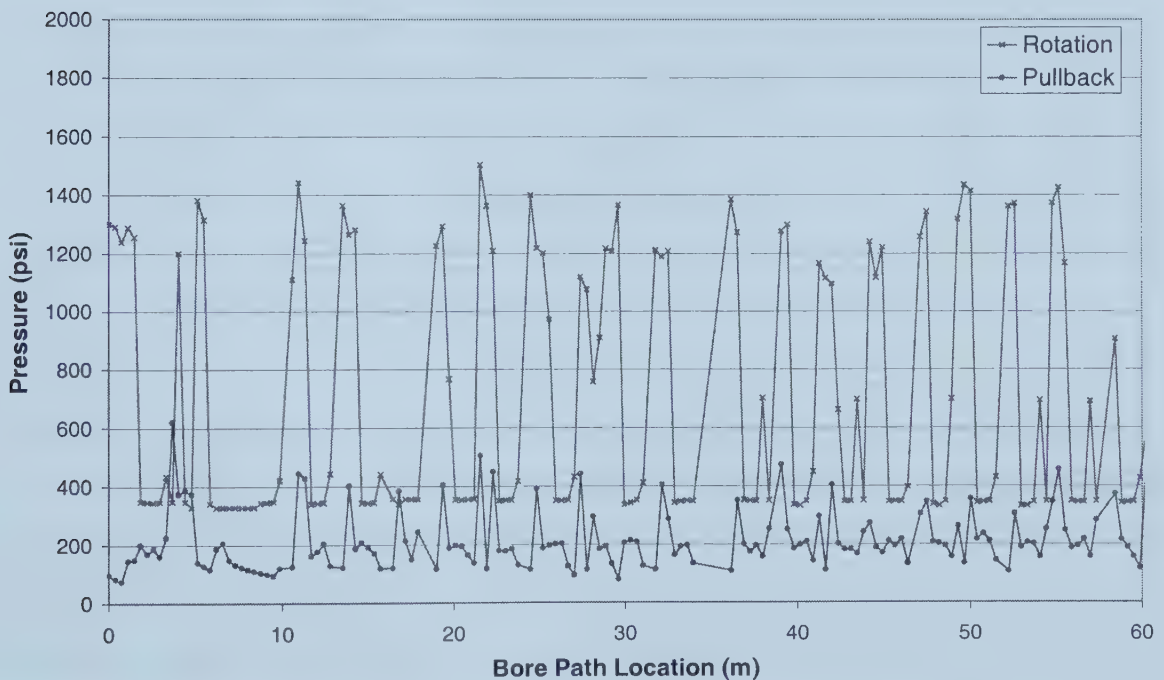


Figure 5.11: 114 mm Rig Pressure During Pullback – Clay 2

The load cell information for the 114 mm installation in the second clay series is shown in Figure 5.12. The absence of the drilling fluid data from the rig pressures also had an

effect on the capability of transforming the load cell data from the time-based approach to the location-based approach. From Figure 5.12 it can be seen that there is a wide variation in the readings given from the load cell with no discernable trends in the data. However, the data does not tend to go beyond the 3 kN mark, which could indicate that the pulling loads on the pipe are almost negligible.

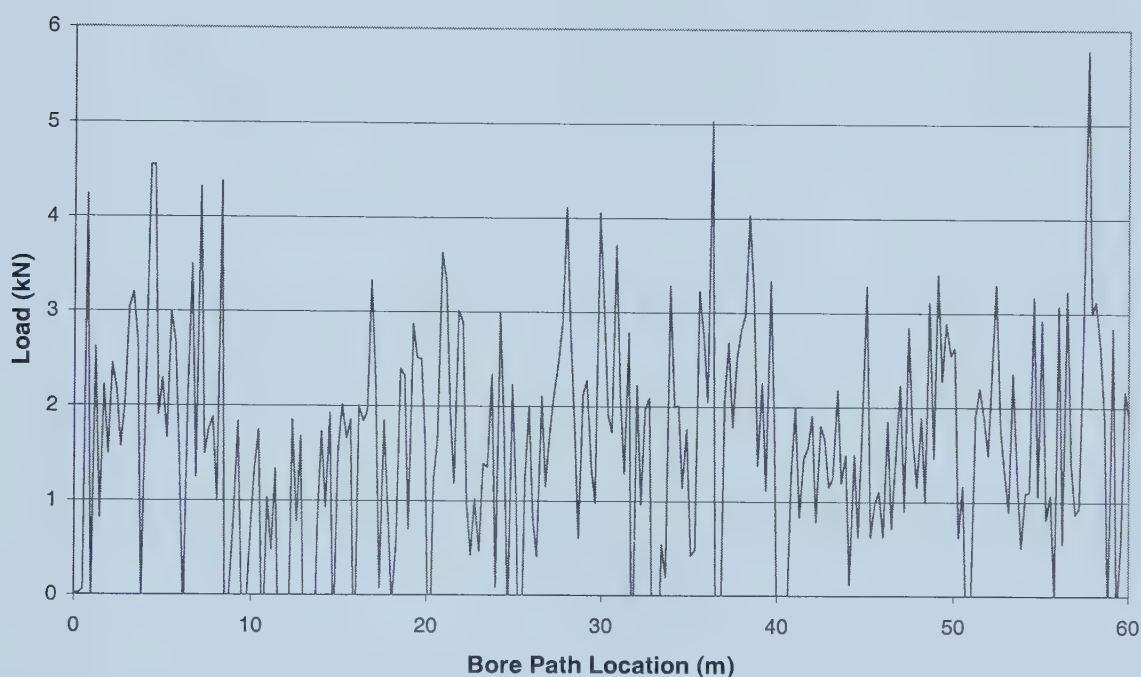


Figure 5.12: 114 mm Load Cell Results During Pullback – Clay 2

Figure 5.13 contains the strain recording during pullback on the 114 mm pipe installed in the second series of clay installations. A very noticeable peak and subsequent dip are evident on the graph during the initial bending portion of the bore path with strain values of 0.9% and -0.8% respectively. Additionally, following this peak, the strains do not return to a negligible state during the rest of the installation but do follow along a horizontal profile. This is due to the stiffness of the pipe material and the relative ease with which the pipe can be bent; the 114 mm pipe is not very stiff and can be permanently bent following a curve in a bore path profile. Following the installation the removed pipe was significantly bent, causing the results observed on the graph. During the initial bending phase the pipe was permanently deformed and the linear

potentiometers deviated from their initial gauge lengths set prior to the installation. Taking this into account, it can be determined that the strain in the pipe following the permanent deformation was negligible for the remainder of the installation.

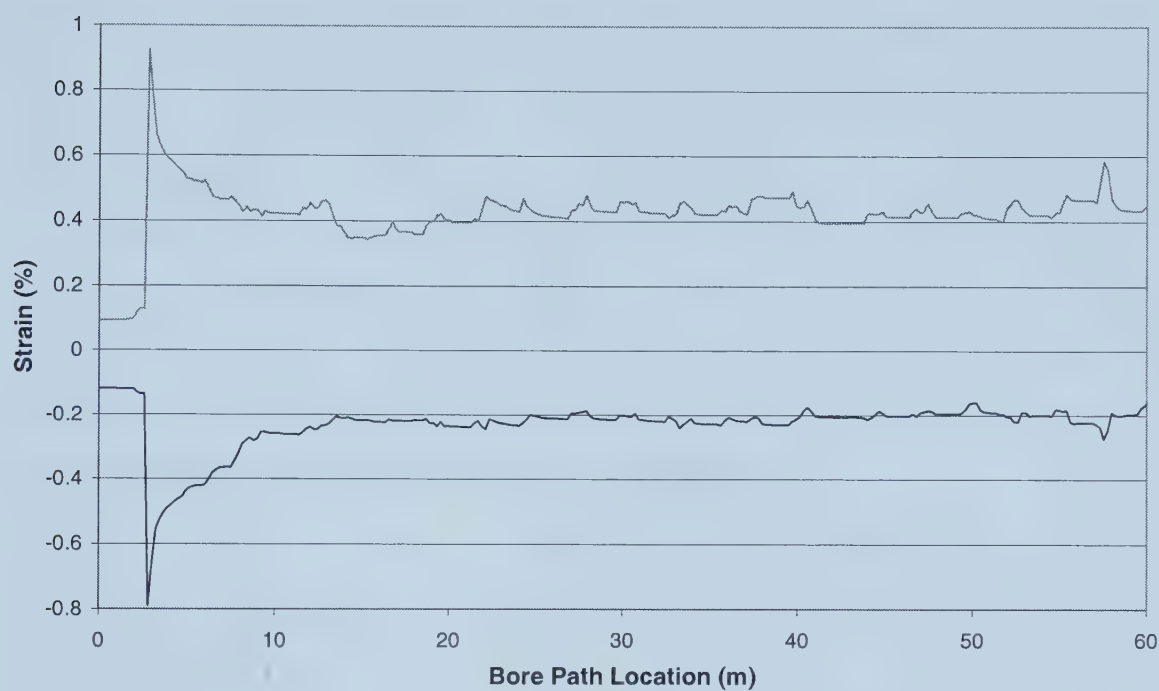


Figure 5.13: 114 mm Strain During Pullback – Clay 2

5.3.2 219 mm Diameter Pipe

The bore path profile for the 219 mm pipe installed in the second clay series is shown in Figure 5.14.

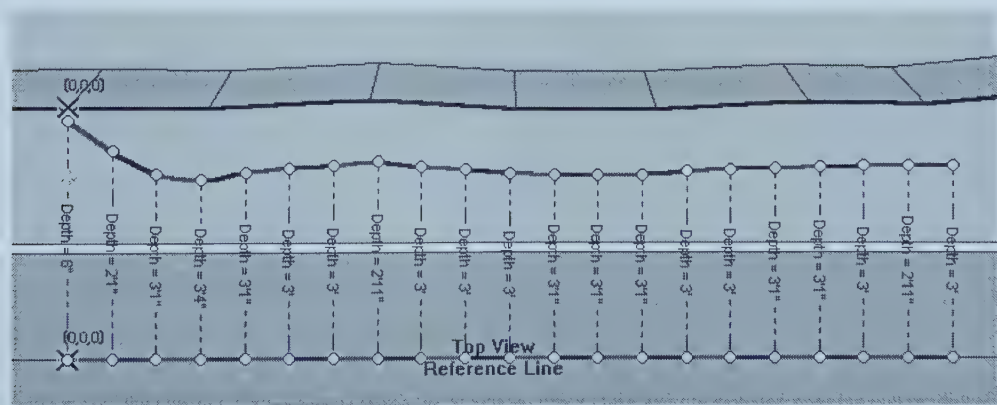


Figure 5.14: 219 mm Bore Path Profile – Clay 2

Figure 5.15 contains the drilling rig pressures experienced during the pullback phase of the 219 mm pipe installed in the second series of clay installations. The drilling fluid increased steadily during the course of the installation from approximately 10 psi to around 100 psi. A number of spikes, peaking above 200 psi, in the drilling fluid pressure were evident nearing the completion of the installation. The pullback pressure increased during the installation with two distinctive trends. The first trend ranged from the starting point of the installation to the 35 m mark of the installation. At the starting point the pressure ranged around the 650 psi point and increased to approximately 900 psi at the 35 m point. Following the 35 m point the trend of the line increased in a greater fashion than prior to the 35 m mark. The pullback pressure peaked at the end of the installation at approximately 2400 psi. The rotational pressure decreased during the length of the installation in a linear fashion. The trend of the pressure started at around 1900 psi and decreased to around 1400 psi at the end of the installation.

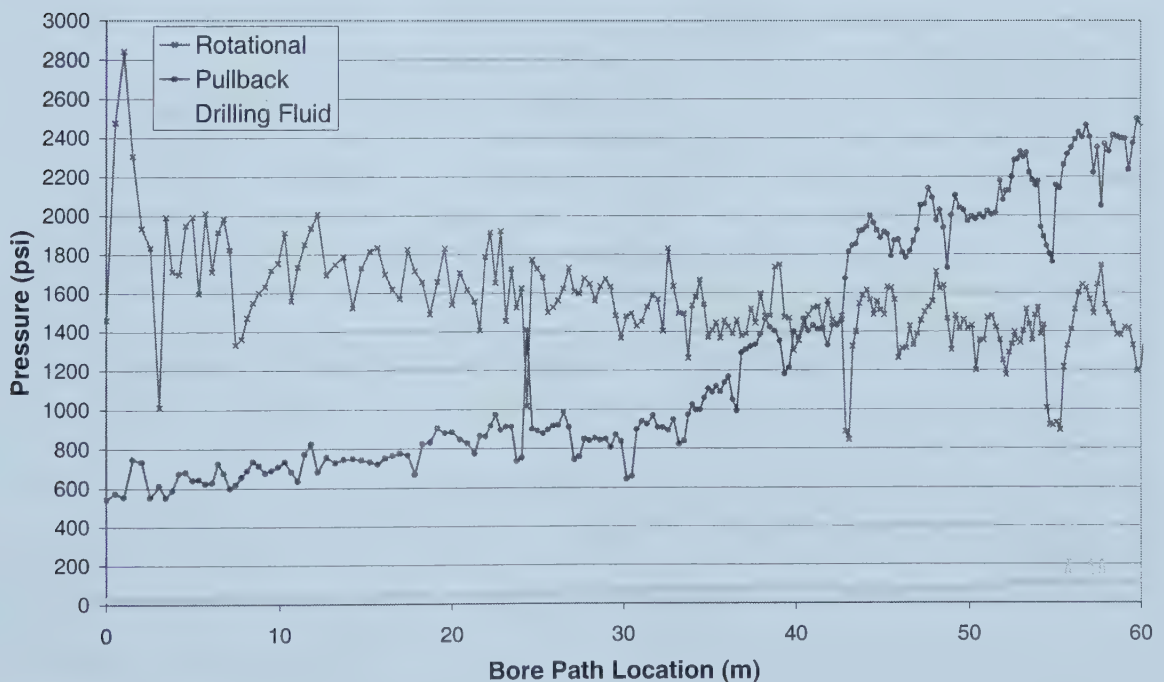


Figure 5.15: 219 mm Rig Pressure During Pullback – Clay 2

The load cell results for the 219 mm pipe installed in the second series of clay installations is displayed in Figure 5.16. There are two distinctive linear trends in the

installation process similar to the trends observed for the pullback pressure experienced by the drilling rig. The first trend starts just after the start of the installation at the 3 m point and continues to approximately the 35 m point. The load increases from around 10 kN to 20 kN at the 35 m point. The next trend continues from the 35 m point but increases in a greater fashion akin to the pullback pressure. The maximum load experienced is at the end of the installation at 70 kN.

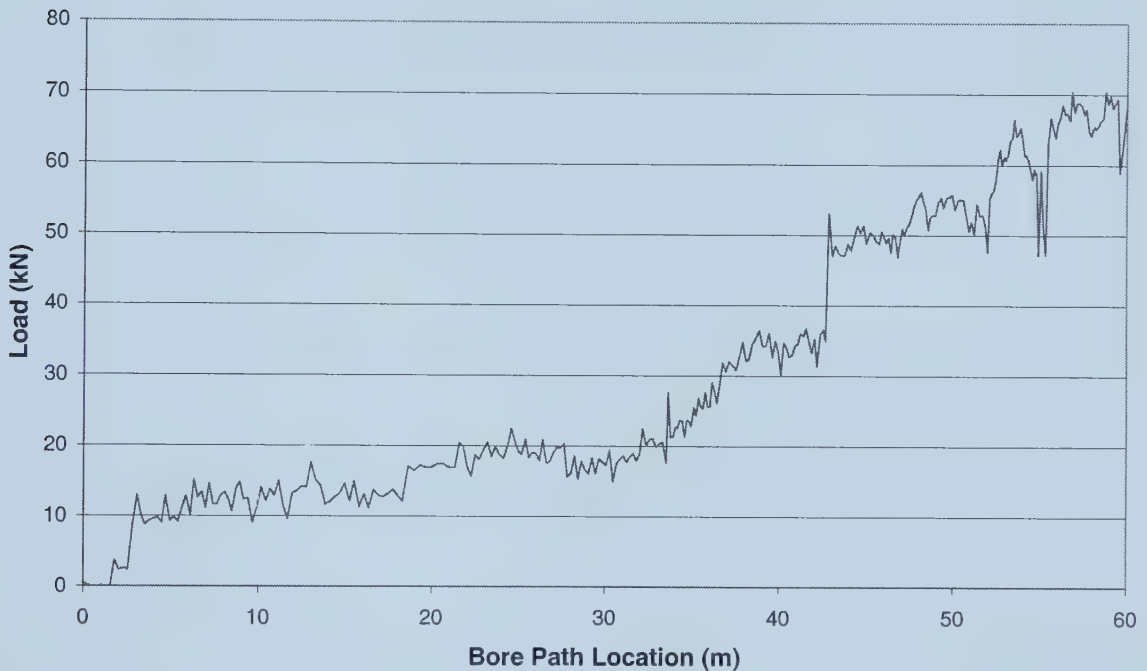


Figure 5.16: 219 mm Load Cell Results During Pullback – Clay 2

Figure 5.17 contains the strain experienced by the 219 mm pipe during the pullback phase of the second series of clay installations. The initial bending stresses impart a maximum value of 0.2 % strain on the pipe. Following the bending portion the strains subside to negligible amounts until the 35 m point of the installation. Following the 35 m point the strains in the pipe steadily increase until the end of the installation. The maximum strain of 1.3% is experienced at the end of the installation.

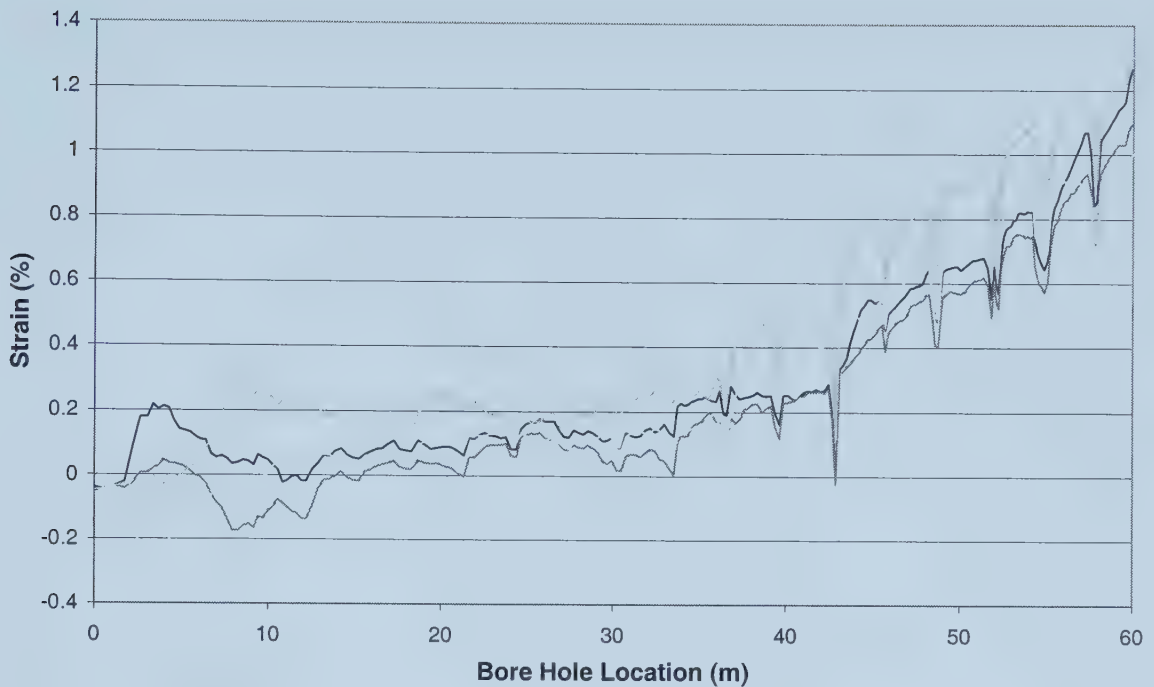


Figure 5.17: 219 mm Strain During Pullback – Clay 2

5.4 SIL SILICA INSTALLATION – SAND

5.4.1 114 mm Diameter Pipe

The bore path profile of the 114 mm pipe installed in sand is shown in Figure 5.18. During the installation, the depth of the pipe was maintained at the 2 ft depth experiencing only 1 in. deviations.

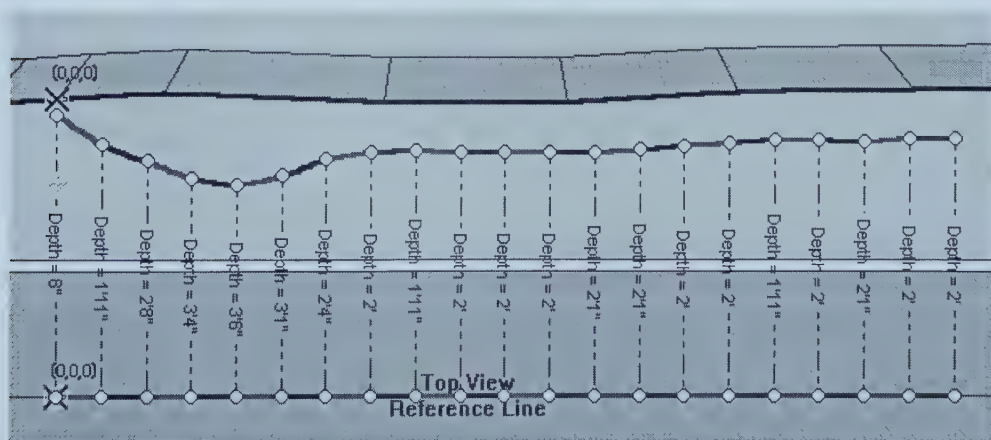


Figure 5.18: 114 mm Diameter Pipe Installed in Sand Bore Path Profile

Figure 5.19 contains the drilling rig pressures experienced during the pipe pullback phase of the 114 mm pipe installed in sand. The drilling fluid pressure during the installation steadily decreased from 130 psi at the beginning of the pullback phase to 60 psi at the end of the installation. One significant dip in pressure was experienced at the 55 m point of the installation. The pullback pressure increased steadily over the length of the installation ranging from 225 psi at the start of the installation to 365 psi at the end of the installation. This increase in pressure was fairly constant across the length of the installation. The rotational pressure also increased along the length of the installation. At the start the rotational pressure was approximately 1050 psi and increased to around 1170 psi at the end of the installation.

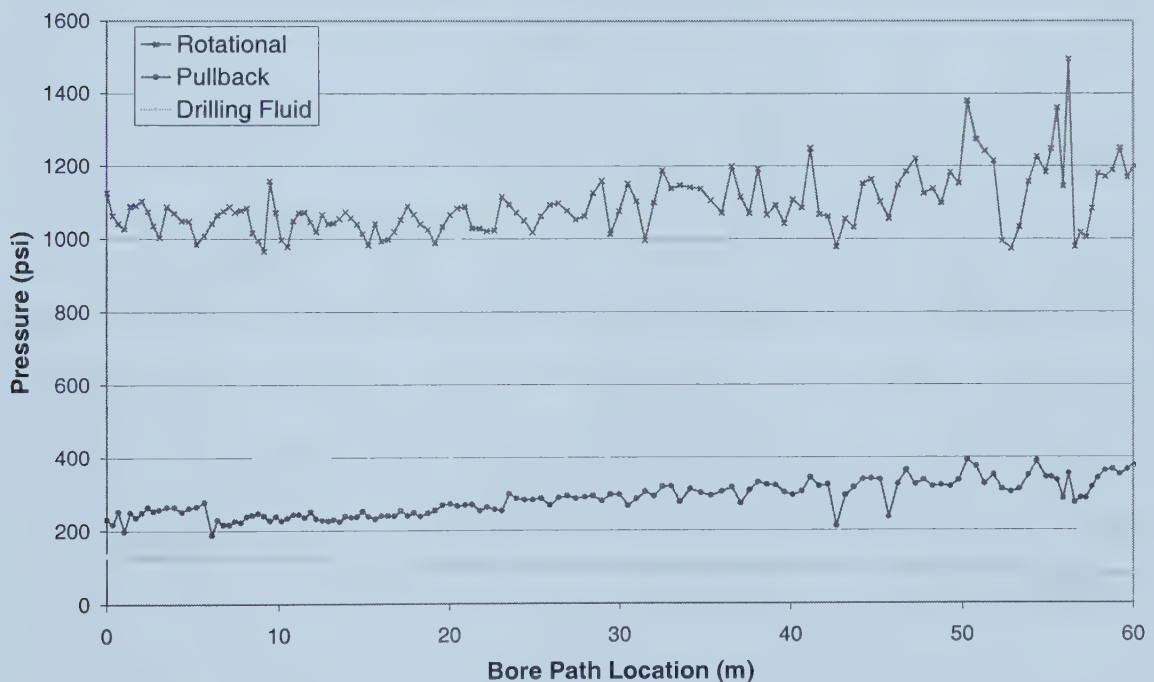


Figure 5.19: 114 mm Rig Pressure During Pullback – Sand

The load cell results for the 114 mm pipe installed in sand are shown in Figure 5.20 for the pipe pullback process. The trend in the data suggests an increase in load as the installation continues along the bore path, with a maximum load of approximately 5 kN experienced by the load cell.

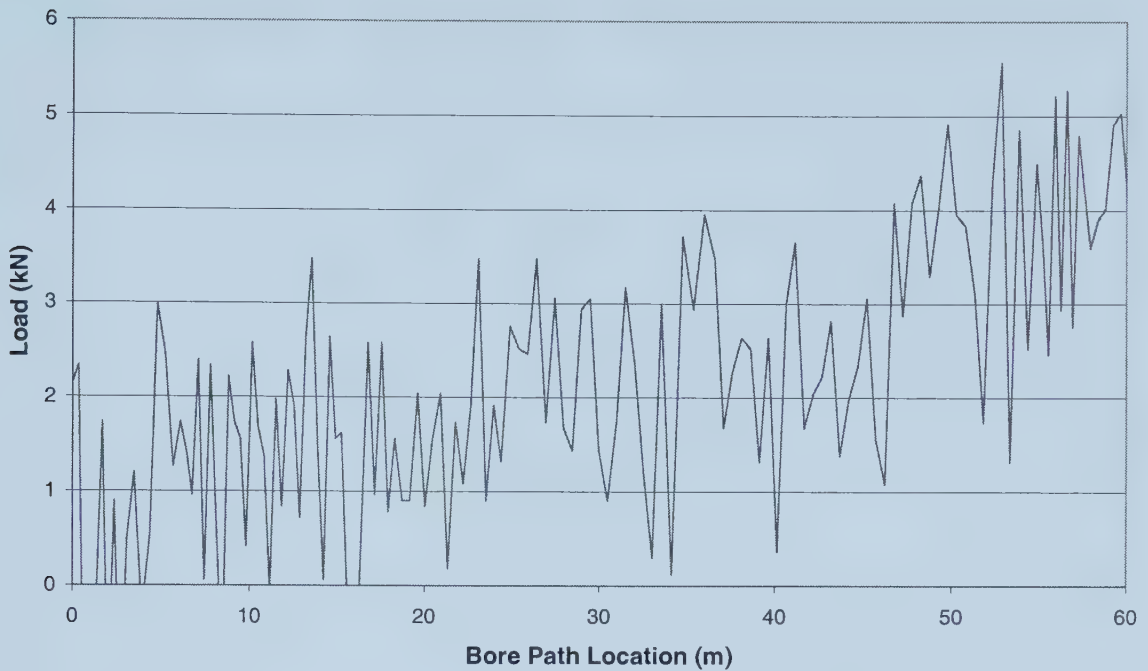


Figure 5.20: 114 mm Load Cell Results During Pullback – Sand

Figure 5.21 illustrates the strain experienced by the 114 mm pipe installed in the sand medium during the pullback phase of the HDD installation. Initial bending strains are exhibited and produce results of approximately 0.05% strain. Initially, following the bending portion, the strains reduce to a negligible amount until the 30 m point of the installation. Following the 30 m point the strains noticeably increase to a maximum of approximately 0.15%.

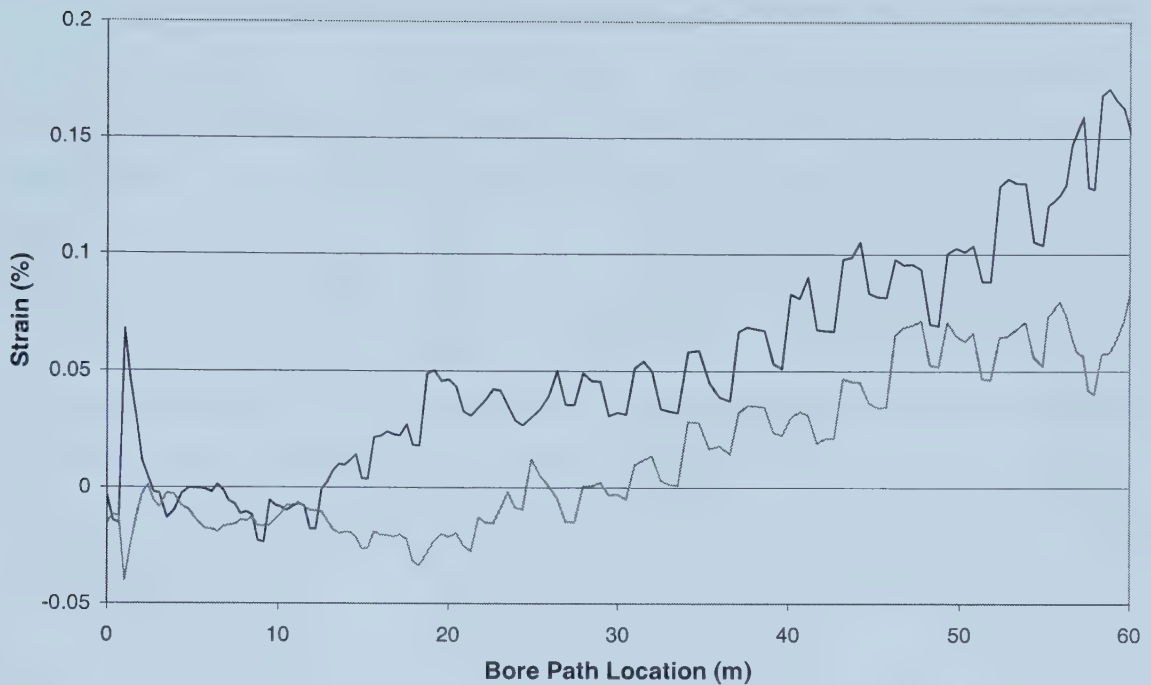


Figure 5.21: 114 mm Strain During Pullback – Sand

5.4.2 219 mm Diameter Pipe

Figure 5.22 contains the bore path profiles for the 219 mm pipe installed in sand. It can be seen from this figure that it took a large portion of the installation length to bring the drill head to the desired depth. Following this, the drilling head remained relatively stable, deviating by a maximum of 1 in. only.

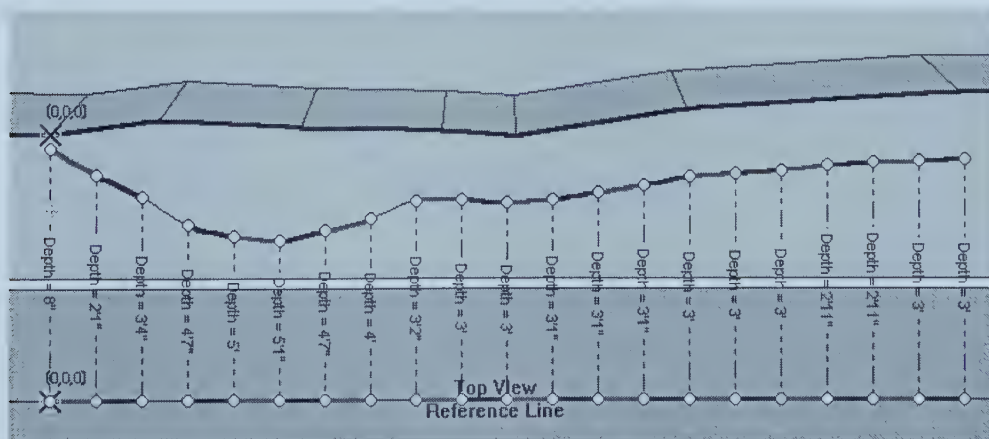


Figure 5.22: 219 mm Bore Path Profile – Sand

The drilling pressures during the pullback phase of the 219 mm pipe installed in sand are shown in Figure 5.23. The drilling fluid pressure exhibited a declining trend during the course of the installation with a number of jumps evident in the later portion. The pressure started at around the 120 psi range and decreased steadily to 80 psi at the 43 m point. Several peaks of around 135 psi occurred, followed by a smaller pressure of 60 psi until it peaked at 180 psi near the end of the installation. The pullback pressure shows an increasing linear trend over the duration of the installation. This pullback pressure started at 200 psi and finished at around 680 psi. The rotational pressure was less erratic during the initial stages of the installation up to the 24 m mark with pressures ranging from 1100 psi to 1600 psi. Following this point the rotational pressure is more erratic ranging from 900 psi to 1900 psi.

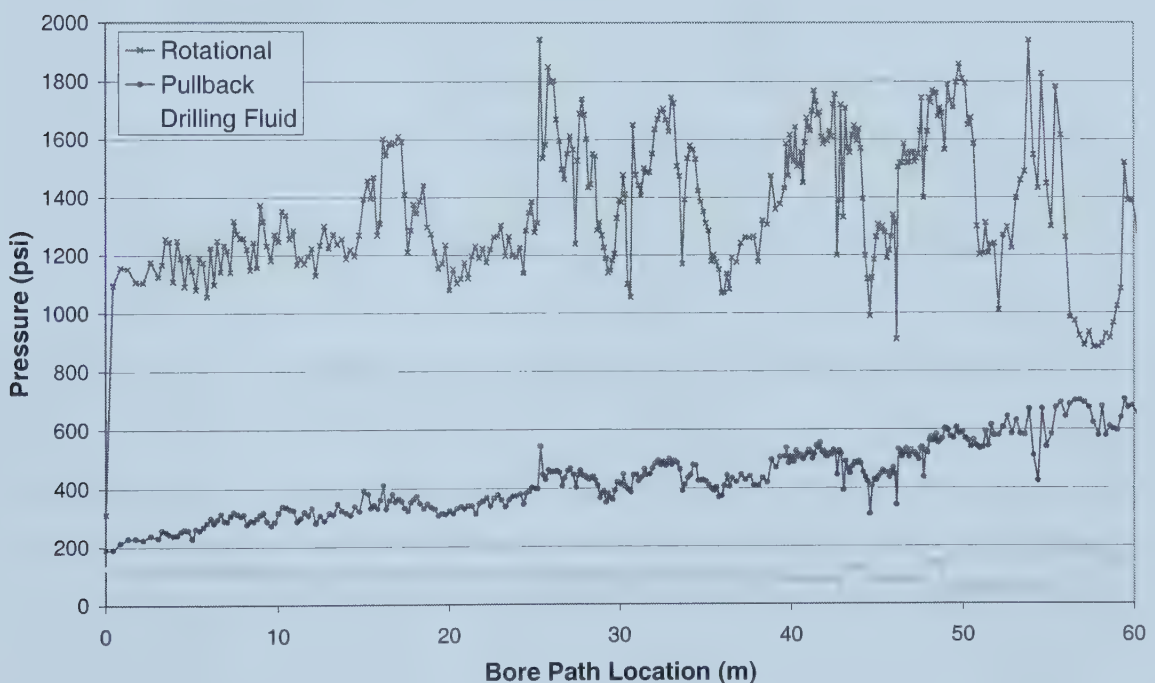


Figure 5.23: 219 mm Rig Pressure During Pullback – Sand

Figure 5.24 contains the load cell results from the 219 mm pipe installed in the sand soil medium. The results of the load cell resemble an increasing linear trend from the beginning to the end of the installation similar to the pullback pressure experienced by

the drilling rig. The maximum loading experienced by the load cell was just slightly over 20 kN.

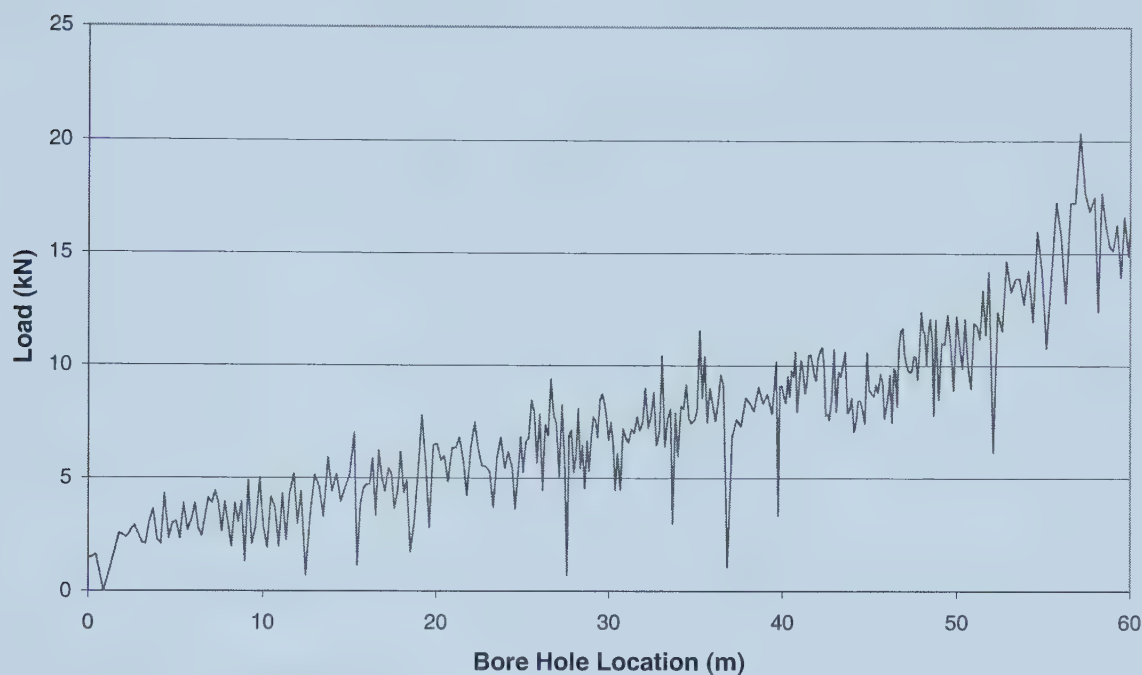


Figure 5.24: 219 mm Load Cell Results During Pullback – Sand

The strain results for the 219 mm pipe installed in sand are shown in Figure 5.25. It can be seen from this graph that the pipe undergoes the initial bending deformation causing a maximum positive and negative strains of 0.1% and –0.15% respectively. Following this, the strain reduces to a negligible amount until the 30 m point of the installation. After the 30 m point the strain increases to a maximum of 0.18% near the end of the installation.

Figure 5.27 shows the drilling rig pressures of the 324 mm pipe installed in sand for the pre-reaming operation. During the pre-ream operation the drilling fluid pressure remained relatively constant at around the 150 psi range. The pullback pressure increased slightly from around 330 psi at the beginning of the installation to around 600 psi at the 55 mm point of the installation. After the 55 mm point the pressure decreases to 400 psi at the end of the installation. The rotational pressure was steadily increasing from the beginning to the 55 m point of the installation, increasing from 600 psi to about 2600 psi. Following the 55 m point, the pressure dropped to around the 1400 psi range for the remainder of the installation.

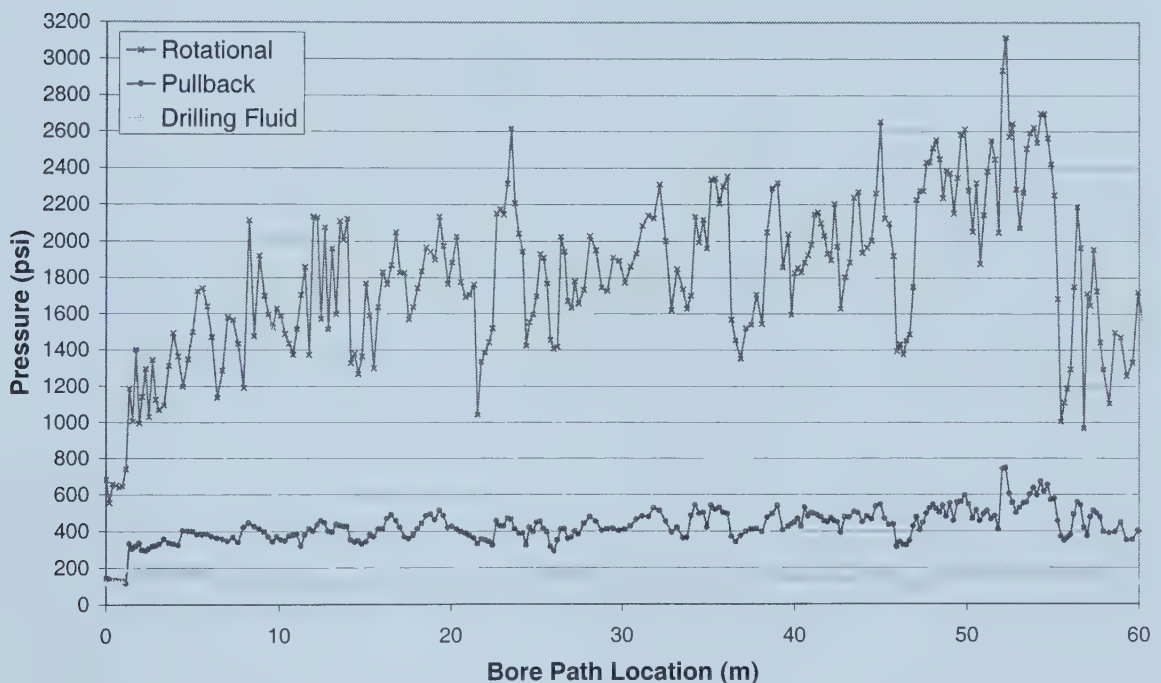


Figure 5.27: 324 mm Drilling Rig Pressure During Pre-Ream - Sand

The drilling fluid pressures for the pullback operation of the 324 mm pipe installed in sand is shown in Figure 5.28. The drilling fluid pressure remained quite constant, at around 200 psi, for the installation with the exception of one dip around the 34 m point. At the 34 m point the pressure dipped to 65 psi for a couple of meters. The pullback pressure increased steadily over the range of the installation increasing from 200 psi to about 975 psi. The rotational pressure was quite erratic over the entire installation but

showed a slightly decreasing trend from start to finish. The maximum pressure experienced was around 200 psi while the minimum was around 800 psi.

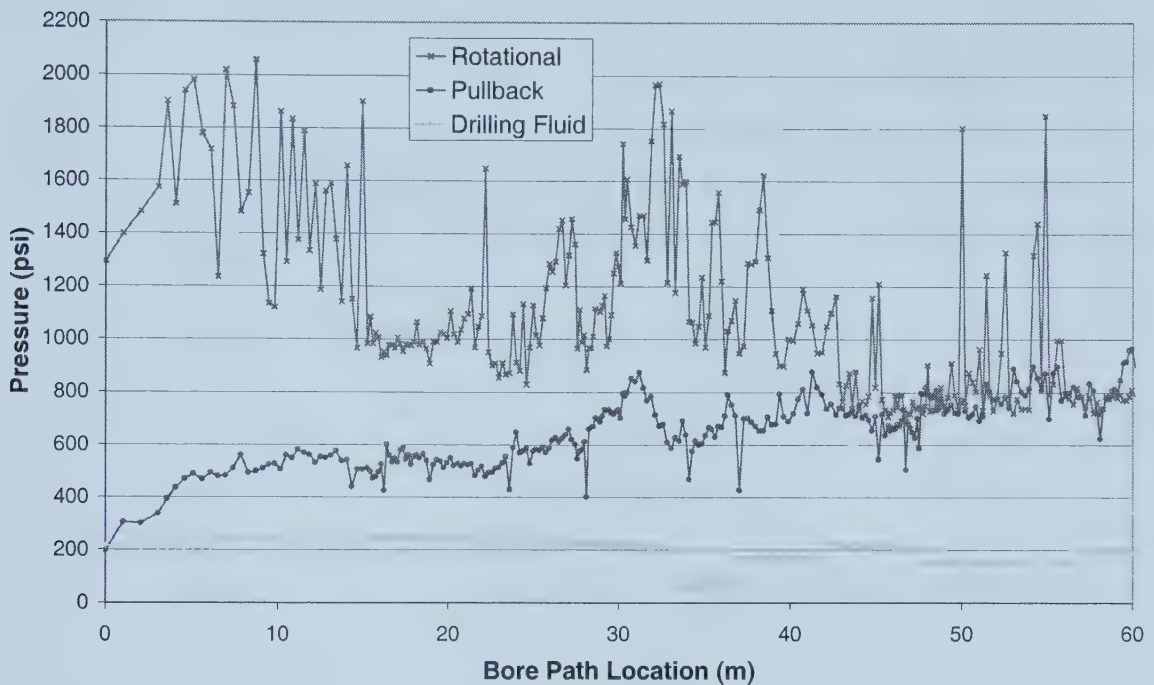


Figure 5.28: 324 mm Drilling Rig Pressure During Pullback - Sand

Figure 5.29 illustrates the load cell results for the pullback phase of the 324 mm pipe installed in the sand soil medium. There was a definite increasing trend experienced over the length of the installation. The maximum load experienced was just over 25 kN at the end point of the installation.

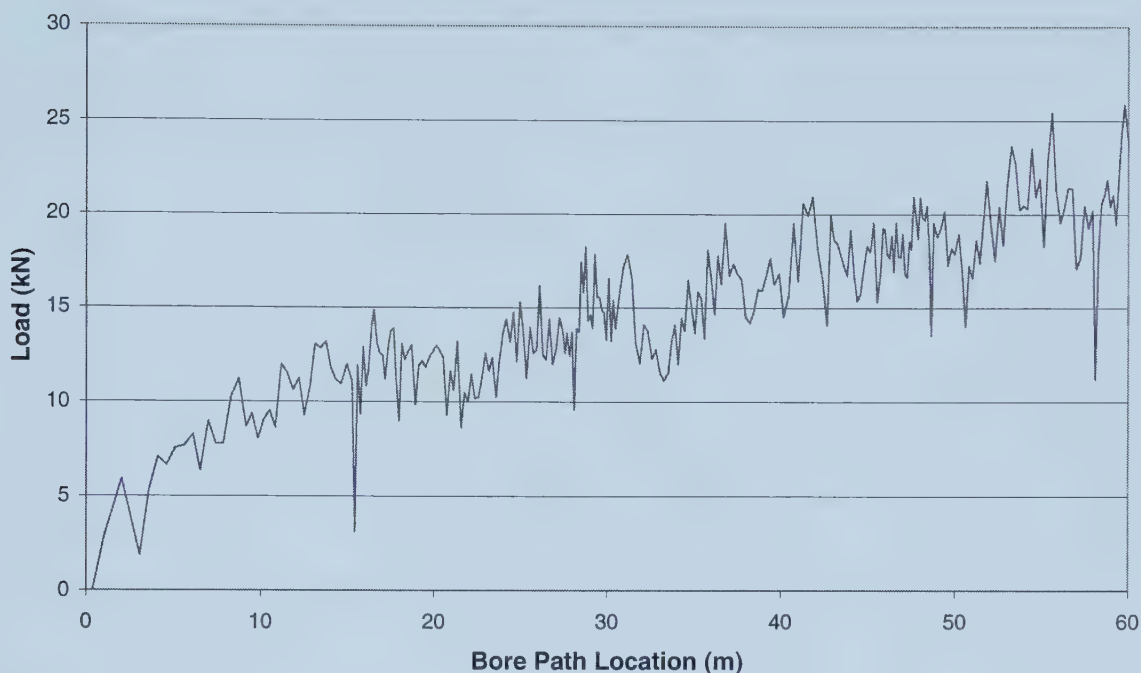


Figure 5.29: 324 mm Load Cell Results During Pullback – Sand

The strain experienced by the 324 mm pipe during the pullback phase in the sand soil medium is shown in Figure 5.30. Initial bending strains peaked at 0.2% for the initial portion of the installation. For the remainder of the installation the strain on the pipe remained within the 0.05% range.

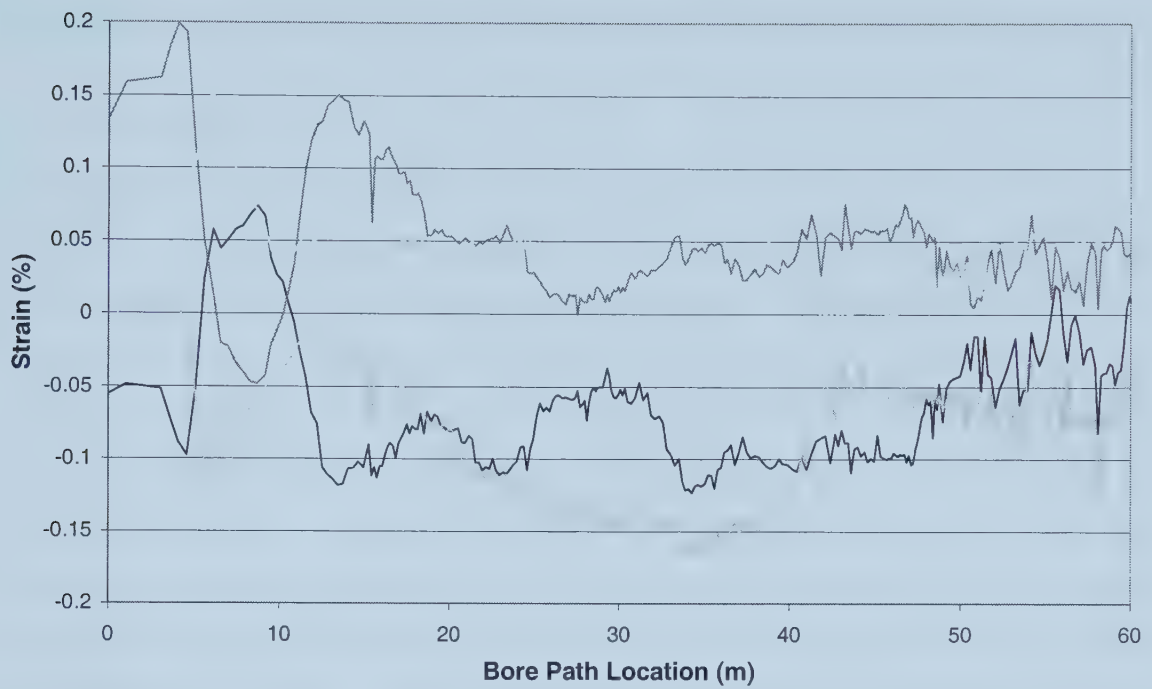


Figure 5.30: 324 mm Strain During Pullback – Sand

Chapter 6 ANALYSIS OF FIELD TESTING RESULTS

6.1 INTRODUCTION

This chapter focuses on the comparisons between the soil mediums and the pipe diameters to determine the effects that they have on the HDD process. Each of the pipe diameters that were installed is compared between each of the soil mediums. The 114 mm diameter pipes are compared first followed by the 219 mm and the 324 mm diameter pipes. For each of the pipe diameter comparisons the drilling rig fluid pressures, drilling rig rotational torque pressures, drilling rig pullback pressures, loading on the load cell, and the average and maximum recorded strain on the HDPE pipe are compared. Following these soil comparisons, the effect of pipe diameter in a soil medium is analyzed. An analysis is conducted for both the clay and the sand soil mediums looking at the following parameters: drilling rig drilling fluid pressure, drilling rig rotational pressure, drilling rig pullback pressure, loading from the load cell, and average and maximum strain on the HDPE pipes. Lastly, an analysis of how the drilling rig pullback pressure relates to both the load cell results and strain results is conducted for both the 219 mm and 324 mm pipes installed in both soil mediums.

6.2 114 mm DIAMETER PIPE - SOIL MEDIUM COMPARISON

6.2.1 Drilling Fluid Pressure

Figure 6.1 gives the drilling rig fluid pressures encountered for the 114 mm pipes installed in the clay and sand soil mediums. For both installations, drilling fluid pressures declined over the length of the installation. The drilling fluid pressures for the sand installation were larger than for the clay installation. The drilling fluid pressure for the sand decreased from around 130 psi at the start of the installation to approximately 80 psi at the end of the installation. Additionally, there was a significant drop in drilling fluid pressure at the 55 m point in the installation. The clay installation started around the 80 psi point and fluctuated down to less than 30 psi at the end of the installation.

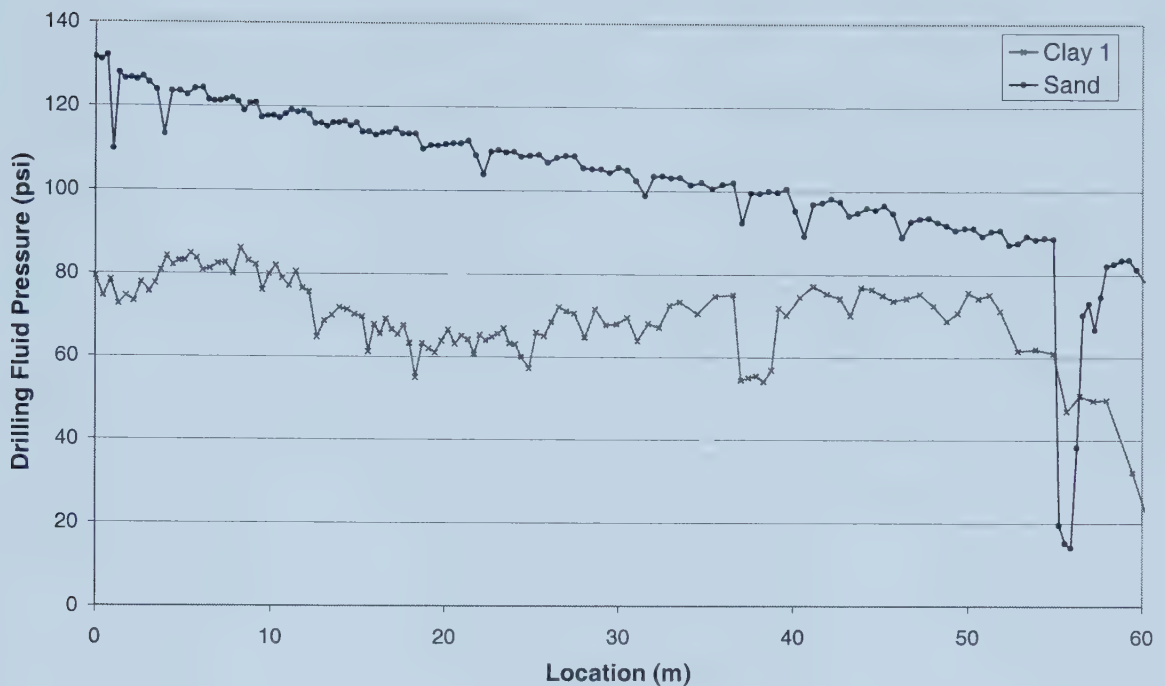


Figure 6.1: Pullback Drilling Fluid Pressures for 114 mm Pipes

6.2.2 Rotational Torque Pressure

The rotational torque pressures experienced by the drilling rig for the 114 mm pipe installations are shown in Figure 6.2. Over the length of the installation the drilling rig rotational pressures remained fairly constant for all three of the installations. Also, the magnitudes of these rotational pressures were very similar between the two soil mediums. The installations in the clay soil medium showed excellent correlation with one another. Both of these installations started around the 1250 psi range and followed a very similar pattern throughout the length of the bore path. For these two installations the rotational pressure varied from a minimum of 800 psi to a maximum of 1550 psi. The rotational pressure for the pipe installed in the sand soil medium was slightly less over the length of the installation in comparison to the two installations in clay. The sand installation ranged from 1000 psi to a maximum of 1500 psi.

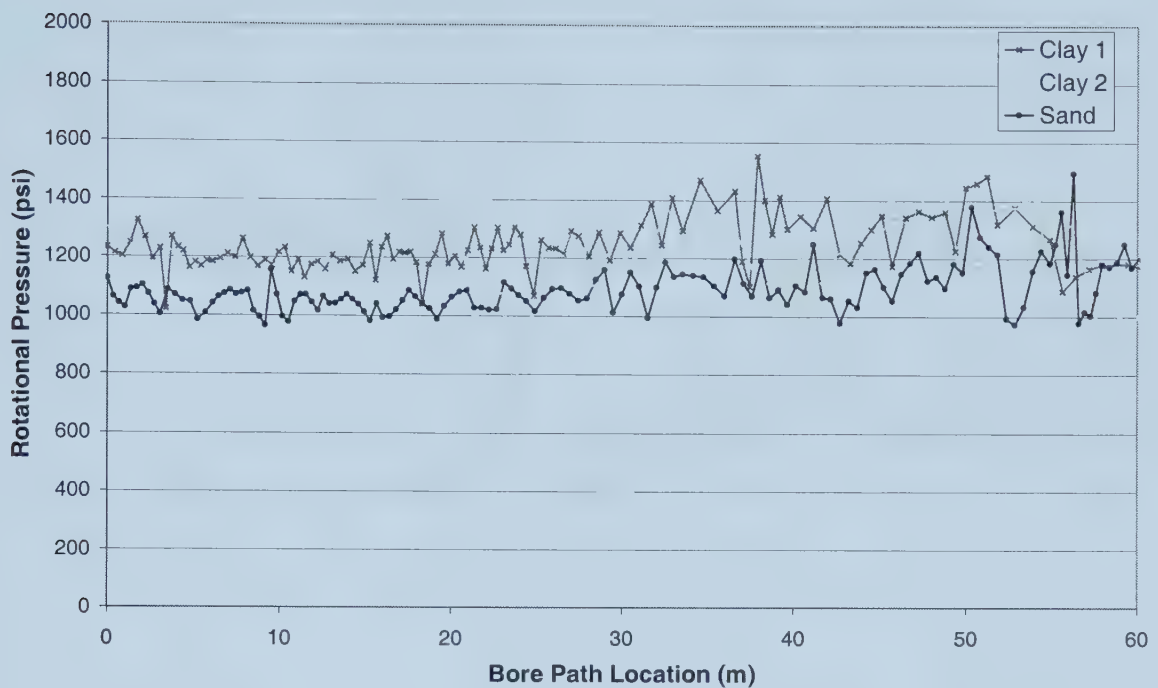


Figure 6.2: Pullback Rotational Pressures for 114 mm Pipes

6.2.3 Pullback Pressure

Figure 6.3 illustrates the pullback pressures experienced by the drilling rig for the 114 mm pipe installations in the two soil mediums. Initially, it can be seen that the installation conducted in sand and the first installation conducted in clay have a good data set. The second installation conducted in the clay soil medium contains very large fluctuations. These large fluctuations can be attributed to the fact that both the drilling rig fluid pressures and the pullback pressures display the same values, which suggests an error in the Data Dolphin collection device during this test. Therefore, this second installation in clay will be ignored during the analysis between the two soil mediums.

Both of the installations, clay 1 and sand, display an increasing trend over the length of the installation. This coincides with more pipe being in the ground and therefore more effort is required to advance this pipe. The pullback pressures for clay started at approximately 300 psi and experienced a maximum pressure of 700 psi at the 39 m point in the installation. The pullback pressure for the sand is less than that experienced during the clay installation with the pressure ranging from 200 to 375 psi.

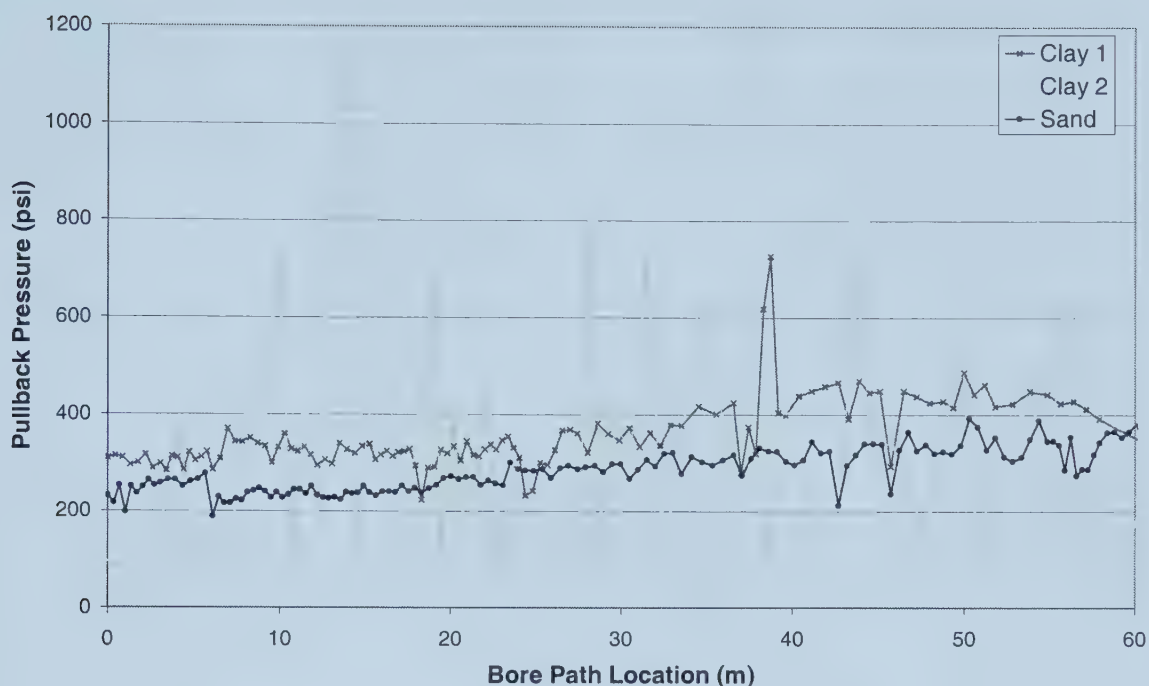


Figure 6.3: Pullback Pressures for 114 mm Pipes

6.2.4 Load Cell

The load cell readings for the 114 mm pipe installations in the two soil mediums are shown in Figure 6.4. The range for the y-axis of this graph was chosen to be larger than required as the fluctuations in the load cell readings made it difficult to ascertain whether any trends existed with a smaller data range. Throughout both of these installations the load cell readings fluctuated widely over the duration of the pullback phase. However, it is still possible to interpret the trend of the data and to observe the reaction of the load during the installation.

The magnitude of loading on both of the pipes is very similar between the two soil mediums. They both experience a range of loading from 0 kN to 6 kN over the bore path length. Although they experience the same loading range, the trend of the load is quite different. For the pipe installed in the clay soil medium, the trend of the load seems to be fluctuating both upwards and downwards over the duration of the installation. However, the pipe installed in the sand soil medium displays an increasing trend over the length of the installation.

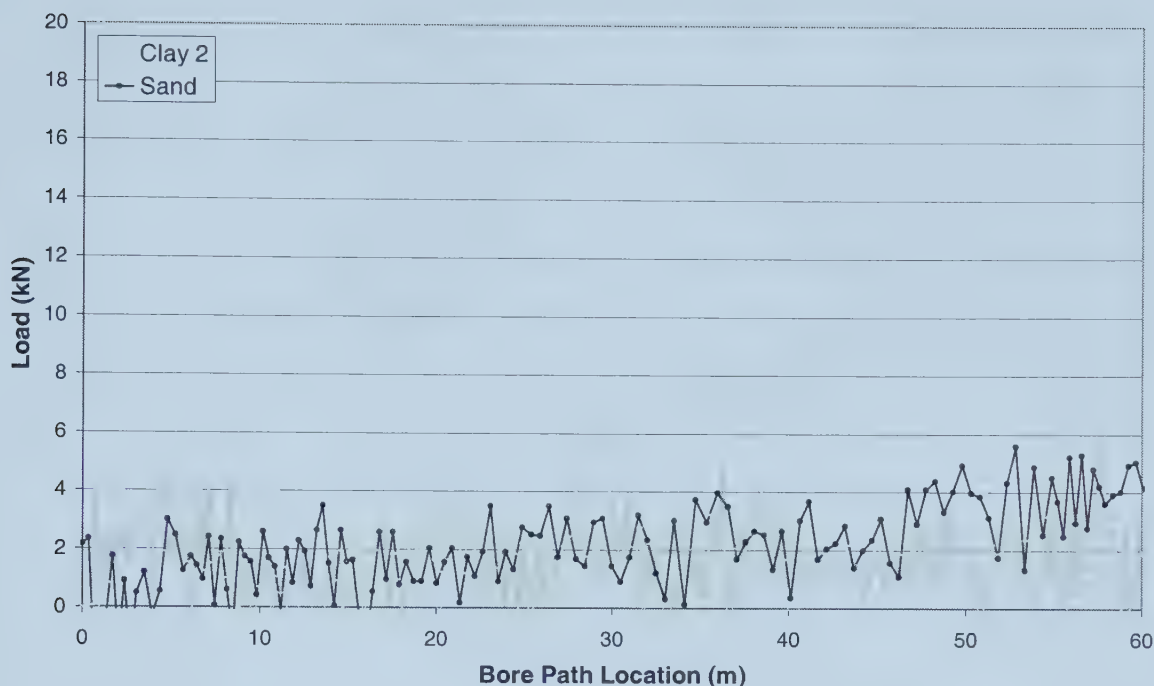


Figure 6.4: Load Cell Comparisons for 114 mm Pipes

6.2.5 Strain Results

Figure 6.5 displays the average strain readings on the 114 mm HDPE pipe recorded during the pullback phase of the HDD operation. The average strain results were calculated by averaging the readings obtained between the two linear potentiometers installed in the HDPE pipe. The average strain for the pipe installed in clay was greater over the bore path length than the average strain experienced for the pipe installed in sand. However, the trend of the strain for the clay installation is less than that of the trend for the sand installation. The reason that the clay experiences greater strain is because the section where the linear potentiometers were installed was permanently deformed during the initial bending portion of the test. This can be seen clearly in Figures 5.13 and 6.6. The maximum strain experienced by the pipe installed in clay was 0.15%. The pipe installed in the sand medium displays a smooth increase in strain over the bore path location, experiencing a maximum average strain of 0.125%.

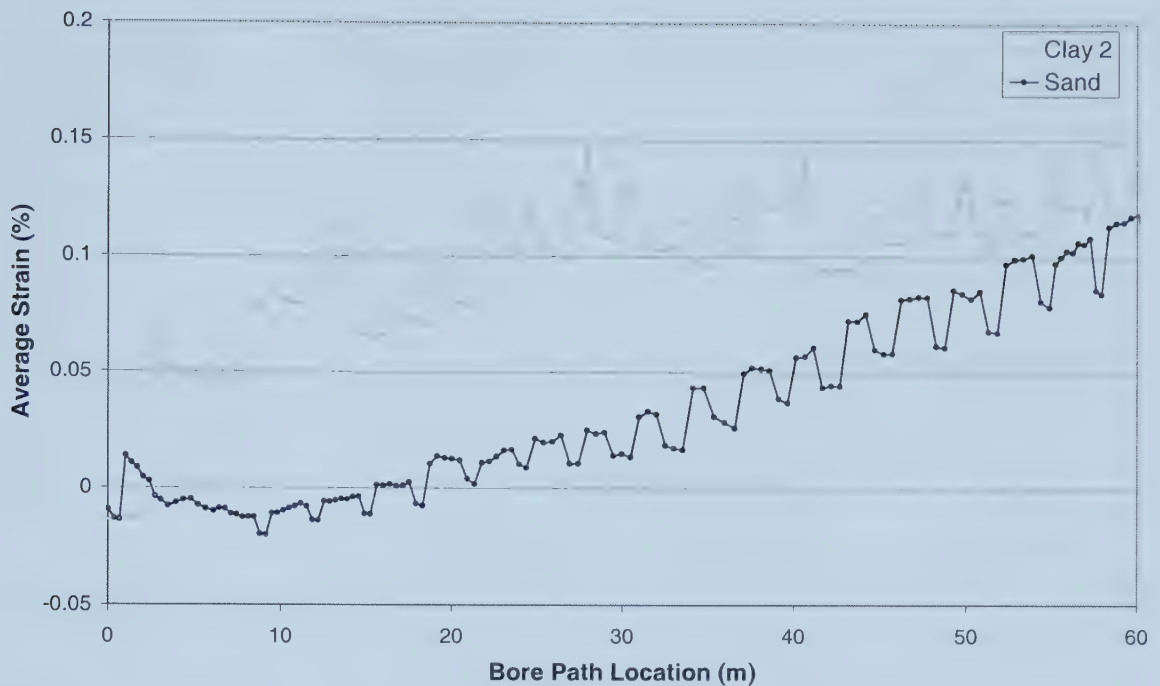


Figure 6.5: Average Strain During Pullback for 114 mm Pipes

The maximum recorded strain experienced by the HDPE pipes installed in the clay and sand soil mediums is shown in Figure 6.6. This maximum recorded strain is the largest strain value, either positive or negative, from all of the linear potentiometers installed in the pipe. This maximum strain provides an illustration of where the maximum strain occurred relative to the bore path location. The maximum absolute strain experienced by the pipe installed in the clay soil medium was larger than the pipe installed in the sand soil medium. Some of this can be attributed to the permanent deformation that was described before, but after this deformation the strain experienced a range from 0.35% to 0.58%. The strain that was experienced by the pipe over this range was essentially 0.23%. In comparison to the pipe that was installed in sand, the strain reached a maximum of around 0.175%. Therefore, the pipe that was installed in the clay soil medium experienced a larger maximum strain even while accounting for the deformation of the pipe. For both of the installed pipes the trend of the strain is increasing over the duration of the installation.

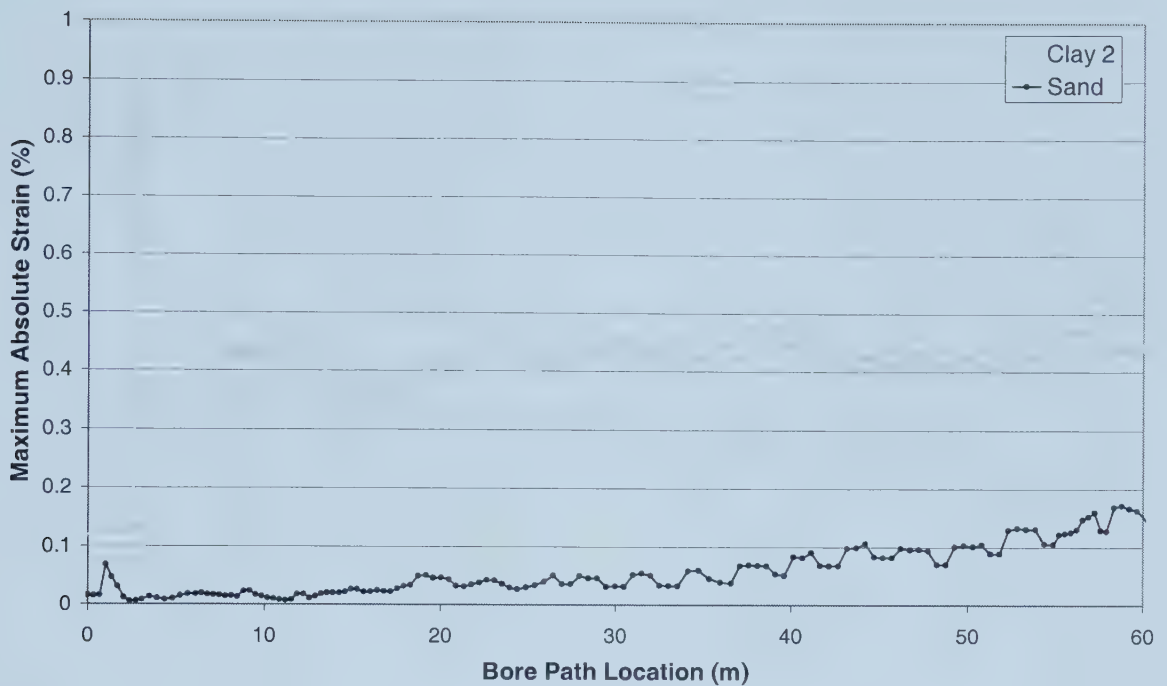


Figure 6.6: Maximum Recorded Strain During Pullback for 114 mm Pipes

6.3 219 mm DIAMETER PIPE - SOIL MEDIUM COMPARISON

6.3.1 Drilling Fluid Pressure

The drilling rig fluid pressures that were experienced during the 219 mm pipe installations are shown in Figure 6.7. Two of the installations follow the same decreasing trend exhibited for the 114 mm pipes while the second installation in clay follows an entirely different profile. Instead of having the drilling pressure decrease over the length of the installation, it was steadily increasing. The first installation in the clay soil medium and the installation in the sand soil medium display very similar trends until the 50 m point in the installation. At the 50 m point of the installation, the pipe installed in the clay soil medium started to become more difficult to pull. Due to this, the drilling rig operator increased the drilling fluid flow into the borehole thus effectively increasing the drilling fluid pressure. For the most part the drilling fluid pressures follow a smooth path during the installation process, although there are a number of instances where sudden peaks are exhibited in the behaviour of the fluid pressure.

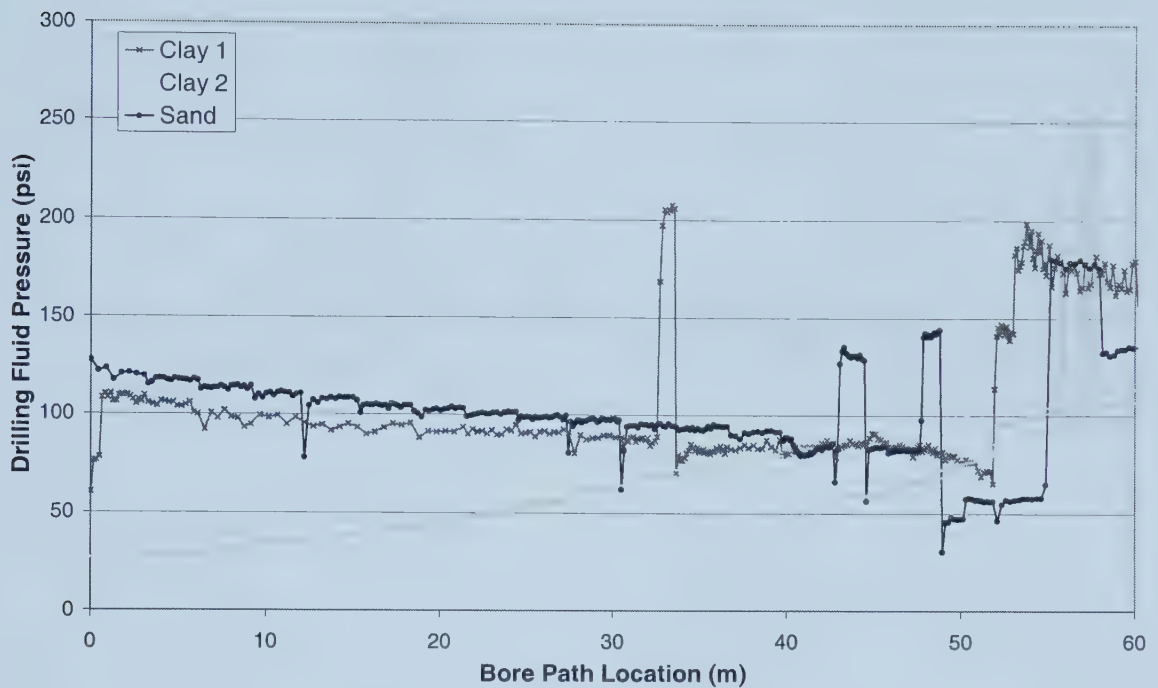


Figure 6.7: Pullback Drilling Fluid Pressures for 219 mm Pipes

6.3.2 Rotational Torque Pressure

Figure 6.8 shows the rotational pressure experienced by the drilling rig for the 219 mm pipe installations. These trends of the rotational pressures are very similar to those experienced during the 114 mm pipe installations. The rotational pressures remain fairly constant over the length of the installation. The difference between the pipes installed in the different soil mediums is small. Additionally, during the installation in the sand soil medium the rotational pressure was smaller than those installed in clay for the first half of the installation. After this point, the rotational pressures were roughly parallel. The two installations in clay have very good correlation as they follow the same profile throughout the length of the installations.

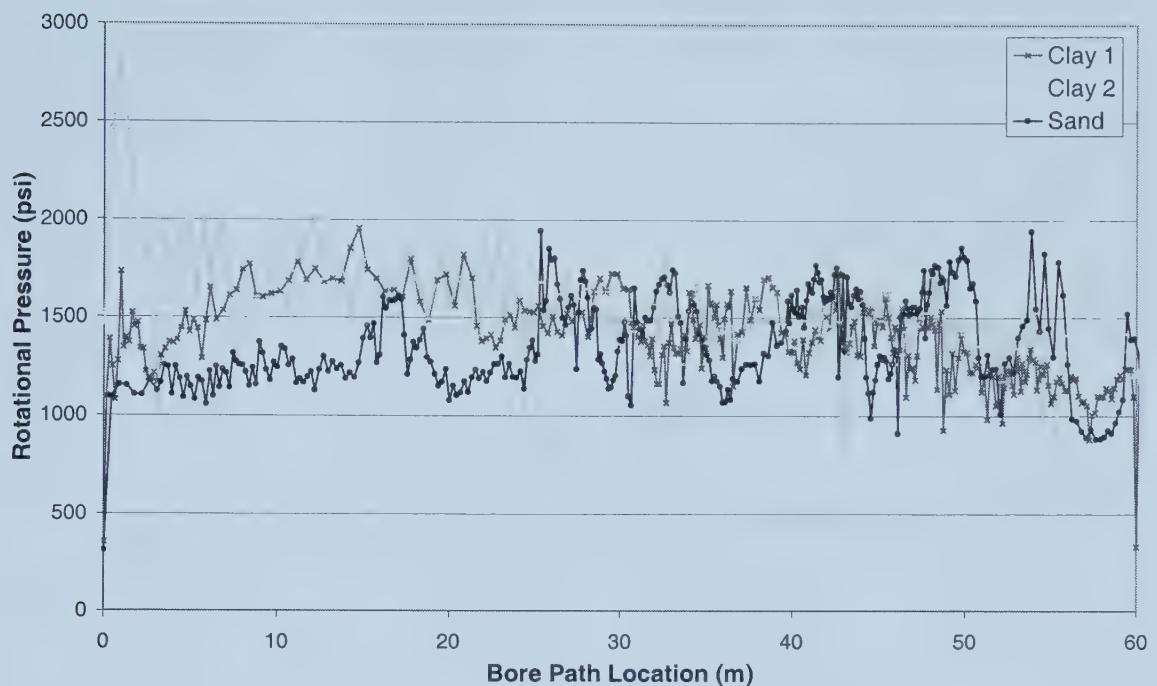


Figure 6.8: Pullback Rotational Pressures for 219 mm Pipes

6.3.3 Pullback Pressure

The pullback pressures experienced by the drilling rig for the 219 mm pipes installed in both the sand and the clay soil mediums are shown in Figure 6.9. Both the installations in clay and the installation in sand display an increasing pullback pressure over the length of the installation. The pullback pressures for the sand pipe followed a very linear trend throughout the length of the installation reaching a maximum of 700 psi. The two installations in clay required much more drilling rig effort than the pipe installed in the sand soil medium. The pressures for these two installations increased with two distinct trends during the pullback. The first trend was evident between the initial entry of the pipe into the borehole to the 30 m point in the installation where the pressure ranged from 500 psi to 750 psi. The slope of this trend appears to follow a linear pattern. Following the 30 m point, the incremental pullback pressure increased, thus impacting the slope of the trend, and the resulting pressure ranged from 750 psi to 2500 psi.

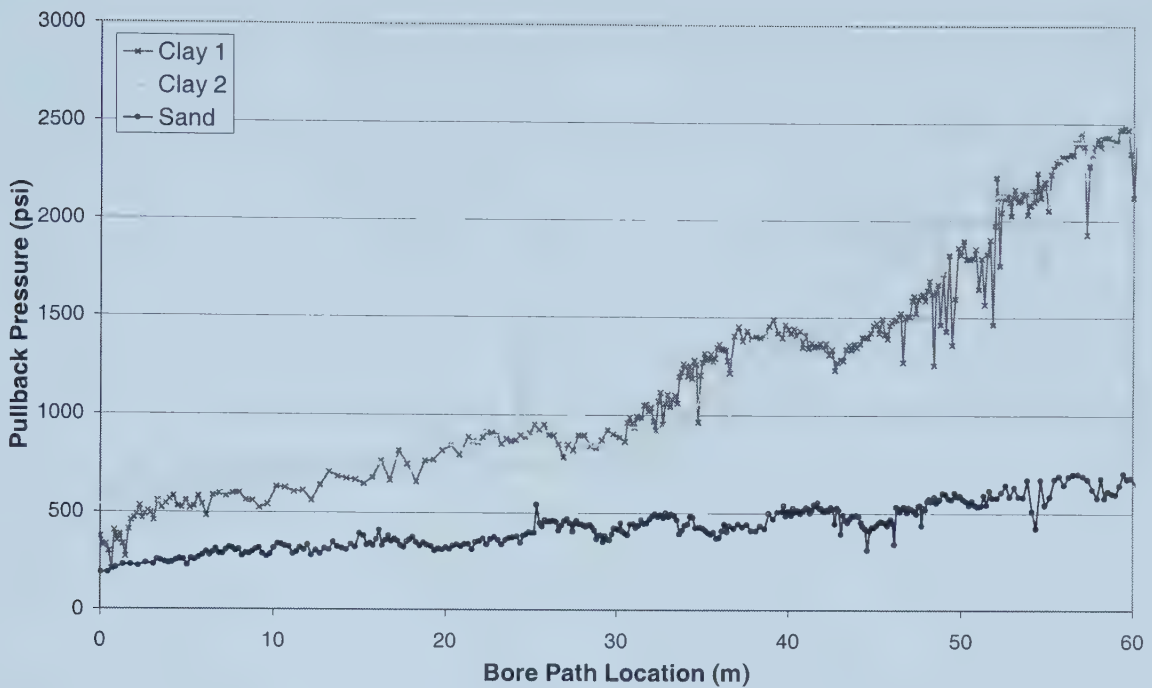


Figure 6.9: Pullback Pressure for 219 mm Pipes

These high pullback pressures for the clay over the sand soil medium can be attributed to a number of factors. The main factor is that clay is a cohesive soil medium and can swell with the application of water. The overall magnitude of this swelling can be mitigated through the use of a properly designed drilling fluid. However, the drilling fluid cannot be guaranteed to prevent the swelling entirely. This swelling process will cause the annular space to become contracted on the pipe and will increase the viscosity of the drilling fluid. During the post-construction evaluation, the first installations in the clay soil medium were excavated at periods of twenty-four hours, one week, two weeks, and four weeks. The drilling fluid in the 219 mm annular space was thicker and stickier than that for the 114 mm and the 324 mm installations, suggesting that swelling had occurred and that the properties of the drilling fluid had changed.

6.3.4 Load Cell

Figure 6.10 contains the load cell readings during the pullback phase for the 219 mm pipes installed in the sand and clay soil mediums. The results from the load cell for these two installations look very similar to the trends of the pullback pressure shown in Figure

6.9. First, the loading is increasing on both pipes in the different soil mediums over the length of the installation. The pipe installed in the sand soil medium exhibited a linear progression of loading throughout the length of the installation with a maximum load of 20 kN. The pullback pressures from Figure 6.9 also exhibited this linear trend. The loading on the pipe in the clay soil medium was larger than the pipe in the sand soil medium. The pipe in the clay soil medium displayed two trends similar to the pullback pressure. The first trend was from the beginning of the installation to the 30 m point where the load reached approximately 20 kN. Following the 30 m point the slope of the trend increased and the load reached a maximum of 70 kN.

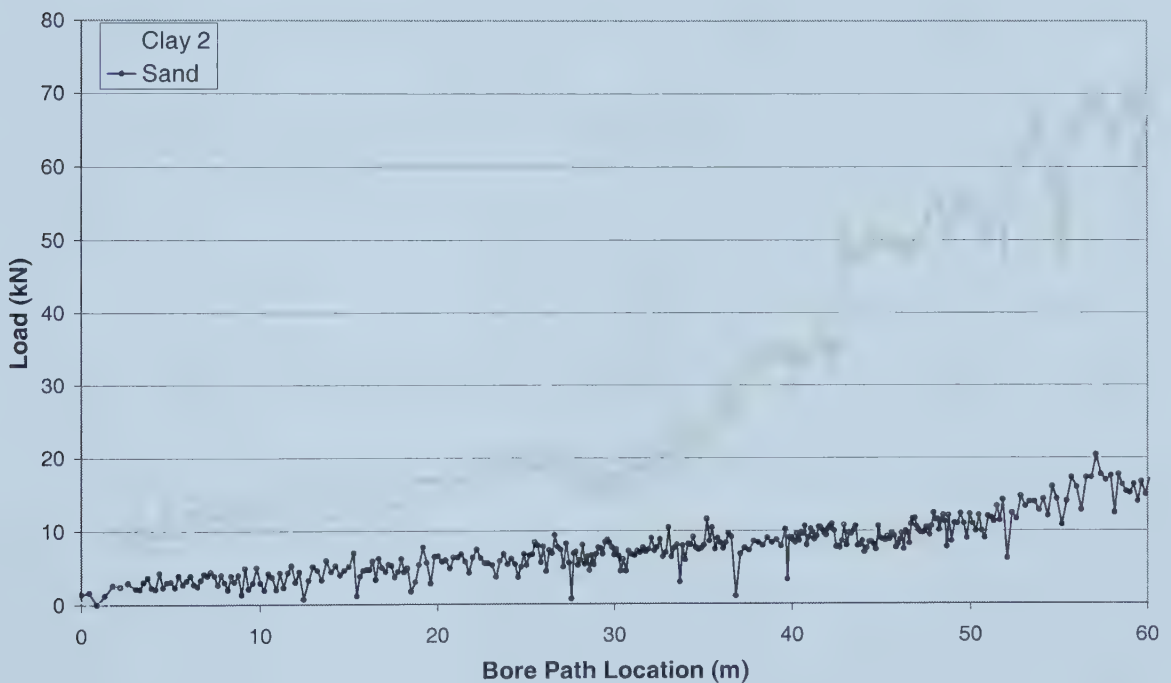


Figure 6.10: Load Cell Comparisons for 219 mm Pipes

6.3.5 Strain Results

The average strain results from the three 219 mm pipe installations are shown in Figure 6.11. All of the strain results show an increasing strain from the beginning of the pullback phase to the exit pit location. The average strain for the sand soil medium reaches a maximum of 0.18% near the end of the installation. In comparison, the clay soil medium installations experience a greater magnitude of strain. The first installation in the clay soil

medium reached a maximum strain of 0.8% while the second installation reached a maximum of 1.2%.

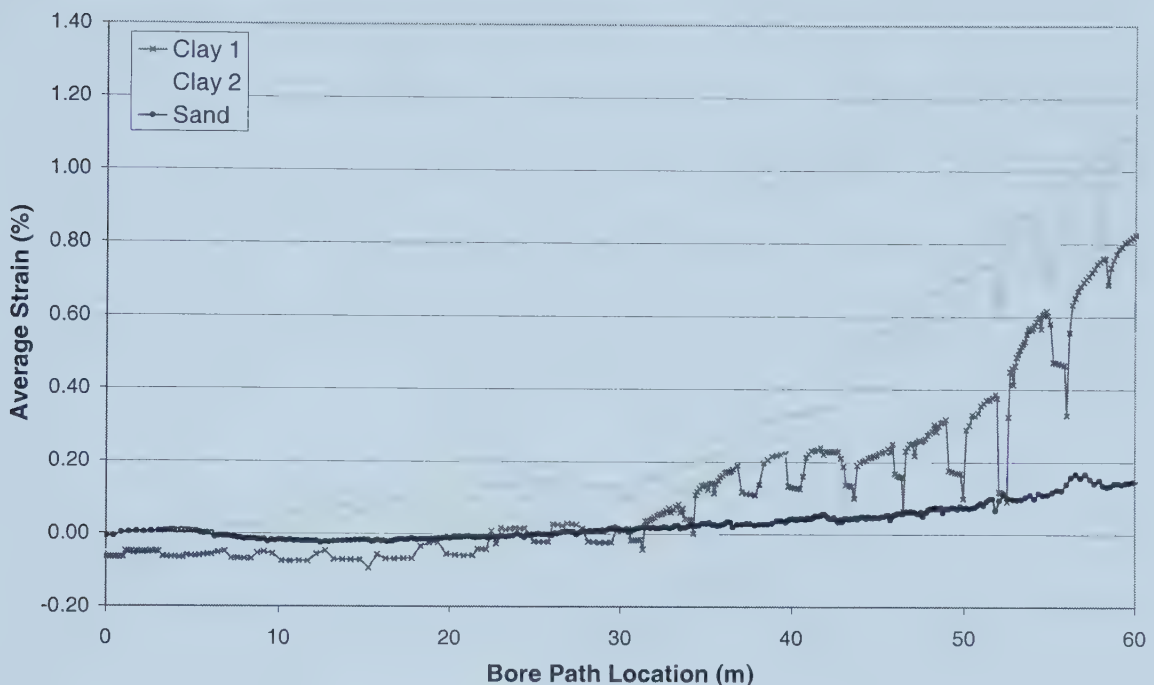


Figure 6.11: Average Strain During Pullback for 219 mm Pipes

From Figure 6.11, several drops can be observed in the strain amounts during the duration of the installation. These drops are from the conversion of the time based system to the bore path based system. These drops are an indication of when the drilling rig was performing rod-loading operations. The drop in strain is not representative of the strain effects while pulling but do show the ability of the HDPE pipe to recover from an applied loading. The viscoelastic nature of HDPE allows it to recover very quickly when a load is removed.

Figure 6.12 contains the maximum recorded strain experienced by the 219 mm pipe during the pullback phase of the HDD process. The maximum strain for each of the installed pipelines follows the same trend as experienced for the average strain. During the pullback process, the strains are increasing as the length of the pipe in the ground increases. The pipes installed in the clay soil medium experience higher strains than for

the pipe installed in the sand soil medium. The clay soil medium test 1 and test 2 experienced maximum strains of 0.9% and 1.3%, respectively. The sand soil medium experienced a maximum strain of approximately 0.2%.

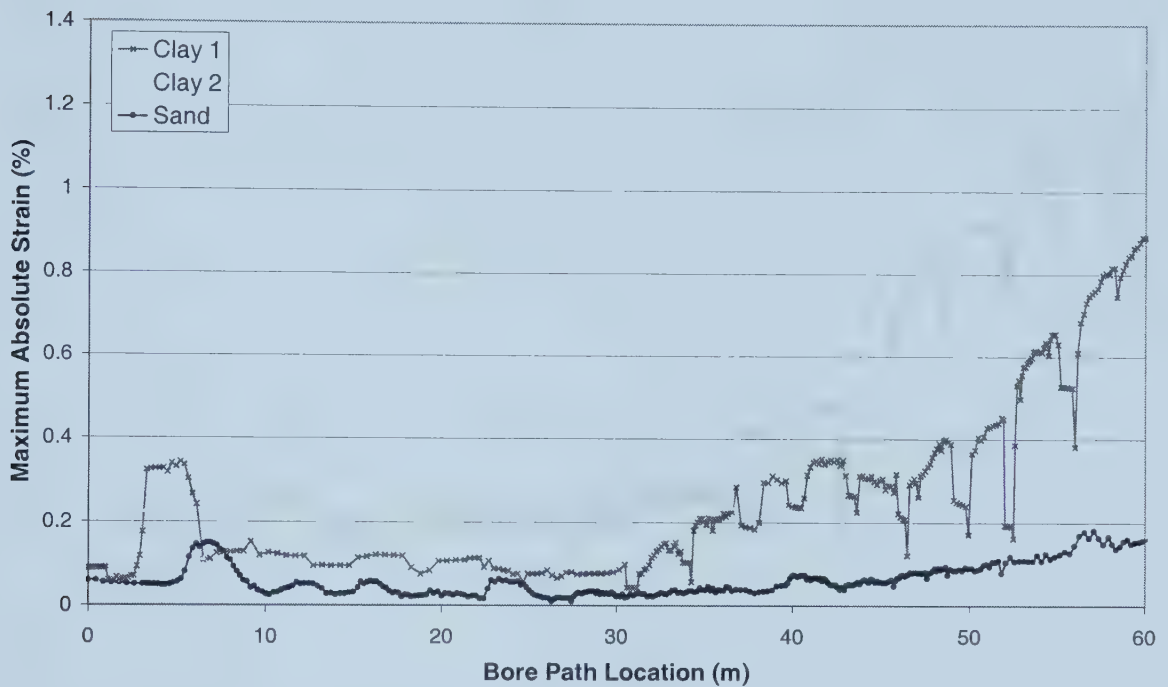


Figure 6.12: Maximum Recorded Strain During Pullback for 219 mm Pipes

6.4 324 mm DIAMETER PIPE - SOIL MEDIUM COMPARISON

6.4.1 Drilling Fluid Pressure

The drilling fluid pressure for the pre-reaming operation of the 324 mm pipe installed in the sand soil medium is shown in Figure 6.13. Only the sand soil medium is shown because the drilling fluid pressures were not collected for the 324 mm pipe that was installed in the clay soil medium. Therefore no comparisons can be made across the soil mediums. However, the observations of the behaviour of the sand soil medium can be noted. Through the installation the drilling fluid pressure is tending to decrease over the length of the installation. Additionally, there are a number of jumps and dips during various locations in the bore path. The maximum observed pressure was 230 psi and this contrasts with the minimum pressure of approximately 80 psi.

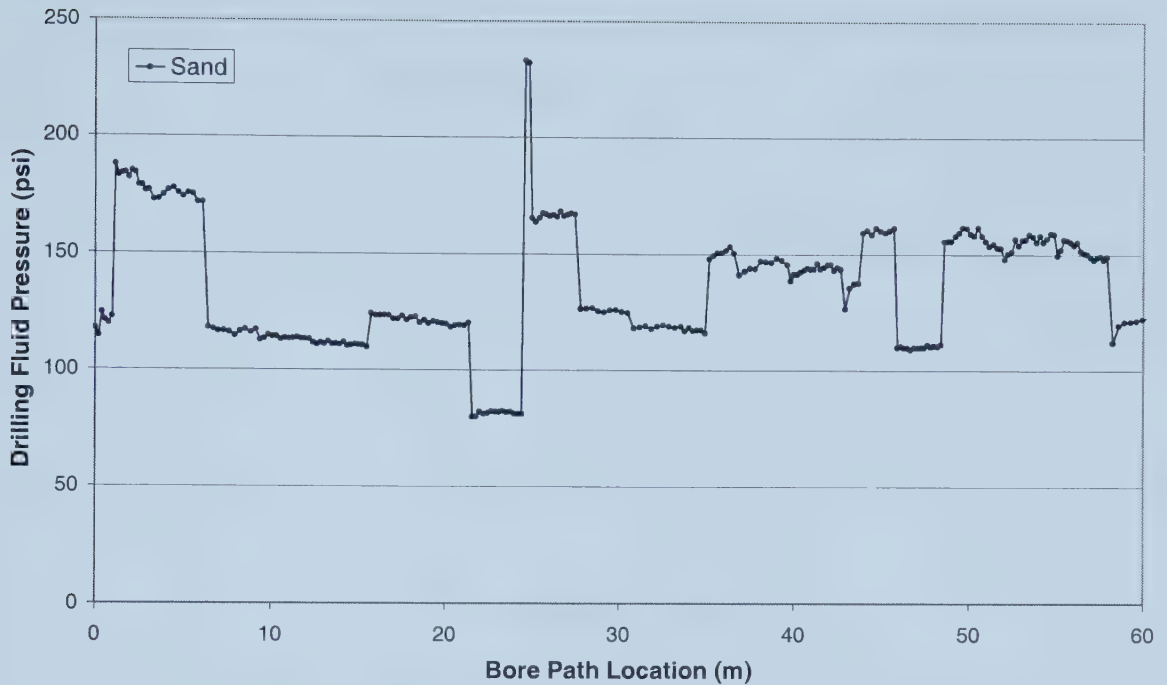


Figure 6.13: Pre-Ream Drilling Fluid Pressures for 324 mm Pipes

The drilling fluid pressures for the pullback of the 324 mm pipe installed in the sand soil medium is shown in Figure 6.14. Again, there is a decreasing trend over the length of the installation with one significant dip experienced after the middle point. The range of fluid pressures during the pullback operation was between 60 psi and 250 psi. In comparison to the pressures experienced by the pre-ream, the pullback pressures are generally larger. This can be attributed to the fact that there was a larger sized reamer for the pullback operation. Larger reamers have a greater mud flow capacity in the borehole.

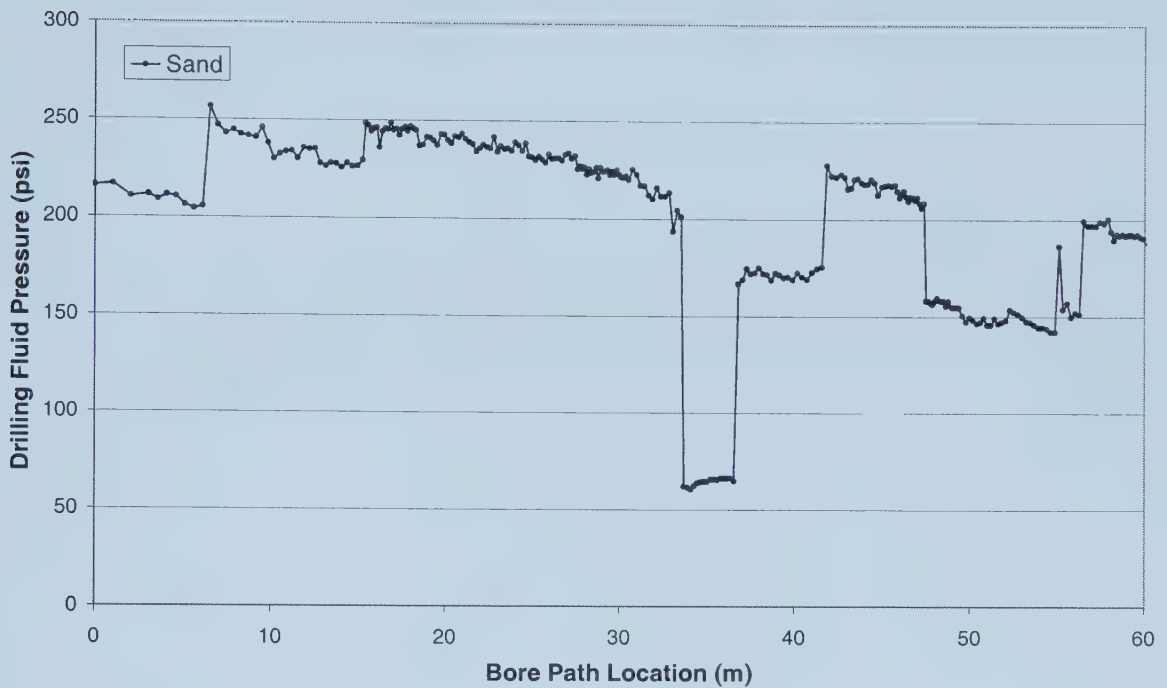


Figure 6.14: Pullback Drilling Fluid Pressures for 324 mm Pipes

6.4.2 Rotational Torque Pressure

Figure 6.15 displays the pre-ream rotational pressures experienced by the drilling rig during the pullback of the 324 mm pipes in the sand and clay soil mediums. Comparing the magnitude of the soil mediums, we can see that the magnitudes are very similar. The clay soil medium ranges from 1000 to 2000 psi and the sand soil medium ranges from 500 psi to above 3000 psi. The rotational pressure for the clay soil medium tends to stay relatively even over the length of the installation showing some decline near the latter stages. The rotational pressures for the sand show an increasing trend over most of the installation with a large drop over the last 10 m. Basically, the rotational pressures follow the same pattern except for the discrepancy near the 50 m point of the installation.

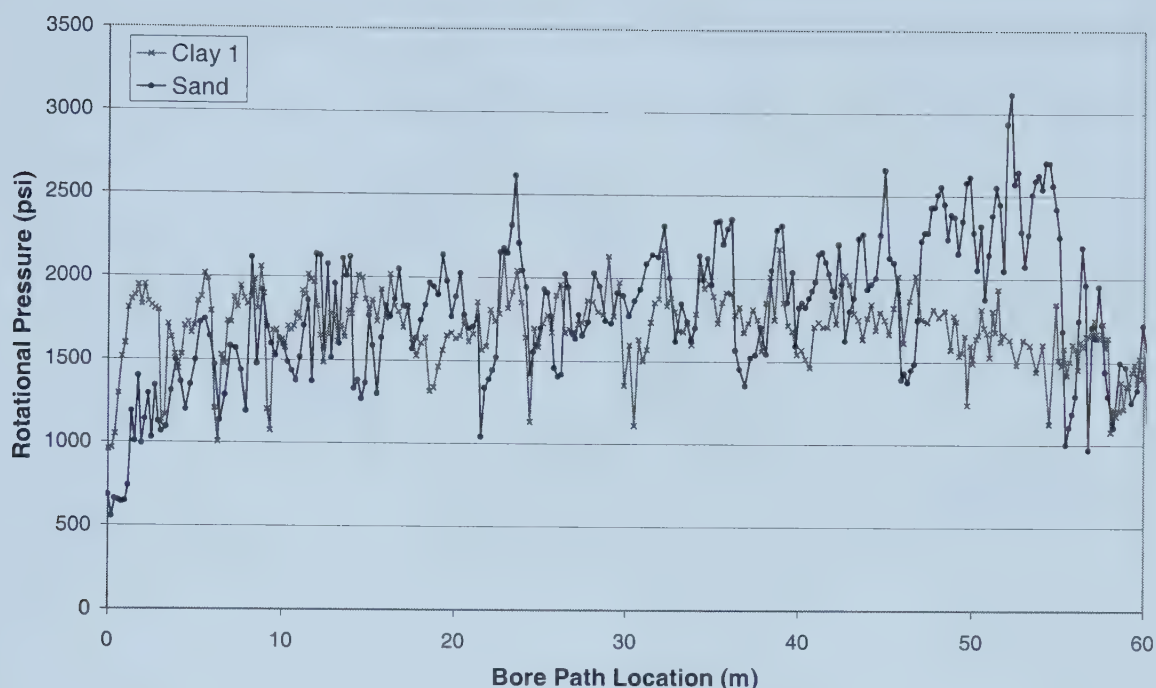


Figure 6.15: Pre-Ream Rotational Pressures for 324 mm Pipes

The rotational pressures experienced during the pullback operation for the 324 mm pipes are displayed in Figure 6.16. The rotational pressures during the pullback exhibit different responses than those experienced during the pre-ream operation. The magnitudes of the pressures are larger than those experienced during the pre-ream. This is to be expected as there was a larger sized reamer utilized during the pullback than the pre-ream in comparing the effects of the different soil mediums, there are a number of observations that we can note. For the clay soil medium the rotational pressures remain fairly constant along the length of the installation, fluctuating from 1000 psi to 3300 psi. Additionally, the rotational pressures for the clay soil medium are larger than those for the sand soil medium, which range from 750 to 2000 psi. Also for the sand soil medium, the rotational pressures were decreasing as more product line entered the borehole. This is in contrast to the pre-ream pressures where the rotational pressures were increasing to the end of the installation.

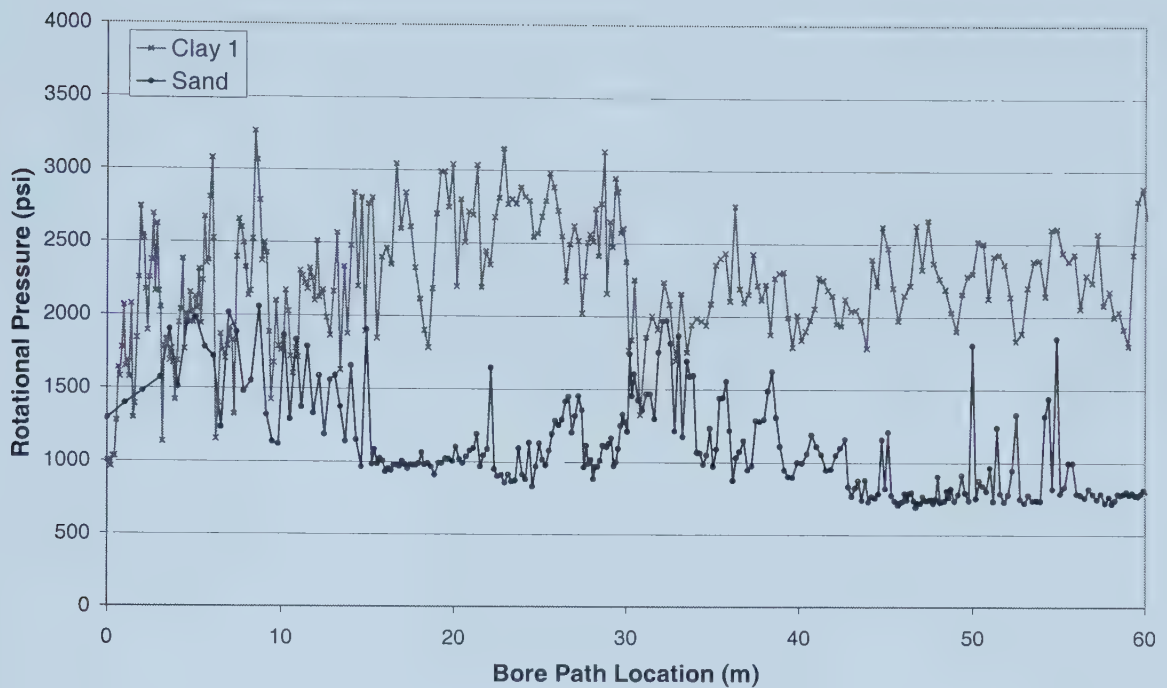


Figure 6.16: Pullback Rotational Pressures for 324 mm Pipes

6.4.3 Pullback Pressure

Figure 6.17 illustrates the pullback pressure experienced during the pre-ream operation for the 324 mm pipes installed in the sand and clay soil mediums. The magnitudes of the pullback pressures are relatively similar for the clay and sand installations. The pullback pressures for the pre-ream in clay display a horizontal trend across the range of the installation with a range of pressure from 300 psi to 650 psi. The sand soil medium displays a slight increasing trend over the length of the installation similar to the rotational pressure for the pre-ream. The range of pressures for the pre-ream pullback pressure in sand was 150 to 750 psi.

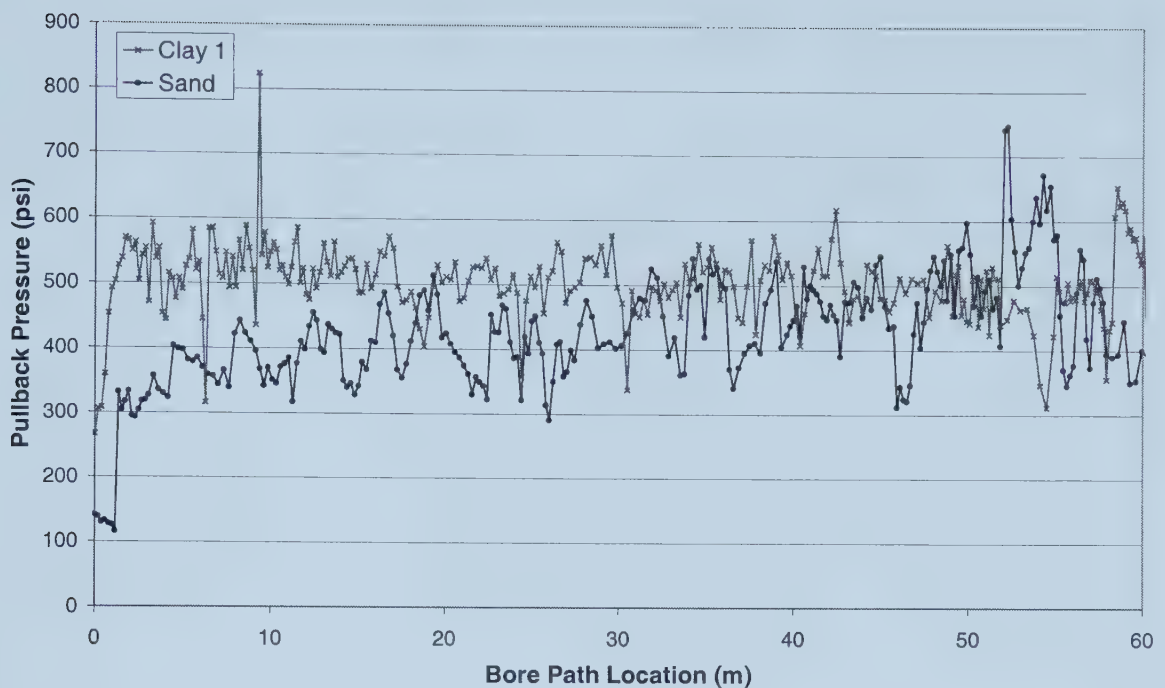


Figure 6.17: Pre-Ream Pullback Pressures for 324 mm Pipes

Figure 6.18 contains the pullback pressures experienced during the pullback stage of the 324 mm pipes. Both of the soil mediums display an increasing pullback pressure over the length of the installation. Comparing the two soil mediums it can be seen that the magnitude of the pressures for the clay soil medium is larger than those for the sand soil medium. However, the slope at the end of the sand soil medium is larger than that for the clay. The range of pressures experienced for the sand installation were 200 psi at the onset of the installation increasing to a maximum of 950 psi at the end of the installation. The pressures for the clay soil medium ranged from 400 to 950 psi.

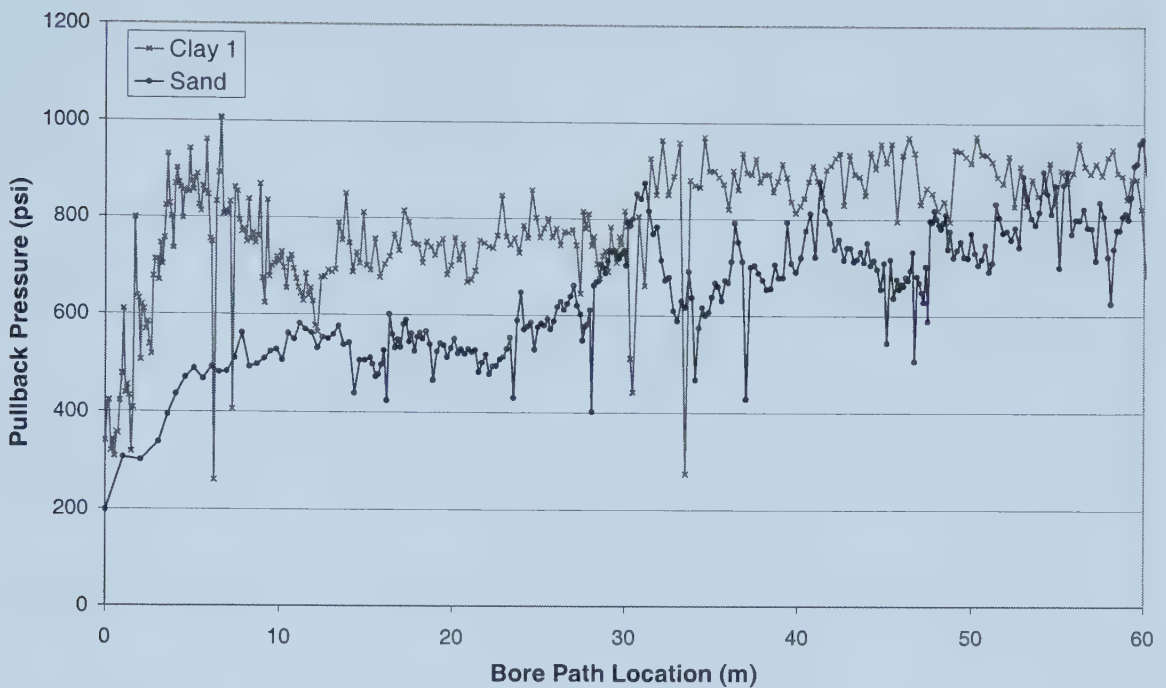


Figure 6.18: Pullback Pressures for 324 mm Pipes

6.4.4 Load Cell

Figure 6.19 gives the load cell results for the 324 mm pipe installed in the sand soil medium. No comparisons can be made with the load cell information, as the load cell was not available for the clay installation. Therefore, the analysis will only focus on the behaviour of the loading on the HDPE pipe installed in the sand soil medium. Throughout the length of the installation the load steadily increased in a linear fashion. The maximum loading on the load cell occurred at the end of the installation and was approximately 25 kN.

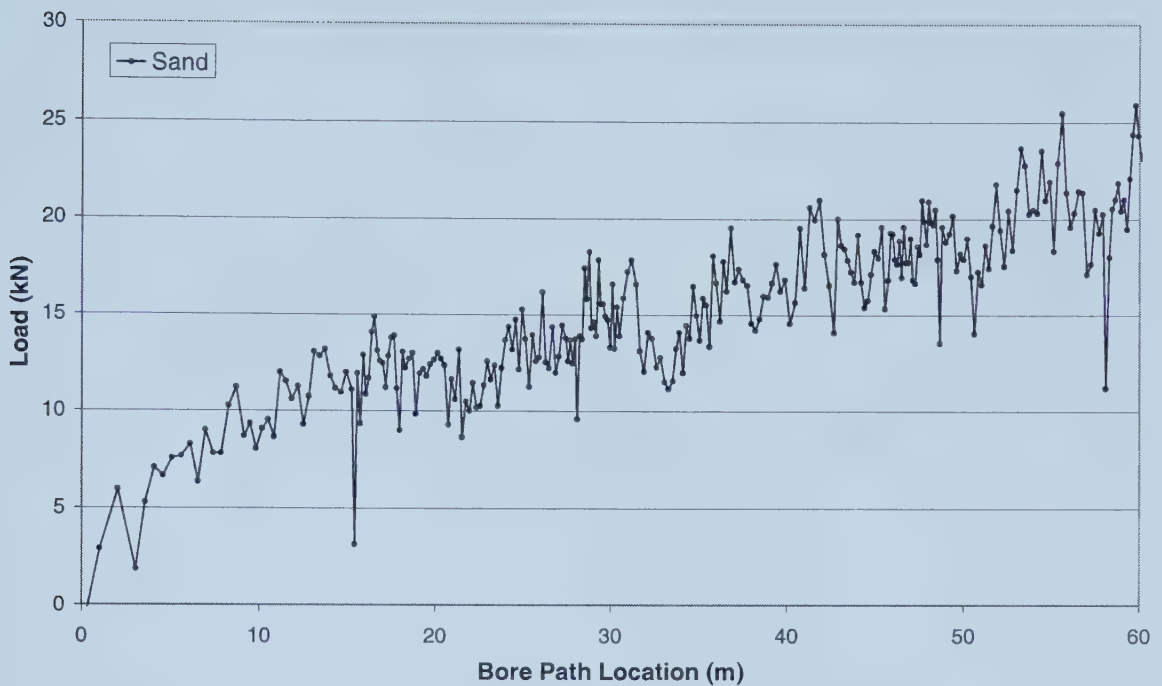


Figure 6.19: Load Cell Comparisons for 324 mm Pipes

6.4.5 Strain Results

The average strain results during the pullback phase of the 324 mm HDPE pipes in the sand and clay soil mediums is shown in Figure 6.20. Before further analysis is performed on the results, it must be noted that the magnitude of the y-axis ranges from 0.06% to – 0.06%. Therefore, the average strain experienced by both of these installations was very small and can be assumed to be negligible over the duration of the installation. The data for both the sand and the clay soil medium does not follow any expected pattern as experienced by the smaller diameter pipelines.

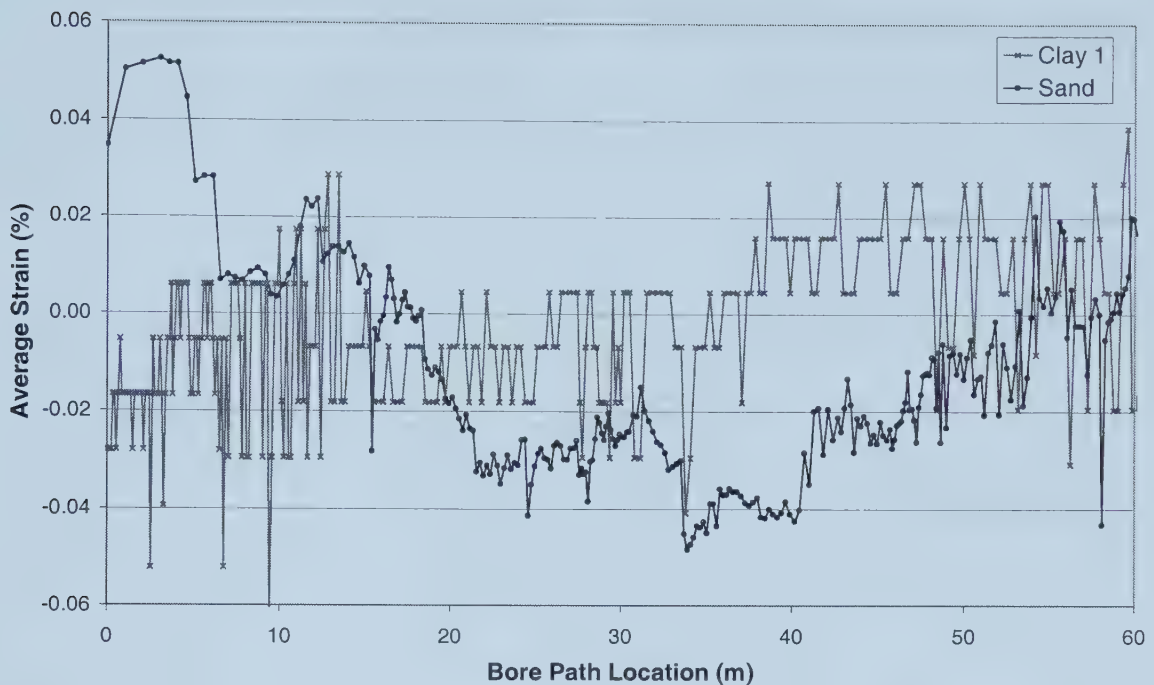


Figure 6.20: Average Strain During Pullback for 324 mm Pipes

The maximum recorded strain on the 324 mm HDPE pipes installed in the sand and clay soil mediums is shown in Figure 6.21. In contrast to the average recorded strain, the maximum strain has some definitive results. There is a definite strain response in the pipe associated with the initial bending portion of the installation. This bending strain is experienced by both of the installations, but there is a greater magnitude of strain in the pipe that was installed in the clay soil medium. In the clay soil medium, the strain in the installed pipe reached a maximum value of approximately 0.4% during this initial bending portion. In the sand soil medium, the maximum value of strain observed was only 0.2%. However, the difference between these strains has more to do with the geometry of the bore path rather than the difference in the soil mediums. Over the length of the installation the pipe that was installed in the sand soil medium experienced more strain than the pipe installed in the clay soil medium. The strain in the length of the installation reached a maximum of approximately 0.16% for the sand and 0.15% for the clay soil mediums.

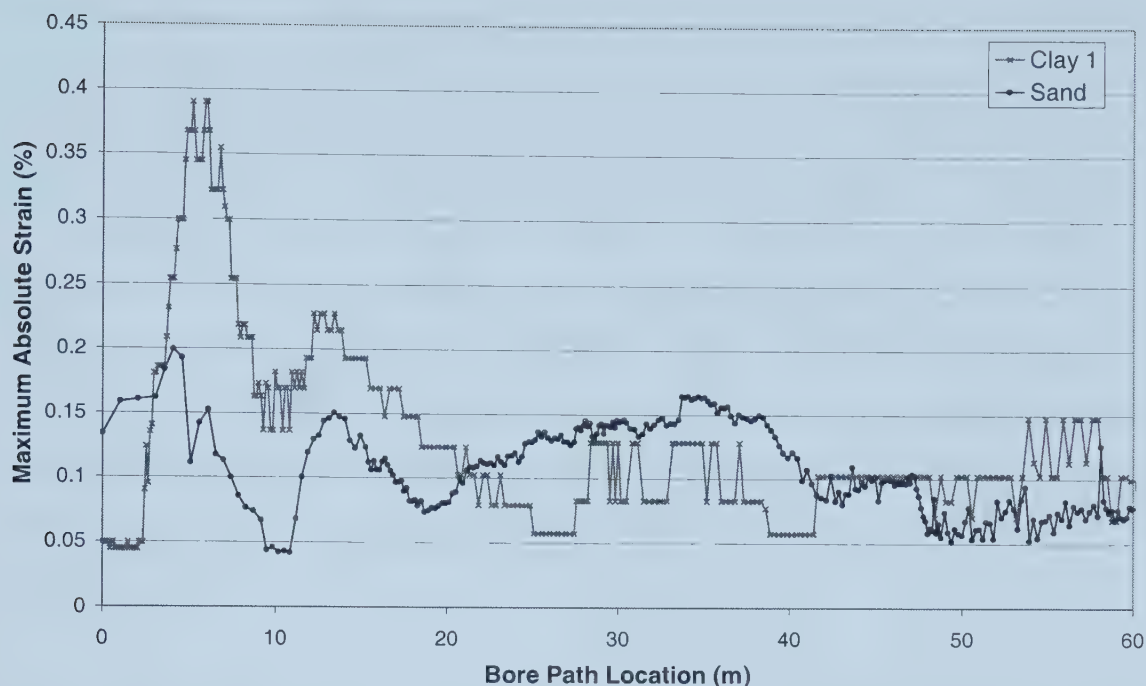


Figure 6.21: Maximum Recorded Strain During Pullback for 324 mm Pipes

6.5 DISCUSSION OF SOIL MEDIUM COMPARISON

Three different diameters of HDPE pipe were installed in both a cohesive and a cohesionless soil medium. The drilling rig pressure, pullback load on the HDPE pipe, and the strain experienced by the pipe are compared between these two soil mediums. A number of conclusions can be drawn about the effect of a cohesionless versus a cohesive soil medium.

A number of observations were made about the nature of the drilling fluid pressures experienced during the field testing. The first observation is that the drilling fluid pressures tend to decrease over the length of the installation. This trend was exhibited in all but one of the eight pipeline installations. The reason for this decreasing drilling pressure is inherent in the pullback process. The drilling fluid is pumped down inside the drilling rods and through the reamer during the pullback phase. During this phase, the number and subsequent length of the drilling rods are decreasing as more pipe is installed in the ground. Therefore, the drilling rig does not have to work as hard to maintain the constant drilling fluid flow over the decreasing rod length. The second observation is that

the cohesionless soil medium experienced larger drilling fluid pressures over the length of the installation withstanding any special conditions such as when the 219 mm clay installation became stuck. The magnitudes of these pressures are mainly influenced by the drilling rig operator in determining the quantity of flow required in a given situation. In a cohesionless soil medium, pullback installations require more drilling fluid as the soil medium is more readily washed away during the reaming action. Therefore more drilling fluid volume is required to replace the soil in the annular space and subsequently the drilling rig operator will compensate by providing more flow in these mediums, as experienced during these installations. The final observation is that there can be large fluctuations in the drilling fluid pressure over the observed installations in both soil mediums.

Several conclusions can be made about the response of the drilling rig rotational pressures for the installations in the two soil mediums. Firstly, the trend of the rotational pressure during installations in both the cohesionless and cohesive soil mediums tended to be horizontal across the length of the installation. That is, there were no distinct increasing or decreasing trends evident during the installation process. This can mainly be attributed to the fact that the soil mediums were very uniform along the entire length of the installation. Through this uniformity the reamer would experience the same soil condition along the length of the bore path and no drastic changes in rotational pressure would occur. Secondly, the differences in rotational pressures observed for the installations between the two soil mediums are very small. Basically, the drilling rig was required to exert a similar amount of effort to install the HDPE product pipeline in both soil mediums. Finally, there is excellent correlation between the similar 114 mm and 219 mm pipe installations in the clay soil medium. The rotational pressures for these installations had similar magnitudes and displayed the same trends over the length of the installation.

The pullback pressures experienced by the drilling rig during the pullback phase of the drilling operation were compared between the two soil mediums. Through this comparison a number of conclusions can be drawn about the effect of the soil medium on

the pullback pressure. The first conclusion is about the response of the pullback pressure on the drilling rig regardless of the installation medium. It was shown that the pullback pressure increases as more installed pipe enters the borehole. This was true for both the cohesive and the cohesionless soil medium. This implies that the frictional effects on the pipeline provided by the soil medium are consistent along the bore path and that any additional pipe will require additional effort to advance it further. The comparison of the pullback pressures between the two soil mediums indicated that the pullback pressures for the cohesive soil medium were larger than for the cohesionless soil medium. These higher pullback pressures are related to the ratio of soil that is displaced by the reamer, versus the soil that is cut away and the frictional effects provided by the soil medium. In a cohesive soil medium the reamer will tend to displace more soil than a cohesionless soil medium. Therefore, the pullback force will be greater for the cohesive soil medium as experienced in these field installations.

The pullback load experienced on the HDPE product pipe recorded by the load cell followed the trends experienced by the drilling rig pullback pressure for the comparison between the two soil mediums. Over the length of the installation, the pullback pressure is increasing for both soil mediums as more pipe enters the borehole during the pullback process. Secondly, the load experienced by the HDPE pipes installed in the cohesive soil medium is much larger than that for pipes installed in the cohesionless soil medium. The resulting difference in the applied load on the HDPE pipe is comprised of the swelling nature of clay soil, the frictional effects of the soil medium, and the ability of a cohesionless soil to be eroded during the pullback process. The impact of the swelling of the clay was identified earlier. The ability of a cohesionless soil medium to be eroded during the pullback phase will affect the frictional effects of the soil medium. The erosion happens as the pipe rubs the borehole wall during the pullback phase. When this occurs, the friction applied on the product pipe by the soil medium is reduced through the erosion process.

The comparisons of the resulting strain on the HDPE product pipes installed provide some conclusions on the differences between the cohesive and cohesionless soil

mediums. Initially, the maximum pipe strains experienced by all the pipe diameters in the different soil mediums did not reach the 5% industry suggested strain limit. The closest strain result came from the 219 mm installation in the clay soil medium at a maximum value of 1.3%. But, for longer installations, the strain could surpass the 5% value as the 114 and 219 mm diameter pipes had increasing strain profiles that would probably continue to increase as the bore path length increases. In regards to the differences between the two soil mediums, the 114 and the 219 mm pipe diameters installed in the cohesive soil medium experienced larger strains than those installed in the cohesionless soil medium. This is an extension of the larger load experienced by the pipeline in the cohesive soil medium. But, for the 324 mm pipes, the axial strain effects were relatively negligible in both of the soil mediums. This can be attributed to the fact that the diameter size of the reamer (1.5 times that of the pipe) creates a larger annular space around the product line. In relation to the 114 mm pipe and the 219 mm pipe, the 324 mm pipe is being pulled through a 450 mm borehole thus leaving 63 mm of space between the outside edge of the pipe and the borehole wall (assuming that the pipe is centered in the borehole) while the 114 and 219 mm pipes have 16 mm and 41 mm of space, respectively. Subsequently, the maximum strains experienced by these pipes were due to the curvature of the bore path and the resulting bending stresses that were placed on the pipe during the negotiation of these curves. These curvatures cause instantaneous increases in the strain but are subsequently released following the successful navigation of any local curvature.

6.6 CLAY SOIL MEDIUM - DIAMETER OF PIPE COMPARISON

This section will examine the effects that different pipe diameters have on the drilling rig fluid pressure, drilling rig rotational pressure, drilling rig pullback pressure, load on the product line being installed, and the average and maximum strain experienced by the HDPE product pipe in the cohesive soil medium.

6.6.1 *Drilling Fluid Pressure*

Figure 6.22 contains the drilling fluid pressures recorded during the pullback phase of the HDD operation. Only two of the five installations are shown on this graph for a number

of reasons. The second installation of the 114 mm pipe had an error with the data collection unit and therefore the drilling fluid pressure data was not correct. The second installation of the 219 mm pipe was not shown, as the trend it followed did not correlate with the other installations. The 324 mm pipe was not added as the drilling fluid data was not recorded during the installation. From this figure it can be seen that the drilling fluid pressure for the 219 mm diameter pipe was larger than that experienced by the 114 mm diameter pipe.

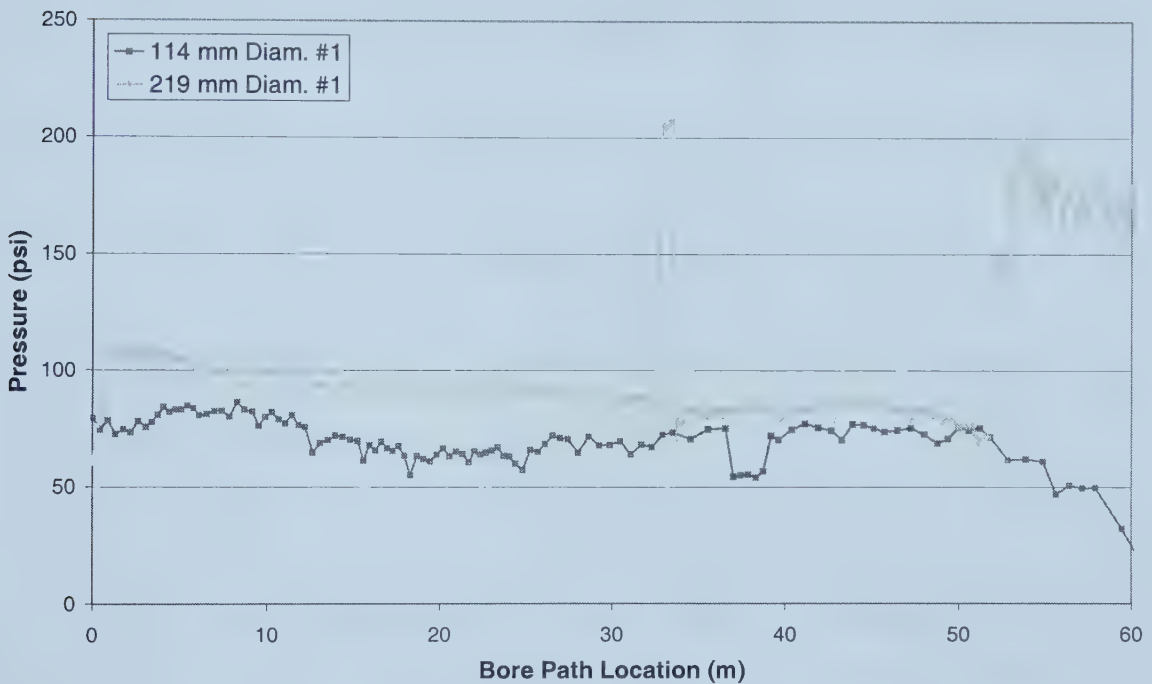


Figure 6.22: Drilling Fluid Pressure by Diameter for the Clay Installations

6.6.2 Rotational Pressure

The rotational pressures experienced by the drilling rig for the installations in the clay soil medium are shown in Figure 6.23. The magnitude of the rotational pressures is tending to increase along with the increasing pipe diameters. The rotational pressure for the 114 mm pipes is around 1250 psi, the rotational pressure for the 219 mm pipes fluctuates around 1250 to 1750 psi, and the rotational pressure for the 324 mm pipe ranges from 2000 to 3000 psi. Additionally, the fluctuations in the rotational pressure are larger for the larger diameter pipelines installed in the clay soil medium.

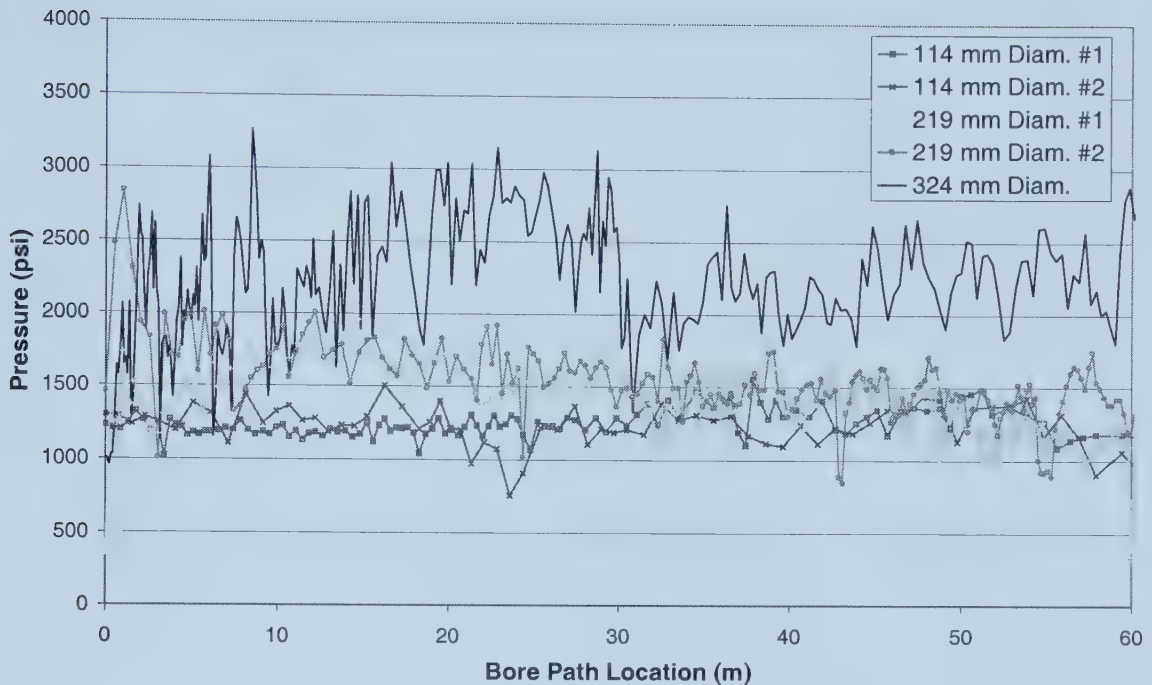


Figure 6.23: Rotational Pressure by Diameter for the Clay Installations

6.6.3 Pullback Pressure

Figure 6.24 illustrates the pullback pressures experienced by the drilling rig for the HDPE pipes installed in the clay soil medium. Initially, it can be seen that the pullback pressures are increasing along the entire length of the installation, as identified earlier in this chapter. However, there are some interesting characteristics displayed by the 219 mm pipelines. The pullback pressures experienced during these two installations are larger than those experienced by the 324 mm pipe. The maximum pullback pressures, neglecting localized spikes, experienced by each of the installations were 500 psi, 2500 psi, and 1000 psi for the 114, 219, and 324 mm pipes respectively. In looking at the slopes and trends of the pressure lines the pullback pressures for the 219 mm pipes again stand out. These two installations have trends that have larger slopes than the other diameters that were installed.

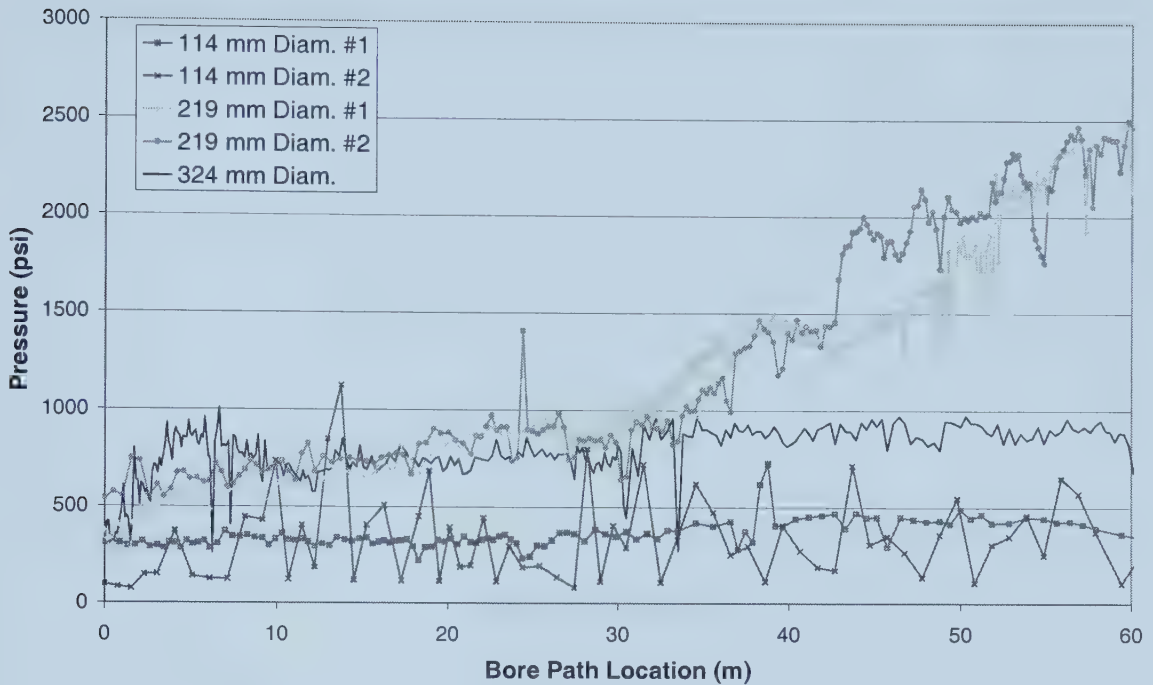


Figure 6.24: Pullback Pressure by Diameter for the Clay Installations

6.6.4 Load Cell

The load cell results for the two HDPE pipes installed in the clay soil medium are shown in Figure 6.25. There are only two sets of data, as the load cell was not fabricated for the first set of installations conducted in the clay soil medium. Unfortunately no comparison can be made for the 324 mm pipe installed in the clay soil medium. The loading on the two product pipelines follows the same trends observed for the drilling rig pullback pressures. For the 114 mm pipe the loading remained relatively horizontal similar to the nature of the pullback pressure. For the 219 mm pipe the loading on the pipe followed the same profile along the pullback phase by experiencing two distinct phases similar to the pullback pressure. In terms of the actual loading on the product pipelines, the 219 mm pipe experienced a much larger loading at 70 kN in comparison to the 5 kN maximum experienced for by the 114 mm pipe.

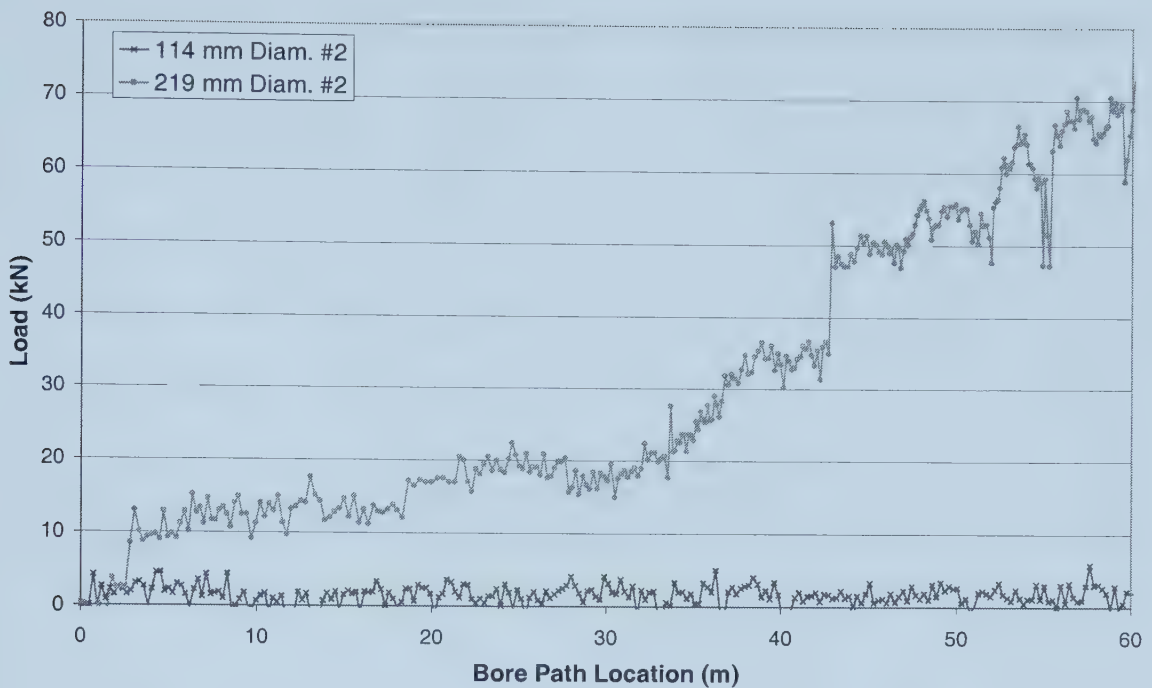


Figure 6.25: Load Cell Results by Diameter for the Clay Installations

6.6.5 Strain Results

Figure 6.26 shows the average strain results experienced by the HDPE pipes installed in the clay soil medium. The maximum average strain experienced by the HDPE pipes was 0.15%, 1.2%, and 0.05% for the 114, 219, and 324 mm diameter pipes respectively. Similar to the pullback pressures, the 219 mm installations had the largest magnitude of strain. Also, the average strains for the 219 mm pipe were increasing over the length of the installation. This suggests that longer installations may exceed the 5% strain in the 219 mm HDPE pipe. The other two pipe diameters, 114 mm and 324 mm, experienced a lower range of strain. The 114 mm pipe only reached the 0.15% range because of the mechanical deformation that was imposed on it during the initial bending curvature of the bore path. Following this deformation the average strain did not rise in any appreciable manner. The 324 mm pipe experienced negligible average strain over the length of the installation. This is due mainly to the thick walls of the 324 mm pipe and because the borehole geometry provides more flexibility for the placement of the pipe in the annular space.

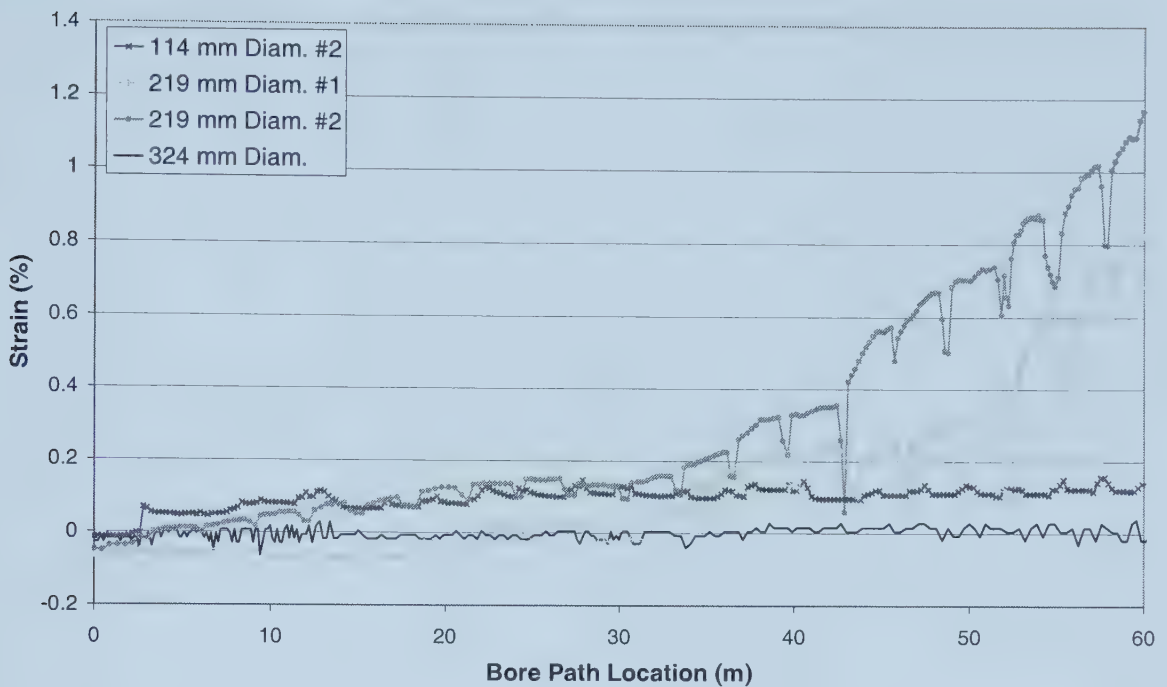


Figure 6.26: Average Strain by Diameter for the Clay Installations

The maximum absolute strain experienced by the HDPE pipes installed in the clay soil medium is shown in Figure 6.27. These maximum strain results display similar trends to those of the average strain with the exception of indicating the bending stress acting on the product line during the installation. These areas of borehole curvature are widely pronounced for all of the HDPE pipelines installed in the clay soil medium. The 219 mm pipelines experience the lowest bending strains from the curvature of the bore path but experience the largest overall strain of 1.3% and 0.9%. The 114 mm HDPE pipe experiences the largest bending strain of 0.95%, which caused permanent deformation of the product line. Finally, the 324 mm diameter pipe experienced a bending strain of 0.4%, which accounted for the maximum strain experienced during the installation. Following the bending portion, the maximum strain in the 324 mm pipe tapered to around 0.1%.

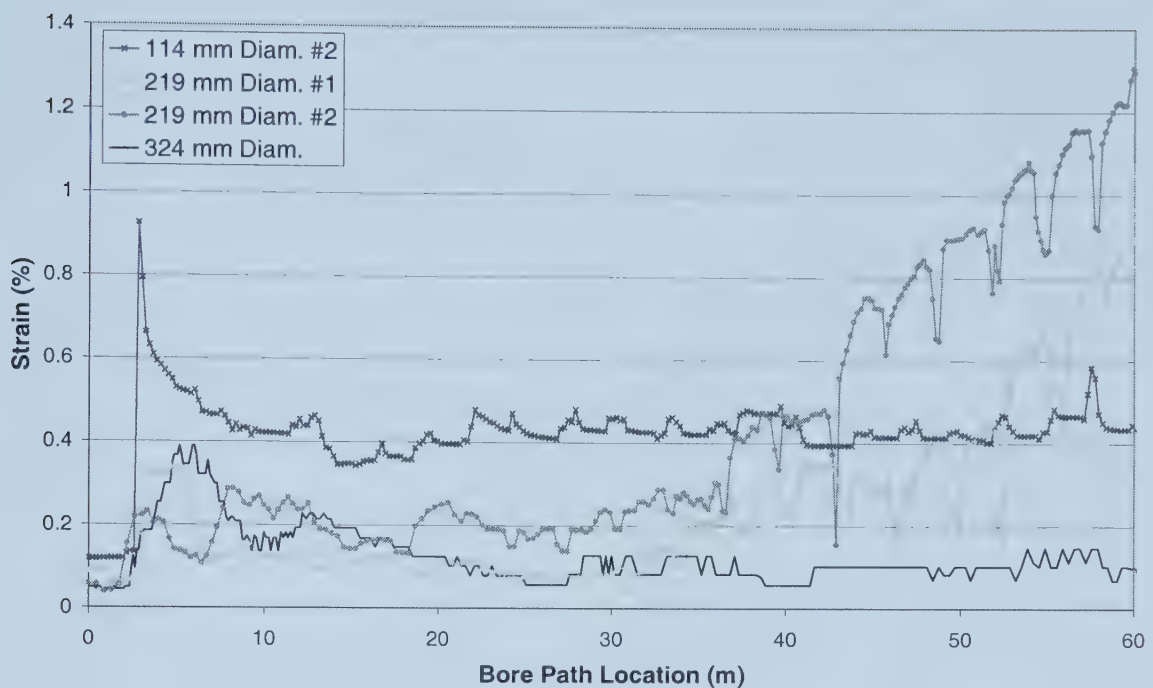


Figure 6.27: Maximum Absolute Strain by Diameter for the Clay Installations

6.7 SAND SOIL MEDIUM - DIAMETER OF PIPE COMPARISON

The following section looks at the effects that different pipe diameters have on the drilling rig fluid pressure, drilling rig rotational pressure, drilling rig pullback pressure, load on the product line being installed, and the average and maximum strain experienced by the HDPE product pipe in the cohesionless soil medium.

6.7.1 Drilling Fluid Pressure

Figure 6.28 contains the drilling fluid pressures experienced during the three installations of HDPE pipe in the cohesionless soil medium. It can be noted that the trend of the drilling fluid pressures is decreasing over the length of the installation. Additionally, there are several jumps and dips that occur in this pressure during the installation process. With respect to the pipe diameters, the drilling fluid pressure experienced during the pullback phase is larger for the 324 mm diameter pipe than for the other two installations. Drilling fluid pressure for both the 114 and the 219 mm pipes was very similar during the length of the installation.

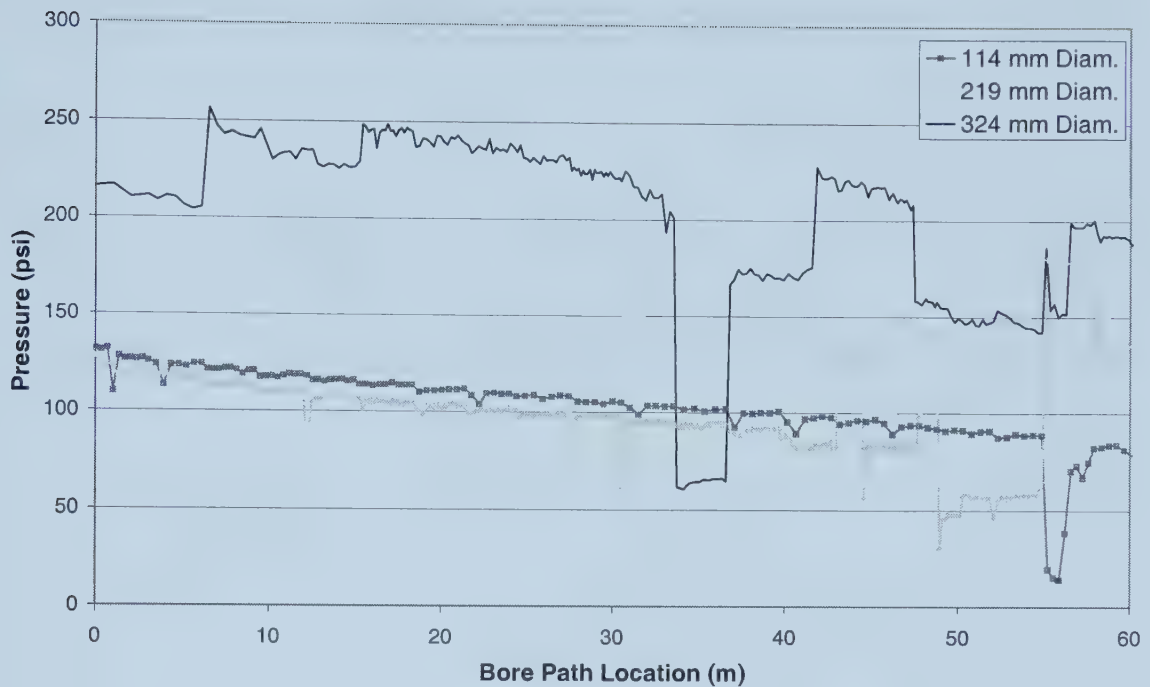


Figure 6.28: Drilling Fluid Pressure by Diameter for the Sand Installations

6.7.2 Rotational Pressure

The drilling rig rotational pressures experienced by the pressure transducers during the pullback operation are shown in Figure 6.29. Again these pressures are plotted in relation to the diameter of the product line that was installed. A number of observations can be made about the rotational pressure during the pullback stage of the directional drilling operation. Initially, it can be seen that the values of the rotational pressures for all of the diameters of HDPE pipe are relatively similar. In relation to the diameter, the fluctuations of the rotational pressure are larger for the larger diameter pipelines. For the 114 mm pipe, the rotational pressures fluctuated between 1000 and 1400 psi. The 219 mm pipe experienced larger fluctuations in the rotational pressure ranging from 1000 to 1900 psi. Finally, for the 324 mm pipe, the rotational pressure ranged from 800 to 2000 psi.

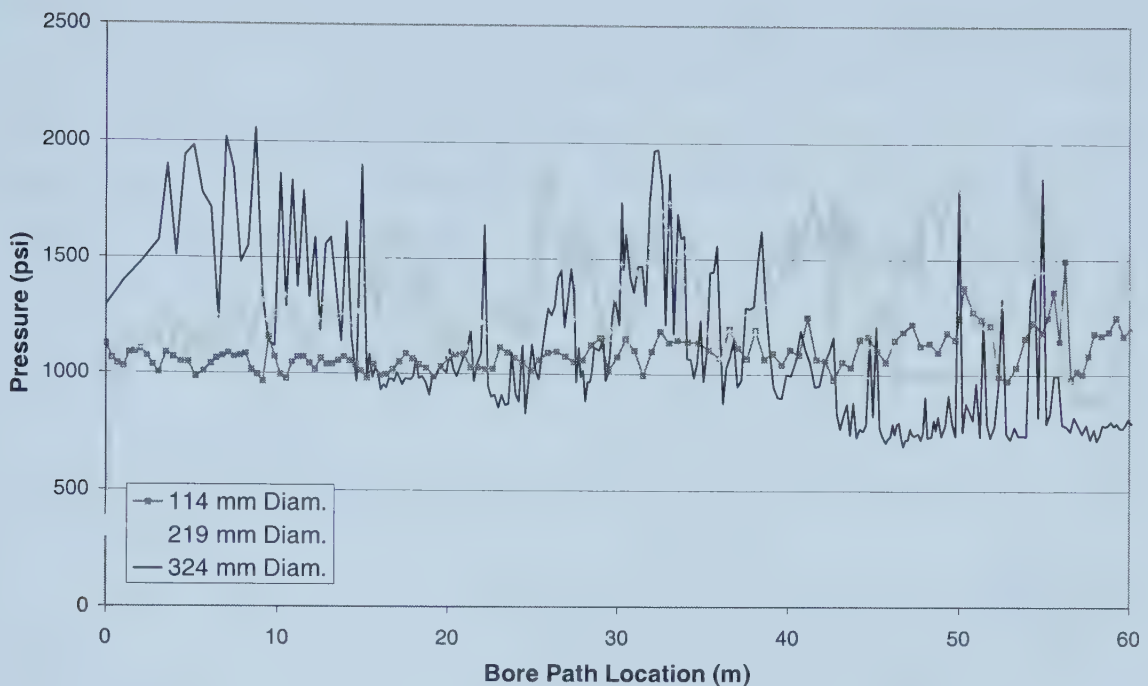


Figure 6.29: Rotational Pressure by Diameter for the Sand Installations

6.7.3 Pullback Pressure

The drilling rig pullback pressures collected by the pressure transducers are shown in Figure 6.30. The pullback pressures are plotted in relation to the diameter of the HDPE product line that was installed. From Figure 6.30, a number of observations can be made about the influence of the pullback pressure during the installation process. Foremost, it can be seen that pullback pressures are increasing as more of the product pipe has entered the bore path for each of the different diameters. This increase in pressure seems to follow a linear trend for all of the installations. The fluctuations away from the linear trend are larger for the larger diameter pipes. In relation to the diameter of the pipe, the drilling rig pressures are greater for a larger diameter pipeline, as the 114 mm, 219 mm, and 324 mm pipes increase from 200 psi at the start of the pullback to approximately 375 psi, 700 psi, and 950 psi at the end of the pullback respectively. In comparing the estimated linear slopes of the pressure lines, it can be noted that the 114 mm diameter pipe has the lowest slope. Interestingly, the 219 mm diameter pipe slope seems to be greater than the 324 mm diameter pipe. This could indicate that incrementally there are greater frictional effects imposed on the 219 mm diameter pipe in relation to the 324 mm

pipe. This can be attributed to the fact that both of the pipes utilized a 1.5 times the diameter upsize for the final ream. With a larger diameter pipe this upsize creates more distance between the pipe and the borehole wall through the larger annular space as mentioned previously. This potentially decreases the frictional forces experienced by the larger pipe during the pullback phase. Additionally, the 324 mm pipe was pre-reamed for one pass prior to the final reaming and pullback operation.

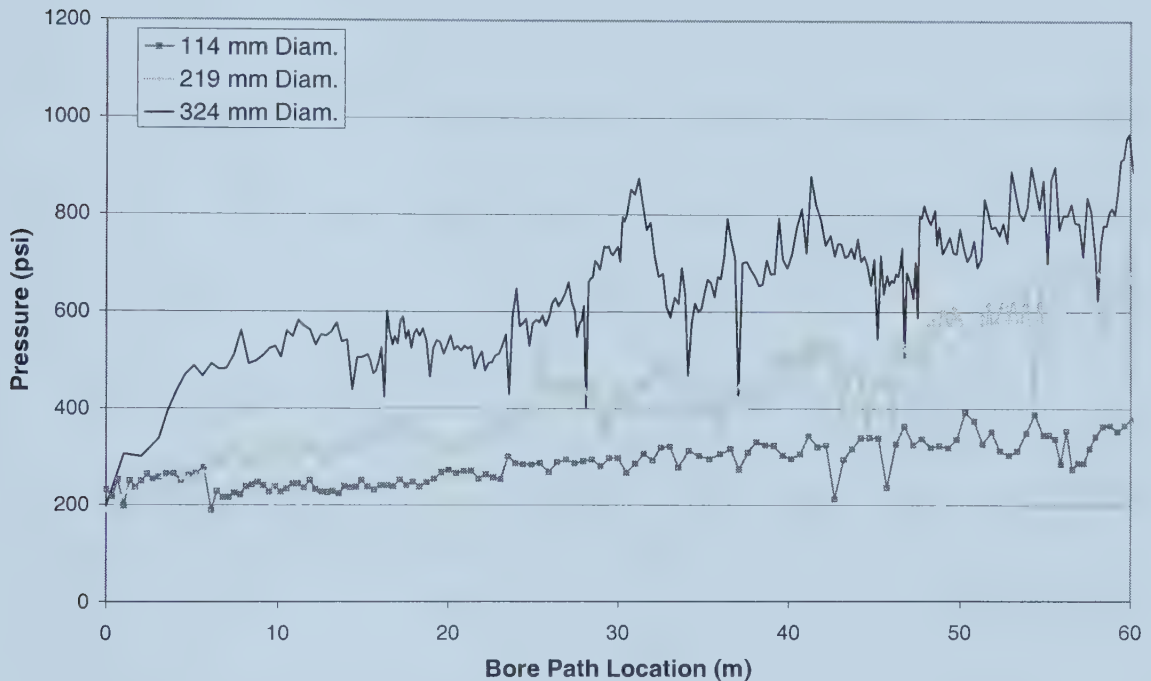


Figure 6.30: Pullback Pressure by Diameter for the Sand Installations

6.7.4 Load Cell

The loading experienced by the load cell for all the installations is shown in Figure 6.31. Akin to the pullback pressures observed earlier, the loading follows the same pattern of increasing load as the diameter of the pipe increases. The trends of each of the installed pipes appear to be linear, which suggests that incrementally, the introduction of additional pipe into the ground translates into a higher pulling force. By comparing the apparent slope of the line it can be noted that the 114 mm pipe has the lowest slope over the length of the installation. The 219 mm and the 324 mm pipes both have a change in the observed trend of the loading. For the 219 mm pipe the trend of the line increases at

around the 45 m point of the installation. The 324 mm pipe has a higher trend during the initial portion of the installation from the start to the 15 m point. Following the 15 m point the trend of the load increases in a smaller manner. The loading on the 114 mm pipe increased to approximately 5 kN at the end of the installation. The loading on the 219 mm pipe increased to a maximum of 20 kN at approximately the 56 m point of the installation

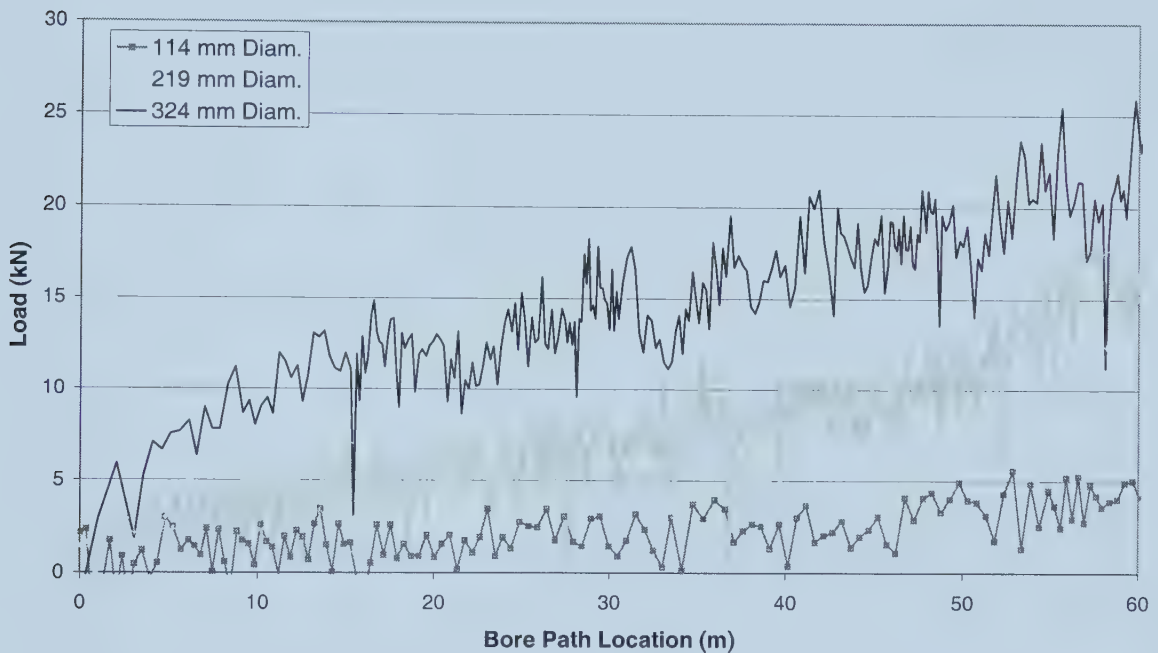


Figure 6.31: Load Cell Results by Diameter for the Sand Installations

The trends of the load cell results (Figure 6.31) mimic the trends observed earlier in the pullback pressures (Figure 6.30). For both of these parameters the larger diameter pipes had increased pullback pressures and loading in relation to the smaller diameters. Additionally, the response of the load on the pipe was related with the pullback pressures experienced by the drilling rig. For the 324 mm pipe, it can be seen that both the load on the pipe and the pullback pressures experienced a higher trend over the first 15 m of the installation. Following the 15 m point the trend of both the pullback pressure and the load on the pipe was smaller than this first section. This type of correlation suggests that estimated values of pipe loading could be determined from the pullback pressures

experienced by the drilling rig during the pullback. Further research is required to determine if a cohesive soil medium will exhibit the same relationship.

6.7.5 Strain Results

The average strain during the pullback process for each of the HDPE pipes installed is shown in Figure 6.32. This average strain was calculated by taking the average of the readings from the two linear potentiometers for the 114 mm pipe, and taking the average of the readings from the four linear potentiometers for both the 219 mm and 324 mm pipes. From Figure 6.32 a number of observations can be made about the average strain experienced by the HDPE pipe during the installation process. The maximum average strain for the HDPE pipes was 0.12%, 0.16%, and 0.05% for the 114 mm, 219 mm, and 324 mm pipes respectively. Both the 114 and 219 mm pipes displayed a smooth increasing strain over the length of the installation. Both of these installations had a relatively small strain imposed on them for the duration of these tests, but could potentially experience strains that could be structurally damaging for longer installations. The 324 mm pipe does not exhibit a smooth transition in the measured strain during the installation process. The measured strains on the 324 mm pipe are very small and the fluctuations in the strain amount can be attributed more to the fluctuations in the voltage sensitivities of the resulting equipment. Essentially, the 324 mm pipe experienced negligible average strain over the length of the installation.

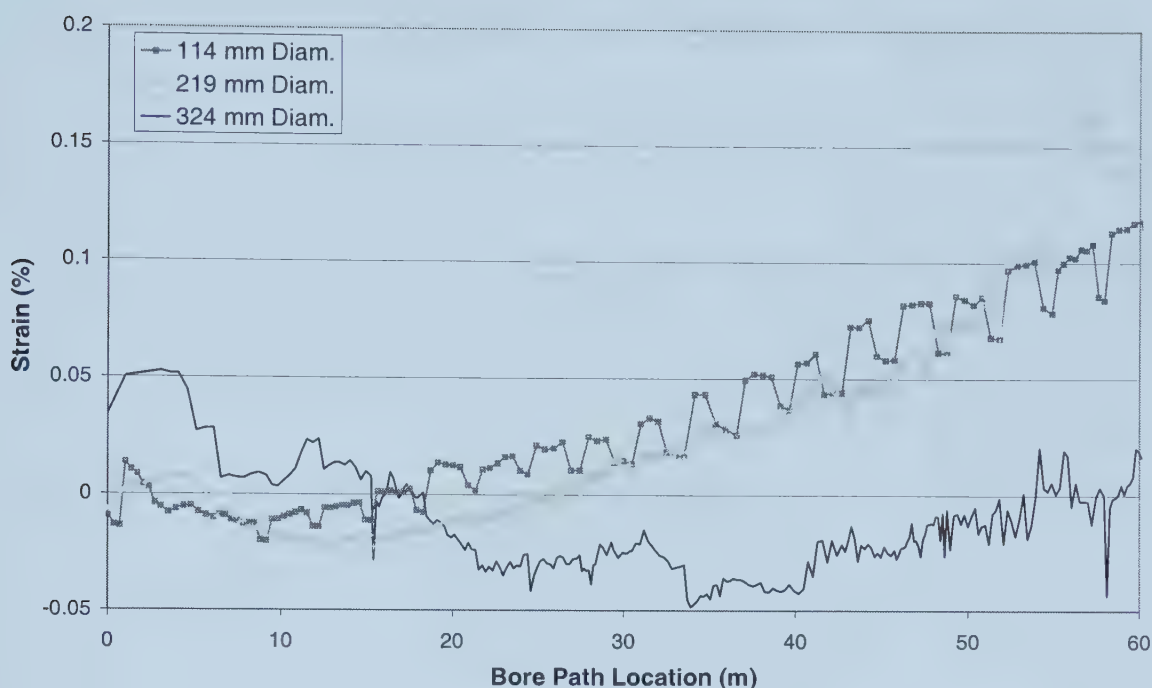


Figure 6.32: Average Strain by Diameter for the Sand Installations

Figure 6.33 contains the maximum absolute strain experienced by each of the product pipes during the pullback process. For the 114 mm pipe an initial spike occurred in the maximum strain for the initial bending portion of the bore profile. Subsequently, the strain increased in a smooth fashion to the end of the installation. The maximum strain experienced by the 114 mm pipe was 0.16%, occurring at the end of the installation. For the 219 mm pipe a peak in the maximum strain occurred at the 7 m point of the installation. Following this peak, the strain responded in a smooth fashion akin to the 114 mm pipe. The maximum strain experienced by the 219 mm pipe was 0.175% at around the 56 m point of the installation. The 324 mm pipe experienced shifts in the strain throughout the length of the installation with no definite trend being established. The maximum strain experienced by the 324 mm pipe was 0.2% and this occurred at the 3 m point in the installation. This strain can be attributed mostly to the bending action of the pipe in the borehole rather than the applied axial strain imparted on the pipe.

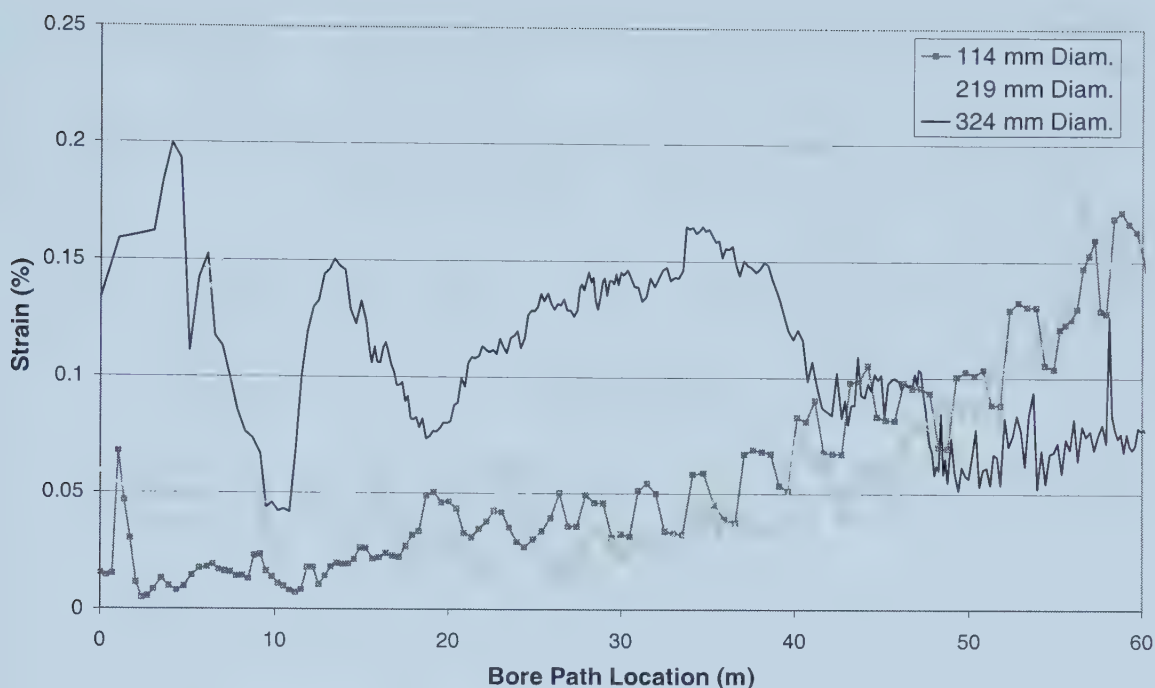


Figure 6.33: Maximum Absolute Strain by Diameter for the Sand Installations

6.8 DISCUSSION OF PIPE DIAMETER COMPARISON

Several conclusions can be drawn about the behaviour of the various testing parameters and how they relate to the diameter of the installed pipeline for the two soil mediums. These conclusions will be separated into how each soil medium behaves through the three different diameters of HDPE pipe installed.

For the clay soil or cohesive medium, the behaviour of the drilling rig pressures, loading on the HDPE pipe, and the strain on the HDPE pipe during pullback were examined in relation to the diameter of the HDPE pipe being installed. The following conclusions can be presented based upon these comparisons:

1. The drilling fluid pressures experienced by the drilling rig during the pullback phase tend to decrease over the length of the installation. Additionally, large increases or decreases may occur in these pressures over the length of the installation.

2. The rotational pressures experienced by the drilling rig tend to be fairly constant over the length of the installation. In respect to the pipe diameter, larger diameter pipelines cause larger rotational pressures on the drilling rig. Additionally, the fluctuations of the rotational pressure increase as the diameter of the installed pipe increases.
3. The pullback pressures experienced by the drilling rig increase as more pipe enters the ground during the pullback phase. There is no direct correlation between the magnitude of the pullback pressure and the diameter of the installed pipe as the 219 mm pipe had larger pressures than the 324 mm pipe. The magnitude of the pullback pressure is influenced by the amount of space between the edge of the pipe and the borehole wall.
4. The loading on the HDPE pipe can only be quantified between the 114 and 219 mm pipes. The loading on the installed pipe was much larger for the 219 mm pipe and followed the pattern experienced by the pullback pressure.
5. Strains on the HDPE pipes during installation never exceeded the 5% recommendation. The frictional effects in the borehole influenced the strains for the 114 and 219 mm diameter pipes. The curvature of the borehole will impose bending strains on the pipe during the installation process.

Again, the behaviour of the same attributes from the cohesive soil medium is examined, but according to their responsiveness to the sand soil or cohesionless soil medium. Several conclusions can be drawn about the effect that the installed pipe diameter has in this soil medium:

1. With respect to bore path length, the drilling fluid pressures tend to decrease as more product pipe is installed in the ground. The 324 mm diameter pipe experienced greater drilling fluid pressures than the smaller two pipes. Additionally, the 114 mm and 219 mm pipes experienced relatively similar magnitudes in the drilling fluid pressures over the duration of the installation.
2. The rotational pressures experienced by the drilling rig during the pullback process remain relatively constant during the length of the installation.

Fluctuations occur in these pressures, and the drilling rig experienced larger fluctuations in rotational pressure for larger diameter installations.

3. The machine pullback pressures increased as more of the product pipe entered the borehole during the pullback process. In relation to the installed pipe diameter the pullback pressures are greater for a larger diameter pipe installed in a cohesionless soil medium.
4. Loading on the pipe during the pullback phase increased as more of the product pipe entered the borehole. The magnitude of the loading was responsive to the installed pipe diameter as the load was greater for a larger diameter pipe. The loading on the pipe displayed the same trends as exhibited by the pullback pressures experienced by the drilling rig during the pullback operation. This suggests that the magnitude of loading on a product line can be estimated through the drilling rig pullback pressures.
5. Strain on all of the installed diameters did not exceed 0.2%. This magnitude of strain is well below the 5% point where permanent structural damage may occur. For the 114 mm and 219 mm pipes the strain increased smoothly over the installation length, suggesting that larger installations may exceed the 5% strain. The maximum strain on the 324 mm pipe was mainly influenced by the geometry of the bore path profile.

6.9 CORRELATIONS OF LOAD, STRAIN, AND PULLBACK PRESSURE

This next section looks at the correlations between the loading on the HDPE pipe, the strains experienced by the pipe, and the pullback pressure experienced by the drilling rig. All of the parameters are plotted on the same chart to allow for comparisons in the trends of the three components.

6.9.1 Clay Soil Medium

Figure 6.34 contains the loading, pullback pressure, and the maximum strain experienced during the installation of the 219 mm pipe in the clay soil medium. These three factors display similar trends over the length of the installation. For this installation, there are two noticeable phases in the installation where there is a change in the slope of the trend

lines of all three variables. The first trend occurs between the start of the installation and the 30 m point of the installation. The second trend occurs following the 30 m point to the end of the installation. Therefore, it is apparent that the load and strain on the HDPE pipe relate to the amount of pullback pressure experienced by the drilling rig. But this relation is not linear; for example, the load cell results are diverging from the pullback pressure. Therefore, this relationship will also depend upon the pipe location in the bore path.

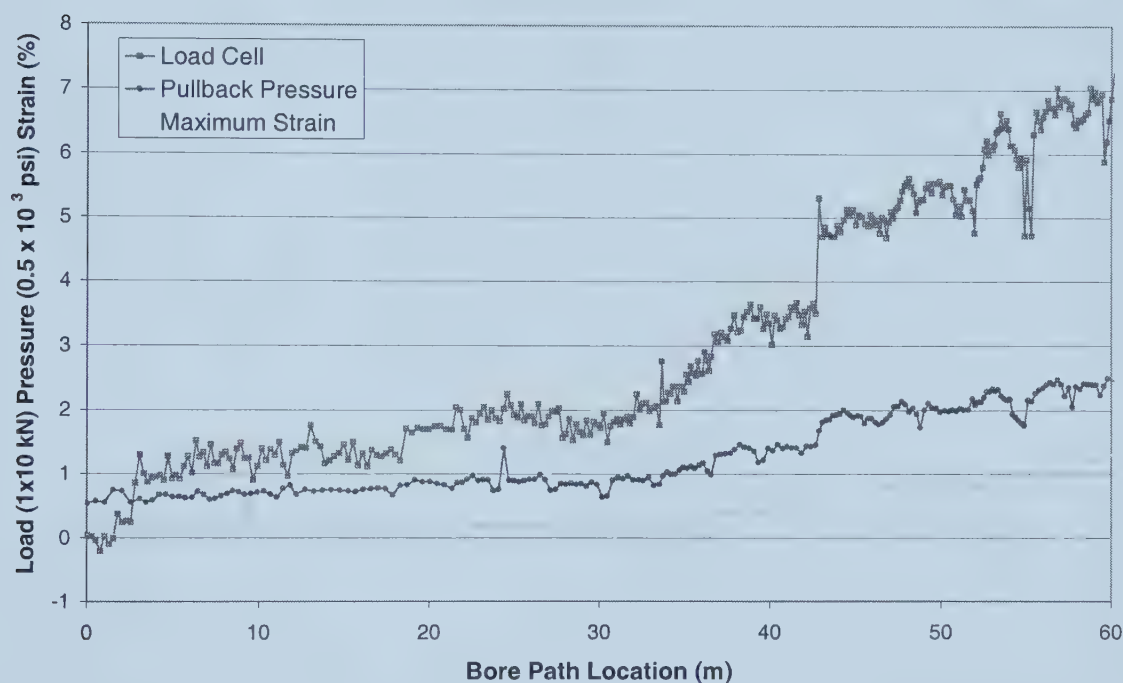


Figure 6.34: Correlation of Installation Results for 219 mm Pipe in Clay

The pullback pressure and the maximum strain experienced by the 324 mm pipe installed in the clay soil medium are shown in Figure 6.35. Similar to the 219 mm pipe, the two parameters show a correlation with one another. The response of the pullback pressure follows a trend similar to the strain experienced by the pipe. During the initial bending portion of the pipe the pullback pressure increased in the same shape as the increase in strain on the pipe. However, following the initial bending portion the pullback pressure on the drilling rig tends to increase while the experienced strain on the pipe remains relatively stable. Additionally, the extent of the curvature in the bore path will directly

affect the strain experienced by the pipe and the magnitude of the resulting pullback pressure is currently unknown.

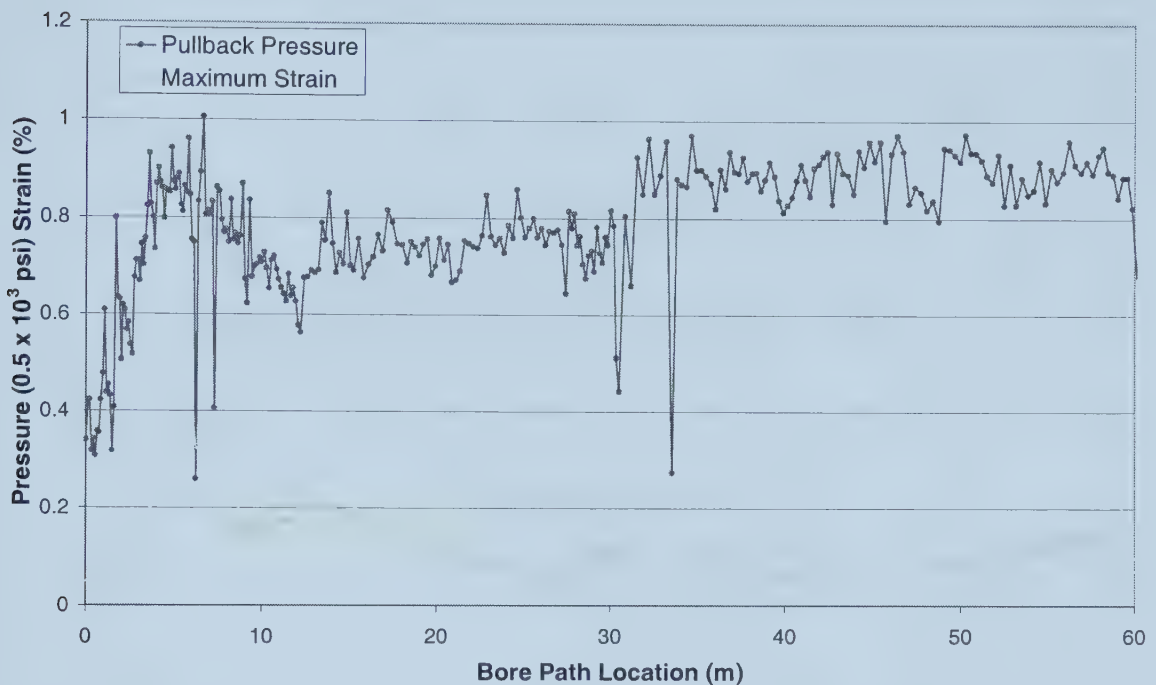


Figure 6.35: Correlation of Installation Results for 324 mm Pipe in Clay

6.9.2 Sand Soil Medium

Figure 6.36 contains the loading, strain, and pullback pressures for the 219 mm diameter pipe installed in the sand soil medium. Akin to the 219 mm pipe installed in the clay soil medium, the three parameter responses during the installation are very similar. There is one similar trend across the installation for the strain, load, and pullback pressure. Also, the ratio between each of the parameters is changing as the length of the installation continues. Therefore, any correlation would need to be respective of the length of the installation for the three parameters.

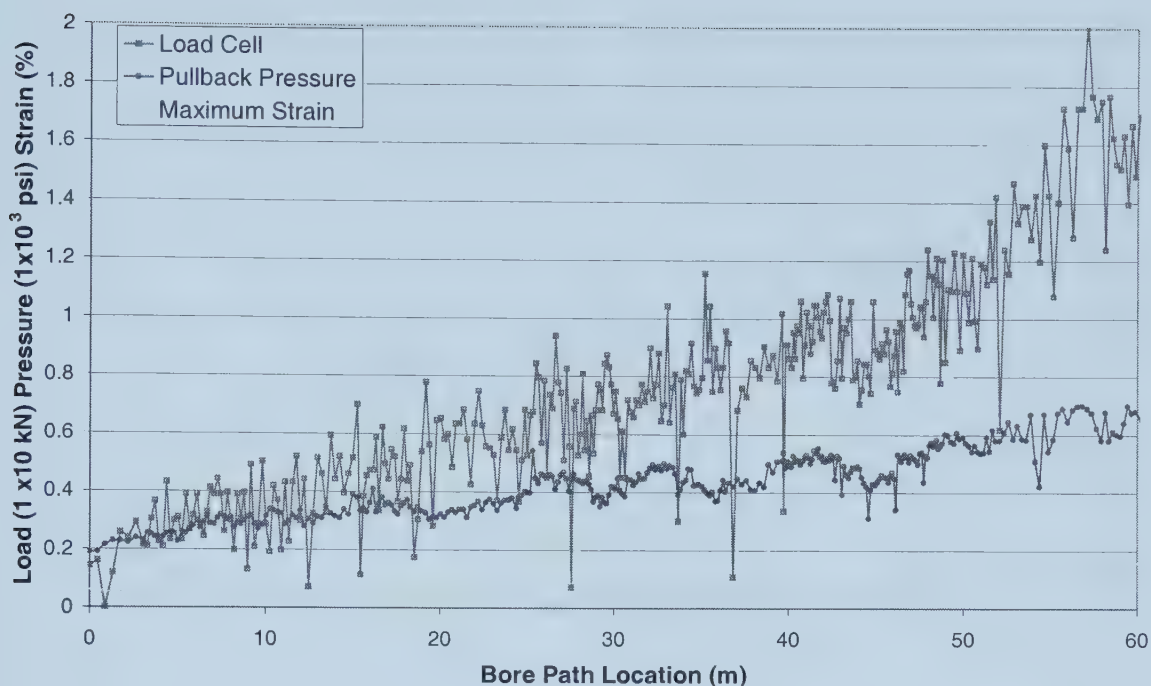


Figure 6.36: Correlation of Installation Results for 219 mm Pipe in Sand

The pullback pressure, load, and strain for the 324 mm pipe installed in the sand soil medium are shown in Figure 6.37. The pullback pressure and the loading of the HDPE pipe show an increasing trend along the length of the installation. The responses of these two parameters are similar to one another, but the magnitude of the ratio between them increases during the length of the installation. In comparing the strain results, it can be seen that the magnitude of the strain does not exhibit the same trend as the pullback pressures or loading experienced by the load cell.

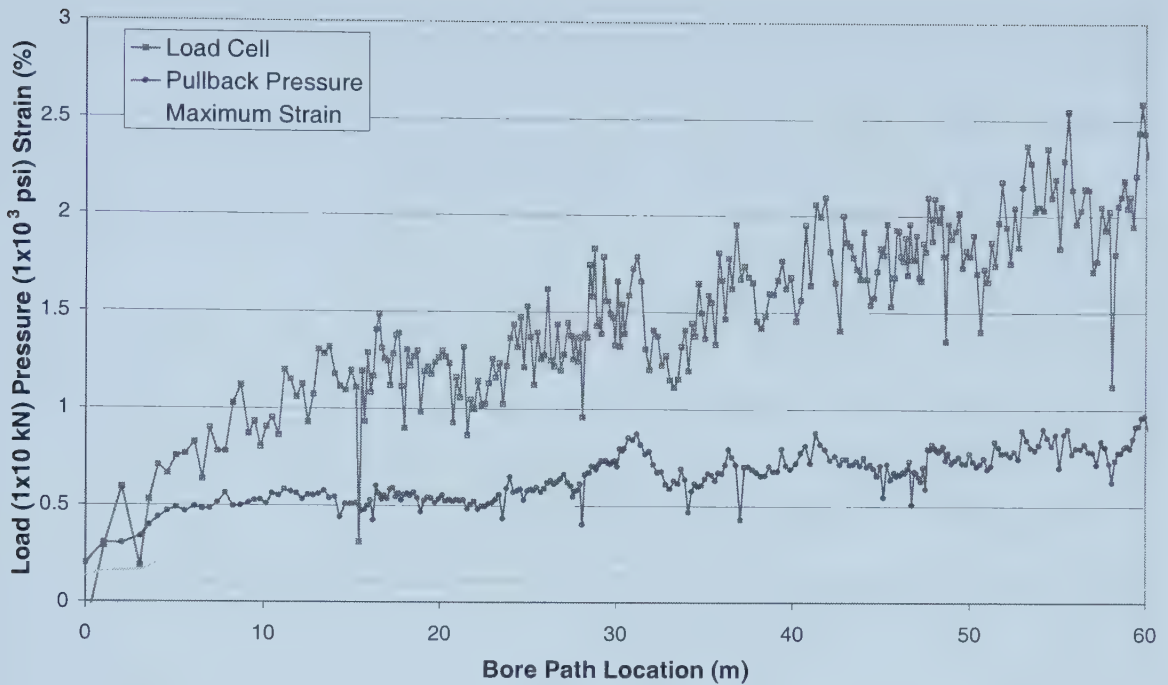


Figure 6.37: Correlation of Installation Results for 324 mm Pipe in Sand

6.10 DISCUSSION OF LOAD, STRAIN, AND PRESSURE CORRELATION

The response of the loading on the pipeline, the strain experienced by the HDPE pipeline, and the pullback pressure experienced during the installation are very similar. It was seen for the 219 mm and 324 mm pipelines installed in the two soil mediums that these parameters behave in a similar manner to one another. This response suggests that an increase in the pullback pressure experienced by the drilling rig translates instantly into the loading experienced by the HDPE product line and the subsequent strain that is experienced by the pipe. Therefore, the magnitude of loading on a product line and the strain experienced by this pipe can be estimated through the pullback pressures that are experienced during the pullback process. However, the ratios of how these parameters interact will vary in differing soil conditions. This ratio changes over the length of the installation. Since soil conditions can change very rapidly, any attempt to specify a relationship for a given soil condition might not be very beneficial. Additionally, these relationships would only be useful for the same installation conditions. Different installation parameters will exist for the following changed parameters: different type or size of drilling rig is used, the standard dimension ratio of the HDPE pipe is changed, the

type of reamer is changed, the upsize of the reamer is larger or smaller, the use of pre-reams, the number of pre-reams, and the properties of the drilling fluid used during the pullback. By changing any one of the above parameters, the condition of the installation would be different and therefore the relationships between the strain, pullback pressure, and load would change.

7.1 INTRODUCTION

This chapter contains the analysis of the laboratory testing results developed through the tensile testing of the HDPE coupons. Twenty-four coupons in total were tested, broken down into the diameter of the HDPE pipe and whether the sample was taken before or following the installation. Stress-strain graphs are presented showing the behaviour of the coupon samples up to the 10% strain point. Additionally, the modulus of elasticity was calculated for each coupon sample using the 2% secant method. Discussion of the difference in the elastic modulus and the tensile testing behaviour between the uninstalled and installed pipe is also presented.

7.2 HDPE PIPE INSTALLED IN CLAY

The tensile testing was conducted until the strain on the coupon reached a value of approximately 10%. This point was chosen arbitrarily and enabled the testing to be conducted in a more efficient fashion than if full tensile failure was required. The Plastics Pipe Institute identifies that the breaking point of HDPE coupons may occur between the 750-1000% strain range (PPI Chapter 3 1993). Additionally, the extensometer utilized during the testing would have been unable to record larger strain values.

7.2.1 219 mm Diameter

Figure 7.1 contains the stress-strain graphs developed from the tensile testing conducted on the 219 mm diameter coupon samples before installation in the clay soil medium. The stress-strain graphs show good correlation between each of the coupon samples and follow the typical shape of HDPE tensile testing illustrated in the literature. All of the tests show a smooth transition from the start of the test to the 10% strain mark, designated as the end point of the test. At this 10% end point the value of the stress on each of the samples range from 14.25 MPa to 17 MPa. From the secant modulus approach the elastic modulus values of 512 MPa, 485 MPa, and 554 MPa were calculated for each of the coupons tested. The mean elastic modulus of these three tests is 517 MPa with a standard deviation of 34.77 MPa.

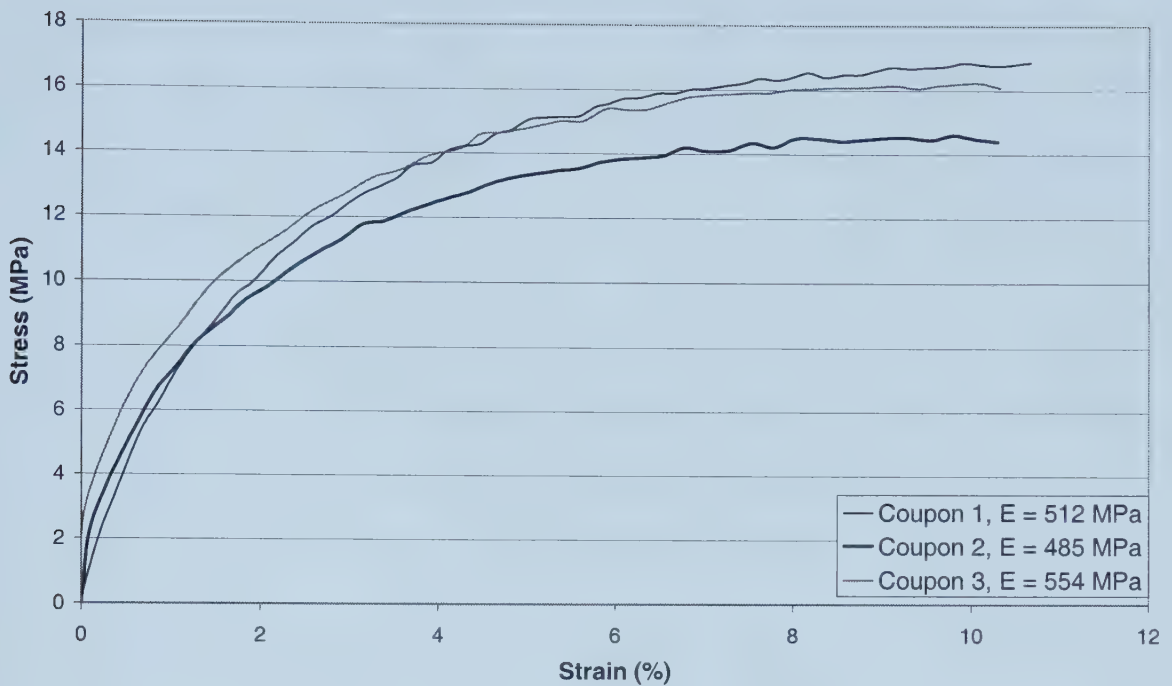


Figure 7.1: Stress-Strain Graphs for 219 mm Coupons – Clay Before Installation

The stress-strain graph for the coupon samples from the 219 mm diameter pipe following installation in the clay soil medium is shown in Figure 7.2. Similar to the three samples taken before installation, there is good correlation between the three plots. Additionally, the stress-strain graphs are smooth over the length of the test with the exception of the first coupon, which experienced a drop in stress at the 7% strain point in the test. This is due to the fact that the piston on the testing machine could no longer continue downward as the full length of travel was realized. Therefore, this caused the stress on the coupon to decrease with no apparent lengthening of the extensometer. For the other two coupons, the end stress values were in the 16 MPa range. The elastic moduli calculated from the three tests were 516 MPa, 465 MPa, and 528 MPa for coupons 1, 2, and 3, respectively. The mean value of the elastic modulus from these three tests was 503 MPa with a standard deviation of 33.45 MPa.

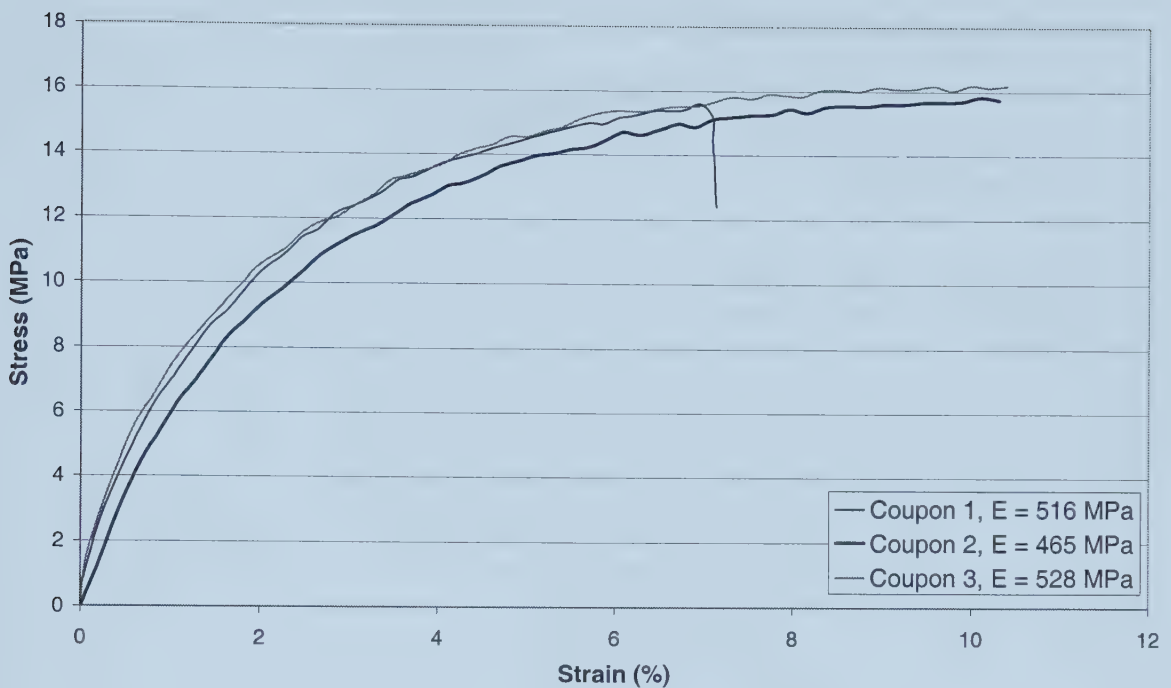


Figure 7.2: Stress-Strain Graphs for 219 mm Coupons – Clay Following Installation

7.2.2 324 mm Diameter

Figure 7.3 contains the stress-strain plots from the 324 mm diameter pipe coupons before installation in the clay soil medium. It can be seen that there are very close correlations between each of the three coupon samples over the entire strain range. At the 10% strain point the values of the stress during the test were approximately 17 MPa. The resulting elastic moduli calculated from these plots were 557 MPa, 522 MPa, and 516 MPa for coupons 1, 2, and 3 respectively. The resulting elastic modulus mean from these three tests was 532 MPa with a standard deviation of 22.14 MPa.

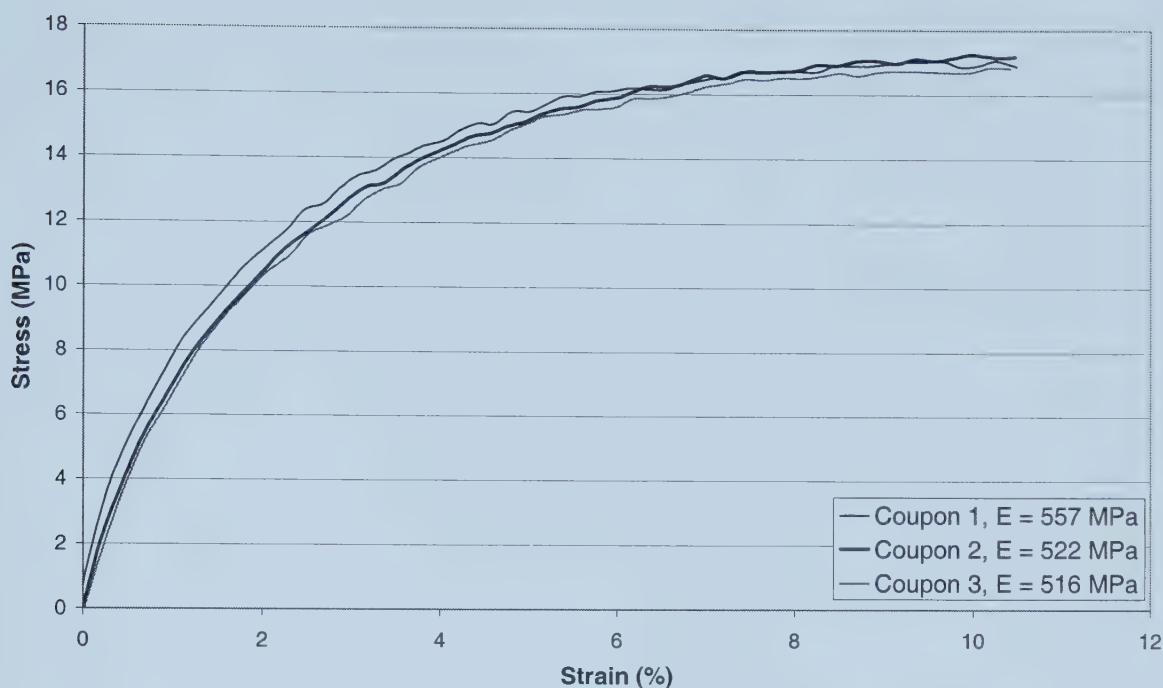


Figure 7.3: Stress-Strain Graphs for 324 mm Coupons – Clay Before Installation

The stress-strain graph for the three coupons tested from the 324 mm diameter pipe installed in the clay soil medium is shown in Figure 7.4. The range of stress values at the end of the tests is larger than that of the previous specimens, which ranged from 16 to 19 MPa. The plot for coupon 1 is flatter than the other two tests yielding an elastic modulus value of 510 MPa. Comparatively, the other two tests were consistent yielding elastic modulus values of 604 MPa and 590 MPa. The mean elastic modulus for these three tests was calculated as 568 MPa with a standard deviation of 50.71 MPa.

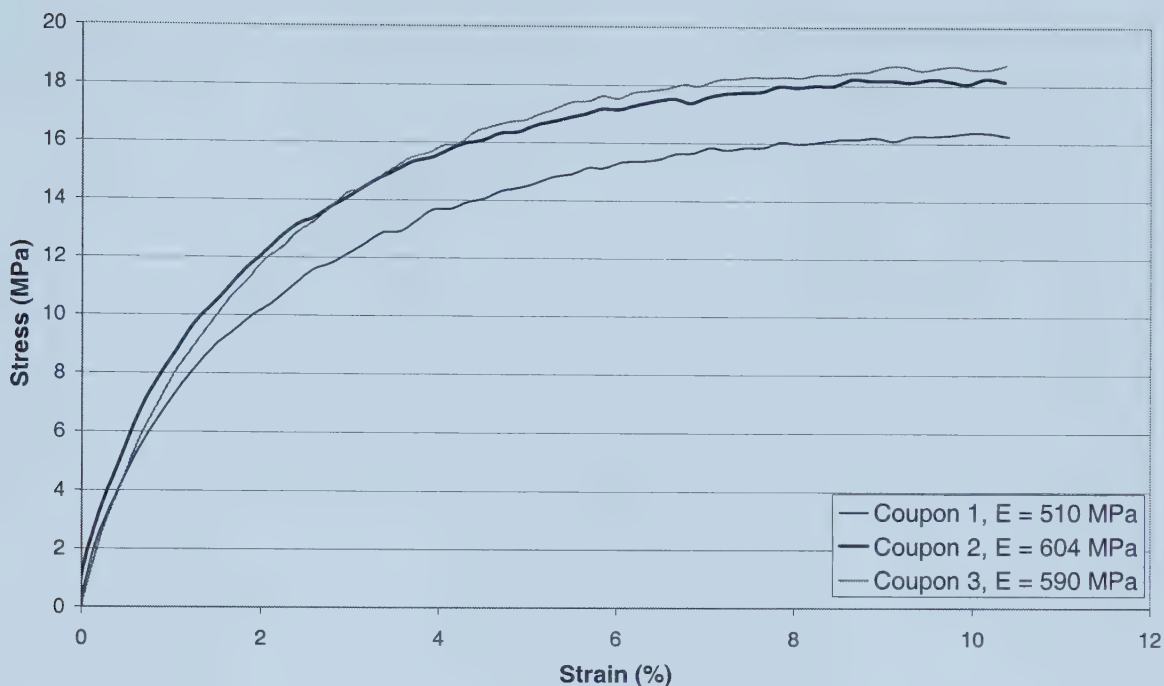


Figure 7.4: Stress-Strain Graphs for 324 mm Coupons – Clay Following Installation

7.3 HDPE PIPE INSTALLED IN SAND

7.3.1 219 mm Diameter

Figure 7.5 contains the stress-strain plots for the coupons manufactured from the 219 mm diameter pipe before installation in the sand soil medium. The results show good correlation over the length of the tensile test with the stress varying around the 16 MPa range at the end of the test. Additionally, the results are consistently smooth for all the coupons during the tensile testing. The values of the elastic modulus for coupon 1, 2, and 3 were as calculated by the secant method were 485 MPa, 490 MPa, and 516 MPa, respectively. The mean elastic modulus for these three coupons was determined to be 497 MPa with a standard deviation of 16.64 MPa.

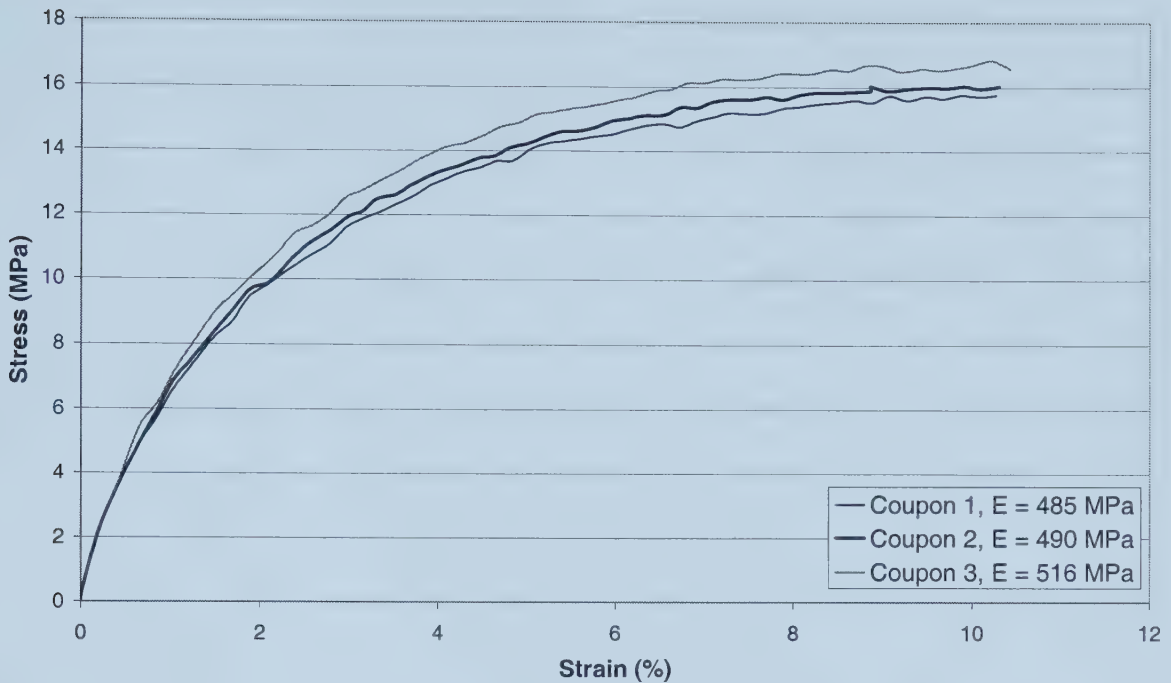


Figure 7.5: Stress-Strain Graphs for 219 mm Coupons – Sand Before Installation

The stress-strain plots for the three coupons manufactured from the 219 mm diameter pipe installed in the sand soil medium are shown in Figure 7.6. The resulting stress-strain profiles are very similar and the resulting stress at the end of the test was around 16 MPa. The elastic modulus calculations yielded results of 480 MPa, 509 MPa, and 519 MPa for coupons 1, 2, and 3 respectively. Subsequently, the mean elastic modulus was determined to be 503 MPa with a standard deviation of 20.26 MPa.

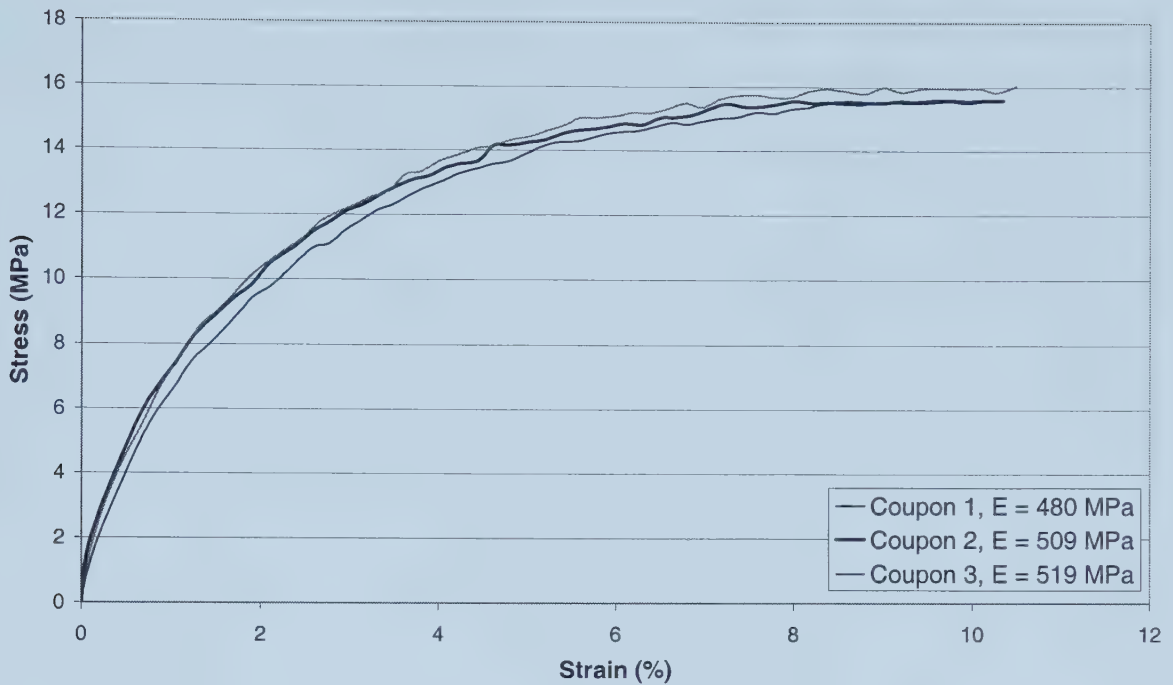


Figure 7.6: Stress-Strain Graphs for 219 mm Coupons – Sand Following Installation

7.3.2 324 mm Diameter

Figure 7.7 contains the stress-strain profiles generated during the tensile testing of the 324 mm diameter coupons prior to installation in the sand soil medium. Similar to the stress-strain graph of the 219 mm coupons in sand following the installation, these tests show exceptional correlation between each test. The resulting elastic modulus values were very close for each of the coupons with 509 MPa for coupon 1, 523 MPa for coupon 2, and 511 MPa for coupon 3. Subsequently, the resulting mean of the elastic modulus was determined as 514 MPa with a standard deviation of 7.57 MPa.

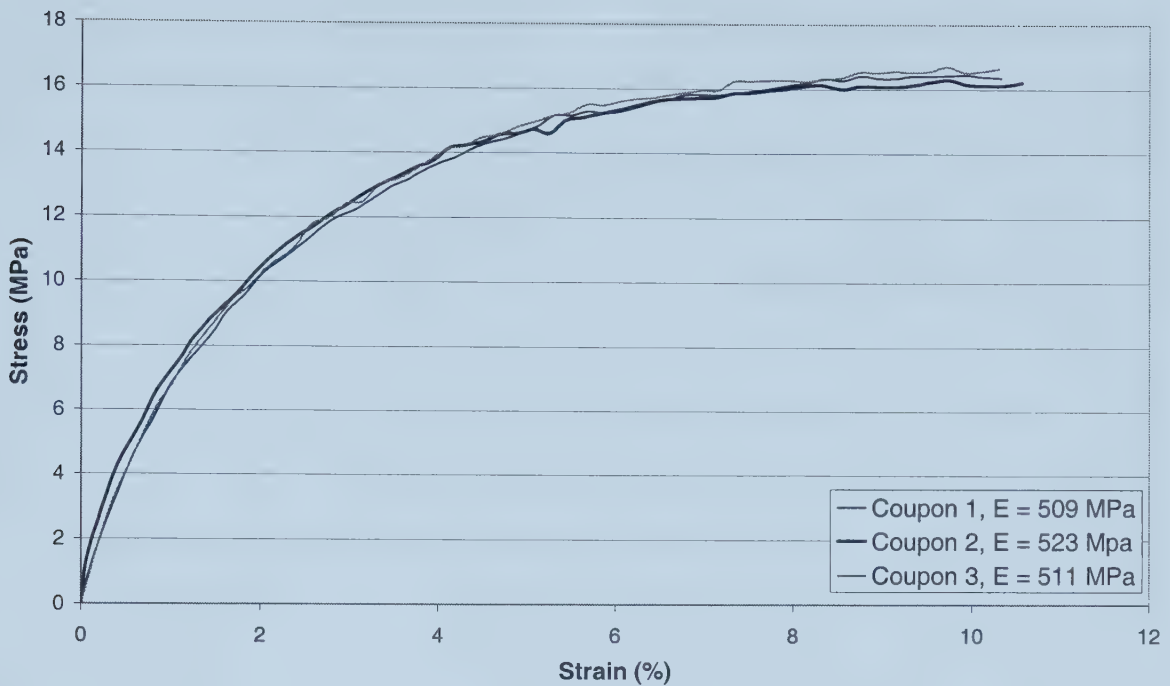


Figure 7.7: Stress-Strain Graphs for 324 mm Coupons – Sand Before Installation

The stress-strain profiles for the coupons manufactured from the 324 mm diameter pipe installed in the sand soil medium are shown in Figure 7.8. Coupon 3 displayed a larger trend over the tensile tests ending with a stress of 19 MPa in comparison to the 16 MPa stress experienced by the other two coupons. Subsequently, the elastic modulus for coupon 3 at 598 MPa was larger than the modulus determined for the other coupons at 485 MPa and 515 MPa for coupon 1 and coupon 2 respectively. The resulting mean of the elastic modulus was determined to be 533 MPa with a standard deviation of 58.53 MPa.

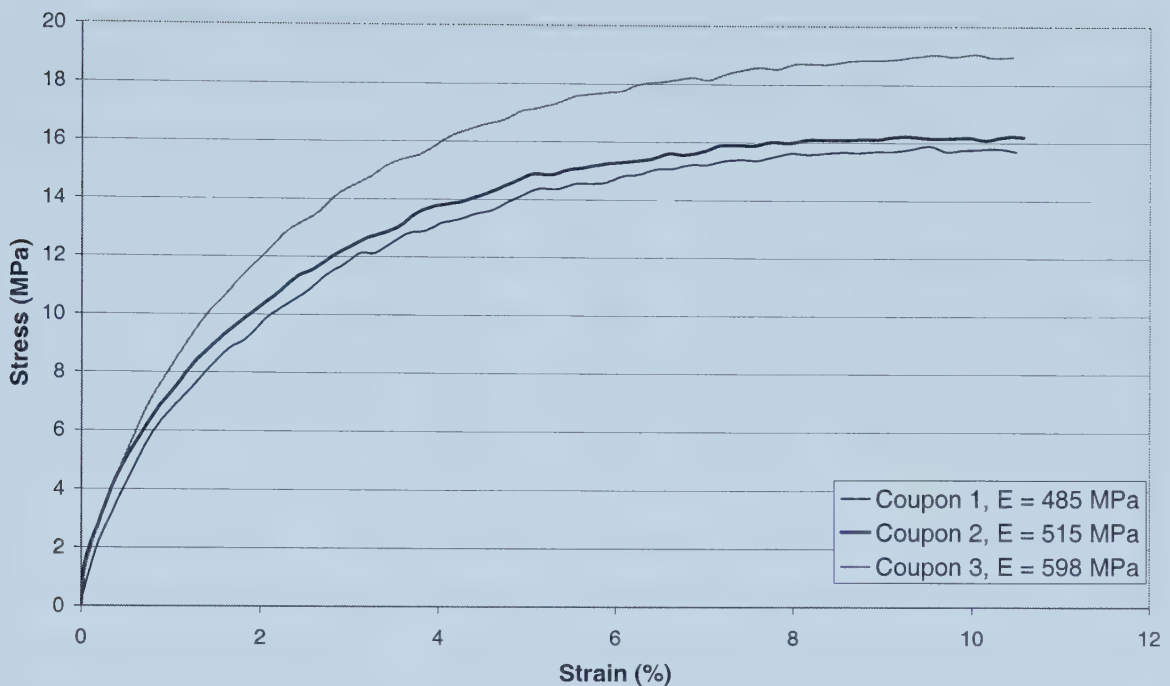


Figure 7.8: Stress-Strain Graphs for 324 mm Coupons – Sand Following Installation

7.4 DISCUSSION OF TENSILE TESTING RESULTS

In total there were twenty-four coupons tested in the tensile testing program covering the 219 mm and 324 mm diameter pipes installed in the both soil mediums. The resulting elastic modulus, mean, and standard deviation from these tests are shown in Table 7.1. The values of the elastic modulus ranged from 465 MPa to 604 MPa over all twenty-four tensile tests. The Plastics Pipe Institute suggests some typical values of the apparent modulus of elasticity for HDPE of 800 MPa, 400 MPa, 350 MPa, and 200 MPa for load durations of short-term, 10 hours, 100 hours, and 50 years respectively (PPI 1998). The elastic modulus values that were calculated from the tensile tests fit quite well between the short-term and 10 hour values given above. Additionally, the speed of testing will affect the results of the test and the Plastic Pipe Institute does not specify the load rate for the above values.

Table 7.1: Summary of Elastic Modulus Values from Tensile Testing

Coupon Classification	Elastic Modulus (MPa)				
	1	2	3	Mean	Std. Dev.
219, Clay, Before	512	485	554	517	34.77
219, Clay, After	516	465	528	503	33.45
324, Clay, Before	557	522	516	532	22.14
324, Clay, After	510	604	590	568	50.71
219, Sand, Before	485	490	516	497	16.64
219, Sand, After	480	509	519	503	20.26
324, Sand, Before	509	523	511	514	7.57
324, Sand, After	485	515	598	533	58.53

In order to determine whether or not the installations in both the sand and the clay soil mediums structurally damaged the pipe, a comparison of the mean elastic modulus determined from the tensile testing will be conducted between the before and after samples. The mean elastic modulus value of the 219 mm pipe installed in the clay soil medium for the before samples was 517 MPa in comparison to 503 MPa for the after samples. These elastic values are very similar and are within 3% of each other. Additionally, the standard deviations of both series of tests are above 30 MPa, which means that the deviation between the same samples is larger than the difference between the two means. For the 324 mm pipe installed in the clay soil medium, the mean elastic modulus values calculated from the tensile tests was 532 MPa and 568 MPa for the before and after samples respectively. The mean value of the after samples is larger than the value for the before samples but also has a higher standard deviation for this mean value. The difference between these two modulus values is about 7%. For the 219 mm pipe installed in the sand soil medium the mean elastic modulus values for the before and after samples were 497 MPa and 503 MPa respectively. These mean values are almost exactly identical, varying by only 1%. Additionally, the standard deviation of the tests was between 16 MPa to 20 MPa. The mean elastic modulus values for the 324 mm pipes installed in the sand soil medium for the before and after samples are 514 MPa and 533 MPa respectively. The difference between these two values is around 4%.

By comparing the differences in the mean elastic moduli and the differences between the standard deviation of the tests with the mean elastic moduli will enable a determination of whether the HDPE pipe was structurally changed during the installation process. Table 7.2 contains the differences in percentages for the mean elastic moduli and the standard deviation in comparison to the elastic modulus of the “before” samples. It can be seen that in all but two cases, the percentage difference between the standard deviation is larger than the percentage difference between the mean elastic moduli values. This suggests that the variability in the testing methodology mainly influences the difference between the mean elastic modulus values of the HDPE coupon samples.

Table 7.2: Percent Difference Between the Mean Elastic Modulus Values

Diameter and Soil	219 - Clay	324 - Clay	219 - Sand	324 - Sand
% Difference - Mean Values	3%	7%	1%	4%
% Diff. - Std. Dev. Before to Mean Before	7%	4%	3%	1%
% Diff. - Std. Dev. After to Mean Before	6%	10%	4%	11%

The variation from the standard deviation during the coupon tests was larger than the differences between the before and after pipe samples for most of the cases. The variability in the pipe samples is due to a number of factors that relate to the manufacturing of the coupons and the tensile testing methodology. First, the coupons were not perfectly identical to one another. There were slight variations in the widths and thickness of the materials, thus affecting the cross-sectional area and the stress experienced during the tensile testing. Second, the coupons that were tested first in the tensile testing machine had greater variability between each of the samples. This can be attributed to the learning curve in using the machine and understanding the nuances of the testing procedure. Additionally, the bottom grip on the machine was not tight against the loading piston. This created a gap in the machine and a slight load was required to be applied in order to close this gap. It was difficult to ensure that the same loading was applied on each of the coupon samples during this procedure.

8.1 CONCLUSIONS

The main objective of this research was to observe the strain behaviour that occurred on the HDPE pipelines during installation in the two different soil mediums. This main objective was broken down into three subcomponents. The first component comprised the observation of the changes in response of drilling rig, loading, and subsequent strain on the HDPE pipe between a cohesive and a cohesionless soil medium. The second component analyzed the effect of pipeline diameter on the aforementioned parameters. Finally, the determination of whether or not the mechanical properties of the HDPE were changed through the pullback process was conducted. The conclusions for this research will be summarized into four areas: strain experienced by the product pipelines in both soil mediums and general observations through all installations, comparison between the cohesive and cohesionless soil medium, effect of pipe diameter in the soil mediums, tensile testing of the HDPE coupons.

8.1.1 Applied Strain and General Observations

For all of the pipeline installations the strain recorded in the HDPE pipe during the pullback process never exceeded 1.5%. This maximum value is well below the industry threshold value of 5%. However, the profiles of the strain observed for the 114 mm and 219 mm diameter pipelines in both soil mediums were increasing as more pipe entered the borehole. This suggests that longer installations may have strain values that exceed 5%. In regards to the differences between the two soil mediums, the pipelines installed in the cohesive soil medium experienced larger strains than those pipelines installed in the cohesionless soil medium. An increase in pipe diameter did not automatically coincide with increased strain on the product line. The 219 mm pipelines experienced greater strain than the 114 mm and 324 mm pipelines. The distance between the outside of the installed pipeline and the borehole wall influences the magnitude of strain experienced by the HDPE pipe.

The effects of curvature in the borehole were observed through the pipeline installations in the two soil mediums. These curvatures caused bending deformations in the HDPE pipelines, which translated into an increase in strain in the pipe. For some of the installed pipelines the effects of bending created larger or similar magnitudes of strain than those experienced solely through the axial loading. For the 324 mm diameter pipelines the maximum strain that was experienced during the pullback phase in both soil mediums was due mainly to the curvature of the borehole.

Several observations on the drilling fluid pressure, rotational pressure, and pullback pressure experienced by the drilling rig during the pullback phase of the installation process can be summarized. The first observation is that the trend of the drilling fluid pressure decreases over the length of the installation. Additionally, large fluctuations can occur in this drilling fluid pressure during the scope of the installation. Secondly, the rotational pressure during all installations tended to remain fairly constant over the length of each respective installation. Lastly, the pullback pressure experienced by the drilling rig increased linearly as more of the installed pipe entered the borehole for both soil mediums.

The pullback loading experienced by the load cell followed the same trends observed for the pullback pressures on the drilling rig. That is, the loading increased in a linear fashion as more of the pipeline entered the borehole. A comparison was conducted between the pullback pressures and the loading experienced by the load cell. Through this comparison it was observed that increases in the pullback effort by the drilling rig will immediately be transferred to the product pipe being installed. Due to this correlation, it may be possible to estimate the pulling load on the product line through the observation of the pullback pressure. However, the ratio between these two parameters increases as more pipe enters the ground and would be susceptible to any change in tooling, procedure, drilling fluid, equipment utilized, and bore path profile.

8.1.2 Cohesionless Versus Cohesive Soil Medium

Several conclusions were reached regarding the effect of different soil mediums on the HDD installation parameters. The drilling fluid pressures observed during the pullback phase of the directional drilling operation were larger in the cohesionless soil medium than in the cohesive soil medium. The magnitudes of the rotational pressures exerted by the drilling rig were very similar between the two soil mediums. Therefore, the drilling rig experienced the same amount of effort for a pipeline of similar diameter installed in the cohesive and cohesionless soil mediums. In regards to the pullback pressures, the pressures experienced in the cohesive soil medium for a given pipe diameter were larger than those experienced in the cohesionless soil medium. Additionally, the loading that is transferred to the product pipeline through the reamer is larger in the cohesive soil medium than in the cohesionless soil medium for the same diameter installation. Therefore, the cohesive soil medium imparts greater frictional effects on the product pipeline, which are then translated into an increased pulling force required to advance the pipeline and subsequent increase in drilling rig effort.

8.1.3 Effect of Pipe Diameter

In the cohesive soil medium, several conclusions were determined about the effect of pipe diameter on the installation parameters. These include:

1. Larger drilling fluid pressures were observed for the larger diameter pipelines.
2. Larger diameter pipelines caused larger rotational pressures on the drilling rig and the fluctuations in rotational pressure for these pipes are greater than for the smaller diameter pipelines.
3. The pullback pressure experienced by the drilling rig was largest for the 219 mm diameter pipeline.
4. The loading trend on the installed HDPE pipe was greater for the 219 mm diameter pipeline than that of the 114 mm pipeline.

In the cohesionless soil medium, conclusions were developed for the behaviour of the drilling rig pressures and the loading on the product pipeline:

1. The 324 mm diameter pipeline experienced the largest drilling fluid pressures during the installation. Both the 114 mm and 219 mm diameter pipelines experienced a similar magnitude of pressure.
2. The magnitude of the fluctuations in the rotational pressures during the pullback phase was greater for a larger diameter pipeline.
3. Pullback pressures are greater for a larger diameter pipeline installed in this soil medium.
4. Loading on the pipe during the pullback phase follows the same trend as the pullback pressure. That is, the loading on the pipe is greater for a larger diameter pipeline installed in this soil medium.

8.1.4 Tensile Testing of HDPE Coupons

Tensile testing was conducted on coupon samples manufactured from the 219 mm and 324 mm pipes installed in the two soil mediums. Through this tensile testing program it was found that there was no significant difference in tensile performance between the pipes that had been installed versus samples taken prior to installation. The mean elastic modulus values determined through this testing were very similar between the before and after pipe samples. The largest difference between the before and after pipe samples was observed for the 324 mm pipe installed in the clay soil medium at 7%. But, the standard deviation of the after samples had a difference of 10% with the mean value of the elastic modulus for the before samples. Therefore, there was more variability evident between the three sample coupons than for the difference between the mean elastic moduli. The other pipe samples had differences in mean elastic modulus values of 3%, 1%, and 4% for the 219 mm pipe in clay, 219 mm pipe in sand, and 324 mm pipe in sand respectively.

The results from the tensile testing program were expected due to the low strain, and subsequent stress history experienced by the pipelines during the HDD installations. The maximum strain experienced during the pullback did not exceed 1.5% for all of the installations. The HDPE pipe was able to rebound from this strain and maintain structural properties that are very similar to those of a product pipe that hasn't been installed.

8.2 AREAS FOR FUTURE RESEARCH

This section presents some areas where future research can be directed to further understand the HDD process and how different parameters affect the response of the drilling rig, strain on the product pipeline, loading on the product pipeline, and the material properties of polyethylene.

Foremost, the behaviour of the HDPE piping and the response of the drilling rig should be examined for other soil mediums and soil medium parameters. The behaviour in other soil mediums such as silt, gravel, shale, and rock should be observed for instrumented HDPE pipeline installation. These new soil mediums will provide further comparisons to the results that have been obtained in this thesis. Along with the different soil mediums, installations should be conducted in differing soil medium parameters. These parameters should include consistency, moisture content, and relative density of the soil medium. A better understanding of these soil parameters on the behaviour of HDPE pipe and the drilling rig can thus be achieved.

The effect of the diameter of the installed pipeline should be observed for larger diameter HDPE pipelines. Currently, the common installation sizes of HDPE range from 100 mm (4 in.) to 900 mm (36 in.) in diameter. The behaviour of these larger diameter pipelines need to be observed with respect to the response of the drilling rig, applied strain on the product pipeline, and the loading that is transferred between the reamer to the product line during the pullback phase. It was found that in the sand soil medium the pullback pressures and the load on the product pipeline increased with the product diameter from the 100 mm (4 in.) to 300 mm (12 in.) range. The installation of these larger diameter pipelines will be able to confirm if this trend continues.

Further HDD installations should be conducted that vary only one parameter from the tests that were performed for this research. By varying a single parameter, a better understanding can be gained about how that parameter affects the drilling rig response, strain on the HDPE product line, and the loading on the HDPE product line. There are many parameters that can be varied, these include: type of the reamer that is employed

during the pullback phase, upsize ratio that is used for the reamer, utilization of a pre-ream or multiple pre-reams prior to the final pullback, standard dimension ratio of the HDPE pipe, density of the polyethylene pipeline, depth of the installation, vertical and horizontal curvature changes in the bore path, properties of the drilling fluid, type of drilling rig, size of drilling rig, and overall length of the installation.

The response of different pipeline materials in an HDD installation should be examined in the same fashion as for the polyethylene pipeline material. There are many other pipeline materials that are being utilized for HDD installation, including polyvinyl chloride, steel, Permalok (steel pipe with a special connection mechanism), clay tile, and concrete. Each of these materials may behave differently during the pullback process. Additionally, the examination of a linear elastic material, such as steel, could enable the formulation of a load and stress model for the HDD process.

A better understanding of the material properties of HDPE and how the HDD process affects them needs to be addressed. The most common mechanism for failure of a HDPE pipeline installed by HDD is through slow crack growth while the pipeline is in service. Material manufactures test their pipelines for their resistance to slow crack growth through intensive laboratory tests. Unfortunately, these tests are done in the laboratory on virgin pipelines and therefore, would not account for the stress history that is experienced by a pipeline installed through the HDD process. The same type of testing program that was utilized for this research could be followed, but instead of conducting tensile testing on the HDPE samples, slow crack growth testing could be conducted. Samples of the pipeline prior to and following installation could be collected and tested. This would enable a comparison of how the HDD installation process affects the HDPE materials' resistance to slow crack growth.

Since HDPE is a viscoelastic material the apparent modulus of elasticity will change through the continued application of load, temperature, and magnitude of the loading. Models have been created that can predict this response but do not address the unique situation created through the HDD pullback process. The loading that is induced on to the

HDPE pipeline during the pullback phase is not continuous and varies along the length of the installation. Additionally, the loading that is applied to the HDPE pipeline is cyclical in nature. When the drilling rig must stop to remove a drill rod, the force on the product pipeline relaxes until the next segment is ready to be pulled and the force is reapplied to the product pipeline. A laboratory testing program needs to be implemented to perform tests on full segments of HDPE pipes. This process should simulate the cyclical loading conditions that are imparted during field installations. Actual loading data would need to be collected through the use of an external load cell connected to the installed product pipeline. The results from these installations or from the load cell data that was recorded during this research (Appendix A) could be used to design the loading parameters for these tests.

REFERENCES

Allouche, E.N. and Baumert, M.E. (2001). "Application of Statistics in Estimating Pulling Loads for HDD Installations," *Proceedings of the No-Dig 2001 Conference*, Nashville, Tennessee.

Allouche, E.N., Ariaratnam, S.T., and Lueke, J.S. (2000). "Horizontal Directional Drilling: Profile of an Emerging Industry," *ASCE Journal of Construction Engineering and Management*, Vol. 126, No. 1, 68-76.

American Society for Testing and Materials (1998). *ASTM D 638-98 Standard Test Method for Tensile Properties of Plastics*, American National Standards Institute: New York, New York.

Ariaratnam, S.T., Allouche, E.N., and Lueke, J.S. (1998). "Identification of Risk in Horizontal Directional Drilling Operation," *No-Dig Engineering*, Vol. 5, No. 1, 21-24.

Baroid (1998). *Baroid Industrial Drilling Products – Product Brochure*, Baroid Industrial Drilling Products, Denver, Colorado.

Bennett, R.D., Ariaratnam, S.T., and Como, C.E. (2001). *Horizontal Directional Drilling Good Practices Guidelines*, HDD Industry Consortium, Washington, DC.

DCCA (1998). *Guidelines for a Successful Directional Crossing Bid Package*, Directional Crossing Contractors Association, Dallas, Texas, 90-94.

Digital Control (1999). *DigiTrak Directional Drilling Locating System: Operators Manual*, Digital Control Incorporated, Renton, Washington.

Duyvestyn, G., Knight, M.A., and Polak, M.A. (2001). "Measurement of HDPE Pipeline Axial Load During Horizontal Directional Drilling Installation," *Proceedings of the UCT 2001 Conference*, Houston, Texas.

Flugge, W. (1967). *Viscoelasticity*, Blaisdell Publishing Company: Waltham, Massachusetts.

Gelinas, M., Polak, M.A., and McKim, R. (2000). "Field Tests on HDPE Pipes Installed Using Horizontal Directional Drilling," *ASCE Journal of Infrastructure Systems*, Vol. 6, No. 4, 130-137.

Gelinas, M. (1998-a). "Field Monitoring and Analysis of High Density Polyethylene Pipelines Installed Using Horizontal Directional Drilling," MASc. Thesis, *University of Waterloo*, Department of Civil Engineering, Waterloo, Ontario.

Gelinas, M. (1998-b). "Strain in High Density Polyethylene as a Result of Installation Using Horizontal Directional Drilling," *Proceedings of the 1998 No-Dig Conference*, Albuquerque, New Mexico: 57-78.

Harper, R. (1999). "Estimating Directionally Drilled Pipe Loads," HDD Inspector and Certification Academy, CALTRANS-NASTT, Sacramento, California.

Huey, D.P., Hair, J.D., and McLeod, K.B. (1996). "Installation, Loading, and Stress Analysis Involved With Pipelines Installed by Horizontal Directional Drilling," *Proceedings of the 1996 No-Dig Conference*, New Orleans, Louisiana.

Kirby, M., Kramer, S.R., Pittard, G.T., and Mamoun, M. (1996). "Design Guidelines and Procedures for Guided Horizontal Drilling," *Proceedings of the 1996 No-Dig Conference*, New Orleans, Louisiana.

Lueke, J.S, Ariaratnam, S.T., and Colwell, D.A.F. (2001). "Towards the Development of Horizontal Directional Drilling Depth of Cover Guidelines," *Proceedings of the No-Dig 2001 Conference*, Nashville, Tennessee.

May, D. (1994). "The Use of Horizontal Wells for Subsurface Soil and Aquifer Restoration," *Drilling Technology*, Vol. 56, 227-239.

Plexco (1999). "Technical Note: Horizontal Directional Drilling (Guided Boring) with Plexco Pipe," *Chevron Chemical Company*, Trenchless Technology Bulletin No. 1.

PPI (1998). "Polyethylene Pipe For Horizontal Directional Drilling," *Plastics Pipe Institute*, Washington, D.C.

PPI Chapter 3 (1993). "Engineering Properties of Polyethylene," *Plastics Pipe Institute*, Wayne, New Jersey.

PPI Chapter 6 (1993). "Polyethylene Joining Procedures," *Plastics Pipe Institute*, Wayne, New Jersey.

Polak, M.A., Gelinas, M., McKim, R.A., and Knight, M. (1999). "Analysis of Strain Data From Field Tests on HDPE Pipes Installed Using Horizontal Directional Drilling," *Proceedings of the No-Dig 1999 Conference*, Orlando, Florida: 17-28.

Richard, J.E. (1996). "Guidelines Simplify Horizontal Directionally Drilled Crossings," *Pipeline and Gas Journal*, Vol. 223, No. 1, 36-38.

Svetlik, H.E. (1993). "Polyethylene Pipe Design for Directional Drillings and River-Crossings," *Richardson: Phillips Driscopipe Inc.*

Zhang, D.J.Y. (1999). "Predicting Capacity of Helical Screw Piles in Alberta Soils." M.Sc. Thesis, *University of Alberta*, Dept. of Civil and Envir. Eng., Edmonton, Alberta.

BIBLIOGRAPHY

Allouche, E.N. and Baumert, M.E. (2001). "Application of Statistics in Estimating Pulling Loads for HDD Installations," *Proceedings of the No-Dig 2001 Conference*, Nashville, Tennessee.

Allouche, E.N., Ariaratnam, S.T., and Lueke, J.S. (2000). "Horizontal Directional Drilling: Profile of an Emerging Industry," *ASCE Journal of Construction Engineering and Management*, Vol. 126, No. 1, 68-76.

Ariaratnam, S.T., and Allouche, E.N. (2000). "Suggested Practices for Installations Using Horizontal Directional Drilling," *Practice Periodical on Structural Design and Construction*, Vol. 5, No. 4, pp. 142-149.

Ariaratnam, S.T., Lueke, J.S., and Allouche, E.N. (1999). "Utilization of Trenchless Construction Methods by Canadian Municipalities," *ASCE Journal of Construction Engineering and Management*, Vol. 125, No. 2, 76-86.

Ariaratnam, S.T., Allouche, E.N., and Lueke, J.S. (1998). "Identification of Risk in Horizontal Directional Drilling Operation," *No-Dig Engineering*, Vol. 5, No. 1, 21-24.

American Society for Testing and Materials (1998). *ASTM D 638-98 Standard Test Method for Tensile Properties of Plastics*, American National Standards Institute: New York, New York

Baroid (1998). *Baroid Industrial Drilling Products – Product Brochure*, Baroid Industrial Drilling Products, Denver, Colorado.

Bennett, R.D., Ariaratnam, S.T., and Como, C.E. (2001). *Horizontal Directional Drilling Good Practices Guidelines*, HDD Industry Consortium, Washington, DC.

Bennett, R.D., Khan, S., and Iseley, T. (1994). "Mini-Horizontal Directional Drilling: Field Evaluation at WES," Trenchless Technology Center at Louisiana Tech University: Ruston, Louisiana.

Bertani, G., Olcese, A., Vescovo, C., Lazzarini, U., and Milani, G. (1994). "Directional Drilling: Study of the Effects on the Pipeline and the Surrounding Soil," *Proceedings of the No-Dig 1994 International Conference*, Copenhagen, Denmark.

Callister, W.D. (1994). *Materials Science and Engineering: An Introduction Third Edition*, John Wiley & Sons: New York, New York.

Chevron Chemical Company (1999). *Technical Note: Horizontal Directional Drilling (Guided Boring) with Plexco Pipe*, Trenchless Technology Bulletin No. 1.

Christensen, R.M. (1971). *Theory of Viscoelasticity: An Introduction*, Academic Press: New York, New York.

DCCA (1998). *Guidelines for a Successful Directional Crossing Bid Package*, Directional Crossing Contractors Association, Dallas, Texas, 90-94.

Digital Control (1999). *DigiTrak Directional Drilling Locating System: Operators Manual*, Digital Control Incorporated, Renton, Washington.

Driscopipe (1996). *Stress/Strain Relationships of Plastics*, Technical Note #12, Driscopipe.

Duyvestyn, G., Knight, M.A., and Polak, M.A. (2001). "Measurement of HDPE Pipeline Axial Load During Horizontal Directional Drilling Installation," *Proceedings of the UCT 2001 Conference*, Houston, Texas.

Duyvestyn, G., and Knight, M. (2000). "Soil Deformations due to Horizontal Directional Drilling Pipeline Installation," *Proceedings of the 2000 No-Dig Conference*, Anaheim, California: 209-217.

Ferry, J.D. (1970). *Viscoelastic Properties of Polymers Second Edition*, John Wiley & Sons: New York, New York.

Flugge, W. (1967). *Viscoelasticity*, Blaisdell Publishing Company: Waltham, Massachusetts.

Fried, J.R. (1995). *Polymer Science and Technology*, Prentice Hall PTR: Englewood Cliffs, New Jersey.

Garrett, L.D. (1996). "Design of Large Diameter Steel Pipelines for HDD Installations," *No-Dig Engineering*, Vol. 3, No. 4, 2-4.

Gelinas, M., Polak, M.A., and McKim, R. (2000). "Field Tests on HDPE Pipes Installed Using Horizontal Directional Drilling," *ASCE Journal of Infrastructure Systems*, Vol. 6, No. 4, 130-137.

Gelinas, M. (1998). "Field Monitoring and Analysis of High Density Polyethylene Pipelines Installed Using Horizontal Directional Drilling," MASc. Thesis, *University of Waterloo*, Department of Civil Engineering, Waterloo, Ontario.

Gelinas, M. (1998). "Strain in High Density Polyethylene as a Result of Installation Using Horizontal Directional Drilling," *Proceedings of the 1998 No-Dig Conference*, Albuquerque, New Mexico: 57-78.

Hair, J.D. (1995). "Directional Drilling Demands Practical Fluids Knowledge," *Pipeline and Gas Industry*, Vol. 78, No. 8, 37-43.

Hair, J.D. (1995). "Drilling Fluid Criteria for Pipeline Installation by Horizontal Directional Drilling, Part I," *No-Dig Engineering*, Vol. 2, No. 3, 22-24.

Harper, R. (1999). "Estimating Directionally Drilled Pipe Loads," HDD Inspector and Certification Academy, CALTRANS-NASTT, Sacramento, California.

Hillmansen, S., Hobeika, S., Haward, R.N., and Leever, P.S. (2000). "The Effect of Strain Rate, Temperature, and Molecular Mass on the Tensile Deformation of Polyethylene," *Polymer Engineering and Science*, Vol. 40, No. 2, 481-489.

Huey, D.P., Hair, J.D., and McLeod, K.B. (1996). "Installation, Loading, and Stress Analysis Involved With Pipelines Installed by Horizontal Directional Drilling," *Proceedings of the 1996 No-Dig Conference*, New Orleans, Louisiana.

Khan, S., Bennett, D., McCrary, S., and Iseley, T. (1994). "Mini-Horizontal Directional Drilling: State-of-the-Art-Review," *Trenchless Technology Center at Louisiana Tech University*, Ruston, Louisiana.

Kirby, M.J., and Kramer, S.R. (1996). "Design Guidelines and Procedures for Guided Horizontal Drilling, Part II," *No-Dig Engineering*, Vol. 3, No. 4, 13-15.

Kirby, M., Kramer, S.R., Pittard, G.T., and Mamoun, M. (1996). "Design Guidelines and Procedures for Guided Horizontal Drilling," *Proceedings of the 1996 No-Dig Conference*, New Orleans, Louisiana.

Knausenberger, R., Krehwinkel, T., Menges, G., Schmachtenberg, E., and Thebing, U. (1984). "New Findings on the Mechanical Behaviour of Plastics," *Proceedings from the European Meeting of Polymer Processing and Properties*, 239-260.

Knight, M. and Duyvestyn, G. (2001). "Excavation and Analysis of High-Density Polyethylene Pipelines Installed Using a Horizontal Directional Drill," *Proceedings of the UCT 2001 Conference*, Houston, Texas.

Lasheen, A. and Polak, M.A. (2001). "HDD Loads Imposed on a Pipe," *Proceedings of the No-Dig 2001 Conference*, Nashville, Tennessee.

Lueke, J.S, Ariaratnam, S.T., and Colwell, D.A.F. (2001). "Towards the Development of Horizontal Directional Drilling Depth of Cover Guidelines," *Proceedings of the No-Dig 2001 Conference*, Nashville, Tennessee.

May, D. (1994). "The Use of Horizontal Wells for Subsurface Soil and Aquifer Restoration," *Drilling Technology*, Vol. 56, 227-239.

Moore, I.D. and Allouche, E.N. (2001). "Masters and Doctoral Research Related to Trenchless Technology: The University of Western Ontario, London, Canada," *Proceedings of the No-Dig 2001 Conference*, Nashville, Tennessee.

Petroff, L.J. (2000). "Polyethylene (PE) Pipe in Trenchless Applications," *Proceedings of the UCT 2000 Conference*, Houston, Texas.

Petroff, L.J. (1990). "Stress Relaxation Characteristics of the HDPE Pipe-Soil System," *Proceedings of the ASCE International Conference on Pipeline Design and Installation*, Las Vegas, Nevada, 280-294.

PPI (1998). "Polyethylene Pipe For Horizontal Directional Drilling," *Plastics Pipe Institute*, Washington, D.C.

PPI Chapter 3 (1993). "Engineering Properties of Polyethylene," *Plastics Pipe Institute*, Wayne, New Jersey.

PPI Chapter 6 (1993). "Polyethylene Joining Procedures," *Plastics Pipe Institute*, Wayne, New Jersey.

Polak, M.A., Gelinas, M., McKim, R.A., and Knight, M. (1999). "Analysis of Strain Data From Field Tests on HDPE Pipes Installed Using Horizontal Directional Drilling," *Proceedings of the No-Dig 1999 Conference*, Orlando, Florida, 17-28.

Polak, M.A., McKim, R.A., Gelinas, M.M., and Lasheen, A. (1998). "Structural Behaviour of Polyethylene Pipes in Trenchless Technologies," *Proceedings of the Structural Engineers World Congress*, San Francisco, California.

Popelar, C.F., Popelar, C.H., and Kenner, V.H. (1990). "Viscoelastic Material Characterization and Modeling for Polyethylene," *Polymer Engineering and Science*, Vol. 30, No. 10, pp. 577-586.

Richard, J.E. (1996). "Guidelines Simplify Horizontal Directionally Drilled Crossings," *Pipeline and Gas Journal*, Vol. 223, No. 1, 36-38.

Sandstrum, S.D. (2001). "HDPE Pipe: Is The Party Over?" *Proceedings of the No-Dig 2001 Conference*, Nashville, Tennessee.

Shames, I.H., and Cozzarelli, F.A. (1992). *Elastic and Inelastic Stress Analysis*, Prentice Hall: Englewood Cliffs, New Jersey.

Svetlik, H.E. (1993). "Polyethylene Pipe Design for Directional Drillings and River-Crossings," *Richardson: Phillips Driscopipe Inc.*

Ugural, A.C., and Fenster, S.K. (1995). *Advanced Strength and Applied Elasticity Third Edition*, Prentice Hall PTR: Upper Saddle River, New Jersey.

Van Houwelingen, M. (1999). "Reading Machine Pressures: Taking a Number from a Gauge & Turning It Into Useful Information." Notes from HDD Inspector and Certification Academy, CALTRANS-NASTT, Sacramento, California.

Zhang, C., and Moore, I.D. (1997). "Finite Element Modeling of Inelastic Deformation of Ductile Polymers," *Geosynthetics International*, Vol. 4, No. 2, 137-163.

Zhang, C., and Moore, I.D. (1997). "Nonlinear Mechanical Response of High Density Polyethylene. Part I: Experimental Investigation and Model Evaluation," *Polymer Engineering and Science*, Vol. 37, No. 2, pp. 404-413.

Zhang, C., and Moore, I.D. (1997). "Nonlinear Mechanical Response of High Density Polyethylene. Part II: Uniaxial Constitutive Modeling," *Polymer Engineering and Science*, Vol. 37, No. 2, pp. 414-420.

Zhang, D.J.Y. (1999). "Predicting Capacity of Helical Screw Piles in Alberta Soils." M.Sc. Thesis, *University of Alberta*, Department of Civil and Environmental Engineering, Edmonton, Alberta.

Appendix A

ORIGINAL FIELD TESTING DATA

This appendix contains the original data (strain, load cell, and hydraulic pressure) that was recorded by the Data Dolphin data collection units.

UNIVERSITY OF ALBERTA FARMS CLAY SITE

June 11 & 12 Installations

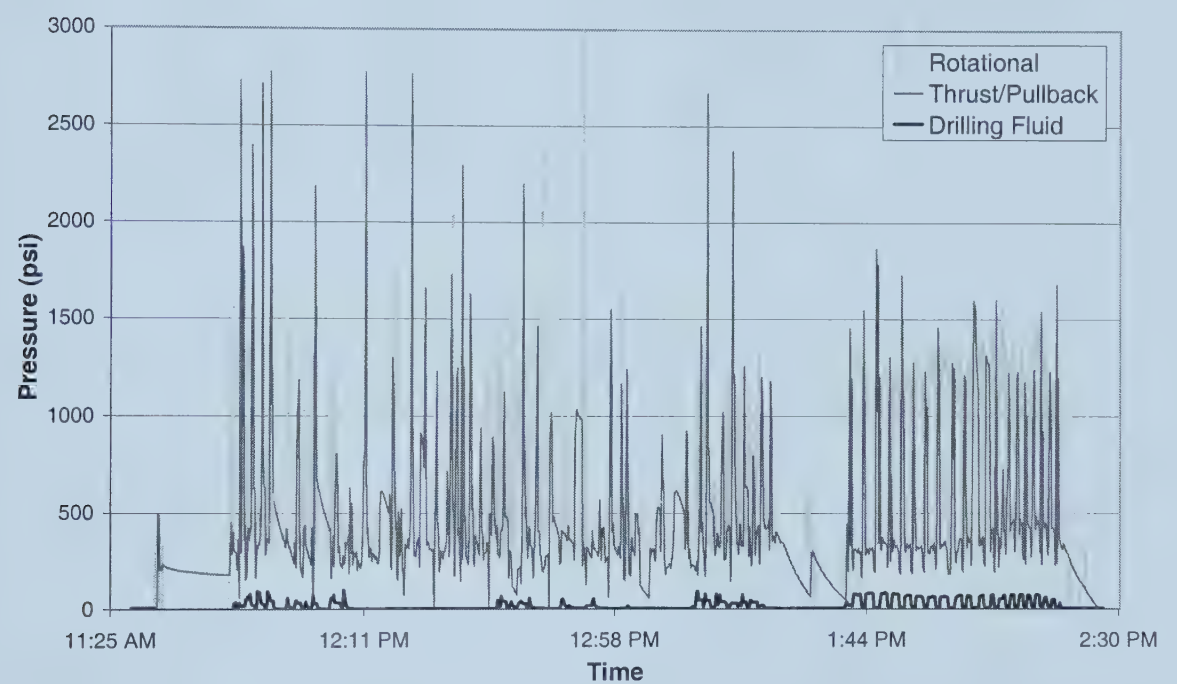


Figure 1: 114 mm (4 in.) Diameter Rig Pressures During Installation

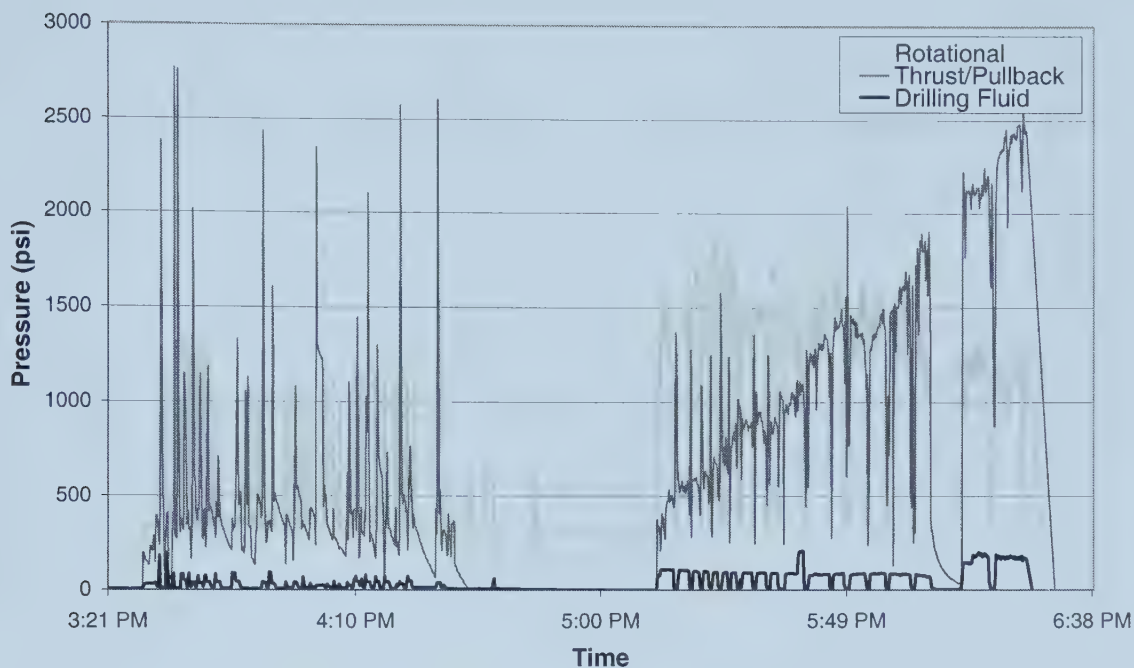


Figure 2: 219 mm Diameter Rig Pressures During Installation

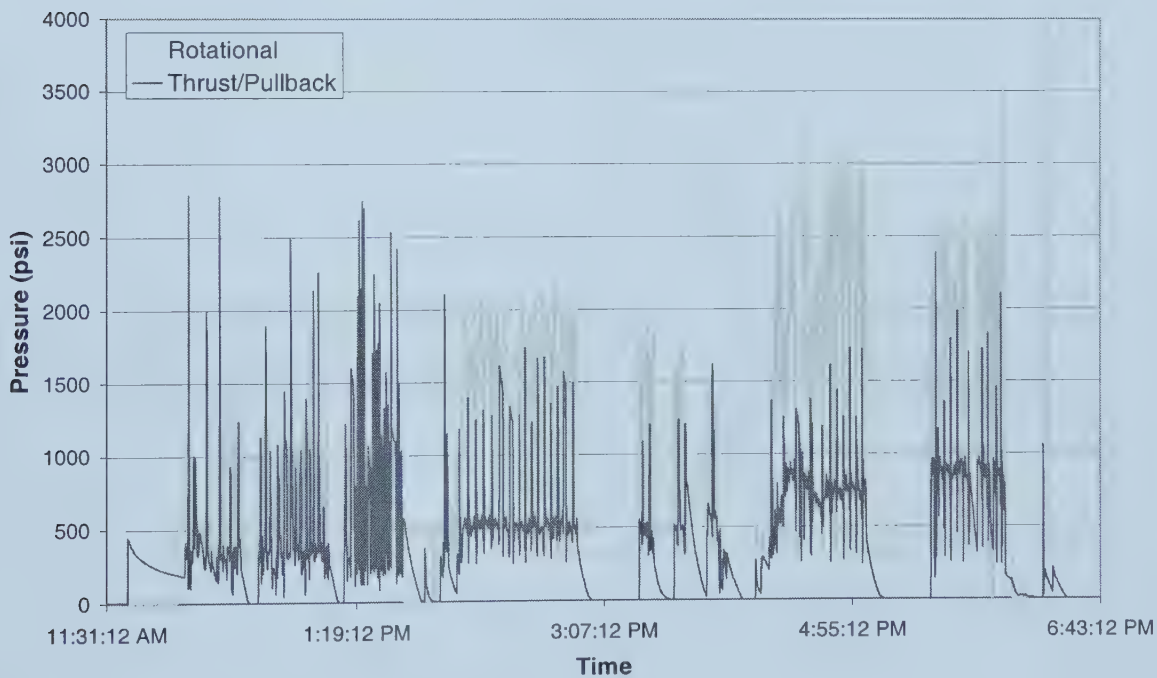


Figure 3: 324 mm Diameter Rig Pressures

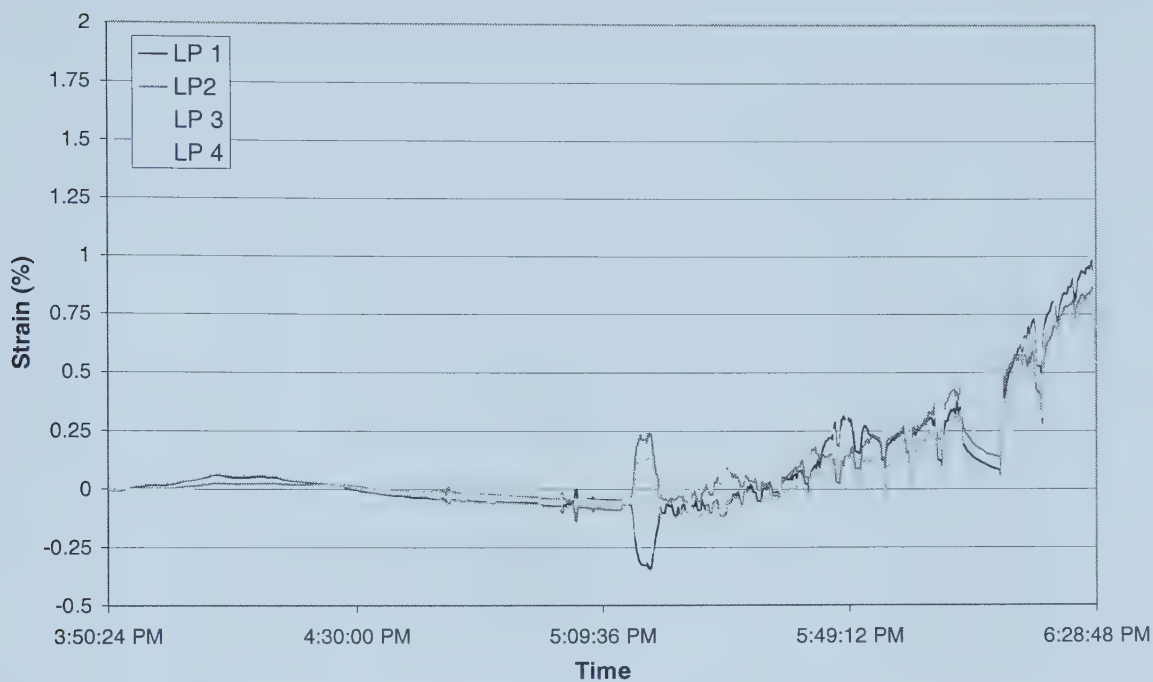


Figure 4: 214 mm Diameter Pipe Strains

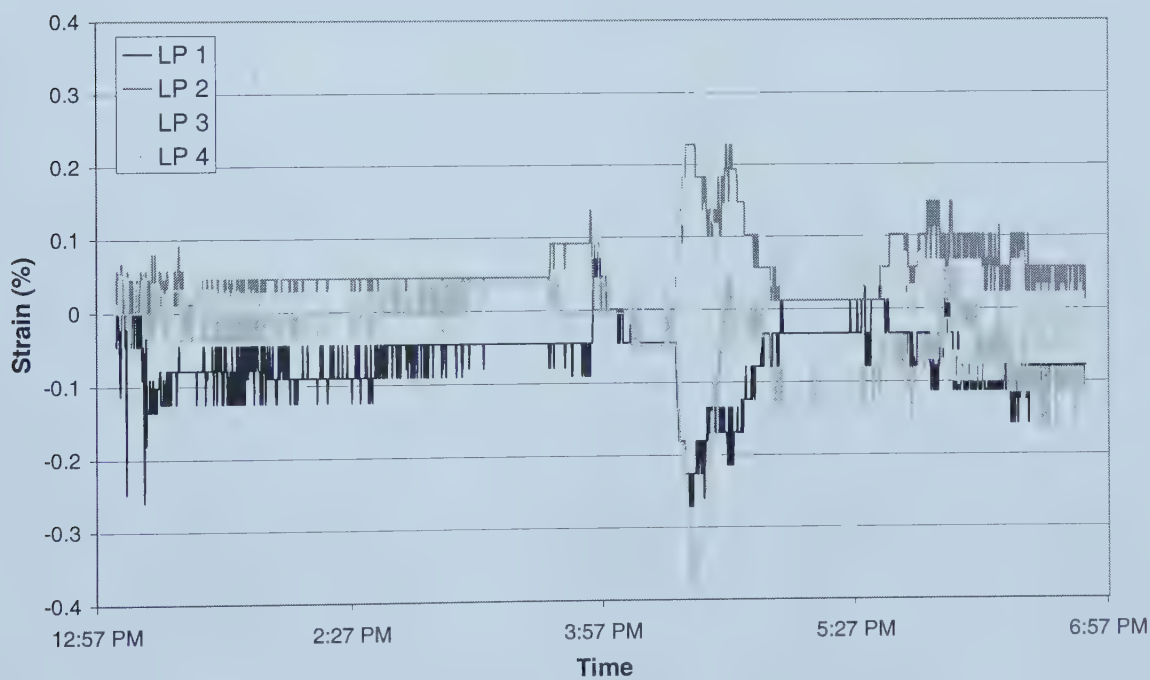


Figure 5: 324 mm Diameter Strain During Pipe Pullback

August 28 Installations

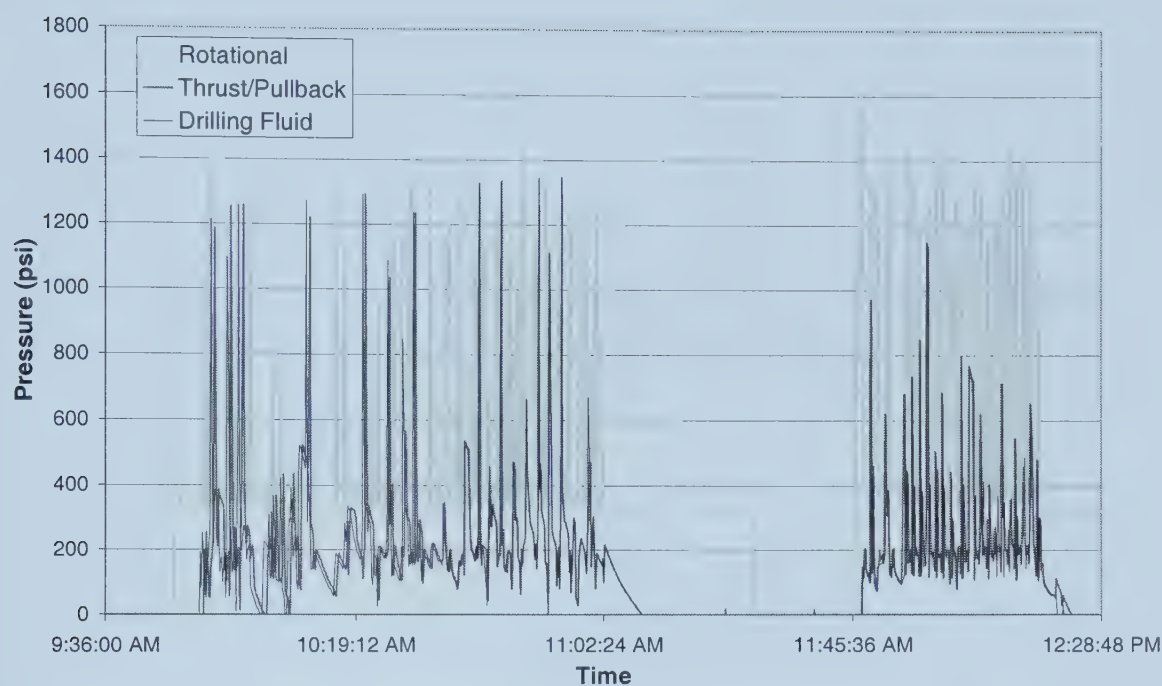


Figure 6: 114 mm Diameter Drilling Rig Pressures

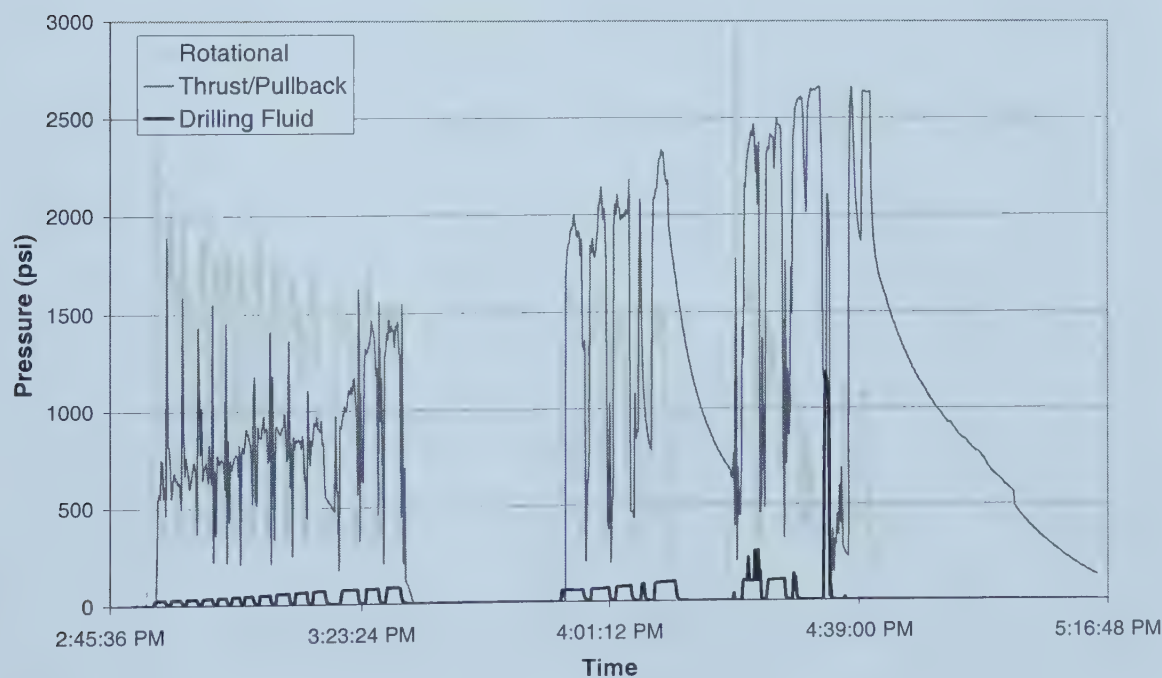


Figure 7: 219 mm Diameter Drilling Rig Pressures

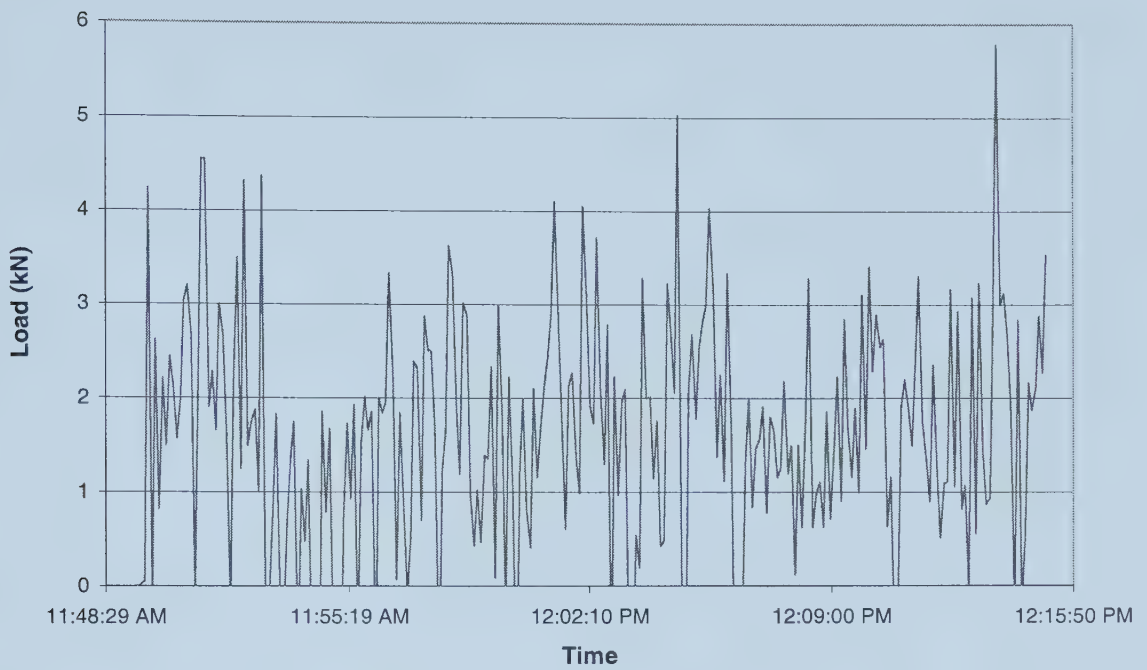


Figure 8: 114 mm Diameter Pipe Load Cell Results

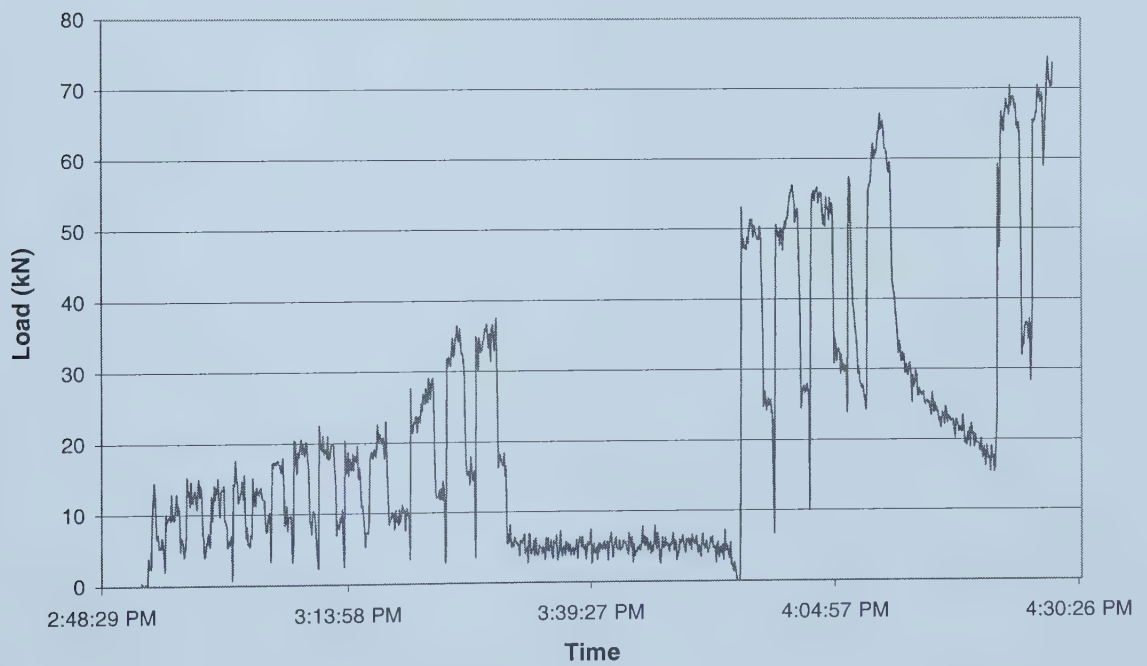


Figure 9: 214 mm Diameter Pipe Load Cell Results

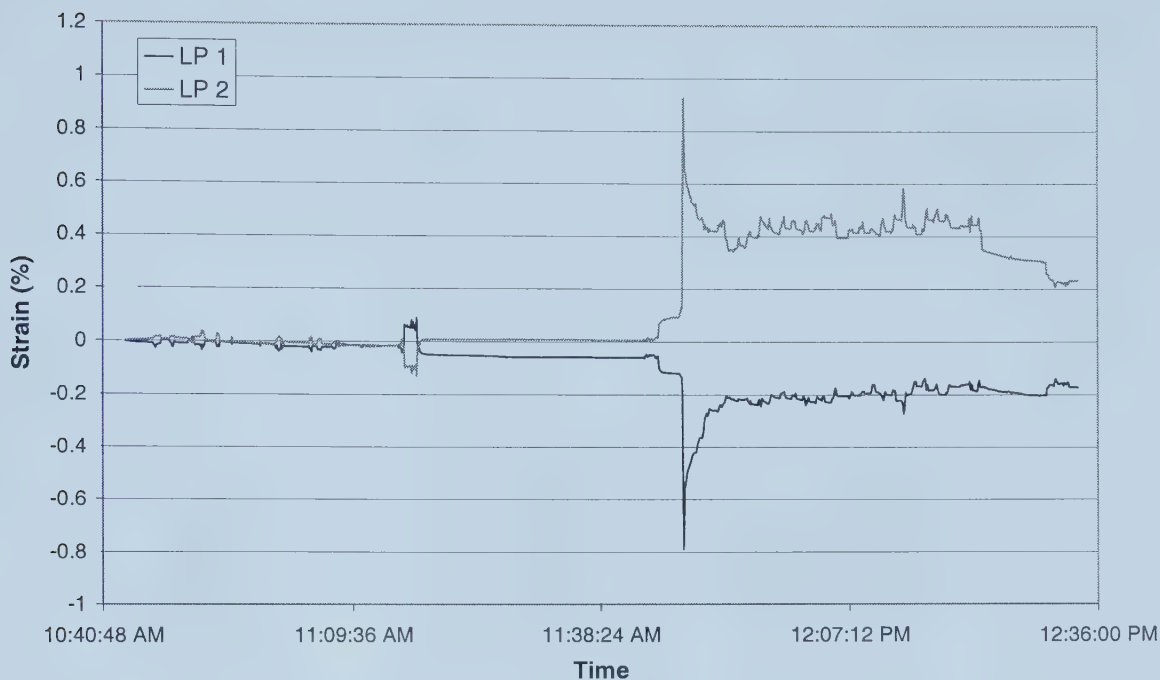


Figure 10: 114 mm Diameter Pipe Strain

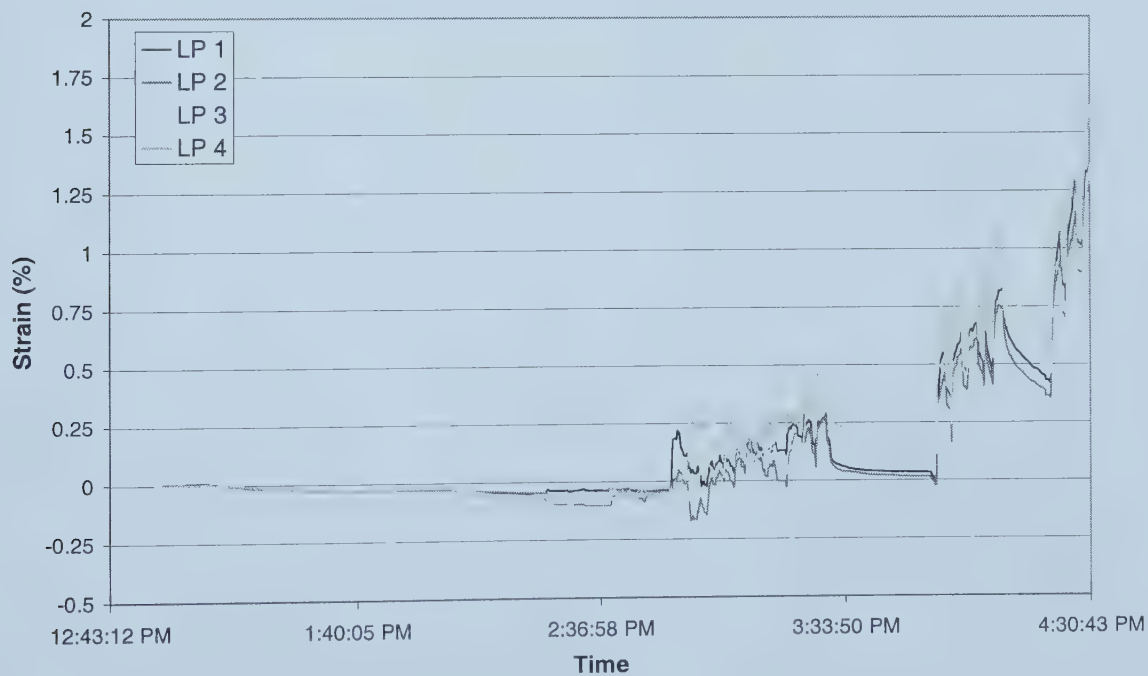


Figure 11: 219 mm Diameter Pipe Strain

SIL SILICA SAND SITE

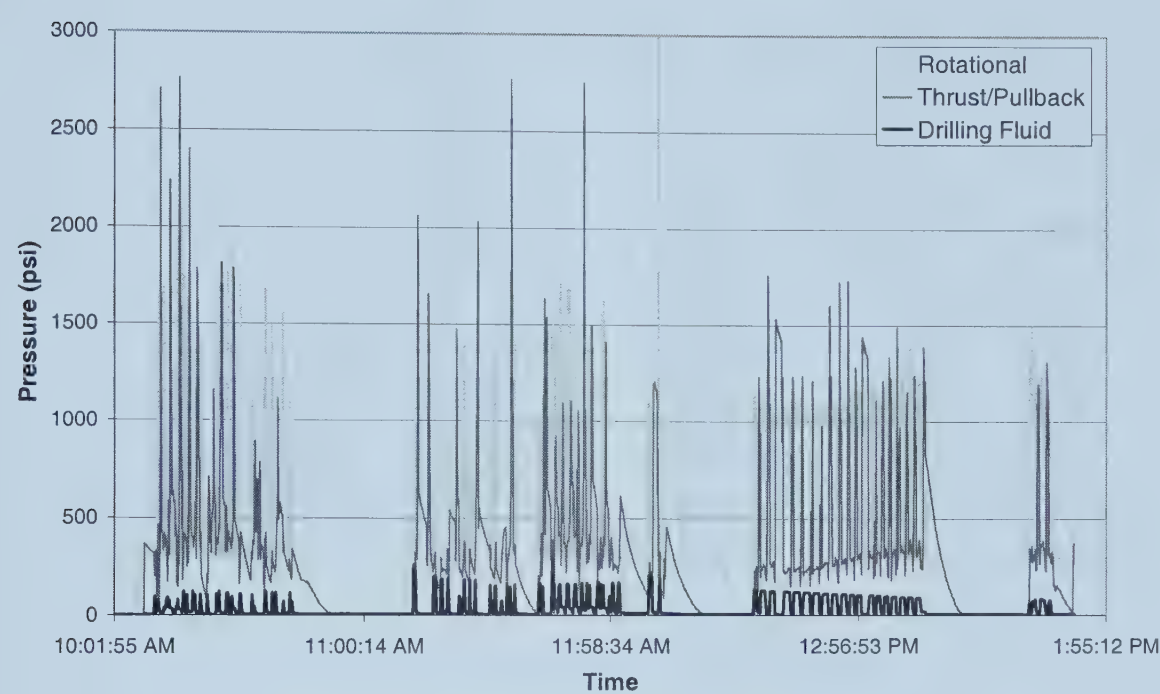


Figure 12: Drilling Rig Pressures 114 mm Diameter

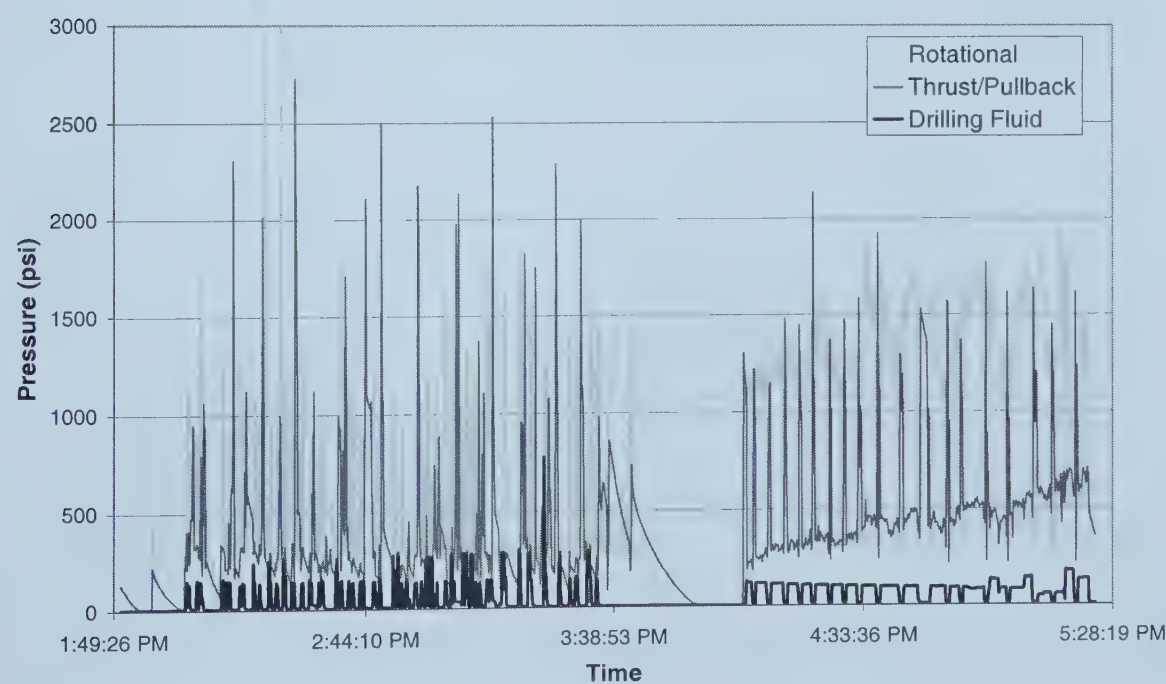


Figure 13: 219 mm Diameter Drilling Rig Pressures

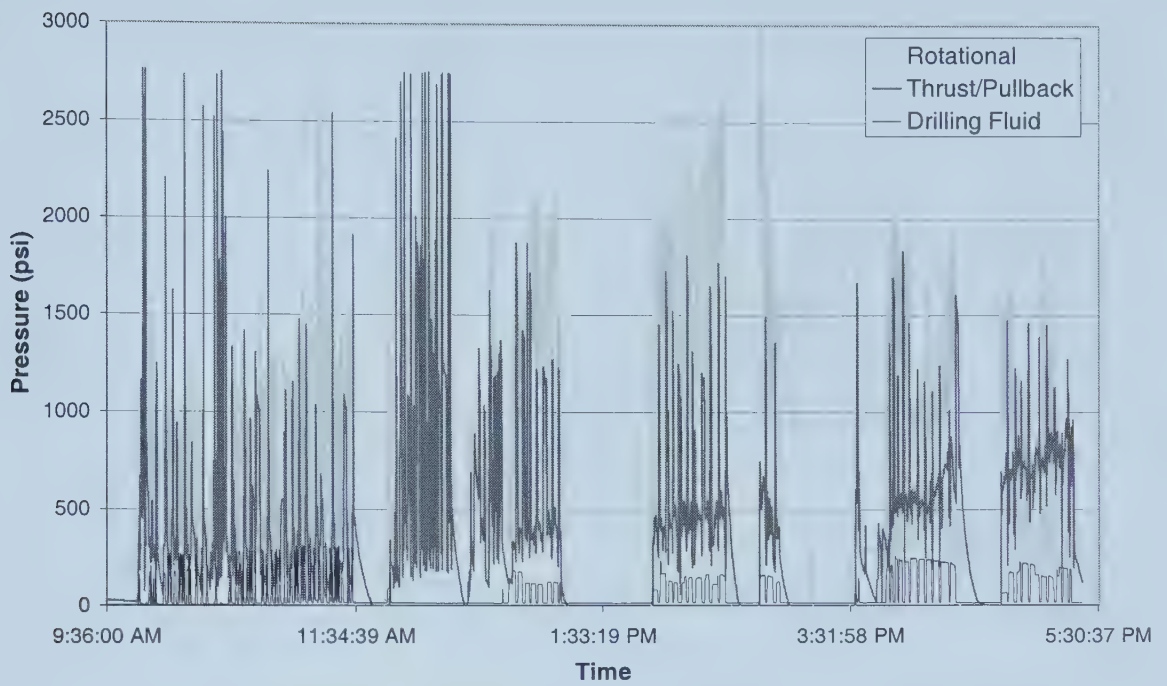


Figure 14: 324 mm Diameter Rig Pressures

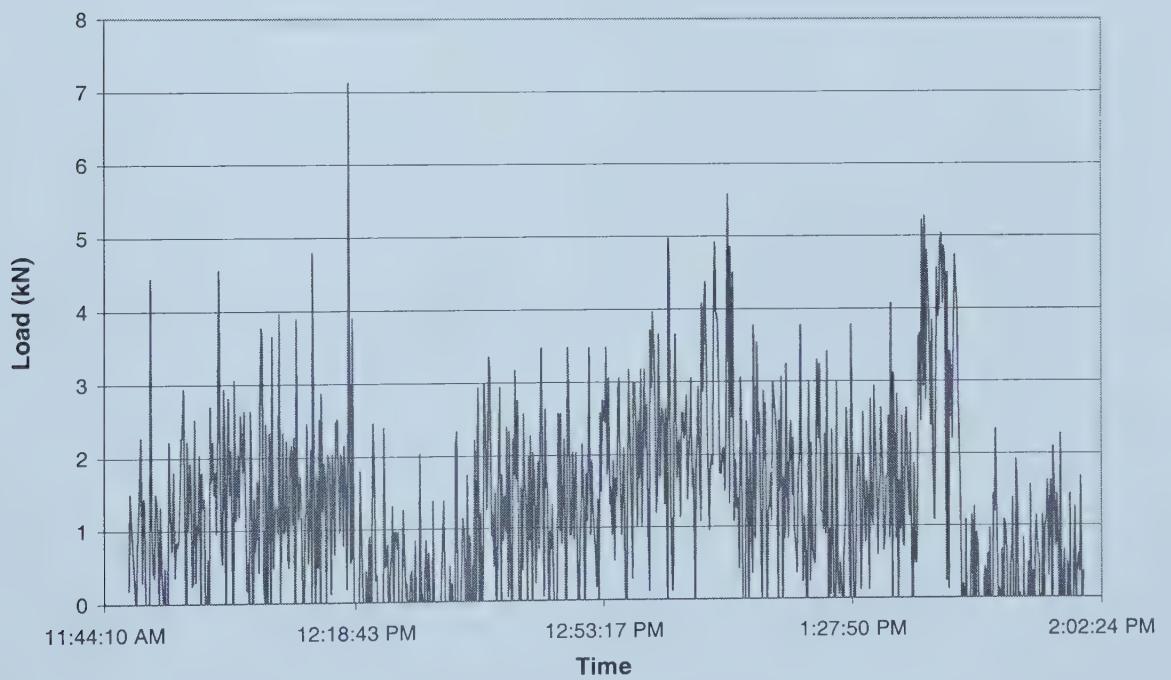


Figure 15: 114 mm Diameter Load Cell

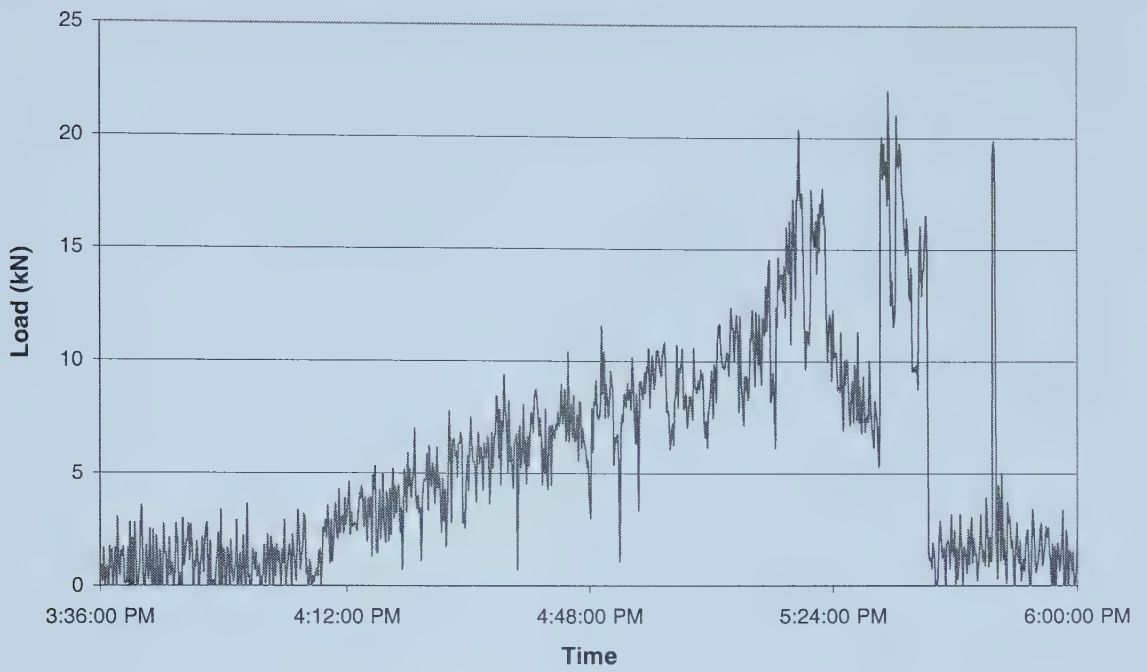


Figure 16: 219 mm Diameter Load Cell

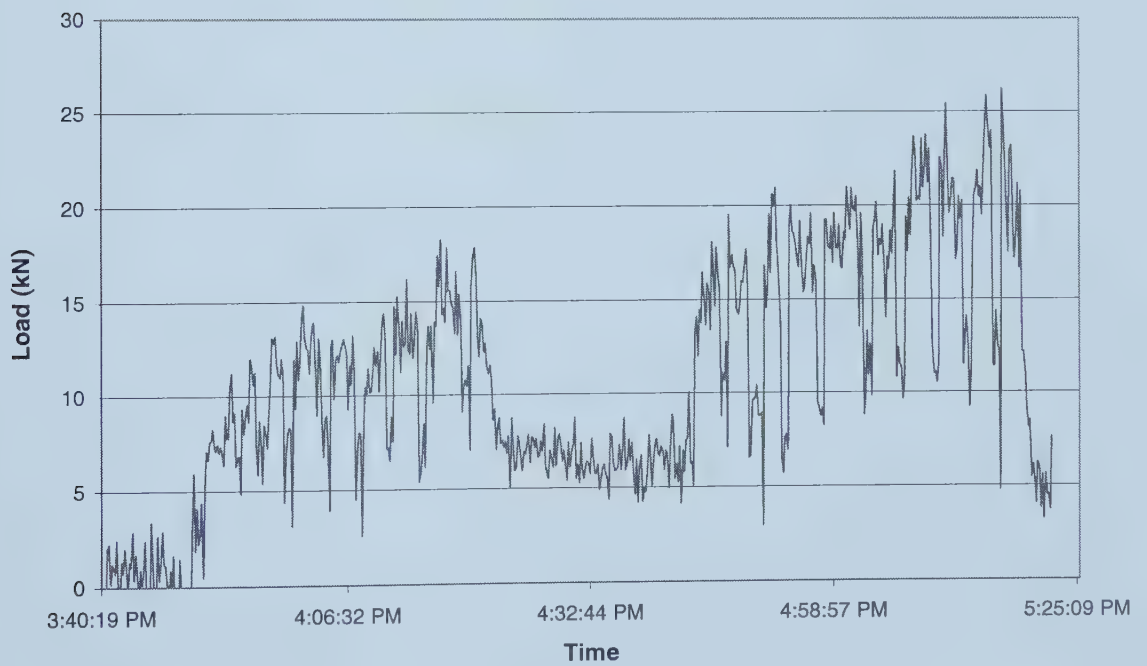


Figure 17: 324 mm Diameter Load Cell Results

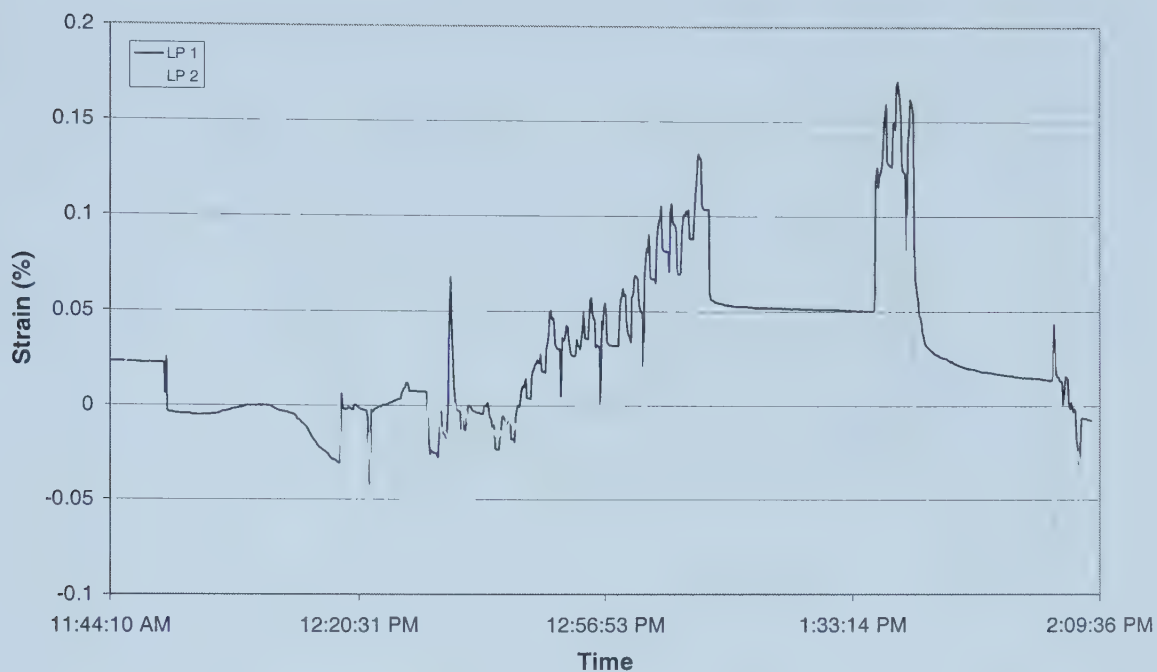


Figure 18: 114 mm Diameter Strain

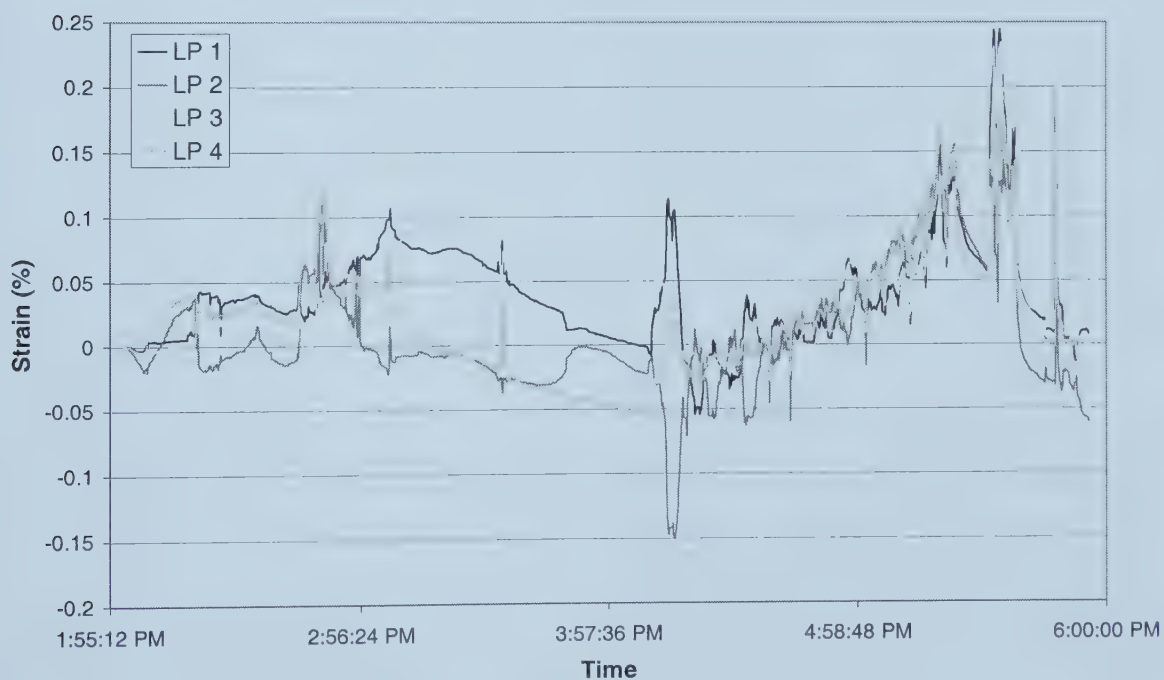


Figure 19: 219 mm Diameter Pipe Strain

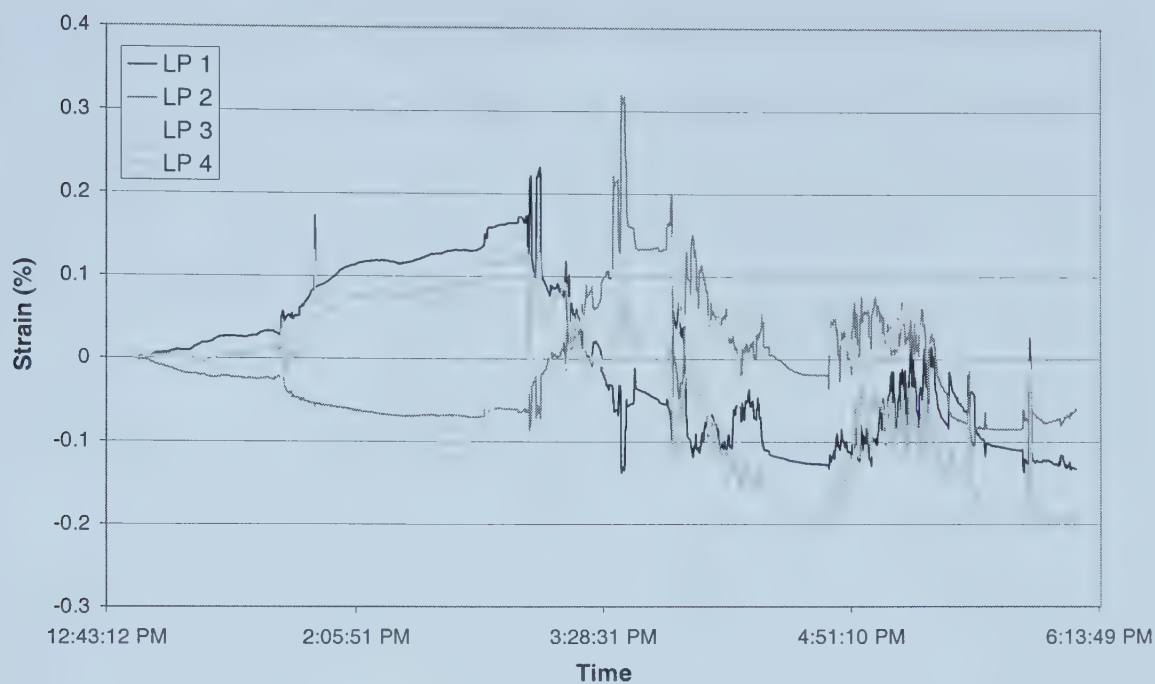


Figure 20: 324 mm Diameter Pipe Strain

Appendix B ORIGINAL TENSILE TESTING DATA

This appendix contains the stress strain curves for each of the coupon specimens that were tested

UNIVERSITY OF ALBERTA FARMS INSTALLATIONS - CLAY

219 mm Diameter Before Installation

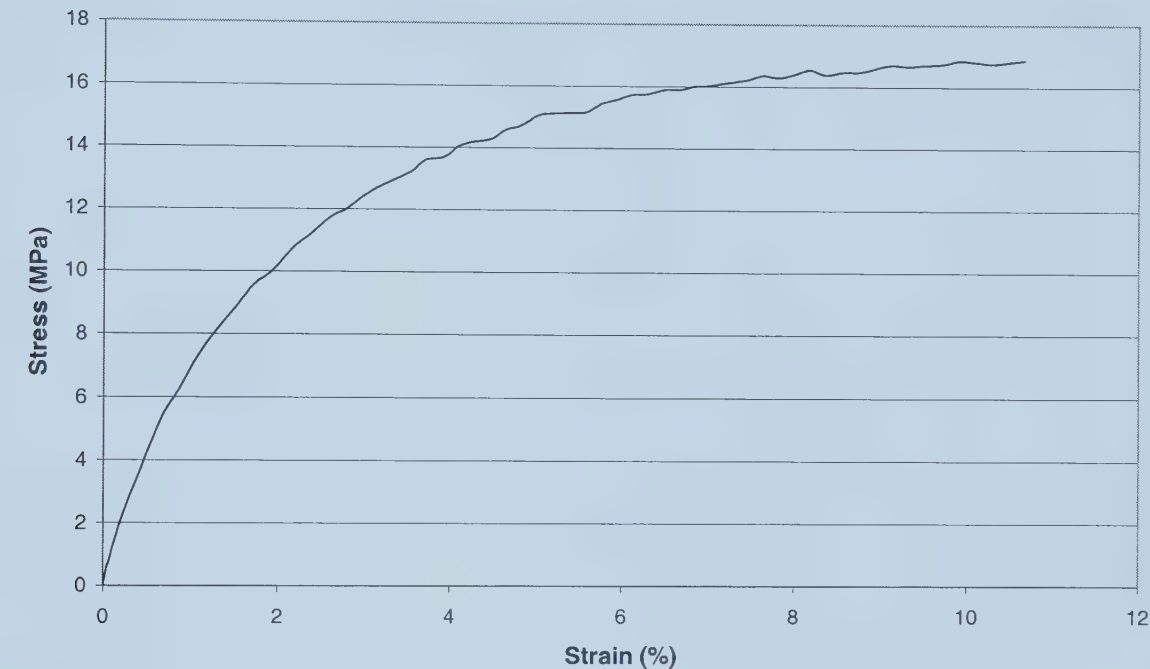


Figure 1: Stress-Strain Graph for Coupon 1 – 219 mm Clay Before Installation

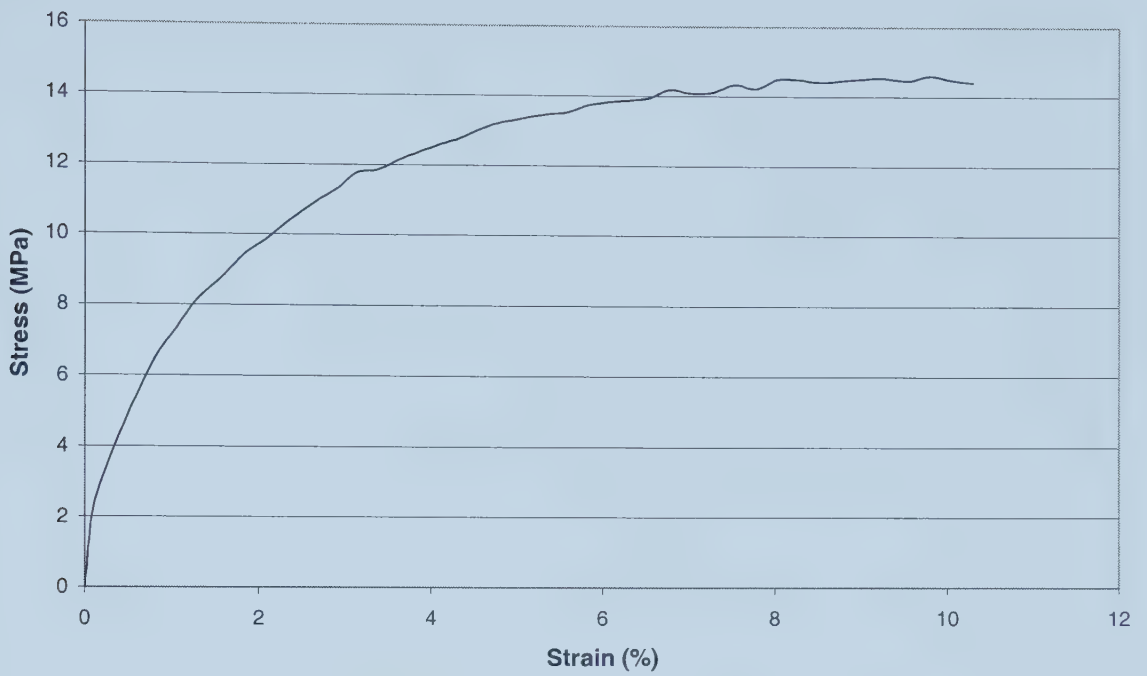


Figure 2: Stress-Strain Graph for Coupon 2 – 219 mm Clay Before Installation

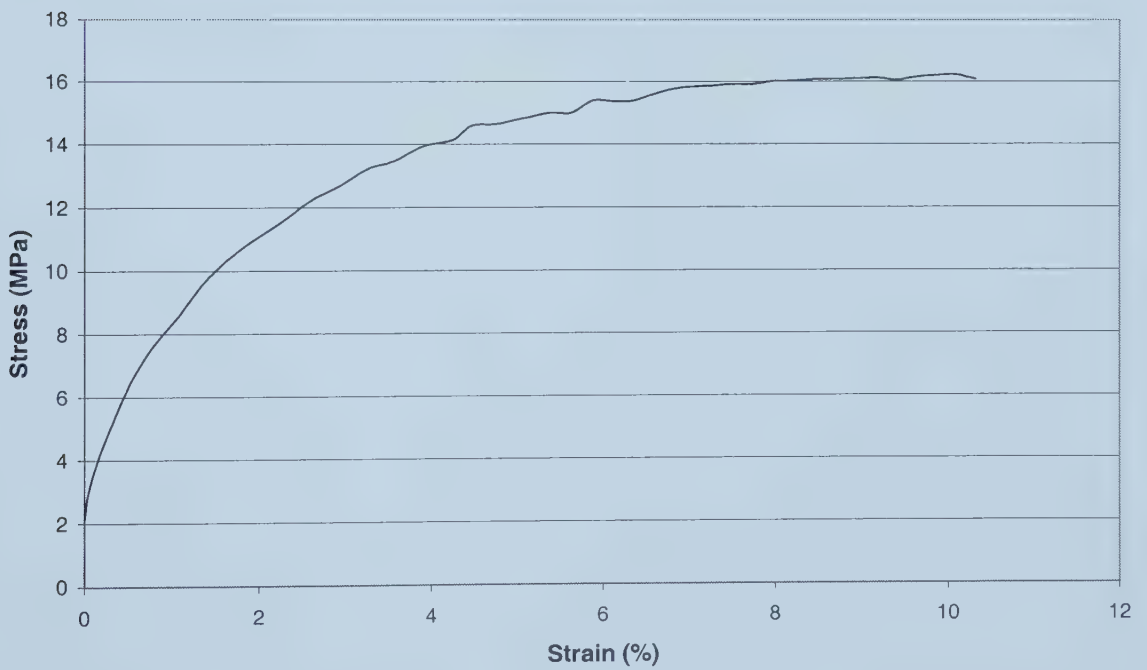


Figure 3: Stress-Strain Graph for Coupon 3 – 219 mm Clay Before Installation

219 mm Diameter Following Installation

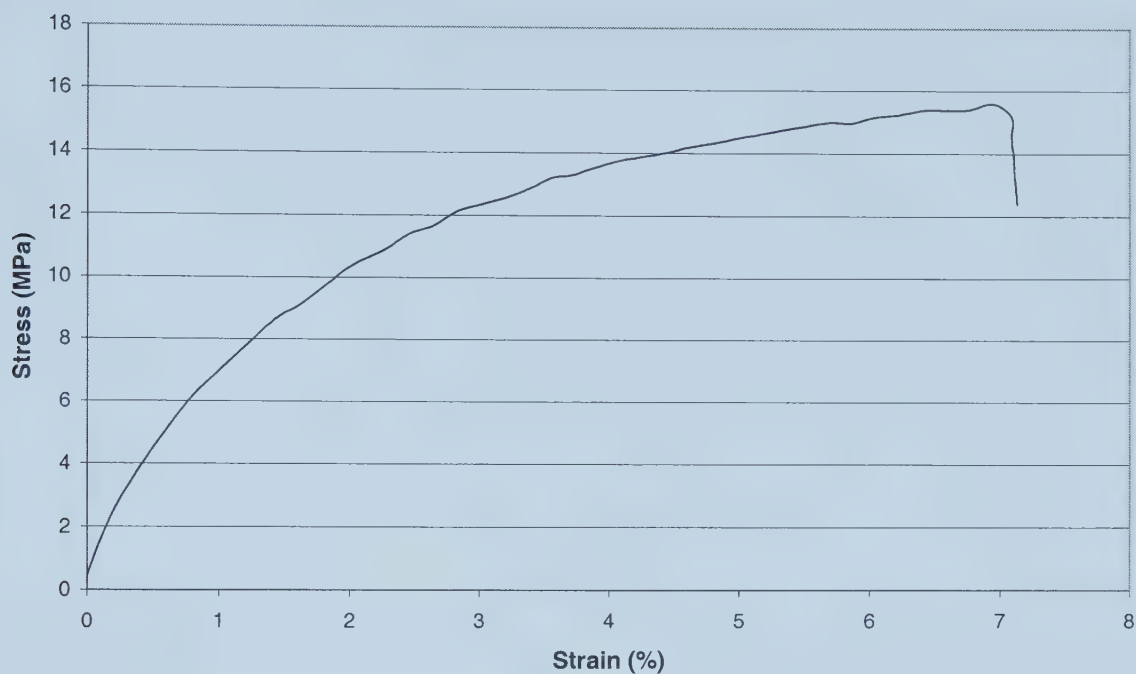


Figure 4: Stress-Strain Graph for Coupon 1 – 219 mm Clay Following Installation

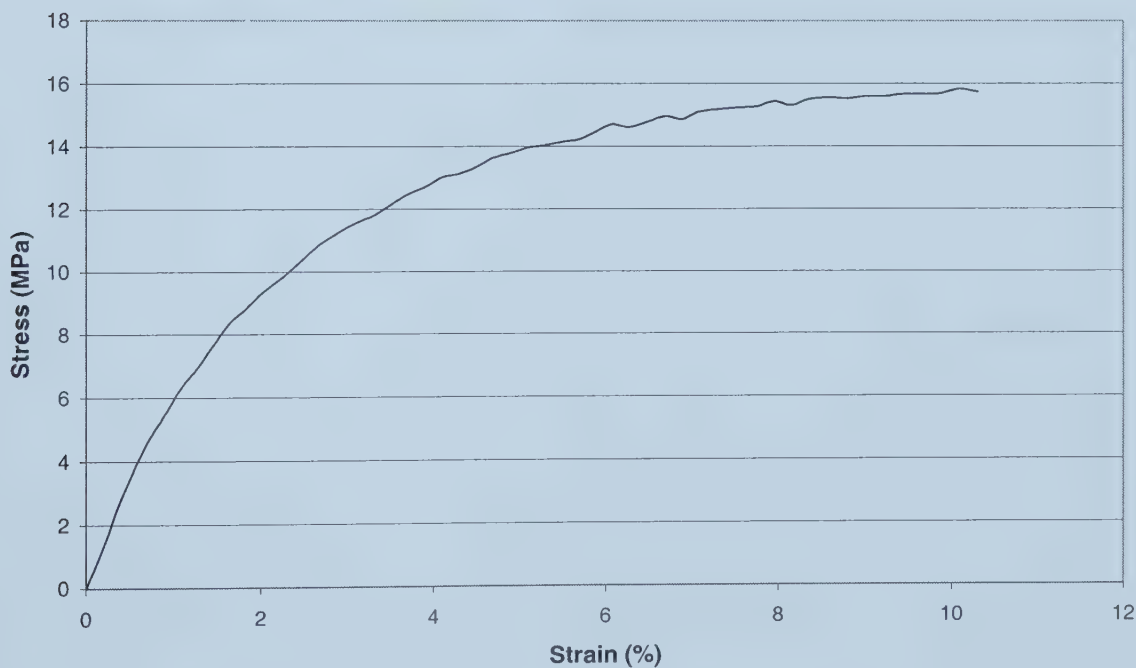


Figure 5: Stress-Strain Graph for Coupon 2 – 219 mm Clay Following Installation

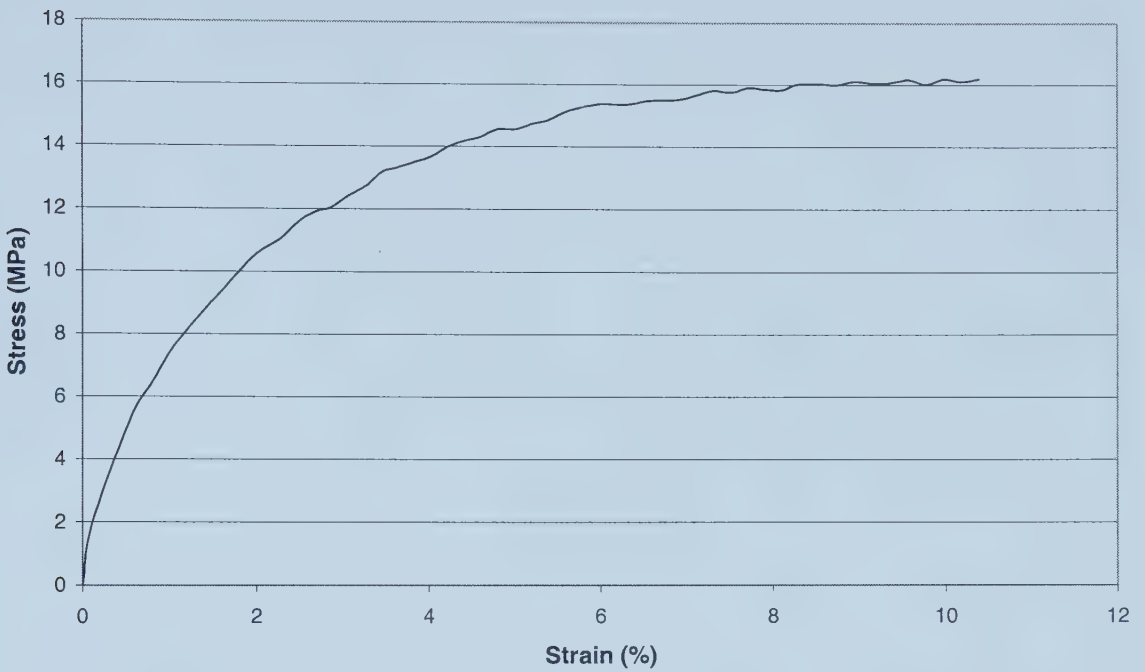


Figure 6: Stress-Strain Graph for Coupon 3 – 219 mm Clay Following Installation

324 mm Diameter Before Installation

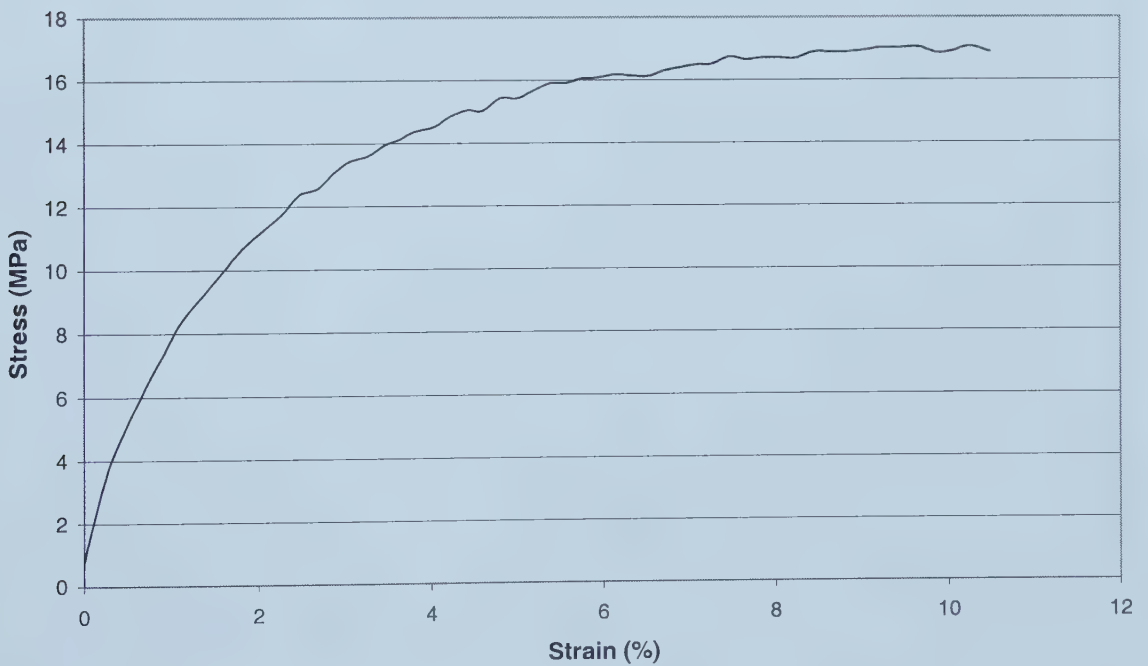


Figure 7: Stress-Strain Graph for Coupon 1 – 324 mm Clay Before Installation

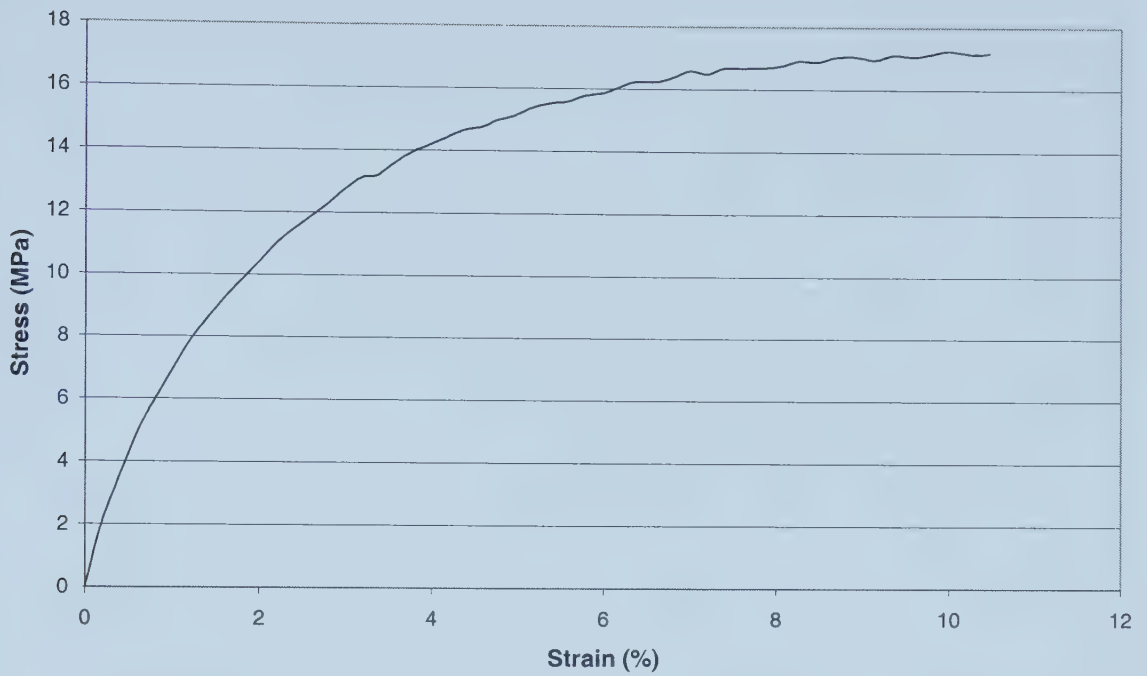


Figure 8: Stress-Strain Graph for Coupon 2 – 324 mm Clay Before Installation

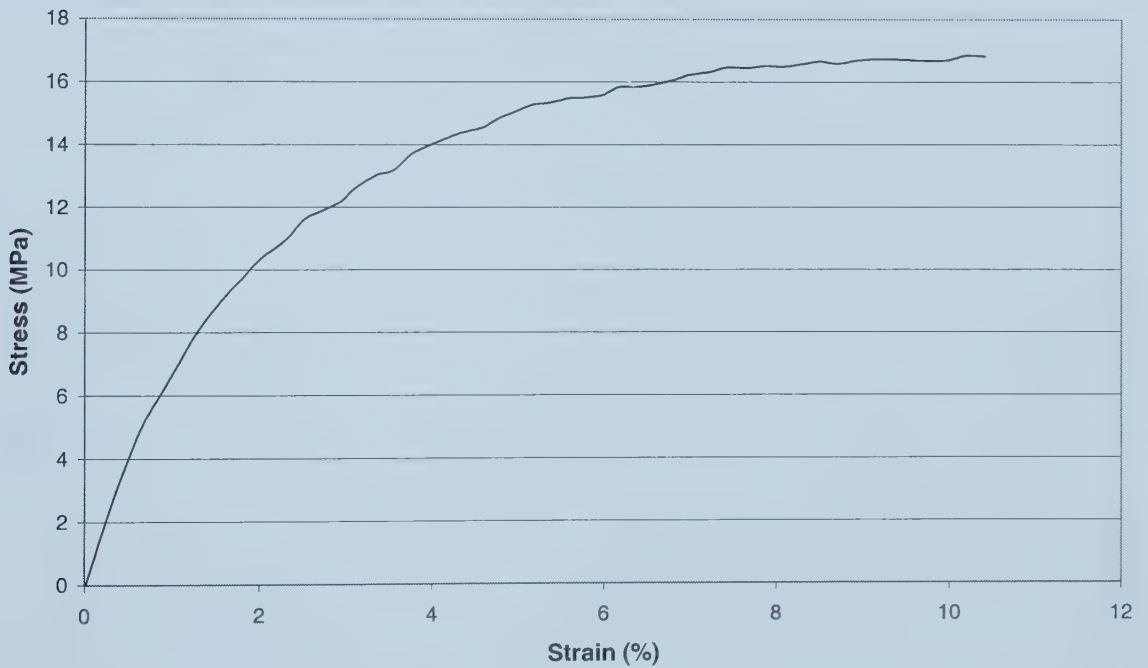


Figure 9: Stress-Strain Graph for Coupon 3 – 324 mm Clay Before Installation

324 mm Diameter Following Installation

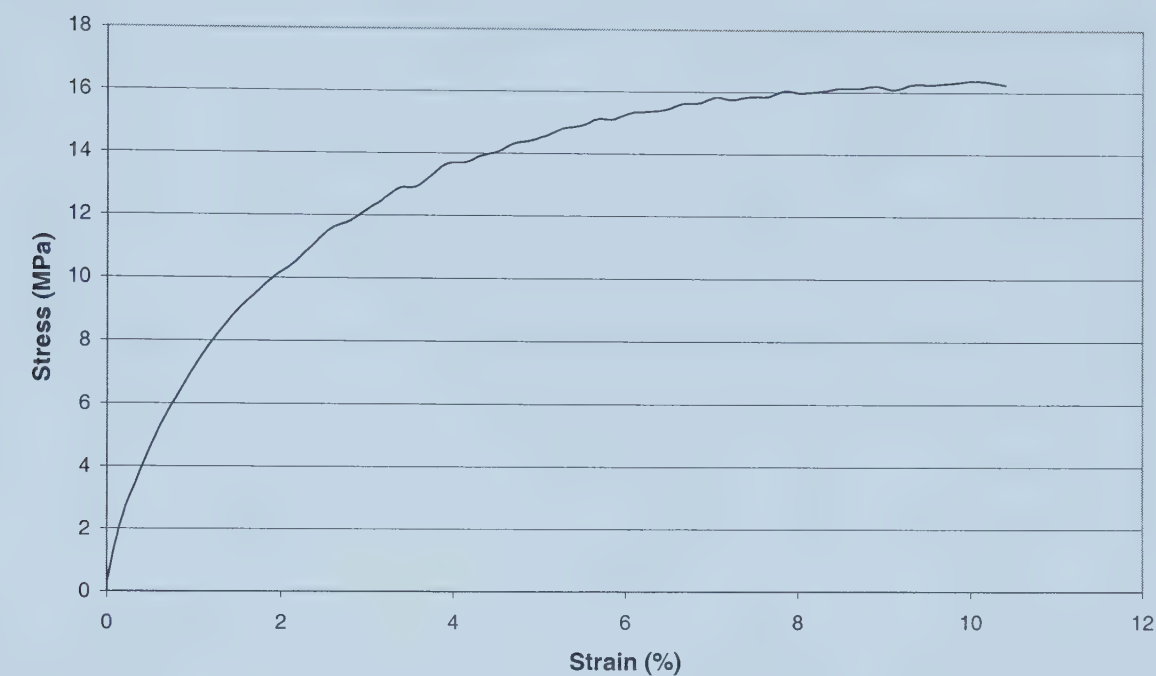


Figure 10: Stress-Strain Graph for Coupon 1 – 324 mm Clay Following Installation

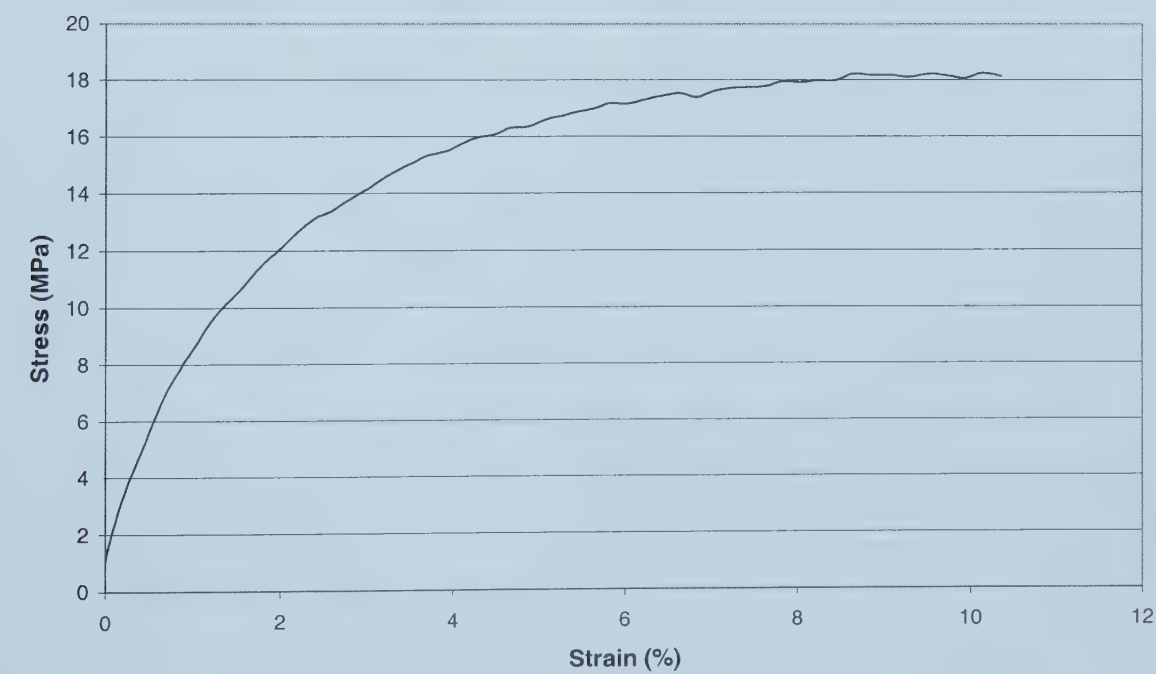


Figure 11: Stress-Strain Graph for Coupon 2 – 324 mm Clay Following Installation

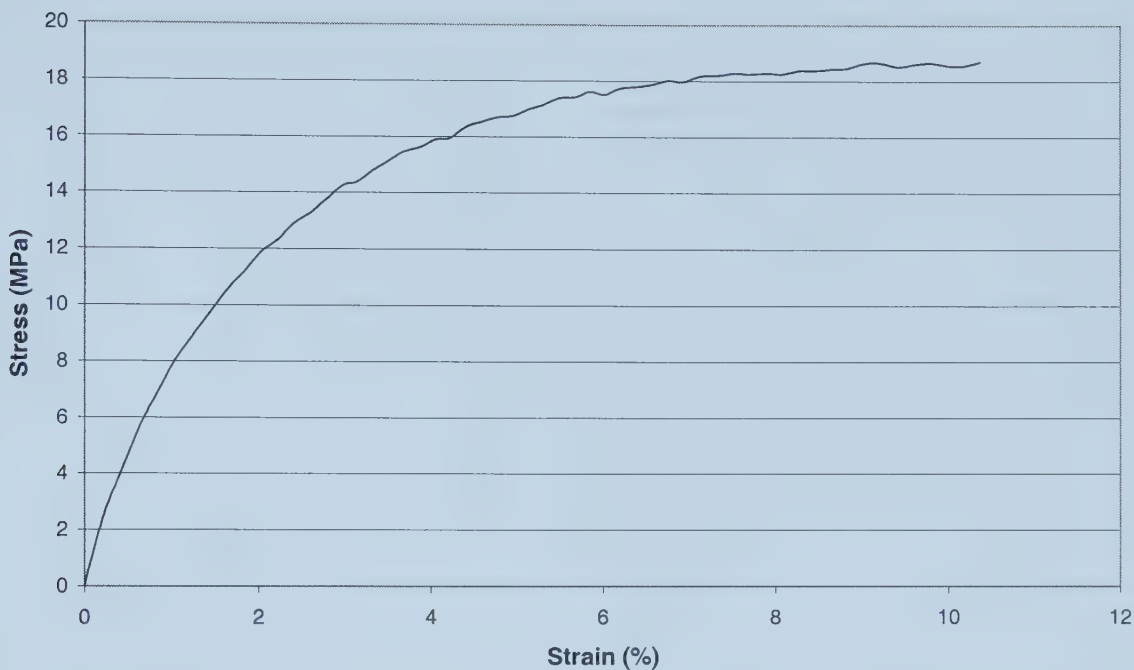


Figure 12: Stress-Strain Graph for Coupon 3 – 324 mm Clay Following Installation

SIL SILICA SAND PIT INSTALLATIONS - SAND

219 mm Diameter Before Installation

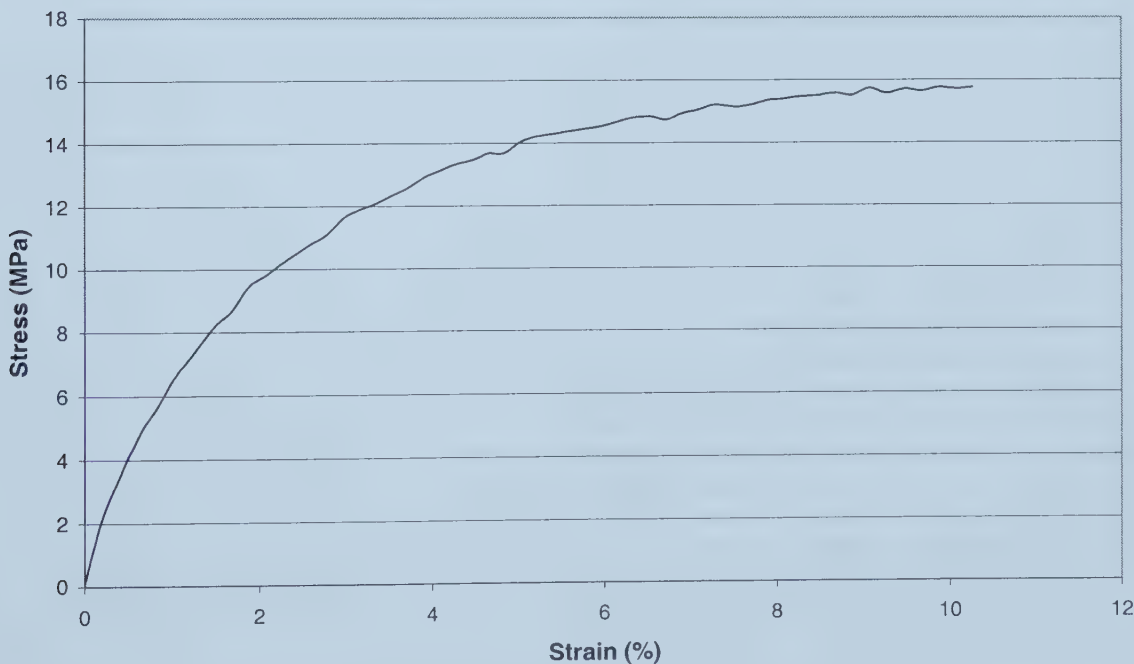


Figure 13: Stress-Strain Graph for Coupon 1 – 219 mm Sand Before Installation

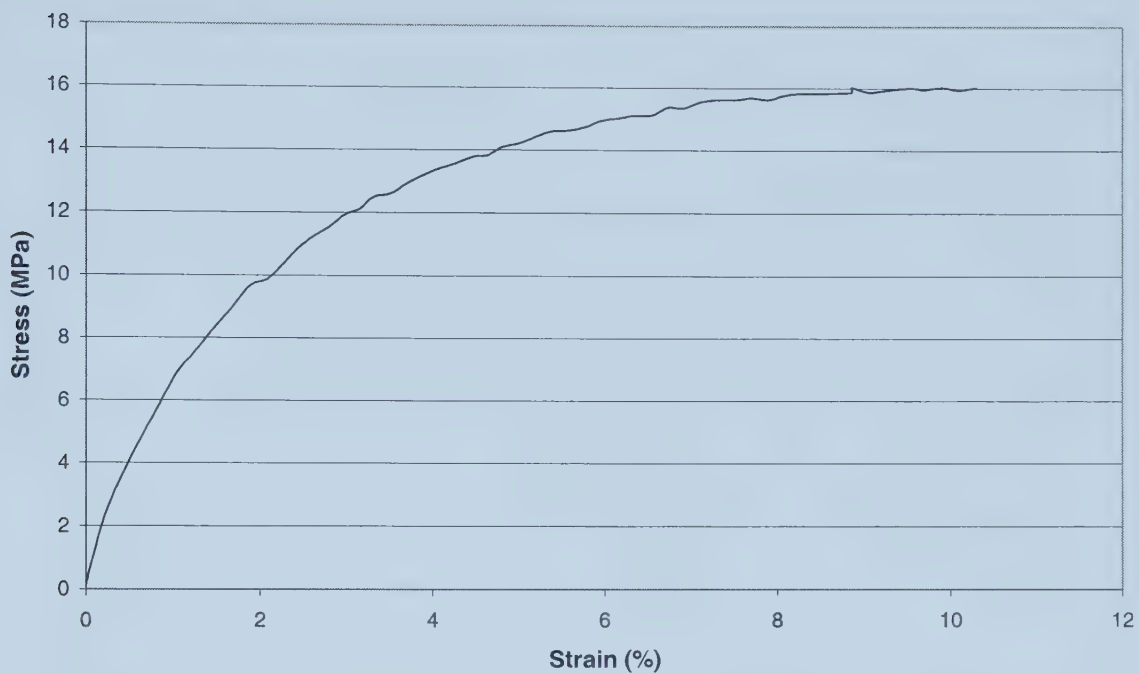


Figure 14: Stress-Strain Graph for Coupon 2 – 219 mm Sand Before Installation

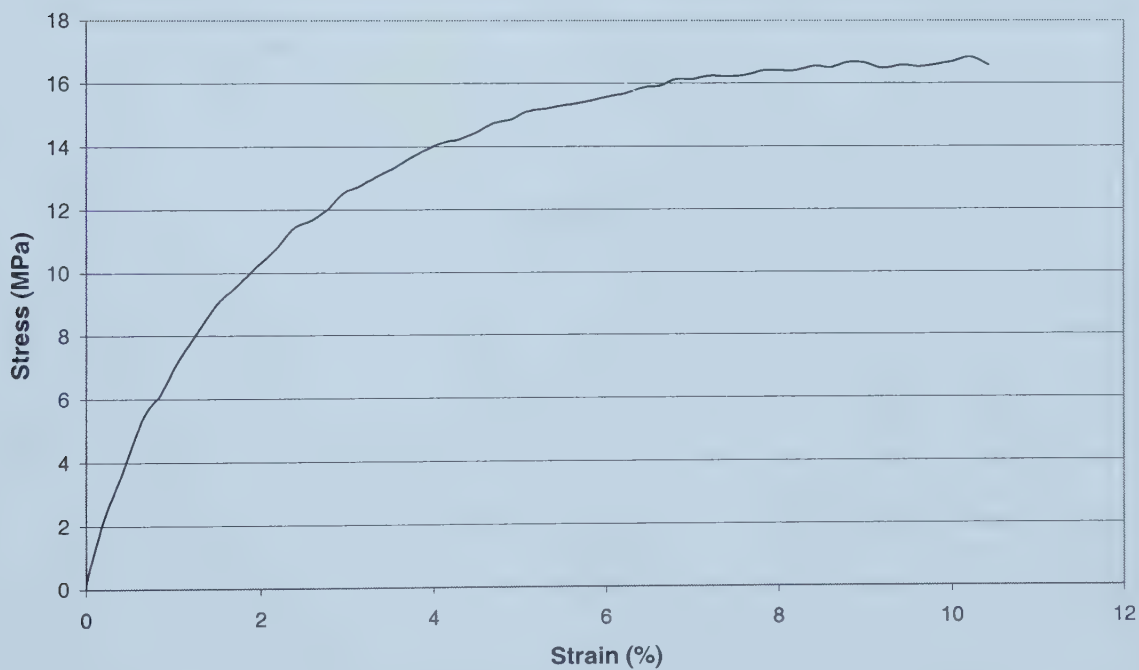


Figure 15: Stress-Strain Graph for Coupon 3 – 219 mm Sand Before Installation

219 mm Diameter Following Installation

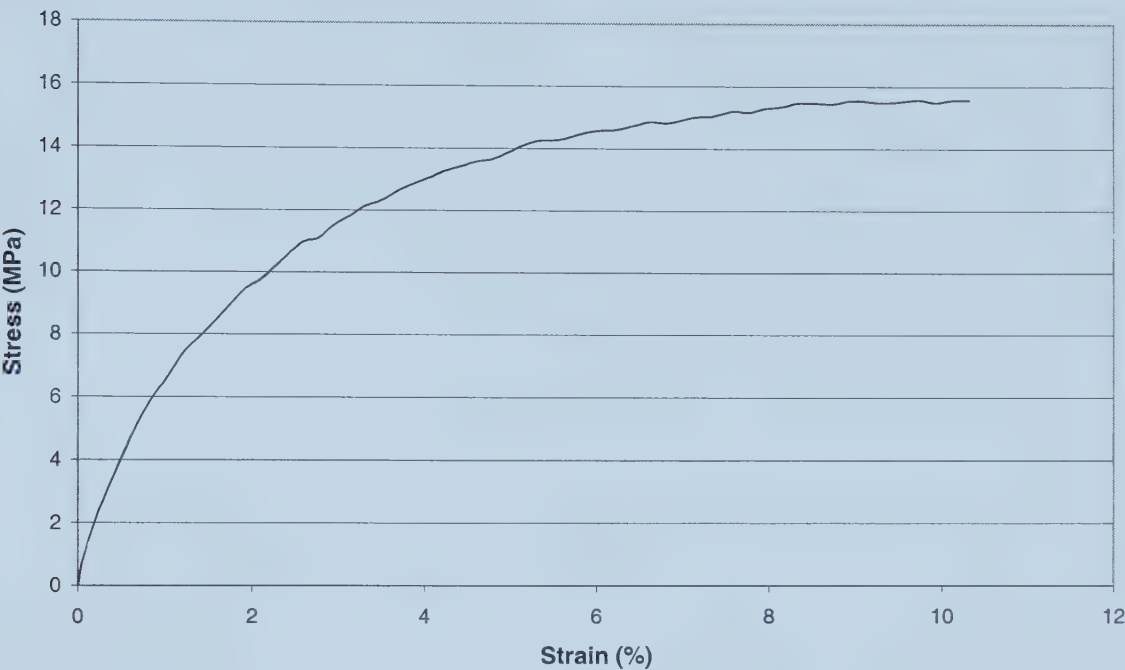


Figure 16: Stress-Strain Graph for Coupon 1 – 219 mm Sand Following Installation

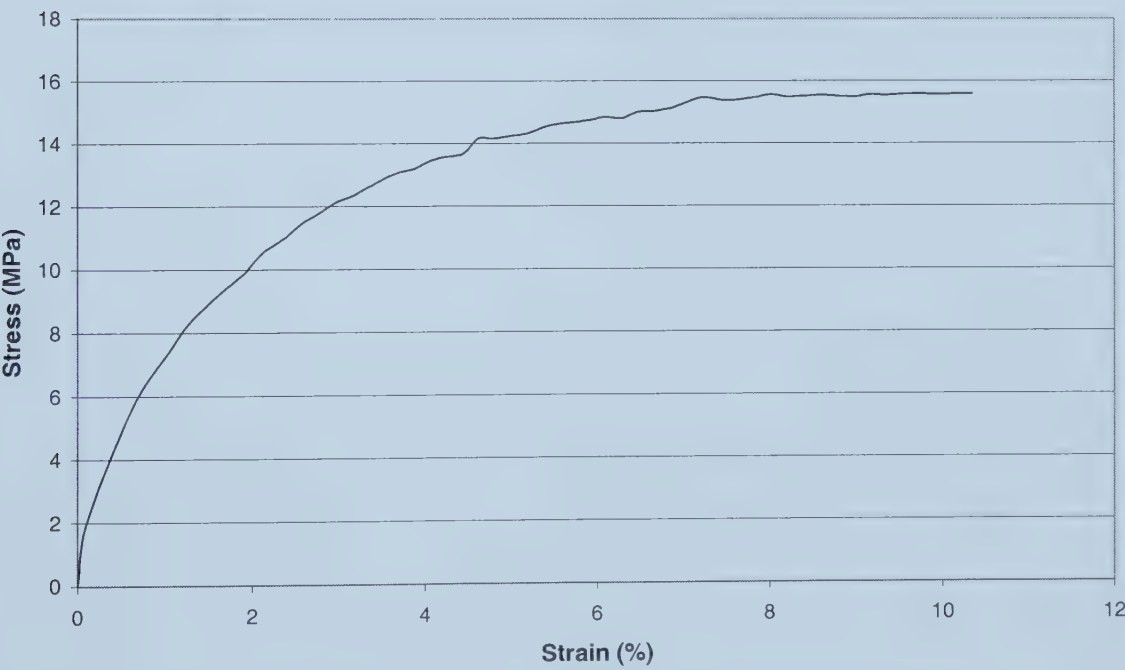


Figure 17: Stress-Strain Graph for Coupon 2 – 219 mm Sand Following Installation

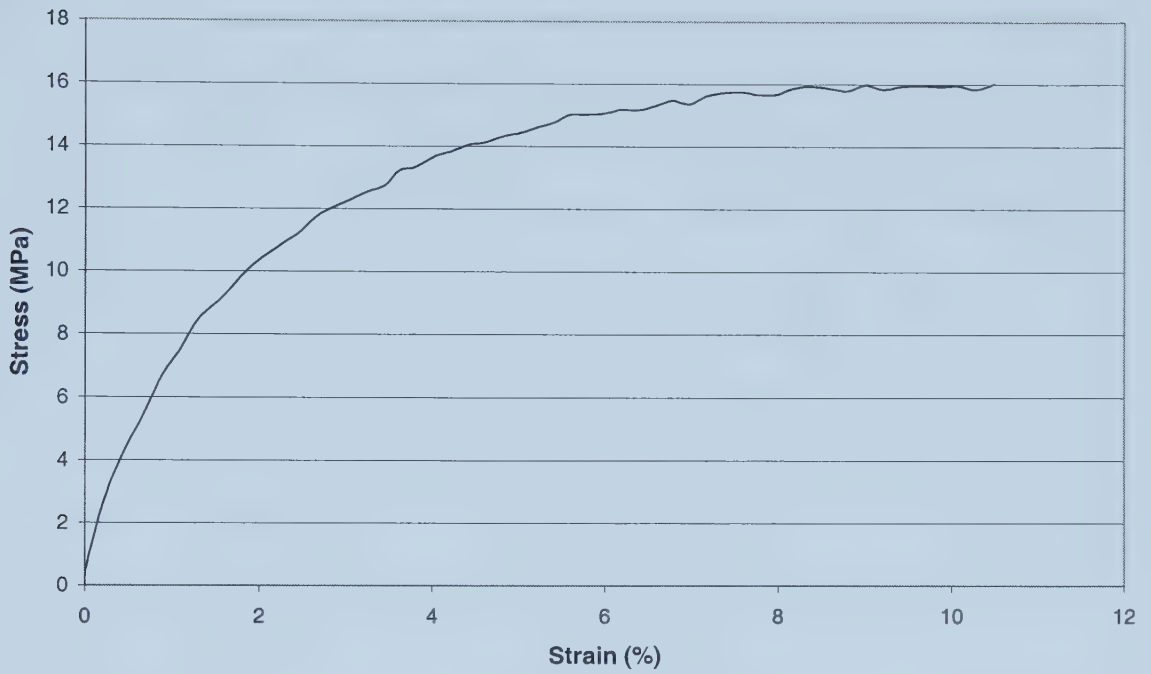


Figure 18: Stress-Strain Graph for Coupon 3 – 219 mm Sand Following Installation

324 mm Diameter Before Installation

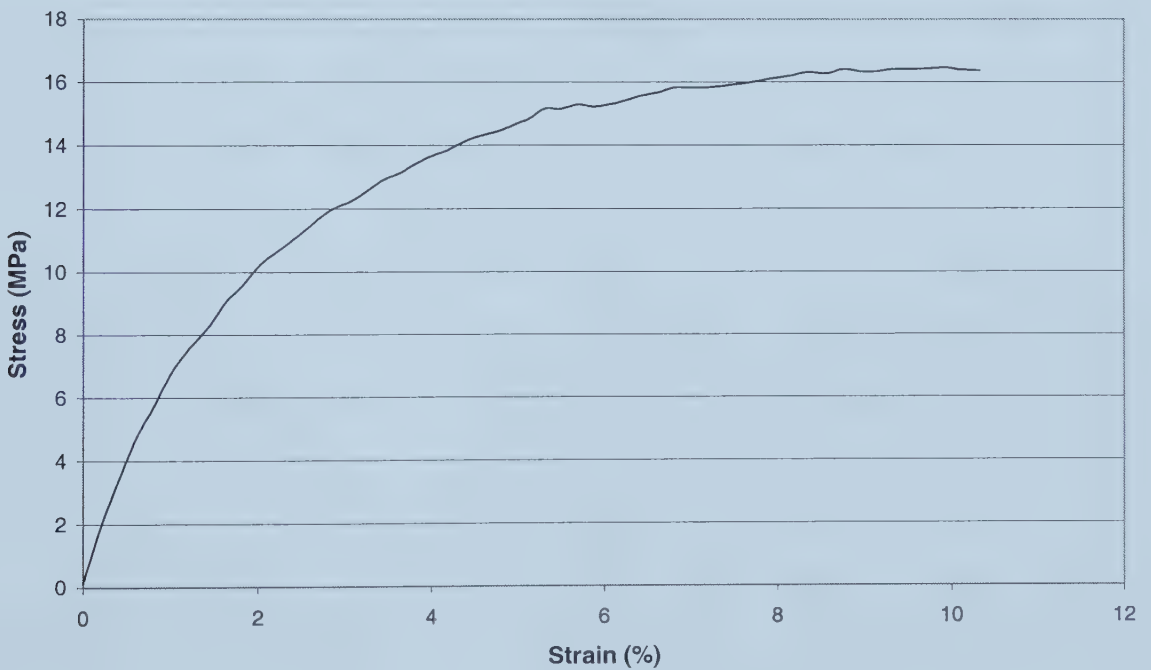


Figure 19: Stress-Strain Graph for Coupon 1 – 324 mm Sand Before Installation

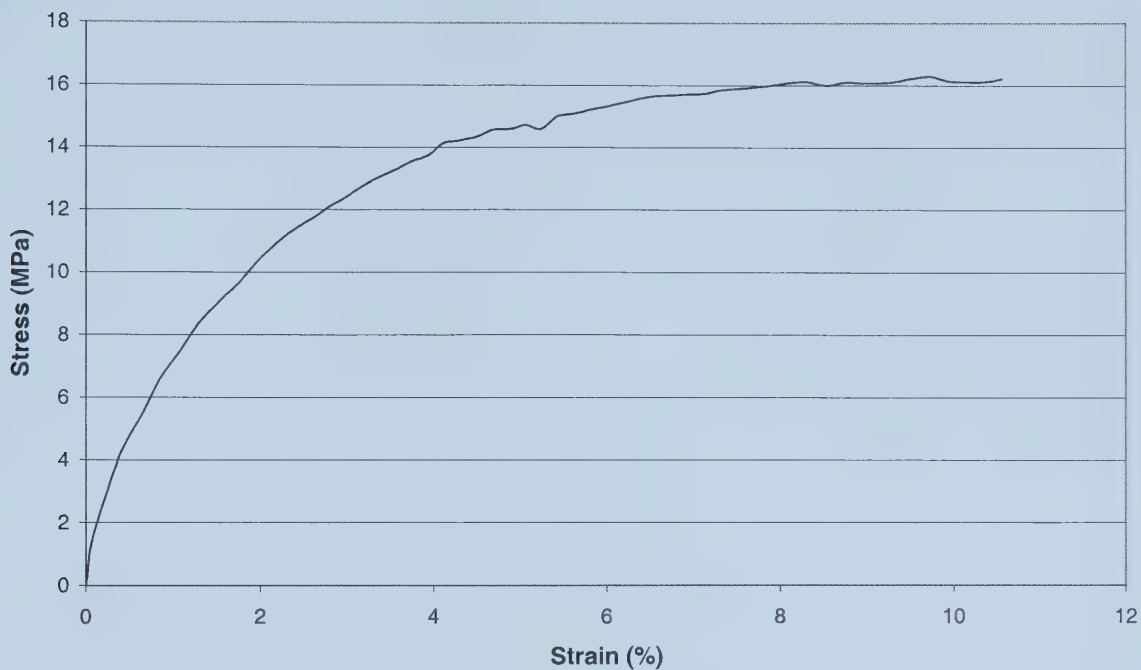


Figure 20: Stress-Strain Graph for Coupon 2 – 324 mm Sand Before Installation

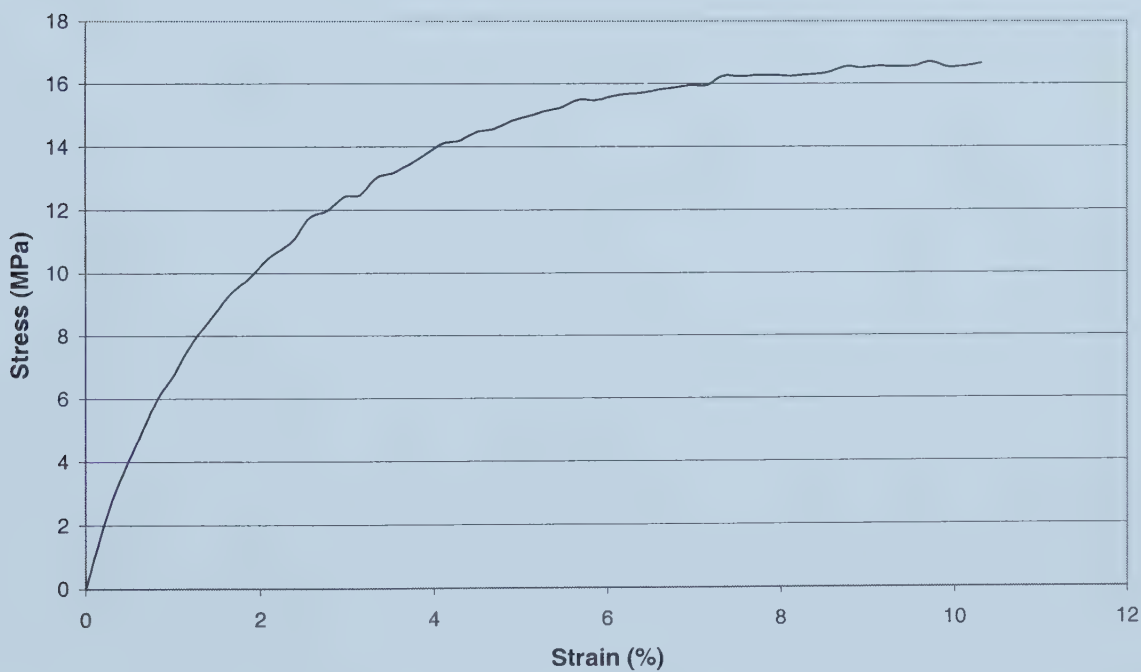


Figure 21: Stress-Strain Graph for Coupon 3 – 324 mm Sand Before Installation

324 mm Diameter Following Installation

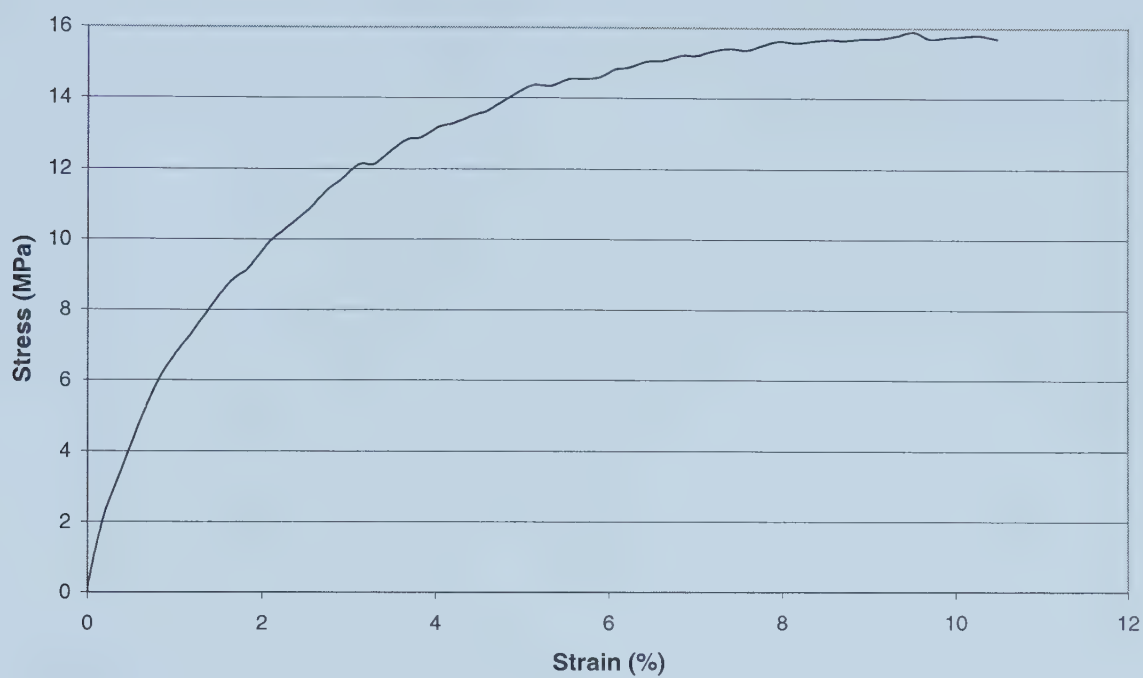


Figure 22: Stress-Strain Graph for Coupon 1 – 324 mm Sand Following Installation

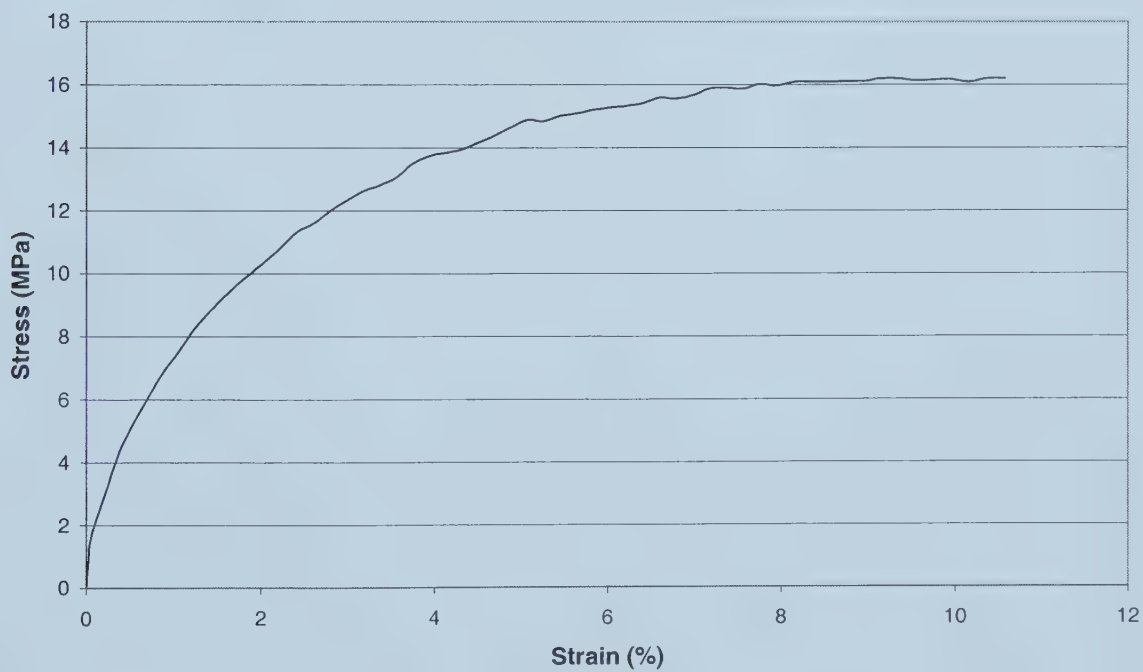


Figure 23: Stress-Strain Graph for Coupon 2 – 324 mm Sand Following Installation

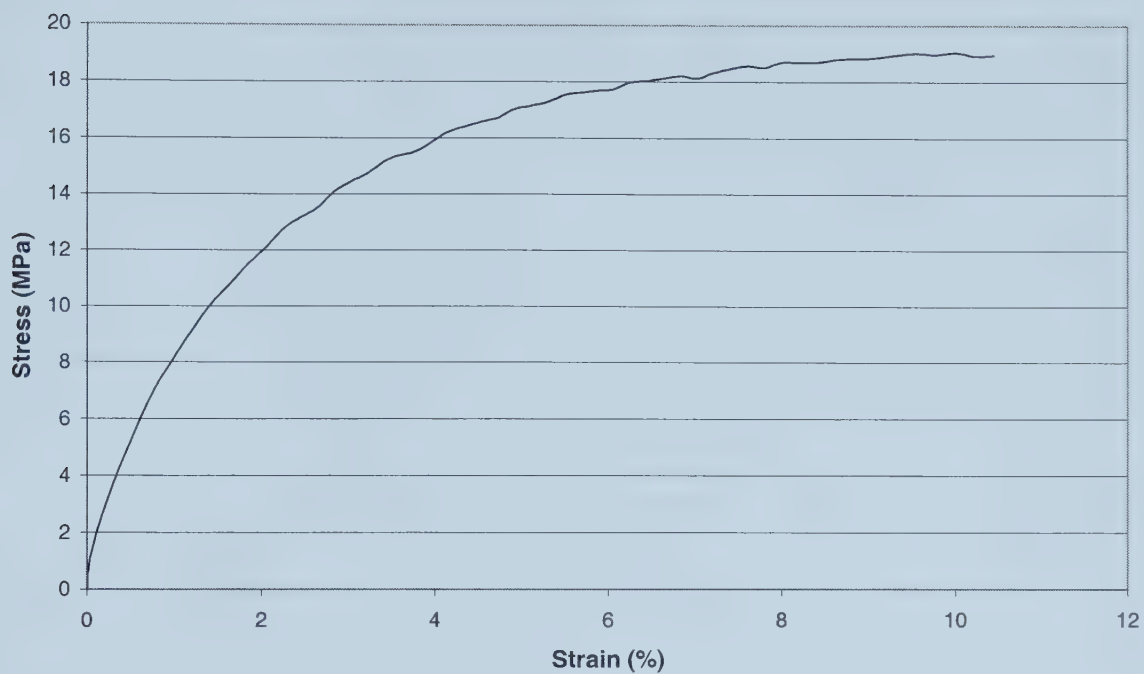


Figure 24: Stress-Strain Graph for Coupon 3 – 324 mm Sand Following Installation

University of Alberta Library



0 1620 1492 0464

B45432